The role of phosphorylation in the control of Ras activity and localisation in *S. cerevisiae*

Thesis submitted to the University of Kent for the degree of

PhD in Cell Biology

Elliot Piper-Brown

Declaration

No part of this thesis has been submitted in support of an application for any degree or other qualification of the University of Kent, or any other University or Institution of learning.

Elliot Piper-Brown

September 2019

Acknowledgements

Firstly, I would like to express my sincere gratitude to my supervisor Dr Campbell Gourlay for giving me the opportunity to conduct this research and for his constant support, guidance patience, and for sharing his vast wisdom in both science and life. The completion of thesis would not have been possible without the support and belief from my friends. I would like to thank Peter, Joey, Melisa, Sophie T, Zakary, and Daniel for being so wonderfully supportive and caring, I am forever in your debt.

As this research was funded by the BBSRC, I would like to thank them for their financial support which made this research possible. Many thanks to Tea pot hill and the gents from CHS. 'Floreat Domus Chathamensis'

Finally, I would like to express my deepest gratitude to my family, who have supported me throughout my life and have always been there for me, I dedicate this thesis to them.

Contents

List of Figures

List of tables

Abbreviations

Aa	Amino acid
ADP	Adenosine diphosphate
Amp	Ampicillin
AntA	Antimycin A
APS	Ammonium persulfate
ATP	Adenosine triphosphate
ATPase	Protein that hydrolyses adenosine triphosphate
Bp	Base pairs
cAMP	Cyclic adenosine monophosphate
CWG	Campbell Wallace Gourlay
Da	Dalton
dH_20	Deionised water
DMSO	Dimethyl sulphoxide
DNA	Deoxyribonucleic acid
dNTP	Deoxyribonucleotide triphosphate
E. coli	*Escherichia coli*
ECL	Enhanced chemiluminescence
EDTA	Ethylenediaminetetraacetic acid
ER	Endoplasmic reticulum
Et al	Et allia (and others)
Etbr	Ethidium bromide

ETC	Electron transport chain
ETS	Electron transport system
FACS	Fluorescence-activated cell sorting
FCCP	carbonyl cyanide p-trifluoromethoxy phenylhydrazone
GDP	Guanosine diphosphate
GEF	Guanosine exchange factor
GFP	Green fluorescent protein
GO	Gene ontology
GPCR	G-protein coupled receptor
GTF	General transcription complex
GTP	Guanosine triphosphate
IMS	Intermembrane space of mitochondria
kDa	Kilo Dalton
Kg	Kilogram
LB	Lysogeny broth
Leu	Leucine
LiAc	Lithium acetate
M	Molar
MAPK	Mitogen activated protein kinase
MAPKK	Mitogen activated protein kinase kinase
MAPKKK	Mitogen activated protein kinase kinase kinase
mRNA	Messenger RNA
mQ	Milli-Q

NADH	Nicotinamide adenine dinucleotide
OD_{600}	Optical density measured at 600 nm
ORF	Open reading frame
PBS	Phosphate buffered saline
PCR	Polymerase chain reaction
PEG	Polyethylene glycol
Pep	Peptone
Pi	Inorganic phosphate
PI	Propidium iodide
PDS	Post-diauxic shift
PKA	Protein Kinase A
PVDF	Polyvinylidene fluoride
PTM	Post-translational modification
RFP	Red-fluorescent protein
RNA	Ribose nucleic acid
RNA-Seq	Ribose nucleic acid sequencing
ROS	Reactive oxygen species
RPM	Revolutions per minute
S. cerevisiae	*Saccharomyces cerevisiae*
SD	Synthetic Dropout
SDS	Sodium dodecyl sulphate
STRE	Stress response elements

TE	Tris EDTA
TEMED	N, N, N', N'-Tetramethyl ethylenediamine
TF	Transcription factor
TOR	Target of rapamycin
Tris	Tris(hydroxymethyl)aminomethane
U	Units
URA	Uracil
UTR	Untranslated region
UV	Ultraviolet
V	Volts
WT	Wild type
YPD	Yeast extract dextrose
YT	Yeast extract tryptone
µ	Micron
µg	Microgram (10^{-6} gram)
µl	Microliter (10^{-6} litre)

Abstract

Ras proteins are small GTPases that act as molecular switches within cells that link extracellular stimuli to intracellular effectors. Ras proteins play a conserved role in the control of both cell growth and proliferation. As a result, mutations that induce the constitutive activation of Ras proteins are often associated with changes in cell behaviour that can lead to disease, such as human cancer. The localisation of Ras is crucial for its function and this is controlled by post-translational modifications. However, the roles for such modifications in regulating Ras localisation and its activity are poorly understood. We have identified that the phosphorylation of Serine^{225} of Ras2, a protein that is essential for the control of both growth and proliferation in *S. cerevisiae,* plays an important role in the regulation of its localisation and activity. Modification of this residue leads to changes in the distribution of GTP-bound Ras2 within the cell. This drives cells towards a novel state of growth cessation that is dependent upon the activity of the cAMP/PKA signalling pathway. We show that this quiescent state is characterised by an uncoupling of cytoplasmic and nuclear process that govern cell growth and division. We suggest that cells can escape growth arrest and re-engage in the cell cycle if the Ras/cAMP/PKA pathway activity is reduced, additional nutritional supplementation is provided or if nutrient uptake processes are elevated. Thus, the Serine^{225} reside plays an important role in the control of Ras2 localisation and activity that allows the cell to co-ordinate nutritional availability with growth and cell division. My thesis highlights that post-translational modifications in regions outside of the highly conserved Ras GTPase domain may be targeted to change cell fate, for example by switching a pro-growth signalling programme to one that drives a growth cessation. This has implications for the development of novel therapeutic approaches for cancers driven by oncogenic Ras proteins.

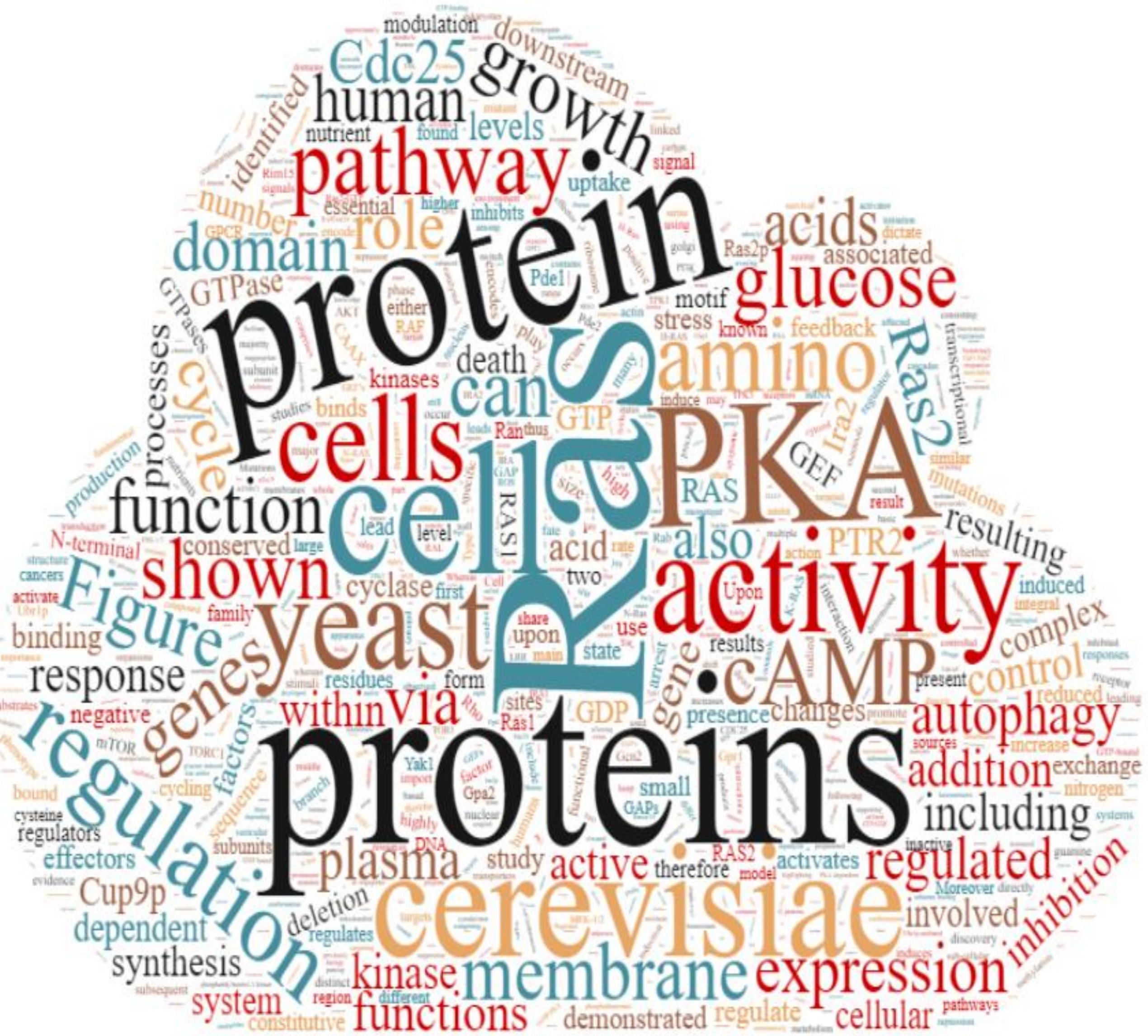

A word cloud generated from the contents of this thesis.

Chapter 1
Introduction

1.1 *S. cerevisiae* as a model organism

The exploitation of eukaryotic organisms as biological models has been fundamental for biological discovery. Model organisms such as yeast, nematodes and flies can be utilized to rapidly elucidate the function of genes and their role in cellular pathways, processes, and compartments. Enhancing the understanding of how genes function is crucial if we are to understand basic cell biology and why mutation can lead to dysfunction that underlies disease.

Saccharomyces cerevisiae (*S. cerevisiae*) is a single-celled eukaryote and therefore shares the cellular structure and organisation of higher eukaryote cells. Coupled with the relative simplicity of genetic manipulation, short-doubling time and broad range of molecular tools and resources available, *S. cerevisiae* is regarded as an important model organism [1][2]. In 1996, *S. cerevisiae* became the first eukaryote to have its complete genome sequenced and published [2]. A wide range of genetic and molecular tools have been developed to facilitate research using *S. cerevisiae*. For instance, a collection of yeast strains comprising deletions of non-essential open reading frames (ORF) was generated and made accessible [3][4]. Furthermore, other collections exist with genome-wide coverage such as a collection comprising of GFP-fused chimera proteins that aid in the visualisation of endogenous yeast proteins [5][6]. Supporting these resources is a freely accessible online database; 'The Saccharomyces genome database (SGD)" which provides key biological information on *S. cerevisiae* along with research and analytical tools to enable investigations on the relationship between gene sequence and gene function (www.yeastgenome.org/).

The available resources have enabled the roles of almost 85 % of the 5800 protein-coding genes of *S. cerevisiae* to be determined. Such annotation, coupled with the advantages of the system as a whole offers an important resource, for example it has been shown that ~ 17 % of yeast genes exist as members of orthologous gene families associated with human diseases [7]. The expression of human proteins in yeast cells can also be instrumental for the discovery of chemical or protein inhibitors of their activity using high throughput screening methods [8]. Such assays are based on the principle that demonstrable functions of human proteins may be manipulated by chemical compounds or further genetic manipulation [9][10]. As such research conducted on *S. cerevisiae* has been instrumental in uncovering the role of many proteins in higher eukaryotes, including humans [9]. A good example lies in the study of small GTPase proteins of the Ras superfamily

1.2 The Ras superfamily

The Ras superfamily comprises of small Guanosine Triphosphate Hydrolases (GTPases), which range from 20 to 40 kDa in size. The Ras superfamily includes over 150 members in humans with evolutionary conserved orthologues present in several organisms including *Drosophila melanogaster*, *Caenorhabditis elegans* and *S. cerevisiae*. The superfamily is divided into five main branches based on sequence and functional similarities; Ras, Rho, Arf/Sar, Rab and Ran [11]. While similar to the heterotrimeric G protein α subunits in biochemistry and function, Ras family proteins act as monomeric G proteins, functioning as molecular control switches [12]. Post-translational modifications and structural differences dictate their subcellular localisation and the proteins that serve as their regulators enable GTPases to function as efficient modulators of complex cellular processes.

Rab family proteins make up the largest branch of the Ras superfamily with 61 members currently identified [13]. Rab proteins are associated with membrane organisation due to their regulatory role in intracellular vesicular transport between organelles in both the endocytic and secretory pathway [14]. The second branch of the superfamily comprises of the ADP-ribosylation factor (Arf) family proteins and like Rab proteins, have been implicated in the regulation of vesicular transport [13][14]. The regulation of Arf GDP/GTP cycling is controlled by distinct GEF's and GAP's [15].

Rho proteins form the third branch of the superfamily with twenty known Rho proteins identified with RhoA, Rac1 and cdc42 being the most studied. Rho proteins function as vital regulators of extracellular-stimulus-mediated signalling networks which regulate gene expression, cell cycle progression and actin organization [16]. Moreover, Rho GTPases are also involved in cell polarity, cell shape and cell-matrix interactions [17].

The fourth branch encompassing the most abundant small GTPase in the cell, is the Ras-like nuclear (Ran) protein. Ran is best characterised for its role in nucleocytoplasmic transport of RNA and proteins [18]. Unlike other small GTPases, Ran activity is dependent on a spatial gradient of the GTP-bound form of Ran. A single human Ran protein is regulated by a Ran-specific nuclear GEF and cytoplasmic GAP. The resulting effect is a high concentration of Ran-GTP in the nucleus, facilitating the directionality of nuclear import and export within cells [19].

1.3 The Ras protein subfamily

The final branch of the Ras superfamily and the focus for this study are the Ras proteins. The activation of Ras proteins, as with all G proteins, is dependent on the exchange of bound GDP for GTP and is deactivated through the hydrolysis of GTP to GDP [20] (Figure 1). Ras proteins function as intracellular signalling molecules transforming extracellular stimuli into intracellular responses at a given target via the utilization of complex intracellular signalling pathways.

All Ras proteins share a conserved G-domain, the functional domain that binds to GTP/GDP, therefor it is not surprising that all Ras proteins present a common mechanism of action. Ras proteins function as binary molecules switching between an inactive GPD-bound state and an active GTP-bound state. The activation of Ras proteins leads to subsequent activation of signalling cascades which differ depending on the organism and specific Ras protein activated [21][22]. Most proteins who interact with Ras to activate downstream signalling pathways, share a conserved domain known as the RAS-binding-domain, or RAS association (RA) domain. The presence of this domain was exploited and used for the identification of novel Ras effectors which were found via cDNA library screens by probing for the presence of RA domains [21]. The conserved mechanism of action shared between Ras proteins is reliant on a conserved sequence consisting of a set (1-5) of G box GDP/GTP- binding motif elements which begins at the N-terminal domain and form a G-domain of approximately 20 kDA in size [23]. The N-terminal domain contains short sequences of amino acids involved in the recognition of phosphates and guanine nucleotides. Important motifs within the G-box domain include switch I and switch II, which regulate the conformational changes between GTP- and GDP-bound Ras proteins [24][25]. The conformations of active and inactive sites

present significant changes which correspond to the switch I and II regions with these small variations leading to different affinities for active or inactive Ras proteins towards Ras regulators and effectors [20].

As with all G-proteins, Ras activation is dependent on the exchange of bound GDP for GTP and is deactivated through the hydrolysis of GTP to GDP; this cycling between active and non-active states is regulated by GEF's and GAPs *(Figure 1)* [26]. The Guanine Exchange Factors (GEFs) regulate Ras activation via the exchange of GDP bound to the Ras nucleotide binding pocket for GTP and GTPase Activating Proteins (GAPS) regulate the subsequent deactivation [26]. The cycling between activation and deactivation of Ras proteins is integral for the coupling of external stimuli to effector proteins within signal transduction cascades.

An example of such an effector protein found in higher eukaryotic systems is RAF, a serine-threonine kinase which interacts with Ras through the previously mentioned RBD, the Raf1 protein binds to active GTP-bound Ras making it a very useful tool for the investigation of Ras activation within living cells [27]. Ras1 and Ras2 guanine nucleotide binding and GTPase activities have been characterised and the C-terminal third of the nucleotide sequence of yeast Ras displays significant overlap with human RAS. Furthermore, human *RAS* suppresses the loss of yeast *RAS* genes, thus supporting functional similarities between yeast and human *RAS* genes [28].

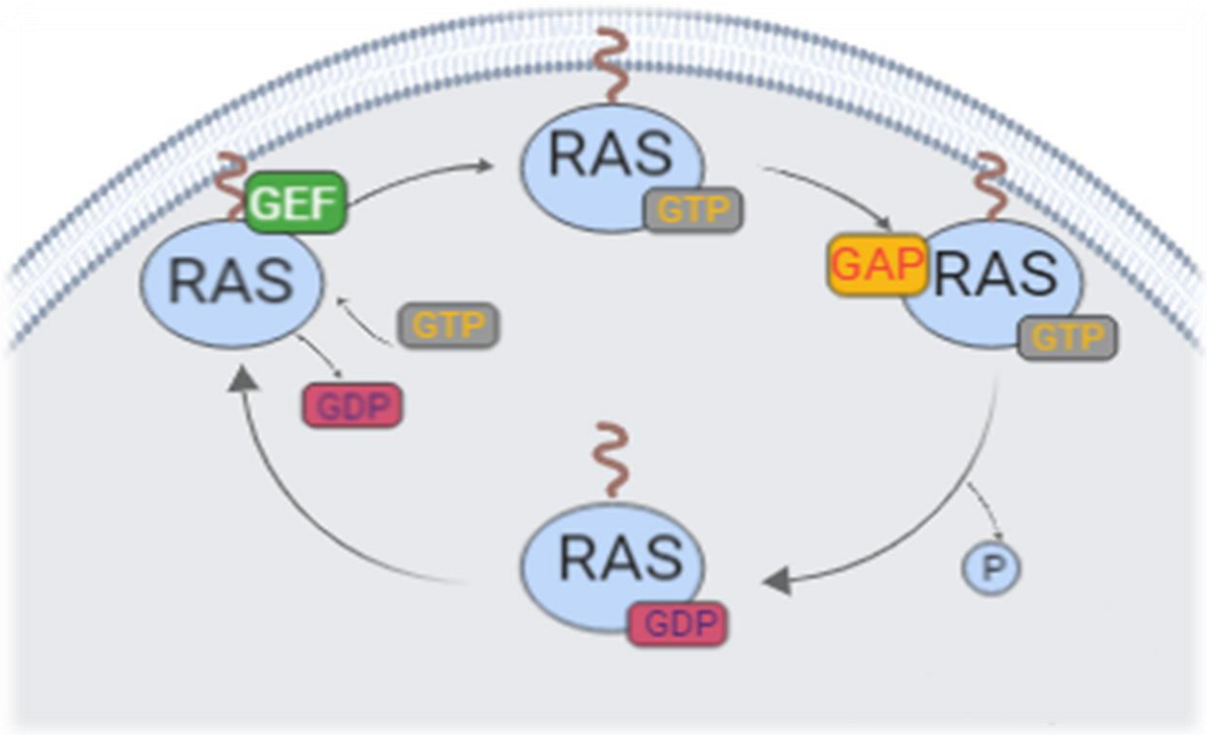

Figure 1. Ras protein cycling between active and inactive states through the action of GEF and GAP proteins.
Active Ras interacts with the downstream targets in signalling cascades to induce a cellular response. Ras activation is dependent on the exchange of bound GDP for GTP and is deactivated through the hydrolysis of GTP to GDP; this cycling between active and non-active states is regulated by GEF's and GAPs [26].

In *S. cerevisiae* two proteins are expressed which are homologous to human Ras, Ras1 and Ras2. The *RAS1* and *RAS2* genes are located on chromosome XV and XIV [29], respectively, and encode two highly similar proteins of 309 and 322 amino acids in size [29] [30].

Ras proteins function as GTP-binding proteins which regulate the nitrogen starvation response, sporulation, and filamentous growth in yeast. In *S. cerevisiae*, *RAS2* has a paralog, *RAS1*, which arose from the whole genome duplication [31]. Ras1p and Ras2p share the same function, but differ in their levels of gene expression [32][33].

Figure 2. A 3D representation of the crystal structure of the human Ras protein in its GDP-bound conformation.
Courtesy of http://www.rcsb.org/structure/2ERY.

Previously, the yeast Ras proteins were thought to have exclusive roles within the cell as Ras1 was unable to complement growth defects caused by the deletion of *RAS2*, such as reduced growth on non-fermentable carbon sources and decreased levels of intracellular cAMP [34][35]. However, these questions have been explained by the differential regulation of the mRNA production and protein translation of *RAS1*. The level of *RAS1* mRNA and protein synthesis are reduced during the mid-logarithmic growth phase and during growth on non-fermentable carbon sources [32], while *RAS2* mRNA levels are high during all growth phases on both fermentable and non-fermentable carbon sources [36][32]. To confirm that *RAS1* and *RAS2* differ only by their level of expression, *RAS1* was put under the constitutive ADH1 promotor. Here, *RAS1* was able to fully supress the phenotype of a *Δras2* strain and the

hyperactive mutant of *RAS1* replicated the phenotypes observed in an constitutively expressed *RAS2* strain [37].

In humans the Ras protein family is comprised of 25 members, which are predominantly localised to the plasma membrane. These proteins are highly conserved within the GTPase domain, but mutations can lead to the constitutive activation of Ras. Investigations have estimated that ~50 % of all tumours are result of mutations involved in the constitutive activation of Ras signalling [26]. A number of human oncogenes implicated in a variety of cancers have been identified including *N-RAS*, *H-RAS* and *K-RAS* [38][39][40][29].

Proto-oncogenes play an essential role in signal transduction and the execution of mitogenic signals, therefore when over-activated they become tumour-inducing agents. Ras genes are examples of proto-oncogenes, which encode for proteins involved in the regulation of cell proliferation and differentiation. Ras plays an important role in the cell cycle and is linked to several human cancers and as such has been extensively researched in recent years. Previous investigations have identified that mutant alleles of the human Ras protein are linked to a number of human cancers, further highlighting Ras as an important target for cancer research [41]. Sequence analyses have revealed the importance of the amino acids at positions 12, 13 and 61 in Ras proteins. Mutations that cause the alternation of residues can lead to the over-activation of Ras via GAP impairment [41].

The proto-oncogenes *K-RAS*, *H-RAS* and *N-RAS* are often termed as the 'classical' mammalian Ras proto-oncogenes and as such are the most extensively studied among all the Ras superfamily members due to their direct involvement in tumorigenesis. *H-RAS* mutants are present in 12 % of cases of bladder carcinoma whereas *N-RAS* mutations are predominantly found in malignant melanomas and hematopoietic tumours [42]. Mutations in *K-RAS* are the

most common mutation associated with cancer disease with 60 % of pancreatic cancers, 34 % of colorectal and 16 % of lung cancers expressing oncogenic *K-RAS* isoforms [43].

1.4 Posttranslational modifications of Ras

Posttranslational modifications such as methylation, ubiquitination and most commonly phosphorylation can diversify protein function and enhance regulation [44]. The regulation of yeast Ras proteins is not explicitly regulated by their GTP/GDP binding state, but also by post translational modifications, which can dictate Ras sub-cellular localisation. The sub-cellular localisation of Ras proteins determines the class of effectors and regulators that are available and thus determines the downstream signalling activity [22][21].

Ras proteins undergo a series of posttranslational modifications which are important to control both activation and its localisation to the cytoplasmic side of the plasma membrane [21]. The C-terminal domain of the Ras protein contains a CAAX (C= cysteine, A = aliphatic amino acid, x + terminal amino acid) motif, which is essential for membrane targeting and activity [44][45][46][47]. The first posttranslational modification of Ras processing is farnesylation. The cysteine in the CAAX motif is targeted by farnesyltransferase, which catalyses the addition of a farnesyl isoprenoid [48]. It has been shown that the addition of geranylgeranyl isoprenoid to the CAAX motif can substitute farnesylation but only when farnesyltransferase is blocked by specific inhibitors [49][49][47]. Following this modification, Ras membrane interaction is initiated and Ras is targeted to the endoplasmic reticulum (ER) [50]. After farnesylation the proteolytic removal of the AAX amino acids from the CAAX motif via the enzyme Rec1 occurs, leaving a prenyl cysteine at the C-terminus [51]. Isoprenylcysteine Carboxymethyltransferase (ICMT) performs carboxyl methylation on the prenyl cysteine, which has been hypothesised to play an essential role in Ras signalling [52].

The previously mentioned posttranslational modifications are the minimum signals required for movement and tenure to the plasma membrane.

1.5 Ras protein trafficking

Ras proteins are most frequently found associated with membranes and research has focused upon its function at the plasma membrane. Importantly, the site of Ras localisation can dictate its function via its interaction with regulatory partners and downstream effectors [21][53].

In *S. cerevisiae*, the precise mechanism of Ras trafficking from cytosol to endomembranes has yet to be elucidated but in the mammalian system it is known that *N-Ras* and *H-Ras* transit to the plasma membranes occurs via vesicular transport following palmitoylation [54][55]. Experimental evidence exists to suggest that *N-Ras* and *H-Ras* localised on the plasma membrane can also be depalmitoylated which promotes its translocation back to the golgi apparatus [56]. Due to the lack of palmitoylation sites in *K-Ras (Figure 3)*, the mechanisms controlling its movement to the plasma membrane is unknown but it is known to be dependent on a poly-lysine region close to the hypervariable region that does not rely on golgi/endomembrane trafficking [53]. A fluorescent probe consisting of the Ras Binding Domain (RBD) of Raf-1 fused to GFP was developed to confirm that signalling occurs from Ras proteins on the surface of the golgi apparatus. The probe binds specifically to active Ras proteins, revealing that Ras activation can be found to occur at both the ER and golgi apparatus [57]. Furthermore, in addition to signalling from the golgi, studies have shown Ras activation at the ER compartment when *N-Ras* and *H-Ras* proteins deficient in palmitoylation accumulate on the ER and in the cytosol [53][50]. Collectively these studies highlight the importance of the regulation of Ras localisation for its activity.

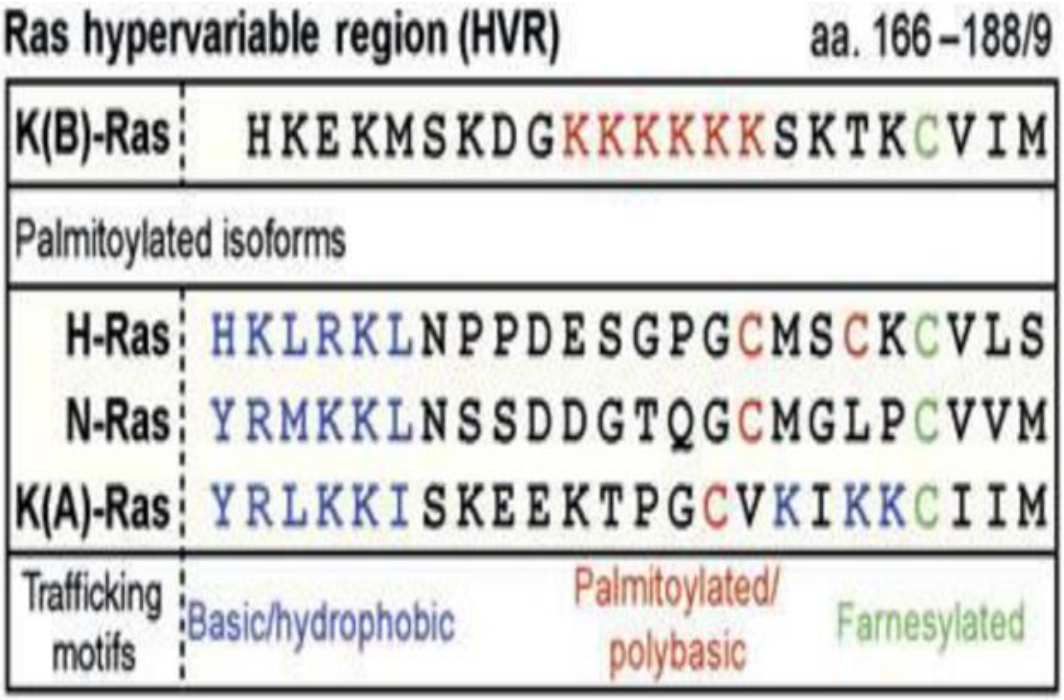

Figure 3. The human Ras protein hypervariable region (HVR).
The HVR influences the variability in function between the Ras isoforms, it undergoes PTM's to allow membrane interaction and localisation.

In yeast, Ras proteins also undergo PTM to regulate their localisation and activity [50][58]. The initial PTM observed for both Ras1 and Ras2 is the removal of a methionine at the N-terminus, followed by C-terminal modifications such as carboxyl methylation, farnesylation and palmitic acid addition [59][60][61]. Ras1p and Ras2p farnesylation at the cysteine of the CAAX box motif is catalysed by a farnesyltransferase, comprised of α and β subunits encoded by *RAM2* and *DPR1/RAM*2. Experimental evidence has shown that Ras protein localisation in mutants of either *RAM1* or *DPR1* present a cytoplasmic localisation [62]. In *S. cerevisiae* the palmitoylation of Ras proteins is catalysed by Palmitoyltransferase (PAT), encoded by the *ERF2* and *ERF4* genes [60]. The protein products of these genes are localised in the ER and perform palmitoylation using palmitoyl-CoA [62].

Through the use of fluorescent labelling of Ras proteins and their partners, it has been shown that Cdc25, Ira2 and Cyr1 are localized on endomembrane's although the activation of adenylyl cyclase by Ras2 occurs solely on the plasma membrane in *S. cerevisiae* [63][64] . Ras has been shown to be anchored to the ER by the Ras inhibitor, Eri1 [65]. More current studies highlight that the localisation of active Ras is dependent on the activity of Protein Kinase A (PKA). A feedback regulation on Ras2 localisation has been suggested, based on PKA-dependent phosphorylation; Ras2 was shown to localize mainly on the plasma membrane in glycerol-growing cells, while glucose-addition causes a rapid re-localisation of large part of the protein to the cytoplasm [66]. The overexpression of the *TPK1* subunit drives both Cdc25 and Ras2 away from the plasma membrane [67]. Furthermore, active Ras has been shown to localise in the nuclear compartment [68][69].

Other studies reveal a potential role for the mitochondria for correct Ras localisation [70]. For example, an aberrant accumulation of activated Ras at the mitochondria in response to nutritional depletion was reported in cells lacking *whi2*, a protein phosphatase activator involved in the general stress response [70].

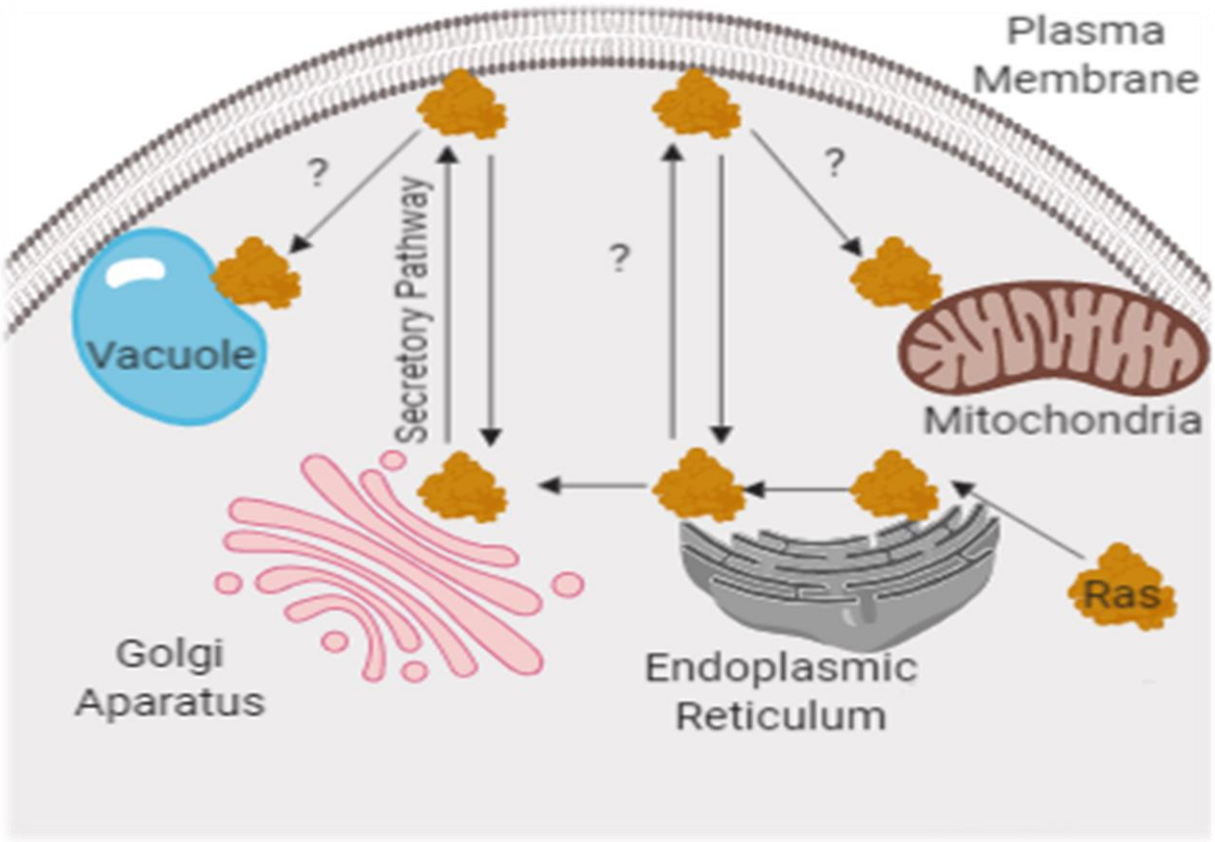

Figure 4. Posttranslational modifications play an important role in dictating sub-cellular Ras trafficking and localisation.
Although the mechanisms of Ras trafficking to many intracellular sites has yet to be determined.

Despite our extensive knowledge on how Ras protein modifications lead to plasma membrane localisation, we know relatively little on how they are targeted to other compartments of the cell *(Figure 4)*. This lack of knowledge necessitates future investigations to elucidate which modifications and mechanisms regulating Ras localisation within eukaryotic cells and the significance of localisation for cell function.

1.6 Ras protein phosphorylation

Phosphorylation is an important posttranslational modification and is used to control the function, localisation, or activity of many proteins [71]. Phosphorylation is the chemical addition of a phosphoryl group to an organic molecule and is catalysed by a kinase. The

subsequent removal of a phosphoryl group is called dephosphorylation and is catalysed by a phosphatase. Protein phosphorylation can occur on serine, threonine and tyrosine residues and is widely considered as the most abundant post-translational modification in eukaryotes [72][73].

In yeast, both Ras1 and Ras2 are phosphorylated and phosphorylation occurs exclusively on serine residues [74]. Tryptic phosphopeptide analysis highlighted only two major phosphorylated tryptic peptides of the Ras2 protein[74][75]. Further investigations showed that phosphorylated Ras2 proteins are predominantly localised in the plasma membrane, where the action of these proteins occurs [74]. Thus, suggesting that phosphorylation may not merely be a random event but rather play a physiologically significant role [74][75].

Specific serine residues have been identified within yeast Ras1 and Ras2 proteins that can be phosphorylated [74][75]. Although there are 31 serine residues in the mature Ras2 protein, it has been shown that only serine residues at positions 6, 198, 202, 207, 214, 224, 225, 235, 238, 262, 275, 285 and 291 are identified as putative Ras2 phosphorylation sites [75]. Interestingly, activated alleles of both *RAS1* and *RAS2* proteins have been shown to be less stable and less phosphorylated than proteins from cells expressing wild-type alleles of *Ras2 [75]*.

Serine^{214} of Ras2 is the preferred site of phosphorylation; however, the protein kinase(s) responsible for Ras2 phosphorylation can phosphorylate a variety of serine residues in the vicinity of serine^{214} when this site is altered [75]. When Ras2^{S214} is replaced by the non-phosphorylatable residue alanine, cells exhibit reduced glycogen accumulation, elevated cAMP levels and increased activation of cAMP signalling by glucose [74]. Furthermore,

increased PKA-dependent activation of Ras2-GTP was observed suggesting that phosphorylation is controlled via feedback regulation of the Ras-cAMP/PKA pathway.

Among *ras* gene products, phosphorylation is not limited to yeast proteins. In humans, the activity of H-Ras mutant proteins can be modulated by phosphorylation. The constitutively activated H-Ras^{G12V} mutant can develop a second mutation resulting in the substitution of alanine for a threonine at position 59. Phosphorylation occurs on the HRAS$^{val12\text{-}Thr59}$ mutant proteins at threonine-59 and functions as a suppressor of the G12V mutation [76]. Furthermore, experimental evidence also shows that PKC agonists induced phosphorylation of serine^{181} resulting in the fast translocation of K-Ras from the plasma to endo-membranes [77].

Although evidence exists to suggest that Ras proteins can undergo phosphorylation events which regulate its activity. Surprisingly, the phosphorylation of Ras2p in *S. cerevisiae* has not been studied regarding its regulation of intracellular localisation despite significant evidence existing linking Ras phosphorylation to its localisation in humans.

1.7 RAS/cAMP/PKA signalling in *S. cerevisiae*

In *S. cerevisiae,* Ras proteins, once activated, interact with adenylate cyclase at the plasma membrane, triggering the synthesis of cAMP from ATP *(Figure 5)* [78]. Adenylyl cyclase, encoded by *CYR1*, is a large protein consisting of 2,026 amino acids. The protein structure comprises of four domains: N-terminal, middle repetitive, catalytic and a C-terminal domain. The middle repeat consists of a 23-residue amphipathic leucine-rich motif called the LRR domain (674-1300 aa). The LRR domain is the principal site of Ras interaction and the N-

terminal domain of the LRR (676-756) has been identified to be a Ras Associating Domain (RAD).

Upon cAMP production by adenylyl cyclase, cAMP binds to the Bcy1 protein, the regulatory subunit of PKA, activating PKA. The regulation of Ras/cAMP/PKA signalling is essential for orchestrating many cellular processes including growth, proliferation, cell cycle progression, stress responses and the control of ageing in yeast cells *(Figure 5)* [79]. Mutations resulting in the inappropriate activation of PKA induce cell cycle arrest in G1, glycogen accumulation and prolonged survival when exposed to starvation [78].

An increase in intracellular cAMP levels results in the activation of PKA via the dissociation of the PKA regulatory subunit Bcy1 [80] and the PKA catalytic subunit(s) encoded by *TPK1*, *TPK2* and *TPK3* [81][78]. The genes *TPK1, TPK2* and *TPK3,* control cAMP-dependant protein kinase activity in *S. cerevisiae*. The PKA subunits Tpk1, 2 and 3 share overlapping functions but also have been shown to be involved in the regulation of several separable functions. Tpk1 has been identified to play a role in the branched chain amino acid biosynthesis pathway, mitochondrial DNA stability and mitochondrial iron homeostasis [82]. Whereas Tpk2 has been shown to impact iron uptake, trehalase synthesis and water homeostasis [82][83]. However, constitutive PKA activity can prove deleterious, with the overexpression of *TPK3* shown to inhibit growth [84].

The production of intracellular cAMP is tightly regulated through feedback loops and the action of phosphodiesterases, which catalyse the degradation of cAMP [85][86]. *Saccharomyces cerevisiae* contains two cAMP phosphodiesterases, *PDE1* and *PDE2*, which encode a low-affinity (Pde1) and a high-affinity cAMP phosphodiesterase (Pde2) that are unrelated in primary sequence [85][86]. Pde2 is an Mg2-requiring, zinc-binding enzyme with

a Km for cAMP of 170 nM [87][88]. It controls the basal cAMP levels in the cell and thereby protects it from changes in the extracellular environment [89].

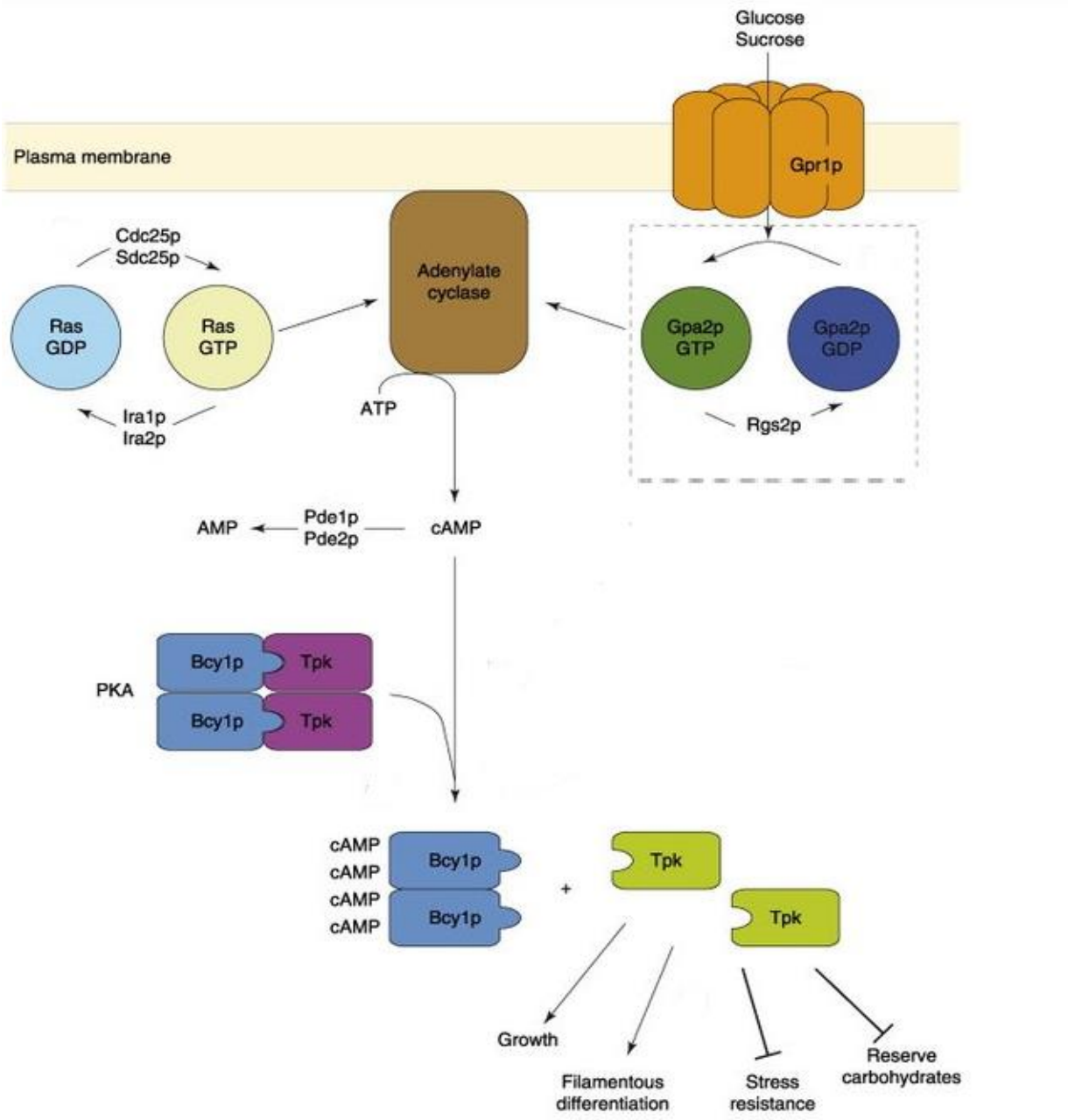

Figure 5. The activation of Ras1 and Ras2 is dependent on nutrient availability.
In the presence of glucose Ras proteins are activated via the GEF proteins cdc25 or Sdc25 which catalyse the liberation of GDP and the binding of GTP. Adenylate cycle is activated inducing the production of cAMP. cAMP functions as a secondary messenger and binds to the inhibitory unit of PKA, releasing the catalytic unit, phosphorylating downstream targets resulting in the activation of multiple downstream cellular processes or the inhibition of transcription factors that control the stress response. This pathway is inhibited by the hydrolysis of cAMP via the action of Pde1 and Pde2 and by the GTPase activity of the GAP's Ira1 and Ira2.

1.8 Regulation of RAS/cAMP/PKA pathway activity

In S*. cerevisiae*, Ras protein activation is finely tuned by two classes of regulatory proteins: Cdc25 and Sdc25 guanine nucleotide exchange factors (GEFs) [90][91][92], and Ira1 and Ira2 GTPase activating proteins (GAPs) *(Figure 6)* [93][94] [95]. The molecular mechanism of the modulation of Ras proteins activity is conserved in higher eukaryotes, as highlighted by the functional interchangeability of Ras proteins and their regulators in yeast and mammals [96].

The *CDC25* gene of *S. cerevisiae* encodes for the Ras protein activator (GEF) and is required to produce cAMP. The Cdc25 gene product is a ~180 kDa polypeptide with a C-terminal highly conserved RAS-GEF catalytic domain (1,121–1,573 aa) [97]. Mutants that result in the constitutive activation of Ras2, such as Ras^{val19}, have been shown to supress the effects of mutations in *CDC25*, as constitutively activated Ras^{val19} does not require the exchange factors for its activation [98]. Furthermore, the gene S*DC25* has also been shown to prevent Ras GEF activity [90].

Despite Cdc25 being the first Ras GEF characterised [99], the precise mechanism of how its activity is regulated and how the Cdc25/Ras/cAMP pathway transduces the signal originated by nutrients is still unclear. Inconsistent reports have put forward either the necessity [100][101] or the dispensability [102] of Cdc25 for Ras and adenylate cyclase activation upon glucose stimulation, however Cdc25 was eventually shown as necessary for Ras2 GTP-loading after glucose refeeding [103].

The Cdc25 protein is tightly bound to membranes [104], although protein solubility increases upon hyper-phosphorylation within the 114-348 amino acid region and results in Cdc25 becoming less available for the association with Ras [105]. Glucose-induced hyper-phosphorylation of Cdc25 upon glucose addition has been shown to directly inhibit Ras GEF

activity rather than affinity for Ras [106][105]. Cdc25 activity modulation by phosphorylation is prevented by nutrient starvation and is hypothesized to be a part of a negative feedback loop resulting from PKA activity *(Figure 6)* [105][106].

The IRA proteins, encoded by the genes *IRA1* and *IRA2* have been shown to inhibit Ras activity in yeast [95].The *IRA1* and *IRA2* genes encode large proteins, 3092 and 3079 amino acids respectively, that share similar amino acid sequence and have related, even if not identical, functions. A region of approximately 360 amino acids in the middle of these gene products, called the GAP domain, is responsible for activating intrinsic GTPase activity of Ras [95]. It has been shown that *IRA1*/*IRA2* gene mutations suppress *CDC25* mutations, double deletion mutant's of Δ*cdc25* and Δ*ira1/Δira2* are viable. Ira2 (Ras-GAP) is regulated by ubiquitination, a posttranslational modification resulting in protein degradation by the proteasome.

More recent studies have shown that the Ubp3 protein interacts with the Ras GTPase-accelerating protein, Ira2, and regulates its level of ubiquitination. Ubp3 is an Ubiquitin-specific protease and regulates PKA activity by controlling the ubiquitination status of Ira2p [107]. It has been suggested that the addition of glucose to the growth media stimulates ubiquitination and Ira2p inactivation resulting in Ras-GTP accumulation and therefore elevated PKA activity. The regulation of Ira2 by ubiquitination is a highly conserved mechanism in Ras signalling [108].

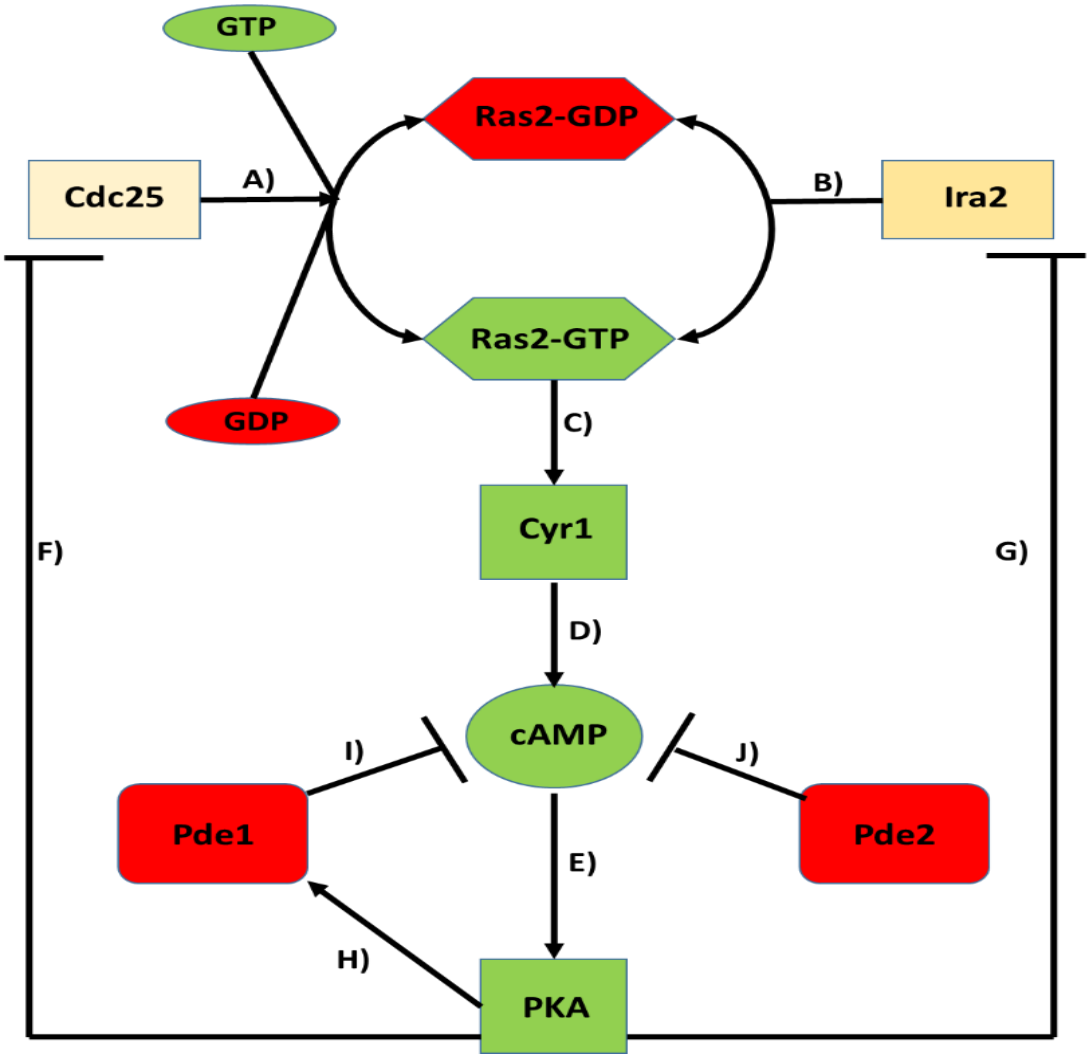

Figure 6. Positive and negative feedback in the Ras/cAMP/PKA pathway.
This schematic shows the relationships among the main components of the Ras/cAMP/PKA pathway. The cycling of the Ras2 protein between its inactive state (Ras2-GDP) and active state (Ras2-GTP) is regulated by Cdc25 (A) and Ira2 (B). Ras2-GTP activates adenylate cyclase Cyr1 (C), which induces the synthesis of the second messenger, cAMP (D). Increased cAMP levels result in PKA activation (E) through binding to the PKA regulatory subunits and liberating its catalytic subunits. The degradation of cAMP is catalysed by Pde1 (I) and Pde2 (J), which functions as a major negative feedback mechanism in this pathway, as both contribute to the decrease in the intracellular level of the second messenger. The active form of PKA performs three main regulations in this pathway via the phosphorylation of different components: a positive regulation of Pde1 (H) and of Ira2 (G), and a negative regulation of Cdc25 (F). The increased activity of the phosphorylated forms of both Pde1 and Ira2 result in switching off the signal—by either a faster degradation of cAMP by Pde1 (I) or to a diminished fraction of active Ras2 by Ira2 proteins (B), both positive regulations result in a negative feedback control of the whole pathway. The negative regulation of Cdc25 by PKA results in a partial inactivation of the GEF activity (A), and therefore a reduced activation of the Ras2 protein, which results in a decreased activity of the adenylate cyclase and therefore contributes to lowering the cAMP level.

1.9 The GPCR System- Regulator of the cAMP/PKA pathway

Working in parallel with Ras to activate PKA is the GPCR (G-protein coupled receptor) glucose-sensing system, composed of the Gpr1 receptor and its cognate G protein, Gpa2 *(Figure 7)* [109][110]. *GPR1* encodes a seven-transmembrane G protein-coupled receptor that interacts with Gpa2 [111][112], a small GTP-binding protein which is homologous to the mammalian Gα subunit of the heterotrimeric G proteins [113]. The binding of glucose to Gpr1 activates Gpa2, which stimulates adenylate cyclase to increase cAMP levels and thus activation of PKA [112]. The Gpr1-Gpa2 system is responsive to both glucose and sucrose but not structurally similar sugars including fructose or glucose analogues [114]. The deletion of *GPA2* has been shown to confer the typical phenotype associated with reduced PKA activity [112], with *GPA2* or *GPR1* inactivation slowing several PKA-controlled processes including the repression of STR responsive genes and the induction of genes encoding ribosomal proteins [115]. Addition of glucose to cells elicits a rapid acidification of the yeast cytoplasm inducing PKA signalling *(Figure 7)* [116]. However the Gpr1-Gpa2 system is not required for intracellular acidification-induced PKA activation and does not play major role in controlling the basal cAMP level [112] [115].

Surprisingly, activation of Ras is dependent on sugar uptake but it does not require the presence of a functional GPCR system [117]. The precise mechanisms by which glucose activates Ras activity is still unknown with no sugar-sensing system identified that could function as an upstream activator of Cdc25 to transmit the glucose signal to the Ras protein [118]. Evidence suggests that Cdc25 may not itself be the signal receiver for the glucose induced cAMP response but instead the glucose induced increase in Ras2 activation may be

mediated through the inhibition of Ira1/2 proteins, thus confirming the early reports indicating Ras as an important mediator in glucose-induced cAMP signalling [102].

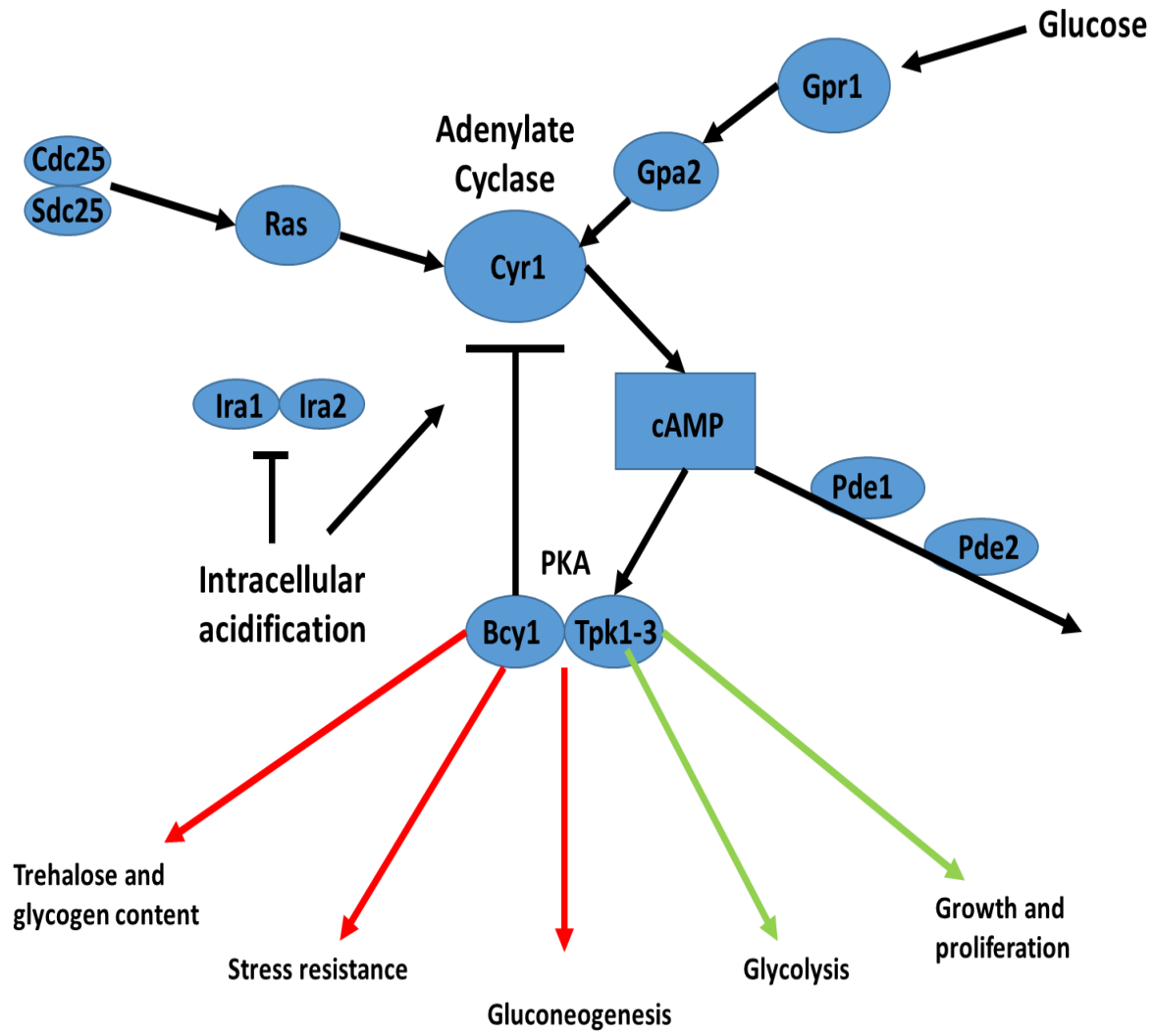

Figure 7. Mechanisms of how glucose and intracellular acidification modulate adenylate cyclase activity.

Glucose binds to the Gpr1 receptor, activating cAMP synthesis through the Gpa2 protein, while intracellular acidification functions through the Ras proteins. Gpr1 and Gpa2 constitute a glucose sensing GPCR system. The transient cAMP accumulation triggered by glucose activates PKA, which causes transient changes in several systems containing components controlled by PKA-mediated phosphorylation. The phosphorylation of downstream targets resulting in the activation of multiple downstream cellular processes or the inhibition of transcription factors that control the stress response. The red arrows represent downregulated process and the green arrows indicate upregulated processes.

1.10 Processes regulated by PKA activity

1.10.1 PKA modulation of ribosome biogenesis

The activation of PKA regulates growth by promoting the expression of the cell's translation machinery. PKA activates Rap1, which in conjunction with the high mobility protein Hmo1, recruits the nutrient-regulated Fhl1-Ifh1 complex to RP gene promotors to induce the expression of the corresponding genes [119][120][121][122][123][124]. Furthermore, PKA inhibits Yak1-mediated activation of the transcriptional repressor Crf1, which, following phosphorylation by Yak1, substitutes the coactivator Ifh1 of the fork head transcription factor Fhl1 to downregulate RP gene expression [123][124]. In addition to the regulation of ribosome biogenesis, PKA functions to control the regulation of the elongation step of RNA Pol II-mediated transcription [125].

1.10.2 PKA modulation of the stress response

As well as stimulating growth, PKA also functions to supresses several stress responses, such as the inhibition of the dual-specificity tyrosine phosphorylation-regulated protein kinase, Yak1. PKA sequesters Yak1 in the cytoplasm through the phosphorylation of Serine^{295} [126][127]. Whereas the downregulation of PKA, as seen during the transition into the diauxic shift, enables Yak1 to enter the nucleus and upregulate its transcriptional targets. These include Pop2 of the Ccr-Pop2-Not1-5 complex, which when phosphorylated by Yak1 results in G_1 arrest and the activation of the zinc-finger transcription factor Msn2, which in combination with its paralog Msn4, induces the expression of ~ 200 stress response element-containing genes in response to a multitude of environment stimuli, including glucose depletion during the diauxic shift (*Figure 8*) [126][128][129]. Moreover, the protein kinase Rim15 has been shown to mediate growth inhibition in the absence of PKA activation. Rim15, a PAS protein

kinase family member, positively controls the initiation of the quiescence program and its kinase activity is directly inhibited through PKA-mediated phosphorylation [130].

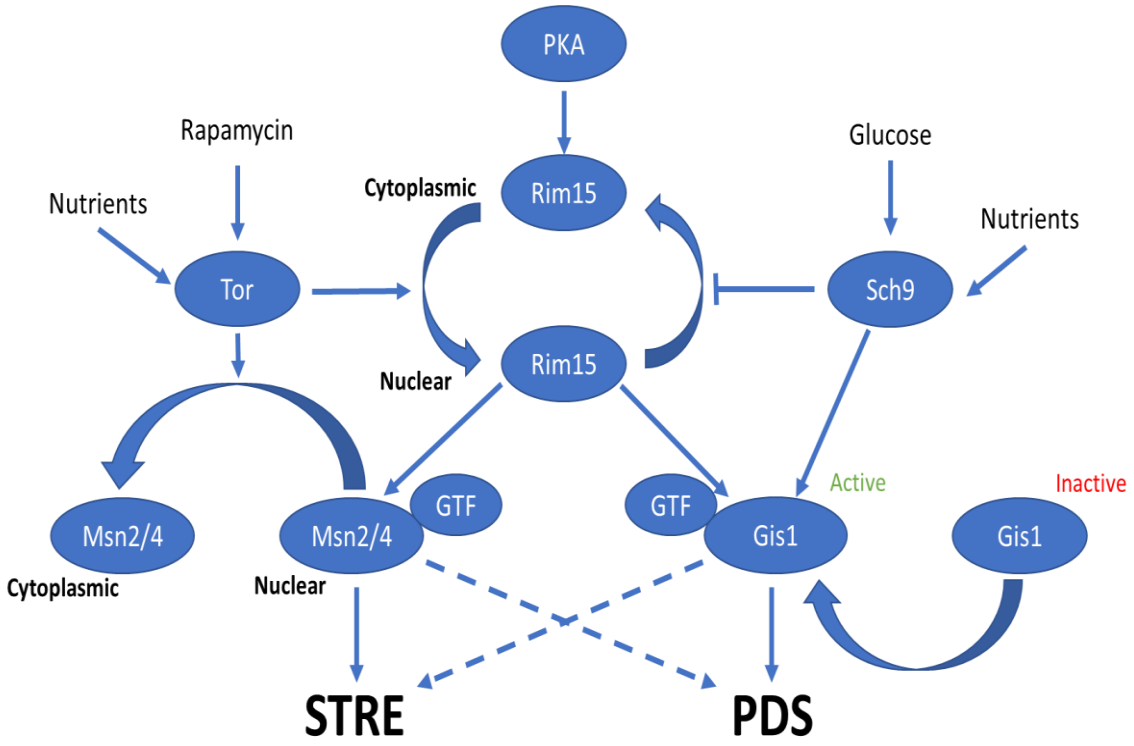

Figure 8. The protein kinase PKA, switches on or off the activities and signals transmitted through the Sch9 and TOR pathways.
Sch9 positively controls the post-diauxic shift (PDS) driven gene expression via Gis1 and Rim15. TOR and PKA control the stress response element (STRE) driven gene expression via Msn2/4 and Rim15. GTF stands for general transcription complex. Arrows and bars refer to positive and negative interactions. Dashed lines refer to potential cross-regulation.

Lastly, PKA inhibits autophagy through the phosphorylation of the protein kinase Atg1 and its regulator Atg13. This inhibits the recruitment of the Atg1–Atg13 complex to the pre-autophagosomal structure, the nucleation site from which autophagy pathway intermediates are formed.

1.10.3 Regulation of metabolism

Many of the physiological changes that occur as cells approach and/or transition into the diauxic shift phase of growth are under the post-transcriptional control of PKA. PKA antagonizes the metabolic transition from glycolysis to gluconeogenesis as well as the induction of trehalose and glycogen synthesis. This is achieved via the activation of the glycolytic 6-phosphofructo-2-kinase, Pfk2 and pyruvate kinases Pyk1/2 [131][132], the inhibition of the gluconeogenic fructose 1,6-bisphosphatase, Fpb1 [133], the activation of the glycogen phosphorylase Gph1 [134] and inhibition of the glycogen synthase Gsy2 [135].

1.11 Ras and the Cell Cycle in *S. cerevisiae*

Ras activation is dependent on the presence of growth factors and pro-survival signals, specifically growth factors in the case of human Ras and glucose in the case of yeast Ras [136][137]. Ras stimulates cell cycle progression which is associated with an increase in cell size and protein synthesis in yeast [138][139][140].

The RAS/cAMP/PKA pathway in yeast regulates several essential intracellular processes including the cell cycle, ribosome production, cells size and mass, and growth rate. These processes are strictly interdependent [109]. The specific growth rate of the cell is determined by the rate of mass accumulation, which in turn depends on nutrient availability, with cell cycle progression and cell size both dependent on growth rate and mass accumulation [141][142][143][144]. The modulation of the cell cycle is also under the influence of the RAS/cAMP/PKA pathway. Ras activation can lead to a change in the expression of cyclins (Clns) [145], which form complexes with cyclin-dependent kinases (Cdks) to promote entry into S phase of the cell cycle. Ras activation leads to the suppression of *CLN1* and *CLN2* expression

but not *CLN3* [145][146]. Moreover, PKA has been shown to directly phosphorylate Whi3, a negative regulator of G1 cyclins leading to progression into S Phase of the cell cycle [147].

Ras signalling has also been identified as a regulator of DNA damage checkpoint recovery. The DNA damage checkpoint functions to maintain genome stability by arresting the cell cycle and promoting DNA repair. Upon the deletion of *ira1/2,* PKA regulatory elements are hyper activated and after checkpoint downregulation cells undergo a permanent mitotic arrest [148].

1.12 Ras and its involvement in Cell fate in Yeast

1.12.1 The involvement of the Ras/cAMP/PKA signalling network in regulating quiescence

Cells spend a large proportion of their life in a temporary non-proliferating cellular state, known as quiescence. Establishing quiescence and maintaining the capacity to re-enter the proliferation cycle are critical for cell survival and must be closely regulated to avoid pathological proliferation. Quiescence is linked with a number of phenotypes, including a reduced rate of protein synthesis, thermo-resistance, and accumulation of storage molecules [149]. Quiescent cells are often considered as G1-arrested cells with only 5-10 % of cells entering quiescence from other cell cycles other than G1 [150]. Although, in both yeast and mammalian systems, a prolonged G1 arrest does not recapitulate the hallmarks of quiescence establishment [151]. Therefore suggesting that quiescent cells are not wholly G1-arrested cells, although the molecular mechanisms linking quiescence entry and cell cycle regulation are still yet to be elucidated [152].

In *S. cerevisiae*, quiescence entry is initiated by nutrient limitation, and is regulated, at least in part, by a complex interplay between nutrient-sensitive protein kinases , PKA and Tor [153].

Both PKA and TORC1 are positive key regulators of cell growth that participate in the cell's decision whether to transition into quiescence. For example, cells with dysregulated, enhanced PKA activity, such as the *RAS2*^{val19} mutant, characteristically fail to acquire many physiological features of the quiescence program as they enter stationary phase growth [154]. Whereas cells with absent or reduced PKA activity, induce growth arrest and hold cells in a G_0-like state [154][147].

1.12.2 Ras and its role in yeast apoptosis and regulated cell death

The RAS/cAMP/PKA signalling has been shown to be an important regulator of cell death in yeast [155][156][157]. An increase in Ras signalling has been correlated with an increase in typical apoptotic markers such as phosphatidylerine externalization, increased reactive oxygen species (ROS) accumulation and DNA fragmentation [158][159]. There are three distinct known stimuli that induce RAS/cAMP/PKA hyper-activation and subsequent cell death and these include; changes in actin cytoskeletal dynamics, exposure to ammonium and osmotin [158][160][161]. Osmotin is a protein synthesized by plants in response to the presence of pathogenic fungi. When in contact with *S. cerevisiae*, osmotic binds to Pho36 – a seven transmembrane domain receptor-like polypeptide that regulates lipid and phosphate metabolism, resulting in the inappropriate inactivation of Ras signalling leading to the induction of regulated cell death [162].

An alternate stimulus for Ras-mediated apoptosis in yeast is mediated by the actin cytoskeleton. Changes in the actin cytoskeleton caused by either the use of drugs or the presence of mutations can lead to the formation of F-actin aggregates, which function as a trigger for the constitutive activation of Ras2 and apoptosis [158]. Ammonia was also shown

to cause programmed cell death in ageing yeast cultures via the activation of the RAS/cAMP/PKA pathway [158][160].

In *S. cerevisiae*, the role of mitochondria is fundamental in the regulation of cell death. When dysfunctional the mitochondria have been shown to be the main source of ROS accumulation in yeast cells [160]. The accumulation of ROS within cells is a central event in the regulation of programmed cell death in yeast as the addition of antioxidants to yeast cells was shown to supress the apoptotic phenotype [156][163][164]. The RAS/cAMP/PKA pathway has also been shown to regulate cell death in acidic environments [164]. Supplementation of acetic acid induces intracellular acidification, which leads to RAS/cAMP/PKA activation and subsequent cell death [164]. Further supporting the integral role of Ras within the regulation of apoptosis, is that the deletion of the *RAS* genes has been shown to suppress the apoptopic phenotype of yeast cells. However, following the suppression the apoptosis, necrosis is induced within these cells. Furthermore, the hyper activation of the Ras pathway by the constitutive active allele $RAS2^{val19}$ or by deletion of *PDE2* increases apoptotic cell death [164][165].

1.13 Ras signalling in the regulation of autophagy

Autophagy is the natural, regulated mechanism of the cell that disassembles unnecessary or dysfunctional cell components allowing the orderly degradation and recycling of cellular products. In *S. cerevisiae,* both macroautophagy and microautophagy take place (*Figure 9*). Macroautophagy occurs when random cytoplasm and dysfunctional organelles are sequestered by an expanding phagophore, resulting in the formation of the autophagosome. The autophagosome fuses with the vacuole membrane, discharging the autophagic body into the vacuole lumen and sequestered cargo is broken down by vacuolar hydrolases.

Microautophagy occurs when cargos are directly taken in by the invagination and exposed to vacuolar hydrolases for degradation

In S. cerevisiae, Ras proteins mediate autophagy through the activity of PKA. Upon activation, PKA phosphorylates Rim15 and Msn2/4 which inhibits the translocation of these proteins to the nucleus to initiate the transcription of autophagy genes [162][163]. Furthermore, PKA activity also inhibits autophagy via the direct inhibition of ATG13, which is integral for autophagy initiation [163].

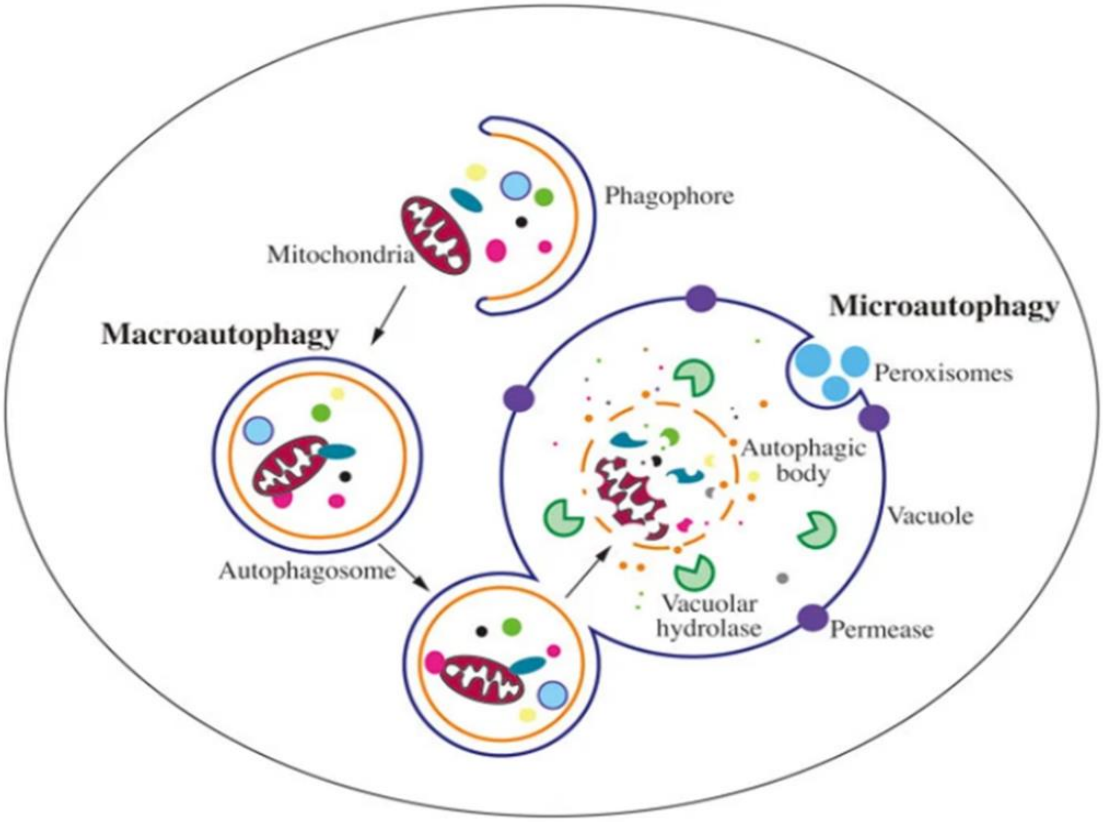

Figure 9. A schematic illustrating the two predominant types of autophagy in yeast – macroautophagy and microautophagy.
Macroautophagy occurs when random cytoplasm and dysfunctional organelles are sequestered by an expanding phagophore, resulting in the formation of the autophagosome. The autophagosome fuses with the vacuole membrane, discharging the autophagic body into the vacuole lumen and sequestered cargo is broken down by vacuolar hydrolases. Microautophagy occurs when cargos are directly taken in by the invagination and exposed to vacuolar hydrolases for degradation.

The RAS/cAMP/PKA pathway has been shown to be highly interconnected with the TOR pathways which are also involved in the regulation of autophagy in yeast. Both Tor and Ras often control overlapping effectors, including effectors involved in autophagy, resulting in a similar cellular response, such as the inhibition of the stress response, cell cycle progression and ageing. *S. cerevisiae* encodes for two Tor kinases, *TOR1* and *TOR2* respectively, with *TOR1* providing the most significant contribution to autophagy [166]. Upon the presence of nitrogen, Tor1 is activated, resulting in the repression of autophagy via the direct inhibition of the Atg1 complex and sequestration of the transcription factors Rim15 and Msn2/4 in the cytosol [167][168]. During starvation conditions or treatment with rapamycin, TOR is inhibited and autophagy is induced [168]. Moreover, the Tor1 complex directly phosphorylates and activates Sch9p, which inhibits the autophagy process. The inactivation of both PKA and Sch9p is sufficient to initiate autophagy, suggesting that both kinases are synergistically involved in the negative regulation of the autophagy process [168][169].

1.14 Ras in nutrient acquisition

The availability of key nutrients, such as amino acids, nitrogen compounds, and sugars, dictate the developmental programs and growth rates of yeast cells. Several overlapping signalling networks including the Ras/cAMP/PKA, AMP-activated kinase, and the TOR1 complex, apprise cells on nutrient availability and influence the cells transcriptional, translational, posttranslational, and metabolic profiles as well as dictating cell fate.

Much of the glucose-induced signalling in yeast functions through the Ras/cAMP/PKA pathway. 90 % of the transcriptional changes that occur on the addition of glucose to glucose depressed cells can be recapitulated by activating this pathway. Conversely, inhibiting this pathway concurrent with glucose addition eliminates most of the glucose induced responses.

Thus, Ras and the PKA pathway is necessary for the majority of the transcription changes of the cell in response to glucose addition [170]. Considering the Ras proteins role in glucose signalling it would not be wrong to postulate that Ras may function within the processes underpinning other nutritional sensing pathways in yeast, including peptide transport.

1.14.1 Di/Tri-peptide uptake mechanisms in *S. cerevisiae*

Peptides are composed of sequences of amino acids and once catabolized provide the essential building blocks required for protein synthesis. In addition, certain peptides and amino acids can be utilized as a nitrogen source and can act as signalling molecules that alter cell behaviour. For example, the branched-chain amino acid leucine, has been shown to control TORC1 activity [171][172]. TORC1 senses and responds to nutrients to promote cell growth and the inhibition of catabolic processes, such as autophagy. Branched-chain amino acids such as leucine function by affecting the 'nucleotide binding status of the Exit from G_0 Complex' (EGOC) GTPase subunits Gtr1 and Gtr2 in *Saccharomyces cerevisiae* [173][174]. Amongst other TORC1-stimulating amino acids, arginine abundance in mammalian cells is proposed to be sensed by the lysosomal transporter SLC38A9 and conveyed to mTORC1 via the Rag GTPases [175][176], while glutamine levels appear to be transduced to control both yeast and mammalian TORC1 independently of the EGO/Rag GTPases [172].

In mammals, amino acids exert a major role on the regulation of protein synthesis through the control of the kinases mTOR and Gcn2, which have been shown to have opposing effects on protein synthesis [172][177]. The regulation of Gcn2 activity by amino acid availability relies on the capacity of Gcn2 to sense the increased levels of uncharged tRNAs upon amino acid scarcity [177]. Gcn2 is activated during scarcity of an essential amino acids and

phosphorylates the α-subunit of eukaryotic initiation factor 2 alpha (eIF2α) [178]. This leads to the general inhibition of protein synthesis.

Due to the multifaceted role of amino acids and peptides in biological systems, it is therefore not surprising that microbes have evolved a multitude of mechanisms to facilitate peptide and amino acid uptake. The study of such mechanisms has been extensively examined in yeast, with amino acid uptake mechanisms presenting high conservation in mammals.

Saccharomyces cerevisiae has two distinct peptide transport mechanisms, a di-/tripeptide (the PTR system) and a tetra-/pentapeptides (the OPT) transport system. The PTR family of peptide transporters transport a number of substrates, including amino acids, nitrates and di/tri-peptides [179]. *PTR2* encodes an integral membrane protein (Ptr2p) involved in the physical translocation of peptides across the plasma membrane.

PTR2 encodes an integral membrane protein of 601 amino acids containing 12 membrane-spanning domains which transport substrates by the means of proton-motive force [180]. The transporter is specific for di-/tripeptides, with a preference for peptides containing hydrophobic amino acids. In *S. cerevisiae* the regulation of *PTR2* expression is strongly affected by the composition of the extracellular environment. In the absence of the preferred nitrogen sources *PTR2* expression is induced [181][182].The import of di/tripeptides composed of basic or bulky hydrophobic N-terminal residues increases *PTR2* expression via reducing cellular levels of Cup9p, the homeodomain-containing transcriptional repressor of *PTR2*. Specific di/tri-peptides function as both as ligands and regulators of the E3 ubiquitin ligase Ubr1p. Ubr1p mediates Cup9p degradation system that is governed by the identity of N-terminal amino acids [183][184]. Most di/tripeptides are too small to be degraded by the proteasome and are assimilated as nutrients by intracellular peptidases. However,

di/tripeptides with basic (Type 1: His, Lys, or Arg) and bulky (Type 2: Ile, Trp, Leu, Tyr, or Phe) N-terminal residues can compete with larger protein substrates and bind at the Type 1 and Type 2 Ubr1p substrate-binding sites. Once bound, Ubr1p-mediated degradation of Cup9p is allosterically activated via the release of the Ubr1p auto inhibitory domain, revealing a substrate-binding domain that binds an internal degron in Cup9p [185]. Relief of Cup9p repression of *PTR2* results in enhanced *PTR2* expression. A positive regulatory feedback loop is created where di/tripeptide uptake perpetuates Ubr1p-mediated Cup9p degradation, upregulating *PTR2* expression and thus increased di/tripeptide uptake.

Although Ptr2p is the major transporter of di/tripeptides in *S. cerevisiae*, di/tripeptides can also be imported with a low efficacy by Dal5, whose primary function is the import of nitrogen sources, such as allantoate and ureidosuccinate [186]. As aforementioned, the peptide transporters Opt1 and Opt2, which have partially overlapping functions, import peptides of 4–5 residues. In addition, Opt1 is a high affinity importer of glutathione, a "noncanonical" tripeptide [187]. In the same way as the Ptr2 transporter of di/tripeptides, the expression of *OTP2* is down-regulated by Cup9p, whereas the expression of *OPT1* is independent of Cup9p [187]. In addition to *PTR2* and *OPT2*, the N-end rule pathway also controls the expression of *DAL5*, but in a manner contrary to that of the other two transporters: whereas Cup9p is a transcriptional repressor of *PTR2* and *OPT2*, Cup9p up-regulates the expression of *DAL5* [179][187].

1.15 Ras signalling in human cells

Human Ras proteins transduce pro-survival signals from the extracellular space to the intracellular compartment via tyrosine kinase receptors (TKRs). Upon ligand binding, the dimerization of the receptors triggers a conformational change that activates the catalytic tyrosine kinase domain, which enables the autophosphorylation of the intracellular carboxyl-terminal domain and therefore induces its activation [188][189]. The phosphorylated domain of the TKR recruits GEFs, activating Ras, allowing it to signal downstream [190]. Active Ras proteins can activate at least 20 different effectors, including the RAF (rapidly-accelerate fibrosarcoma) kinases, phosphatidylinositol-3-kinase (PI3K) and RAL guanine nucleotide-dissociation stimulator (RALGDS) *(Figure 10)*. Other effectors associated with Ras protein activation include RIN1, T-lymphoma invasion and metastasis-inducing 1 (Tiam 1), Af6, Nore1, PLCS and PKC [191][192].

Activated RAF kinases phosphorylate and activate the MAPK/ERK kinase. Signal transduction along the Raf/MEK/ERK pathway starts with the activation of Ras by TKR's, G-protein-coupled receptors and/or intergrins *(Figure 10)* [193]. These membrane proteins form large signalling complexes upon activation and recruit and activate Ras proteins by promoting the exchange of Ras-bound GDP with GTP. The process is regulated by the interaction of Ras with GDP/GTP-exchange factors, such as SOS (son of sevenless). After the small G-proteins recruit the MKKKs c-Raf (and, if present, A- and B-Raf) to the plasma membrane, where RAF is activating causing phosphorylation, changes in its conformation and protein interactions occur [193] . The MEK-1/2 serine residues are phosphorylated by RAF leading to MEK-1/2 activation. ERK-1/2 is then phosphorylated by MEK-1/2 at threonine and tyrosine residues in the TEY motif of the activation loop. This dual phosphorylation event is linked with ERK-1/2 activity and can be

used to measure indirect quantification of the serine/threonine kinase (ERK) activation [194]. Upon activation, ERK can phosphorylate over 80 different substrates in the cytoplasm and nucleus.

In the phosphatidylinositol-3-kinase PI3K pathway, activated PI3K catalyses the production of Pip3 (phosphatidylinositol-3,4-triphosphate) by the phosphorylation of Pip2 (phosphatidylinositol-4,5-diphosphate). Pip3 activates the phosphatidylinositol dependent kinase 1 (PDK1), resulting in the activation and recruitment of AKT to the membrane [195]. The primary downstream effecter of activated AKT is mTOR (the mammalian target of rapamycin), which is a serine/threonine kinase. mTOR can form two distinct complexes, depending on the proteins it interacts with. The mTOR complex (mTORC1) primarily functions to promote the transcription of genes associated with energy metabolism, cell cycle progression and cell proliferation.

The mTOR complex 2 (mTORC2) mainly functions to phosphorylate AKT which results in cell survival and proliferation. Furthermore, AKT phosphorylation promotes telomerase activity, inhibition of apoptosis and blocking the release of cytochrome C from the mitochondria, downregulation of pro-apoptopic factos and pro-caspase 9, and regulates modulators of angiogenesis via activation of nitric oxide synthases [196][137][195].

Ras stimulates the RAL (RAS-like), GTPases, promoting the activation of phospholipase DI (PLD) and CDC42/RAC-GAP RAL binding protein 1 (RALBP1). These, among other pro-survival

functions, promote the progression of the cell cycle, inhibiting transcription factors involved in then cell cycle arrest, including the FORKHEAD transcription factors [191] [197].

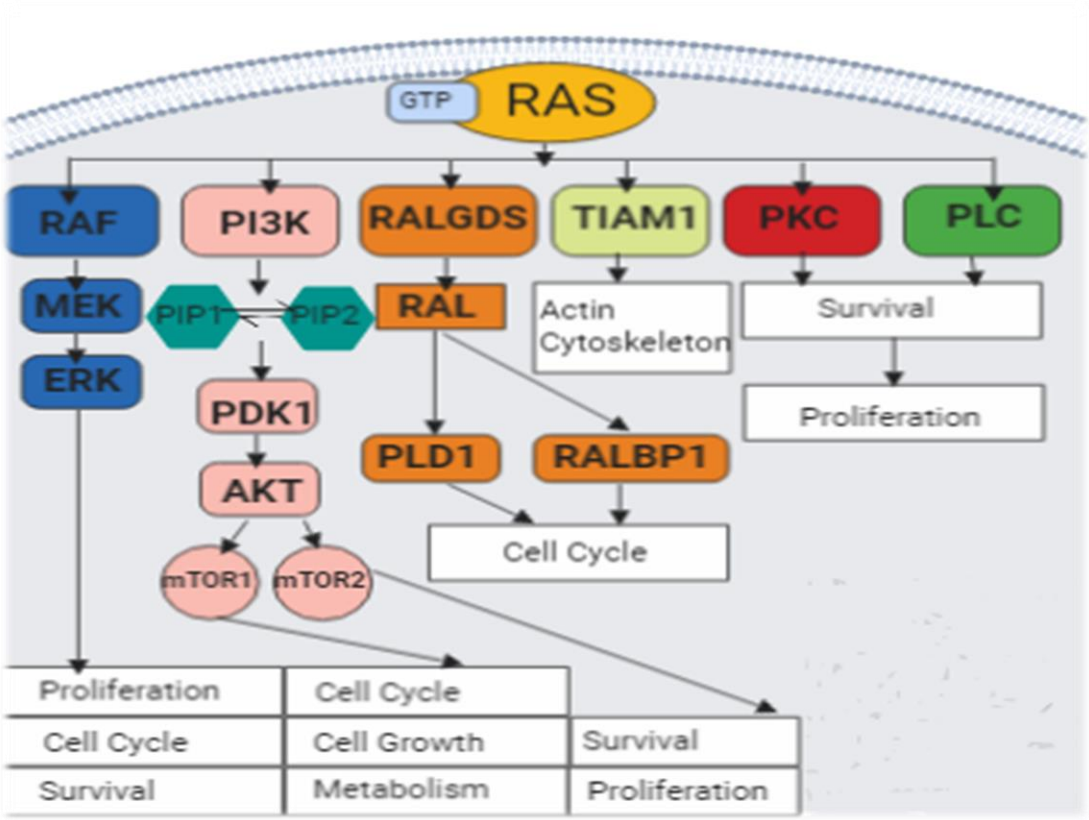

Figure 10. Schematic representation of the multiple effectors activated by human Ras proteins and the different impact these interactions have on cell fate.

1.16 The use of *S. cerevisiae* for the study of human Ras proteins

Human Ras proteins play a fundamental role in tumorigenesis and exhibit sequence homology with yeast Ras homologous [198] [199]. As such efforts have been made to use *S. cerevisiae* to investigate the molecular mechanisms of Ras proteins with the aim of understanding their roles and regulation in higher eukaryotes. The use of *S. cerevisiae* as a model to study the role of Ras proteins has been important for understanding the post-translational processes required for the translocation of Ras proteins to the plasma membrane [200]. Notably, the use of the *S. cerevisiae* mutant, Δ*dpr1*, revealed that the acylation was not the first

translational modification in the processing of Ras proteins [201]. Furthermore, the first Ras effector and first guanine-nucleotide exchange factor (GEF), adenylate cyclase and Cdc25, were identified in yeast [30] [78]. Such discoveries, particularly that of Cdc25, facilitated the identification of analogous proteins in humans [78]. In addition to the discovery of GEF proteins, yeast has been valuable for enhancing our understanding of the GTPase activating proteins (GAPs) through the discovery of *IRA1* and *IRA2*. The functions of the GAP-coding *NF1* gene, which when mutated is responsible for neurofibromatosis type 1, were uncovered thanks to the similarity with the *IRA* genes of *S. cerevisiae* [78]. Moreover, the expression of the *NF1* gene in yeast suppressed the phenotypes associated with the deletion of *IRA* genes, such as heat shock sensitivity, demonstrating that the mammalian and yeast GAPs are interchangeable and therefor highlighting the similarity between yeast and mammalian Ras protein activation [38]. Such examples highlight the importance of the use of *S. cerevisiae* as a model organism in modern biology.

1.17 Aims of this study

The localisation and signalling of Ras on the plasma membrane has been extensively studied. It has been shown that Ras undergoes a series of posttranslational modifications that dictate its subcellular localisation. Evidence exists to suggest that Ras proteins can undergo phosphorylation events which regulate its activity. Surprisingly, the phosphorylation of Ras2p in *S. cerevisiae* has not been studied regarding its regulation of intracellular localisation, despite significant evidence existing linking Ras phosphorylation to its localisation in humans. This study aims to further investigate whether Ras2p phosphorylation provides a mechanism that regulates Ras2p trafficking inside the cell.

In the laboratory of Dr Campbell Gourlay, previous bioinformatics investigations identified potential kinase and phosphatase enzymes that may influence Ras2 protein phosphorylation. This data was generated using the PhosphoPep (v2.0) database, which provides information sourced from tandem mass spectrometry experiments regarding phosphopeptides and phosphoproteins. The PhosphoPep database proposed twelve phosphatase and kinase enzymes that effect Ras2p phosphorylation and identified several serine residues that may be phosphorylated (*Table 1* and *Figure 11*).

Table 1. Phosphatase and kinase enzymes predicted by the PhosphoPep database to effect Ras2p phosphorylation.

Gene deletion	Protein function	Ras2 phospho-peptide level in deletion strain	Identified sequence
YIL035C *(CKA1)*	Protein kinase, functions in cell growth and proliferation	2.2-fold DOWN	R.NAS*IES*KTGL AGNQATNGK.T
YGR262C *(BUD32)*	Protein kinase, required for tRNA modification	2.2-fold DOWN	R.KMS*NAANGK. N
YIL042C *(PKP1)*	Mitochondrial protein kinase, functions in the negative regulation of pyruvate dehydrogenase	1.5-fold DOWN	R.NAS*IES*KTGL AGNQATNGK.T
YLL010C *(PSR1)*	Plasma membrane phosphatase, involved in general stress response	3.1-fold DOWN	R.NAS*IES*KTGL AGNQATNGK.T
YNL307C *(MCK1)*	Protein kinase, involved in chromosome segregation, mitotic entry, genome stability	1.6-fold DOWN	R.NAS*IES*KTGL AGNQATNGK.T
YPL042C *(SSN3)*	Cycline dependant protein kinase, involved in phosphorylation of RNA polymerase, and glucose repression	1.5-fold UP	K.GSGANSVPRNS *GGHR.K
YDL047W *(SIT4)*	Phosphatase, required for golgi to ER traffic, like human PP6	1.6-fold UP	K.NVNSS*TTVVN AR.N
YKL126W *(YPK1)*	Protein kinase; phosphorylates flippase activator Fpk1p, homolog of mammalian kinase SGK	1.6-fold UP	K.NVNSS*TTVVN AR.N

YKL139W *(CTK1)*	Catalytic subunit of C terminal domain kinase, like human CDK12	1.7-fold UP	K.NVNSS*TTVVN AR.N
YPL042C *(SSN3)*	Cycline dependant protein kinase, involved in phosphorylation of RNA polymerase, glucose repression	2.4-fold UP	K.NVNSS*TTVVN AR.N
YPL031C *(PHO85)*	Cyclin-dependent kinase, involved in cellular response to nutrient levels and environmental conditions and cell cycle	1.6-fold UP	R.NASIES*KTGLA GNQATNGK.T
YLR019W *(PSR2)*	Plasma membrane phosphatase involved in general stress response	3.9-fold UP	R.KMS*NAANGK. N
YAR019C *(CDC15)*	Protein kinase of the mitotic exit network	1.7-fold UP	R.KMS*NAANGK. N

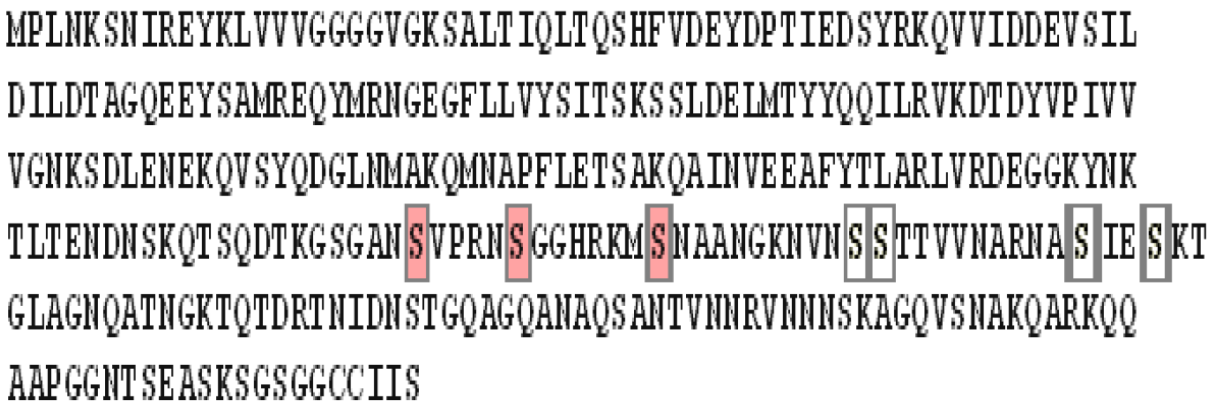

Figure 11. A schematic of the Ras2 protein sequence indicating the location of the phosphorylated serine residues.
Residues circled are those identified to be phosphorylated by the PhosphoPep database.

Previous studies from the laboratory of Dr Campbell Gourlay reported that the deletion of either *Δsit4* or *Δssn3* led to significant changes in GFP-Ras2 protein localisation during both logarithmic and stationary phases of growth. Interestingly, the phosphorylation sites that were predicted to be affected upon the deletion of either *SSN3* or *SIT4* were found to be identical and focussed upon the serine residue at position 225 of Ras2p. Two-dimensional electrophoresis was used to identify whether the deletion of either *SIT4* or *SSN3* resulted in

changes to Ras2 protein phosphorylation. Two-dimensional electrophoresis of *Δsit4*, *Δssn3* and wild type cells identified a putative Ras2 phosphorylation event occurring in both *Δsit4* and *Δssn3* cells that was not present in wild type cells. This was represented by the appearance of a negatively charged spot in *Δsit4* and *Δssn3* cells which disappeared following the treatment with alkaline phosphatase. The negatively charged spot occurring in a similar position in both *Δsit4* and *Δssn3* cells was hypothesized to be the phosphorylation of serine^{225} of the Ras2p.

In the present study, we therefor sought to investigate whether modification of Serine^{225} led to any changes in Ras2 protein localisation or activity within the cell and whether this was accompanied by any phenotypes in cells expressing either *RAS2*^{S225A} or *RAS2*^{S225E}.

Chapter 2
Materials and Methods

2.1 Growth conditions and media for the culture *of Saccharomyces Cerevisiae* and *Escherichia coli*

A Prestige Medical bench-top autoclave was used to sterilise all media. Media was autoclaved at 121 °C, 15 lb/sq.in for 11 mins. All liquid cultures of *Saccharomyces cerevisiae* were incubated at 30 °C with constant rotation at 200 rpm. All liquid cultures of *Escherichia coli* were incubated at 37 °C with constant rotation at 180 rpm. For solid medium 2 % w/v granulated agar (Oxoid technical agar No. 3) was added prior to autoclaving.

2.1.1 Water used in study

Pure deionised water (dH_20) was produced by Thermo Scientific Barnstead NanoPure Diamond water system. dH_20 was then further sterilized via autoclaving.

2.1.2 Yeast extract, peptone, dextrose (YPD) growth media

Ingredients included 2 % w/v glucose (Fisher), 1 % w/v yeast extract (Oxoid) and 2 % w/v bactopeptone (Difco).

2.1.3 Synthetic complete (SC) drop-out medium

This media was prepared as follows; 2 % w/v glucose (Fisher), 0.77 % Yeast Nitrogen Base without amino acids (Kaiser, Formedium), yeast synthetic complete drop-out media supplement (Formedium). The source of nitrogen for yeast cells grown in this media is ammonium sulphate.

Upon the transformation of cells with plasmid DNA, successful transformants were selected for using auxotrophic selection media through the addition of the appropriate Yeast Synthetic Complete Drop-Out Media Supplement (Formedium).

Table 2. Percentage of auxotrophic selection drop-out supplement added to media

Amino acid drop-out	Required %
Uracil	0.19
Leucine	0.164
Uracil and Leucine	0.174

2.1.4 Nitrogen Starvation Media (NS)

The media was prepared as follows; 2 % glucose (Fisher), 0.675 % Yeast Nitrogen base without amino acids and ammonium sulphate (Difco), 0.193 % yeast synthetic dropout Kaiser mixture without Uracil (Formedium).

2.1.5 Yeast extract and Tryptone (YT) Growth Media

YT growth media was prepared as follows; 0.1 % w/v yeast extract (Oxoid), 1 % w/v analytical grade sodium chloride (Fisher) and 1 % w/v bacto-tryptone (Difco).

For the selection of successfully transformed *E. coli* containing the plasmid of interest, antibiotic resistance markers were used. Ampicillin (Sigma-Aldrich) was added to the growth medium after autoclaving to select for successfully transformed *E. coli* containing plasmids with the *AmpR* gene integrated. Ampicillin was added to a final concentration of 100 µg/ml, from a 100 mg/ml stock solution in sterile deionised water. To select for *E. coli* colonies containing the gene for kanamycin resistance, kanamycin (Sigma-Aldrich) was supplemented to the growth media after autoclaving. Kanamycin was added to a final concentration of 50 µg/ml from a 10 mg/ml stock solution in sterile deionised water.

2.2 *Saccharomyces cerevisiae* strains used in this study

Table 3. The Saccharomyces cerevisiae strains used in this study

Strain	Genotype	Source/strain ID
BY4741	*MATa hisΔ1 leu2Δ0 met15Δ0 ura3Δ0*	CGY424
BY4741 *Δcup9*	*MATa his3Δ1 leu2Δ0 met15Δ0 ura3Δ0 ⊿cup9::KANMX*	KO collection*
BY4741 *Δubr1*	*MATa his3Δ1 leu2Δ0 met15Δ0 ura3Δ0 Δubr1::KANMX*	KO collection*
BY4741 *Δptr2*	*MATa his3Δ1 leu2Δ0 met15Δ0 ura3Δ0 Δptr2::KANMX*	KO collection*
BY4741 *Δras2*	*MATa his3Δ1 leu2Δ0 met15Δ0 ura3Δ0 Δras2::KANMX*	KO collection*
BY4741 *Δpde2*	*MATa his3Δ1 leu2Δ0 met15Δ0 ura3Δ0 Δpde2::KANMX*	KO collection*
KAY836 – *wt*	*MATa ura 3-52 leu 2 his4-539*	CGY370
KAY23- *Δras2*	*Δras2::leu2 MATa ura 3-52 leu2 his4-539*	CGY371
BY4741 + *Δcox4*	*MATa his3Δ1 leu2Δ met15Δ ura3Δ Δcox4::HIS*	CGY638
KAY836- *RAS2$^{ala18, val19}$*	*his3Δ1, leu2Δ, ura3Δ, met15Δ, RAS2(ala18, val19)*	CGY372

*****Yeast MATa Collection was purchased from Open Biosystems and was produced by the EUROpean Saccharomyces Cerevisiae Archive for Functional analysis (EUROSCARF).

2.3 *Escherichia coli* strains used in this studyDH5α:

Competent *E. coli* cells were used in this study, the genotype of these cells: *F- endA1 glnV44 thi-1 recA1 relA1 gyrA96 deoR nupG Φ80dlacZΔM15 Δ(lacZYA-argF) U169, hsdR17(rK- mK+), λ–.*

DB3.1: Competent *E. coli* cells were used in this study, the genotype of these cells: F- *gyrA462 endA1 glnV44* Δ(*sr1-recA*) *mcrB mrr hsd*S20(rB-, mB-) *ara14 galK2 lacY1 proA2 rpsL20*(Smr) *xyl5 Δleu mtl1.*

TOP10: Competent *E. coli* cells were used in this study, the genotype of these cells: *F- mcrA Δ(mrr-hsdRMS-mcrBC) Φ80lacZΔM15 ΔlacX74 recA1 araD139 Δ(araleu)7697 galU galK rpsL (StrR) endA1 nupG.*

Strataclone Solopack: Competent *E. coli* cells were used in this study, supplied by Agilent technologies (Product reference: 200184), the genotype is not published.

2.4 DNA Methods

2.4.1 Plasmids used in the study

Table 4. Plasmids used in the study

Strain	Description	Selective marker	Source
pDONR221	Gateway Entry Vector	N/A	Addgene
pAG426GPD-EGFPccdB	Gateway Destination Vector	*URA3*	Addgene
pAG416GPD-EGFPccdB	Gateway Destination Vector	URA3	Addgene
pCG347- Active GFP-Ras2	PYX212 RBD x3GFP URA3- TPI	URA3	Leadsham
pCG46	pYX142-mtGFP	LEU2	(Westermann & Neupert 2000)
pCG381	Gateway entry vector PDONR221 RAS2 KAN^R	URA3	Addgene
pCG502	*PDE2*	LEU2	CWG plasmid collection
pCG557	Gateway Destination Vector 1H2 416-GPD-ccdB- AMP^R	URA3	CWG plasmid collection
pCG558	Gateway Destination Vector 1H3 426-GPD-ccdB - AMP^R	URA3	CWG plasmid collection
pCG565	Gateway Expression Clone $Ras2^{S225E}$ 416-GPD-EGFP- AMP^R	URA3	CWG plasmid collection
pCG566	Gateway Expression Clone	URA3	CWG plasmid collection

	Ras2^{S225A} 416-GPD-EGFPAMP^{R}		
pCG571	Gateway Expression Clone Ras2^{S225E} 426-GPD-EGFPAMP^{R}	URA3	CWG plasmid collection
pCG572	Gateway Expression Clone Ras2^{S225A} 426-GPD-EGFP AMP^{R}	URA3	CWG plasmid collection
pCG582	*RAS2* in PCG557 AMP^{R}	URA3	This study
pCG583	*RAS2* in PCG558 AMP^{R}	URA3	This study
pCG586	*Ras2^{S225E}* in PCG558 AMP^{R}	URA3	This study
pCG587	*Ras2^{S225A}* in PCG558 AMP^{R}	URA3	This Study
pCG588	*Ras2^{S225E}* in PCG557 AMP^{R}	URA3	This Study
pCG589	*Ras2^{S225A}* in PCG558 AMP^{R}	URA3	This Study
PCG593	*N-Ras^{S173A}* in PCG558 AMP^{R}	URA3	This study
PCG594	*N-Ras^{S173E}* in PCG558 AMP^{R}	URA3	This study
PCG595	*N-Ras* in PCG558 AMP^{R}	URA3	This Study
PCG597	Gateway Expression Vector *N-Ras* 416-GPD-EGFP- AMP^{R}	URA3	This Study
PCG598	Gateway Expression Vector *N-Ras^{S173A}* 416-GPD-EGFP- AMP^{R}	URA3	This Study
PCG599	Gateway Expression Vector *N-Ras^{S173E}* 416-GPD-EGFP- AMP^{R}	URA3	This Study
PCG600	Gateway Expression Vector *N-Ras* 426-GPD-EGFP AMP	URA3	This Study
PCG601	Gateway Expression Vector *N-Ras^{S173A}* 426-GPD-EGFP AMP^{R}	URA3	This Study
PCG602	Gateway Expression Vector *N-Ras^{S173E}* 426-GPD-EGFP AMP^{R}	URA3	This Study
PCG636	Low copy plasmid expressing *GFP-ATG8*	URA3	Professor Frank Madeo, University of Graz.

A)

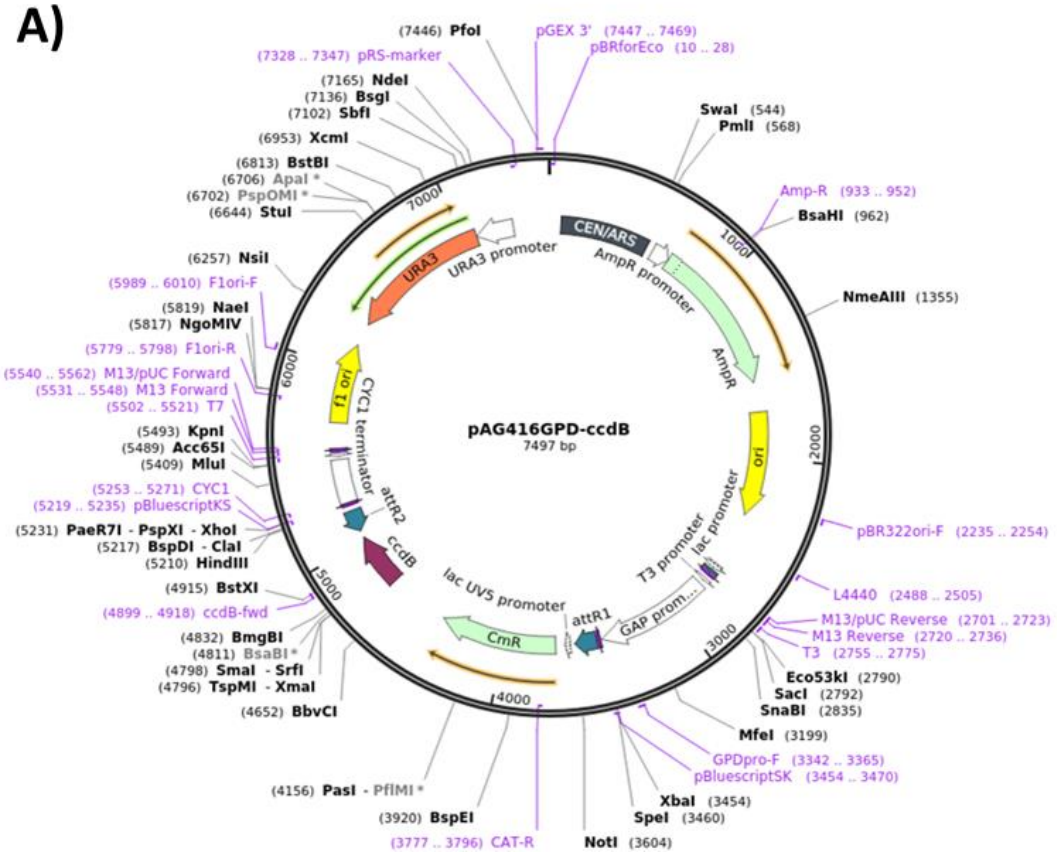

B)

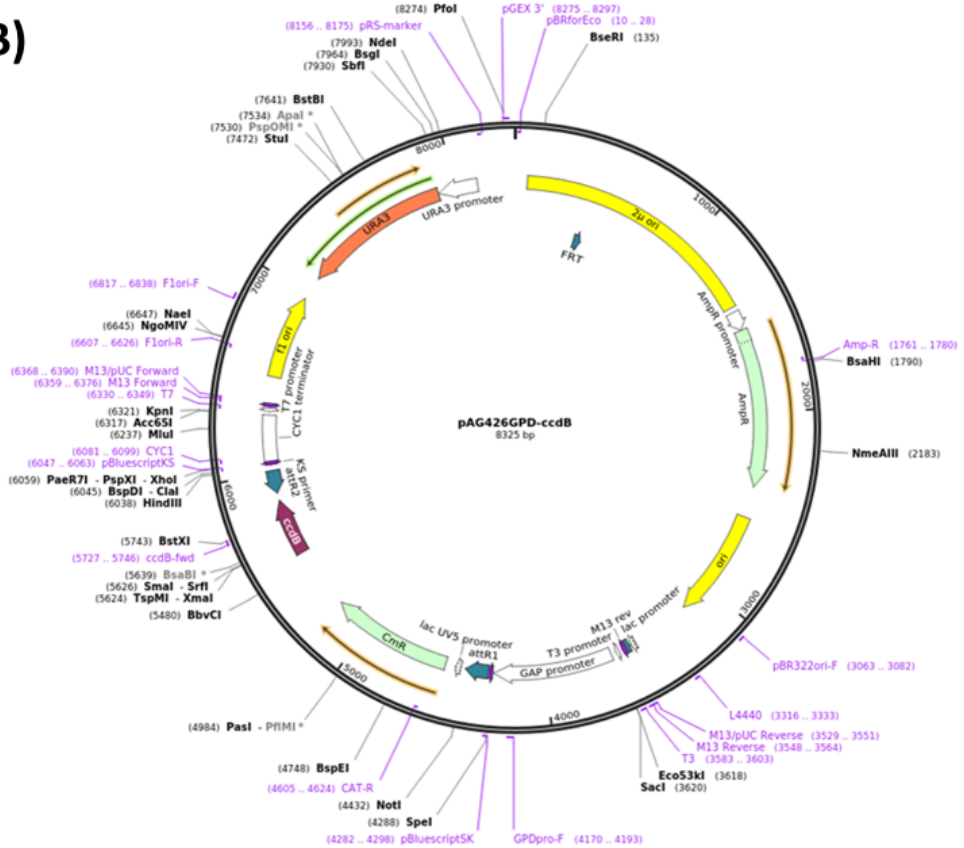

C)

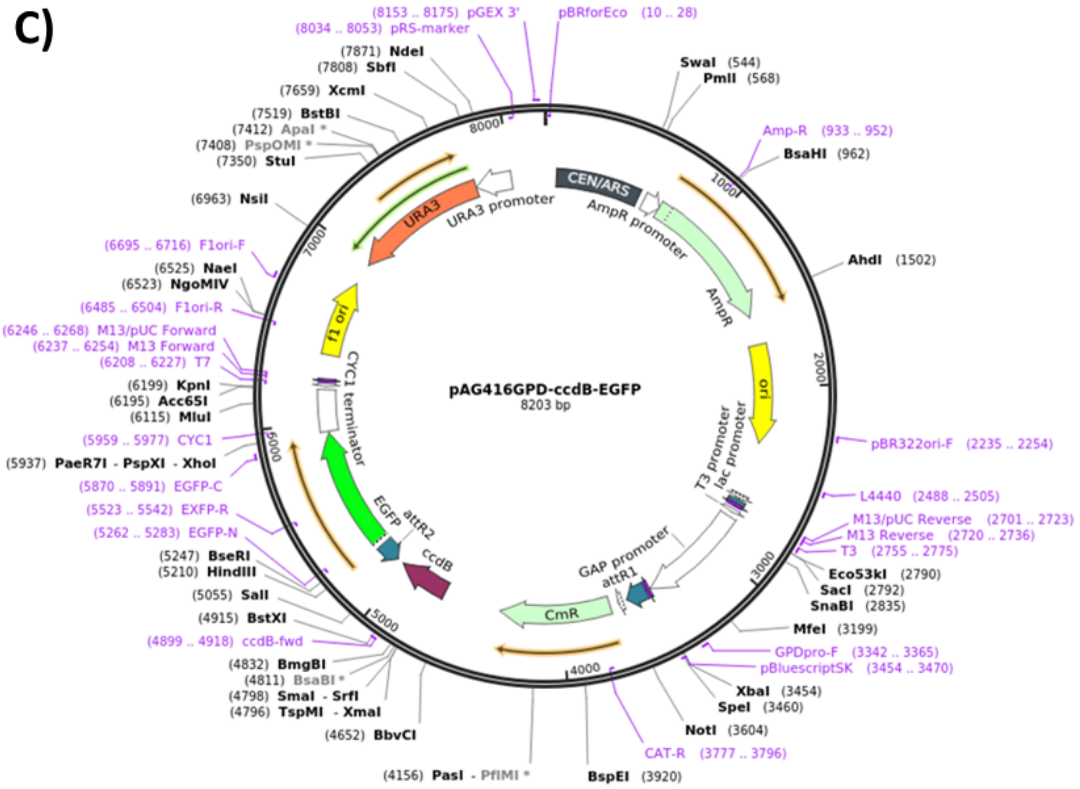

D)

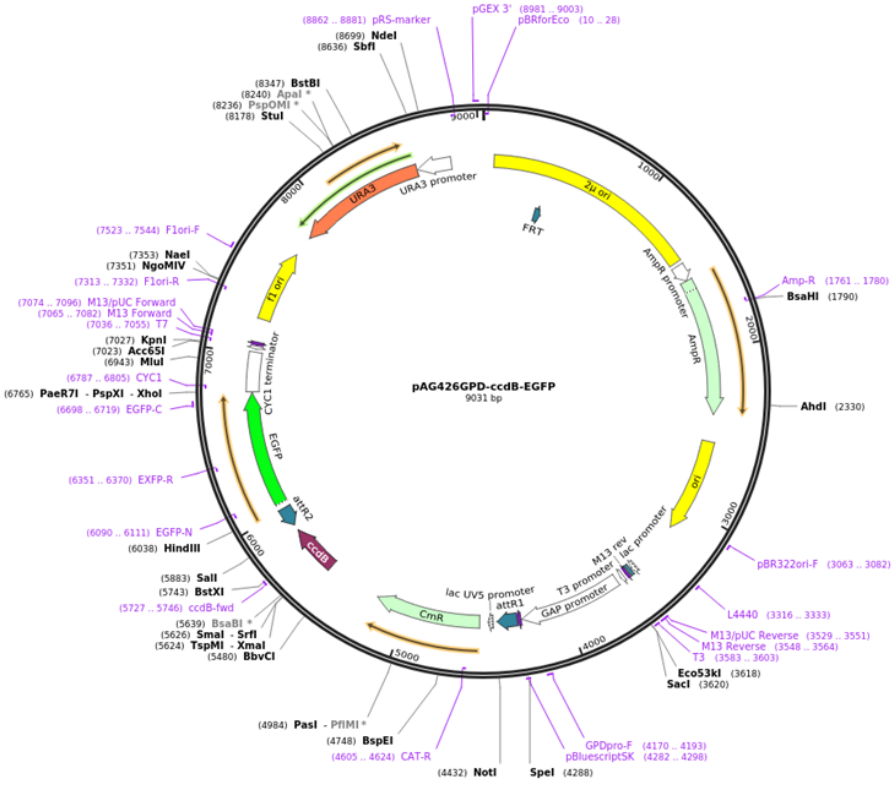

Figure 12. Maps of the plasmids used in the Gateway cloning reaction.
A) pAG416GPDccdB destination vector. B) pAG426GPD destination vector. C) pAG426GPD-ccdB-EGFP destination vector. D) pAG416GPD-ccdB-EGFP destination vector.

2.5 Transformation of plasmid DNA into *S. cerevisiae* and *Escherichia coli*

2.5.1 Transformation of *S. cerevisiae* using the lithium acetate method

A sterile inoculation loop was used to pick a fresh colony of yeast. The colony was inoculated into 5 ml of appropriate medium and grown overnight at 30 °C with shaking at 200 rpm. A 1 ml volume of fresh overnight culture was transferred to a 1.5 ml microcentrifuge tube and harvested in a bench-top centrifuge at 3000 rpm for 4 min at room temperature. The supernatant was discarded, and the pellet resuspended in 1 ml of 1x TE buffer at pH 8.0. The cells were pelleted as previously described and resuspended in 1 ml of 1M lithium acetate (LiAc) in TE at pH 8. Cells were pelleted again and resuspended in 0.1 ml of 0.1 M lithium acetate (LiAc) in TE at pH 8. 15 µl of single stranded carrier DNA (boiled herring sperm DNA, 10 mg/ml) was added to the suspension and mixed. 2µl of plasmid DNA at 100 ng/µl was added to the mixture and the mixture vortexed briefly. 700 µl of 40 % polyethylene glycol (PEG 4000 [Sigma]) in 0.1 M LiAc in TE was added and the mixture vortexed briefly. The microcentrifuge tube was then incubated at room temperature for 90 mins with rotation. A 42 °C heat shock for 20 mins followed. Cells were pelleted by centrifugation as previously described and resuspended in 200 µl of sterile deionised water. The cell suspension was spread onto agar plates with the appropriate selective media and incubated at 30 °C for at least 2 days to allow colony growth.

2.5.2 Transformation of S. *cerevisiae* using the lithium acetate method without heat shock

For some strains that displayed sensitivity to heat shock an alternative protocol was used. In these cases, a sterile inoculation loop was used to pick a fresh colony of yeast. The colony was inoculated into 5 ml of appropriate medium and grown overnight at 30 °C with shaking at 200 rpm. A 2 ml volume of fresh overnight culture was transferred to a 1.5 ml microcentrifuge tube and harvested in a bench-top centrifuge at 3000 rpm for 4 mins at room temperature. The supernatant was removed, and the pellet was resuspended, using a bench top vortex, in the reagent cocktail listed in **Table 2.5**. The microcentrifuge tube was incubated at room temperature overnight. The supernatant was removed, and the pellet was resuspended in 200 µl of sterile water and plated on the appropriate media. Plates were incubated at 30 °C for at least 2 days to allow colonies to grow.

Table 5. Yeast transformation reagents for the heat sensitive transformation protocol

Transformation reagents
37 % polyethylene glycol (PEG)-4000 from a 50 % w/v stock
0.1 M LiAc from a 1 M stock
0.1mg ssDNA from a 10 mg/ml stock
0.11 M 2-Mercaptoethnaol (Sigma M6250)
0.4 – 1 µg plasmid DNA
Sterile Deionised water to a volume of 324 µl

2.5.3 Transformation of *Escherichia coli* with plasmid DNA

A 50 µl aliquot of competent cell (for preparation protocol refer to Materials and Methods, Section 2.6) suspension was thawed on ice. A volume of plasmid DNA at a concentration of at least 20 ng/ml was added to the solution of competent cells and mixed gently. The suspension was incubated on ice for 1 hour and then incubated at 42 °C for 90 secs. 200 µl of YT media was added and the suspension was incubated at 37 °C for 30 mins. The suspension was then spread onto YT agar containing the appropriate antibiotic to select for transformants and incubated at 37 °C overnight. Plates were checked for colony growth the following morning.

2.6 *Escherichia coli* competent cell preparation

E. coli cells (DH5α) were grown overnight in 10 ml of YT at 37 °C with constant shaking at 180 rpm. The overnight culture was subcultured and diluted in 28 ml YT media to 0.2 OD_{600}. The culture was incubated at 37 °C with constant shaking at 180 rpm until the culture reached an OD_{600} of ~0.7. The time at which the culture would reach the required OD_{600} was calculated using the following formula.

[(Log (OD_{600} wanted) – Log (OD_{600} read))/Log2] x doubling time = time to required OD_{600}

A 3.75 ml aliquot of pre-heated glycerol (35 °C) was slowly added to the culture. The cell suspension was then incubated on ice for 10 mins. Cells were then harvested by centrifugation at 4000 rpm for 10 mins at 4 °C. Harvested cells were then resuspended in 28 ml of ice cold $MgCl_2$/ glycerol solution (0.1 M $MgCl_2$, 15 % glycerol [v/v]). After resuspension, cells were harvested by centrifugation at 3800 rpm for 8 mins at 4 °C and resuspended in 6.25 ml of iced T-salts solution (0.0075 M $CaCl_2$, 0.006 M $MgCl_2$, 15 % glycerol [v/v]). A 20-minute incubation period followed. Cells were harvested via centrifugation at 3600 rpm for 6 mins

and resuspended in 1.35 ml of T-salts solution. The cell suspension was then aliquot into pre-chilled microcentrifuge tubes and stored immediately at -80 °C. Competent cells were ready for use after 24 hours.

2.7 Molecular Biology methods

2.7.1 Plasmid DNA purification from *Escherichia coli* (mini prep)

A sterile inoculation loop was used to pick a fresh colony of *E. coli* which contained the plasmid of interest. The colony was inoculated into 5 ml of YT media supplemented with the appropriate antibiotic and grown overnight at 37 °C with constant rotation at 180 rpm. Cells were harvested in a benchtop centrifuge at 8000 rpm for 3 mins at room temperature and the supernatant removed. The plasmid DNA of interest was extracted from the cell pellet using a Qiagen QIAprep Spin Miniprep Kit according to the manufactures' instructions.

2.7.2 Plasmid purification from *S. cerevisiae*

To isolate plasmid DNA from a yeast strain, the Invitrogen ChargeSwitch plasmid yeast mini kit was used. A sterile inoculation loop was used to pick a fresh colony of yeast containing the plasmid of interest. The colony was inoculated into 5 ml of appropriate medium and grown overnight at 30 °C with shaking at 200 rpm. A 1 ml aliquot of the overnight culture was taken and placed in a sterile 1.5 ml Eppendorf. Cells were then spheroplasted and lysed. The lysate is extracted and placed in a fresh 1.5 ml Eppendorf in a low pH buffer and ChargeSwitch beads are added. The ChargeSwitch beads bind DNA of specific sizes in a low pH environment. The sample is then placed into a magnetic platform (MagnaRack). The beads and DNA are retained in the Eppendorf tubes containing them, and the remaining lysate is washed through and discarded. Following the wash phases, the DNA is eluted by the addition of a low salt buffer.

The addition of the low salt buffer raises the pH in solution and neutralizes the surface charge on the beads, causing the DNA to disassociate from the beads. The concentration of plasmid DNA isolated from yeast using this methodology is relatively low for any future processing or downstream applications. Therefore, the extracted plasmid DNA was then amplified by transforming into bacterial cells (Materials and Methods, Section 2.5.3).

2.7.3 Yeast genomic DNA extraction

Following the yeast transformation protocol described in Materials and Methods, Section 2.5.1**,** individual colonies were re-streaked onto separate plates containing the appropriate media and labelled as individual clones. A sterile inoculation loop was used to pick a fresh colony of the clone of interest. The colony was inoculated into 5 ml of appropriate medium and grown overnight at 30 °C with shaking at 180 rpm. 1 ml of the overnight culture was aliquot into a fresh 1.5 ml Eppendorf tube and cells were harvested using a benchtop centrifuge spinning at 13 000 rpm for 1 minute. The supernatant was discarded, and cells were washed with 1 ml of sterile de-ionised water using the same centrifuge settings as previously described. The supernatant was discarded, and cells were re-suspended in 500 µl of lysis buffer (100mM Tris pH 8, 50 mM EDTA, 1% SDS). 50 mg of acid washed glass beads were added to each sample, bringing the sample volume up to 1.25 ml. Samples were then vortexed for 1 minute to lyse the cells. To separate the lysed cell debris from the glass beads; a heated needle was inserted into the bottom of the Eppendorf, the existing Eppendorf was placed into a fresh second Eppendorf and centrifuged at 2 000 rpm for 5 mins. To each sample, 275 µl of 7M ammonium acetate (pH 7) was added. A 5-minute incubation period at 65 °C, then a further 5-minute incubation on ice followed. To each sample, 500 µl of chloroform was added, followed by a brief vortex stage, and then centrifuged at 13 000 rpm for 2 mins. The

supernatant was extracted and moved to a fresh Eppendorf tube and 1 ml isopropanol was added and briefly mixed by inversion and incubated at room temperature for 5 mins. The sample was then centrifuged at 13 000 rpm for 5 mins and the isopropanol facilitates the precipitation of genomic DNA out of solution. The supernatant was discarded, and the pellet was washed in 70 % ethanol. The ethanol was removed, and the pellet was air dried and suspended in 50 µl of sterile deionised water.

2.7.4 Whole cell RNA extraction from *S. cerevisiae*

The extraction of RNA from yeast cells was performed using the E.Z.N.A. Yeast RNA Kit Spin protocol. A sterile inoculation loop was used to pick a fresh colony of yeast. The colony was inoculated into 5 ml of appropriate medium and grown overnight at 30 °C with shaking at 200 rpm. The cells were then subcultured and diluted to a calculated OD_{600} of 0.1 and grown for 24 hours. $5x10^7$ yeast cells were harvested from the overnight culture in a 15 ml Falcon tube via centrifugation at 4 °C for 5 mins at 1000 g. The supernatant was discarded, and cells were resuspended in 480 microliters of SE Buffer/lyticase solution. The pellet was resuspended using a vortex for 1 minute. The cells were then incubated at 30 °C for 1 hour to ensure complete lyses of cells. The spheroplasts were then pelleted via centrifugation at 400 g for 5 mins at room temperature. The supernatant was carefully removed and 350 µl of YRL buffer and 50 mg of glass beads was added to the pellet. Using a vortex at 13 000 rpm for 5 mins, the suspension was mixed to lyse and homogenize the sample. The homogenised suspension was then centrifuged at 13,000 g for 3 mins at room temperature. The supernatant was carefully removed and transferred into a new Eppendorf tube. An equal volume of 70 % ethanol to the lysate was added and mixed thoroughly using a vortex for 15 secs. The entire sample, which was around 700 µl, was added to a Hibind RNA mini column assembled in a 2

ml Eppendorf. The sample was then centrifuge at 10 000 g for 30 secs at room temperature and the flow through was discarded. 350 µl of RNA wash buffer 1 was added to the column and the sample was centrifuged as above.

A DNA denaturing phase followed to ensure denaturing of any residual DNA in the sample. 75 µl of the DNase1digestion reaction mixture was added onto the surface of the HiBind RNA membrane in each column and incubated at room temperature for 15 mins. 350 µl of the RNA Wash Buffer 1 was added onto the surface of the HiBind RNA membrane and allowed to soak for at least 5 mins. The sample was centrifuged at 10 000 g for 15 secs and the flow through was discarded. 500 µl of RNA Wash Buffer II was added to the column and centrifuged and flow through discarded, as in the preceding step. Using the same collection tube, the spin cartridge was centrifuged at 10 000 g for 1 minute to dry the HiBind matrix. The column was transferred to a sterile RNase free 1.5 ml Eppendorf and the RNA was eluted with 50 µl of DEPC water. Samples were then stored at -80 °C until required for downstream applications.

2.7.5 Illumina library preparation and sequencing

Before library preparation, the quality and quantification of RNA samples were evaluated with TapeStation (Agilent) and Qubit (Thermal Fisher) at the Centre of Genome-Enabled Biology (Aberdeen) by Dr Jin Pu. The samples with the minimum RIN of 8.0 was proceeded. The input of RNA was based on the specifically measured RNA concentration by Qubit. The mRNA-Seq libraries were prepared using TruSq Sample Preparation Kit (Illumina) according to the manufacturer's instructions. Briefly, Poly-A RNA were purified from 500 ng of total RNA with 1ul (1:100) ERCC spike (Thermal Fisher) as an internal control using RNA purification oligo(dT) beads, fragmented and retrotranscribed using random primers. Complementary-DNAs were end-repaired, and 3-adenylated, indexed adapters were then ligated. 15 cycles of PCR

amplification were performed, and the PCR products were cleaned up with AMPure beads (Beckman Coulter). Libraries were validated for quality on Agilent DNA1000 Kit and quantified with the qPCR NGS Library Quantification kit (Roche). The final libraries were equimolar pooling and sequenced using the High Output 1X75 kit on the Illumina NextSeq 500 platform producing 75 bp single end reads. For each library, a depth 20-30 M reads were generated. The quality of sequencing was analysed by FastQC and MultiQC.

2.7.6 Analysis of RNA-Seq data

The analysis of RNA–Seq samples was performed using the Galaxy web platform (www.usegalaxy.org) [202]. The quality of the RNA sequencing reads was checked using FastQC v0.11.5 [203] with default settings. Low quality ends (Phred score < 20) and any adaptor sequences were trimmed using TrimGalore! v0.4.3 [204]. Reads which became shorter than 40 bp after trimming were not progressed for further analysis. After trimming, the quality was checked again using FastQC v0.11.5 [203] to ensure correct trimming. There were no Poly-A reads (more than 90 % of the bases equal A), low quality reads (more than 50 % of the bases with a Phred score < 25) or ambiguous reads (containing N). After processing, the mean Phred score per read was 37. Processed reads were aligned with the reference *S. cerevisiae* genome S288C version R64-2-1_20150113 (SacCer3) using HISAT2 v2.1.0 [205] with single-end reads and reverse strand settings, remainder of settings were set to default. After alignment, the number of mapped reads which overlapped CDS features in the genome (using *S. cerevisiae* genome S288C version R64-2-1_20150113 (SacCer3) were determined using featureCounts plug-in v1.6.3 with default settings [206]. Reads aligning to multiple positions or overlapping more than one gene were discarded, counting only reads mapping unambiguously to a single gene. Differential gene expression analysis between conditions was

performed using DESeq2 v1.18.1 [207] with default settings. To identify the cellular pathways which differentially expressed genes are within we conducted Gene Set Enrichment Analysis (GSEA; Broad Institute) [208]. To conduct a GSEA analysis, a list of significantly ($q \leq 0.05$) differentially expressed genes, ranked from the most upregulated to the most downregulated were uploaded into the GSEA database and compared to a gene set data base (S288C version R64-2-1_20150113_features gtf annotation file).

2.7.7 Quantification of nucleic acid samples

The concentration of DNA in samples was obtained using either a Thermo Scientific Nanodrop-1000, Biophotometer (Eppendorf) or a Spectrostar Nano UV/Vis spectrum absorbance microplate reader (BMG Labtech). To determine the DNA/RNA concentration from the OD_{260} reading from the Biophotometer, the following equation was used: DNA/RNA concentration (µg/mL) = OD_{260}/OD_{280} ratio dilution factor. No dilution of sample was required for use of the Nanodrop-1000 and readings were obtained from an analysis of a 1µl aliquot sample.

2.7.8 Restriction enzyme digest of DNA

Enzymatic scission of DNA at specific sequence points was achieved using restriction endonucleases from New England Biolabs, Promega and Roche. The buffers used were supplied by the manufactures and the recommended protocols were used.

Table 6. The basic reaction mixture for a restriction digest used in this study

Reagent	Volume
Restriction digest buffer (10x)	2 µl
Bovine Serum Albumin (BSA)	0.2 µl
Restriction Endonuclease	1 µl
Plasmid DNA	1.5 µl
Sterile water	Up to a final volume of 22 µl

The reagents listed above were added to the pre-determined volume of sterile water required for a 22 µl reaction mix. All digests underwent a 2-hour incubation at 37 °C. For analyses of the digested products, 10 µl of the sample was loaded onto an agarose gel.

2.7.9 Agarose gel electrophoresis

For the analysis of DNA fragments and plasmids, agarose gel electrophoresis was undertaken. Typically, agarose gels were composed of 0.8 % (w/v) agarose (Melford, MB12000) in TAE buffer.

Recipe for 1x TAE Buffer: Tris base 4.84 g, Glacial acetic acid 1.14 ml, 0.5 M EDTA, pH 8.0 2 mL, Milli-Q water to 1 L final volume.

For higher percentage agarose gels, up to 1.5 % gels were used to better resolve smaller fragments. The agarose was dissolved in 1x TAE by heating in a microwave oven until the solution became clear. The solution was cooled to ~60 °C before ethidium bromide (10 mg/ml)

was added at a concentration of 0.0167 µg/ml. The mixture was poured carefully into a gel forming cassette, and a comb was inserted. The gel was left to cool and set for up to an hour.

Once the gel had solidified, it was placed in an electrophoresis tank and 1x TAE buffer was added in sufficient quantity to cover the gel surface by 2-3 mm. The comb was then removed. A Promega 1 kb DNA ladder (G57511) was added to the first well and 6x loading buffer containing bromophenol blue was mixed 1 in 6 with the DNA samples. Typically, 10 µl of sample was loaded into the subsequent wells. For analysis of restriction digestion products, 10 µl of sample was loaded. A voltage of 80 V was applied to the tank for 30-60 mins until the DNA bands had migrated the desired distance. The DNA fragments were visualised by short wavelength (312 nm) UV transillumination.

2.7.10 Polymerase Chain Reaction (PCR)

For the amplification of DNA sequences, the polymerase chain reaction (PCR) was utilized. The PCR reaction was performed using the Roche 'High Fidelity PCR System and Techno TC-3000 thermal cycler.

1-5 µl of plasmid DNA was used as the source of the template for PCR reaction. The following reagents were mixed on ice in an Eppendorf PCR tube:

Table 7. Standard PCR reaction composition used in this study

Reagent	Volume Added	Final concentration
(10x) High Fidelity Buffer + 15 mL $MgCL_2$	5 µl	1x (1.5 ml $MgCl_2$)
Reverse Primer, 100 pmol/ µl	1-5 µl	300 nM
Forward Primer, 100 pmol/ µl	1-5 µl	300 nM
Template DNA	1-5 µl	0.1-250 ng
dNTP mix, 10 mM each dNTP	1 µl	200 µM each dNTP
High Fidelity Enzyme Mix	1 µl	3.4 U/reaction
Sterile Deionised water	Up to 50 µl	-

PCR reactions were conducted using the cycling conditions described in Materials and Methods, Table 2.7.10.2. After the completion of the reaction, a 5 µl aliquot of the PCR product was run on an agarose gel. The products of the PCR reactions were purified with the Qiagen 'PCR Purification' kit according to manufactures instructions.

Table 8. Standard 3-step PCR cycling protocol used in this study

Cycle Step	Cycle Temperature (°C)	Time (mins)	Number of Cycles
Initial Denaturation	94 °C	5 mins	1
Denaturation and Annealing/Extension	1) 96 °C 2) 52 °C 3) 72 °C	1 min 1 min 1 min	30
Final Extension	72 °C	5 mins	5

2.7.11 Generation of yeast gene knock outs using LoxP marker cassettes

This procedure was taken from Gueldener et al (2002) [209]. For the generation of yeast strains that contained deletions of specific genes, DNA cassettes were created that recombined with specific regions of the genome to replace the genes encoded within that region.

PCR primers were designed to incorporate 19 or 22 nucleotides that are adjacent to the LoxP sequences flanking the marker, as well as 45 5'nucleotides that anneal with sites on the beginning and end of the target gene to be deleted. The newly designed primers are used in a PCR reaction to generate a DNA sequence consisting of a selection marker flanked by the LoxP sites and a sequence corresponding to regions close to the start and end of the ORF of the target gene. Following the completion of the PCR reaction, the disruption DNA cassette was purified using the genomic DNA extraction (Materials and Methods, Section 2.7.3). The purified disruption cassette was transformed into yeast cells (Materials and Methods, Section 2.5.1). The transformation of the disruption cassette leads to a recombination event allowing the selection marker to replace the target gene. This is achieved due to the recombination driven specificity of the 45 nucleotides flanking the selection marker that are specific for the ORF of the target gene. A successful transformation procedure therefore should produce null mutants of the target gene.

2.7.12 Invitrogen Gateway Cloning Reaction

The Invitrogen Gateway© cloning method was used for the generation of plasmids used in this study. The Gateway system is a cloning method based upon the site-specific recombination of the *lambda bacteriophage*. Two types of recombination sites have been engineered to recombine uniquely between the two ends of a source sequence and a host

vector. The sites have been constricted to enable the recombination reaction to be completely reversible using two sets of catalytic proteins. These two reactions are called LR and BP, so named because of the recombination sites involved in each reaction: LR recombines attL and attR sites, BP recombines attB and attP sites. The recombined sites transform by swapping opposite halves into the opposite set, so attL and attR become attB and attP and vice versa. Vectors engineered to contain these sites have been given the names: Entry Clone, Expression Clone, Donor Vector, and Destination Vector.

2.7.13 BP Cloning Reaction

For the generation of the entry vectors used in this study the Invitrogen Gateway BP cloning reaction was performed. The plasmid containing the *RAS2* nucleotide sequence was extracted and purified using a Qiagen Spin Miniprep Kit and sequenced by Source Bioscience. 0.5 µl of the purified plasmid DNA was mixed with 0.5 µl of pDONR221 and 4 µl of TE buffer in a clean PCR tube. The BP clonase II enzyme was thawed on ice for ~ 2 mins and then vortexed for 2 secs. 1 µl of BP clonase II was added to the reaction mixture and incubated at room temperature for 1 hour. To terminate the reaction, 0.5 µl of Proteinase K solution was added to the reaction mixture. The mixture was then vortexed briefly and incubated at 37 °C for 10 mins. Samples were incubated at -20 °C for 24 hours

2.7.14 LR Cloning Reaction

For the generation of the expression clones used in this study, an Invitrogen Gateway LR cloning reaction was used. The LR reaction enables the recombination of the gene of interest contained within an entry clone with a destination vector.

Table 9. LR Cloning reaction

Reagent	Volume/Mass
Entry Clone Plasmid DNA	75 ng/µl
Destination Vector	50 ng/µl
LR Clonase II	0.5 µl
LR Reaction Buffer (5x)	2 µl
TE Buffer pH 8	2.75 µl

The LR reaction mixture listed above was incubated at room temperature for 1 hour. 0.5 µl of proteinase K was added followed by a 10-minute incubation period at 37 °C. All destination vectors used in this study contain ampicillin and chloramphenicol resistance genes. *RAS2* expression clones with a GPD promotor were sequenced with the GPDPro-F primers and the entry clones with M13F.

2.7.15 DNA sequencing

The sequencing of purified plasmid DNA samples was carried out by Source Bioscience Lifesciences, based in Cambridge. The plasmid DNA was sequenced via the Sanger sequencing methodology. Purified by plasmid DNA samples a concentration of 100 ng/µl were sent for sequencing with the associated primers at a concentration of 5 µM. The data from the sequencing reaction was received electronically and analysis of data was carried using ApE- a plasmid editor V.1.17 Copyright © 2003-2008 by M. Wayne Davis.

2.8 Biochemical Methods

2.8.1 Whole cell protein extraction for SDS PAGE

The generation of protein samples required for polyacrylamide gel electrophoresis was achieved using the methodology described in von der Haar et al, (2007) [210]. The concentration of cells in a culture was estimated from the optical density. 2 x 10^8 cells were harvested via centrifugation for 2 mins at 13 000 rpm. For log phase cultures at an OD_{600} of 0.7 this was around 10 ml. If quantitative electrophoretic analysis was required, the number of cells in a culture was counted under a microscope using a haemocytometer. The volume containing a defined number of cells was harvested using the centrifugation procedure as described above.

Harvested cells were resuspended in 200 µl of lysis buffer (0.05 M EDTA, 0.1 M NaOH, 2% w/v SDS, 2% v/v β-mercaptoethanol) and incubated at 90 °C for 10 mins. After incubation, 5 µl of 4 M acetic acid was added and the sample was vortexed for 30 secs before a second 10-minute incubation at 90 °C. 50 µl of loading buffer (50 % glycerol, 0.25 M Tris-HCl pH 6.8, 0.05 % bromophenol blue) was added to the sample. The sample was then centrifuged for 90 secs at 13 000 rpm in a bench microcentrifuge prior to loading.

2.8.2 Polyacrylamide gel electrophoresis

Polyacrylamide gels were prepared using the recipe listed in Materials and Methods, Table 2.8.2. Each gel was composed of a standard 5 % acrylamide stacking gel and a 7.5-12 % resolving gel. SDSPAGE gels were casted in 0.75 mm glass cassettes (Bio-Rad). The resolving layer was poured into the cassette and allowed to set for 20-30 mins and layered with 1 ml of isopropanol to provide an even top layer surface after solidification of the gel. The

isopropanol was discarded, and the stacking gel solution was then poured into the cassette and an appropriately sized comb was inserted. The stacking layer set for 20 mins.

Table 10. SDS-Page reagents

Stacking gel	Resolving gel	SDS running buffer
126 mM Tris pH 8.8 **0.1 % SDS** **12 % acrylamide (29:1)** **0.15 % ammonium persulphate** **0.07 % TEMED**	240 mM Tris pH 6.8 0.1 % SDS 4.3 % acrylamide (29.1) 0.23 % ammonium persulphate 0.07 % TEMED	0.3 % (w/v) Tris-HCL 1.44 % (w/v) glycine 0.15 % (w/v) SDS

Polyacrylamide gels were mixed in sterile 50 ml falcon tubes. Ammonium persulfate was freshly dissolved in water at 10% (w/v).

After the final incubation period the comb and gasket were carefully removed, and the cassette was inserted into a gel tank and sealed against the central column. 1x TGS was then added to the gel tank and wells were submerged in TGS buffer. A protein standard (ColorPlus marker p7709S, New England Biolabs) was loaded into the first well of each gel. Protein samples in loading buffer were then loaded into subsequent wells. The electrodes were connected to a BioRad power pack and a voltage of 90 V was applied until the protein front entered the resolving layer, at this point the voltage was increased to 130 V. Once the protein front had migrated through the acrylamide gel to ensure sufficient separation, the voltage was stopped. Careful notice was taken to ensure the protein front did not run off the gel. The gel tank was disconnected from the power pack and the cassettes removed. The gels used in this process were either used for staining with Coomassie blue, or the western blot protocol described in Materials and Methods, Section 2.8.5.

2.8.3 Coomassie staining of SDS-PAGE gels

SDS-PAGE gels were visualised following a 20-minute shaking incubation phase at room temperature with Coomassie brilliant blue stain (40 % (v/v) Methanol, 20 % (v/v) Glacial acetic acid, 0.1 % Coomassie brilliant blue R250), followed by a 20-minute shaking incubation phase with de-stain solution (10 % (v/v) methanol, 10 % (v/v) Acetic acid). Gels were then submerged overnight in sterile water, shaking at room temperature.

2.8.4 Semi-dry transfer of proteins to PVDF membranes

Proteins were separated via molecular mass by SDS-PAGE. The polyacrylamide gel containing the protein samples was removed from the cassette and the stacking layer was discarded. The resolving gel was removed from the cassette and placed in transfer buffer (0.0058 % w/v Tris base, 0.0029 % w/v glycine, 0.00004 % w/v SDS, 20 % v/v methanol). Four pieces of Whatman blotting paper (Thermo Fisher) was cut into 8x9 cm pieces and soaked in transfer buffer. PVDF western blotting membrane (Thermo Fisher) was wet thoroughly in methanol (Thermo Fisher) and then placed in transfer buffer to 10 mins. Two pieces of blotting paper was placed on the anode plate of a Trans-Blot Semi-Dry Transfer cell (BioRad), followed by the PVDF membrane, the polyacrylamide gel, and the final two pieces of blotting paper. To ensure that there were no significant air bubbles present between layers, a roller was used to roll out any excess air. The cathode plate was place on top and the apparatus was connected to a power pack. A voltage of 25 V was applied for 30 mins. Upon completion of the semi-dry transfer the PVDF membrane was removed for use in the immunoblotting procedure as detailed in Materials and Methods, Section 2.8.5.

2.8.5 Immunoblotting procedure

Following the completion of the semi-dry transfer protocol, the PVDF membrane was placed in 6 ml of blocking solution (5 % w/v Dried Skimmed Milk (Oxoid) and PBS/T (Phosphate Buffered Saline and 0.2 % Tween 20 [Sigma]) and incubated with shaking for 1 hour at room temperature. The membrane was briefly washed twice with PBS/T and placed in a 50 ml falcon tube with 6-12 ml of blocking solution containing the appropriate concentration of primary antibody, for details on primary antibodies used see Materials and Methods, Section 2.8.8. A 1-hour incubation with shaking at room temperature followed. The PVDF was carefully removed from the 50 ml falcon tube and rinsed briefly with PBS/T. The membrane was then incubated with PBS/T and washed via shaking for 15 mins, followed by another two 15 min washes, replacing the PBST/T each time. After the completion of the wash phases, the PVDF membrane was placed in a fresh 50 ml falcon tube containing 6-12 ml of blocking solution containing an appropriate concentration of secondary antibody conjugated to Horse-Radish Peroxidase, for details on secondary antibodies used see Materials and Methods, Section 2.8.8**.** A 30-minute incubation period with shaking at room temperature followed. The PVDF membrane was then washed with PBS/T as previously undertaken after the primary antibody straining. The membrane was then placed in PBS.

2.8.6 ECL detection (Enhanced Chemiluminescence)

The PVDF membrane was placed in a clean polyethylene terephthalate box and the ECL solutions, listed in the table below, were mixed in a 1:1 ration. The PBS used to incubate the PVDF membrane was discarded and the ECL solution was added and incubated for 1 min with constant shaking. The ECL solution was discarded and the membrane was removed and

placed in a Sharon wrap. The membrane was placed into the SYNGENE G: BOX gel doc system and blots were visualised.

The GeneSys Software (Version 1.6.5.0) was used to analyse blots and a Synoptics 6MP camera was used to capture images. To calculate the Ras2p band intensity relative to the Pgk1p loading control, ImageJ version 1.51n was used. Here the integrated intensity of the Ras2p band was calculated and divided by the integrated intensity of the Pgk1p band and normalised to the control strain.

Table 11. Recipes for ECL solutions

Name	Recipe
Solution 1	1 ml luminol 250 mM (3-aminophthalhydrazide from FLUKA No. 09253 0.44 ml p-coumaric acid 90 mM (Sigma No C9008) 10 ml 1 M Tris.HCL (pH 8.5) Water to 100 ml
Solution 2	64 µl 30% hydrogen peroxide 10 ml 1 M Tris.HCL (pH 8.5) Water to 100 ml

2.8.7 Stripping of PVDF membrane

Following the completion of an ECL detection on a PVDF membrane, a loading control was required to ensure an even loading of protein to the gel. Here previously bound antibodies were required to be removed from the PVDF to allow for re-probing with a new antibody. The Restore Western Blot Stripping Buffer (ThermoScientific) solution and protocol was used. The PVDF membrane was carefully removed from the 50 ml falcon tube and rinsed briefly with PBS/T. The membrane was then incubated with PBS/T and washed via shaking for 15 mins, followed by another two 15 min washes replacing the PBST/T each time. After the completion of the wash phases, the PVDF was immersed in 10 ml of stripping buffer and incubated for 30

mins at room temperature with shaking. The stripping buffer was discarded and the PVDF membrane was washed with PBS/T as previously undertaken before addition of stripping buffer. Following the completion of the stripping protocol, the PVDF membrane was placed in 6 ml of blocking solution (5 % w/v Dried Skimmed Milk (Oxoid) and PBS/T (Phosphate Buffered Saline and 0.2 % Tween 20 [Sigma]) and incubated with shaking for 1 hour at room temperature before probing with a fresh primary antibody.

2.8.8 Antibodies used in study

Antibodies were used to perform western blot analysis. The antibodies used within this study are listed below.

Primary antibody used for Ras2p detection: Goat anti-Ras2 polyclonal IgG was purchased from Santa Cruz Biotechnology (Santa Cruz Biotechnology, Inc**.** Bergheimer Str. 89-2, 69115 Heidelberg, Germany) and was used at a dilution of 1/1000.

Secondary antibody for Ras2p detection: Anti-sheep IgG HRP (Sigma, catalogue number A3415) and was used at a dilution of 1/5000.

Primary antibody used for detection Pgk1p: Rabbit anti-Pgk1p (Supplied by Professor Mick Tuite a 1:10 000 dilution and was used as the loading control.

Secondary antibody used for detection Pgk1p: Anti-rabbit (Supplied by Professor Mick Tuite) a 1:500 dilution was used as the following loading control.

Primary antibody used for GFP detection: Mouse anti-GFP (Sigma, catalogue number 1181446000) used at a dilution of 1/1000.

Secondary antibody used for Porin and GFP detection: Anti-Mouse IgG HRP (Sigma, catalogue number #A4416) and was used at a dilution 1/5000.

2.9 Cell biology techniques

2.9.1 Absorbance assays for growth rate analysis of S. cerevisiae cells

A sterile inoculation loop was used to pick a fresh colony of yeast. The colony was inoculated into 5 ml of appropriate medium and grown overnight at 30 °C with shaking at 200 rpm. The optical density of the overnight culture was calculated by absorbance at OD_{600} using an Eppendorf Biophotometer plus. Cultures were diluted to an OD_{600} of 0.1 in 1 ml of the appropriate fresh medium in a sterile 24-well plate (Greiner). Alternatively, cultures were diluted to an OD_{600} of 0.1 in 500 µl of the appropriate fresh medium in a sterile 48-well plate (Greiner). Growth was measured using a BMG LABTECH FLUOstar OPTIMA or a BMG LABTECH SPECTROstar Nano plate reader.

Table 12. The protocol setting used to measure growth rate

Cycle Time	**1800 seconds**
Flashes Per Well	3
Excitation	600 nm
Shaking Frequency	400 nm
Shaking Mode	Double Orbital
Additional Shaking Time	30 Seconds before each cycle
Temperature	30 °C
Positioning Delay	0.5 seconds

For the analysis and processing of the data generated by the plate reader, the BMG LABTECH MARS data analysis software was used. The data processed in this software was then

exported to Microsoft Excel for further analysis. Each growth curve assay displayed in this thesis is the sum of three biological repeats, each of which includes three technical repeats.

Doubling times for each strain were determined by separately plotting sequential 2-hour data sets individually, each overlapping by 30 minutes, with time in hours or mins (x-axis) against the OD_{600} (y-axis) using Microsoft Excel 2010. For each 2-hour plot, an exponential trend line equation was generated, y= c*e^(b*x), which is equivalent to ln(y) = ln(c) + b*x, for which b represents the slope and ln(c) represents the y-axis intercept. The 2 hour plot with the highest x value (which represents the slope) in the exponential line equation was selected, and that x-value was used to generate the doubling time (hours) using the formula LN (2)/x.

2.9.2 Cell counting using a haemocytometer

To perform cells counts, a haemocytometer was used. An overnight culture was diluted 1/25 and log phase cultures were enumerated without dilution. A 50 µL aliquot of culture was loaded onto the haemocytometer and counted under a light microscope using the 100x magnification. When counting budding yeast cells, cells with a bud size greater than one third the size of the mother cell were counted as two cells, if not, buds were not included in the cell count. Only cells existing within, or on the bottom or left-hand line of the box were counted. A minimum of 300 cells were counted when possible.

2.9.3 Viability assay

A sterile inoculation loop was used to pick a fresh colony of yeast. The colony was inoculated into 5 ml of appropriate medium and grown overnight at 30 °C with shaking at 200 rpm. The cell density of the overnight culture was measured using an Eppendorf Biophometer plus. Cells were diluted to an OD_{600} of 0.1 in 5 ml of the appropriate fresh media. Cells were

incubated at 30 °C shaking at 200 rpm for 24 hours. The number of cells in a culture was counted under a microscope using a haemocytometer. Cells were diluted to 2 x 10^3 cells/ml and 150 µl (300 cells) was plated on to the appropriate media. 300 cells from each sample was plated onto an agar plate, which, for 100 % viability, should lead to the growth of 300 colony forming units (CFU). Plates were incubated at 30 °C for 2-4 days before counting to ensure that slow growing strains had sufficient time to grow. The percentage viability was determined by the dividing the number of observed CFU's by the number of expected CFU's and multiplied by 100.

2.9.4 Di/Tri-peptide supplementation viability assay

A sterile inoculation loop was used to pick a fresh colony of yeast. The colony was inoculated into 5 ml of appropriate medium and grown overnight at 30 °C with shaking at 200 rpm. The cell density of the overnight culture was measured using an Eppendorf Biophometer plus. Cells were diluted to an OD_{600} of 0.1 in 5 ml of the appropriate fresh media. Cells were incubated at 30 °C shaking at 200 rpm for 24 hours. The number of cells in a culture was counted under a microscope using a haemocytometer. Cells were diluted to 2 x 10^3 cells/ml and 300 cells were plated onto either SD-URA or SD –URA with the addition of a specific di-peptide at a 1 mM concentration. The di-peptides used in this study; Leucine-Leucine (Sigma), Alanine-Leucine (Sigma), Tyrosine-Alanine (Sigma) or Histadine-Leucine (Sigma). Alternatively, cells were plated on media containing a mix of all the di-peptides listed above, added together at a 1 mM concentration. Plates were incubated at 30 °C for 2-4 days before counting to ensure that slow growing strains had sufficient time to grow. The percentage viability was determined by the dividing the number of observed CFU's by the number of expected CFU's and multiplied by 100.

2.9.5 Hydrogen Peroxide Sensitivity Assay

A sterile inoculation loop was used to pick a fresh colony of yeast. The colony was inoculated into 5 ml of appropriate medium and grown overnight at 30 °C with shaking at 200 rpm. The cell density of the overnight culture was measured using an Eppendorf Biophotometer plus. Overnight cultures were then diluted to OD_{600} 0.1 in 1 ml of the appropriate media. Cells were diluted to 1 x 10^7 cells/ml and were diluted 1000-fold over three serial dilutions. Each 1000-fold dilution of the sample was plated onto four different agar plates differing in concentration of hydrogen peroxide (H_20_2). A 3 % percent working stock of hydrogen peroxide (v/v) was made from a 30 % hydrogen peroxide stock solution (v/v). From this stock, 1 mM, 2 mM, 3 mM, and 4 mM concentrations of hydrogen peroxide was added to 40 ml of agar media. Plates were dried and then incubated at 30 °C and checked after 48 and 72 hours. Following incubation, visual analysis was performed to observe the differences in growth. Images were taken on a scanner (CANOscan 4000), 48 hours after plating.

2.9.6 Copper Sensitivity Assay

A sterile inoculation loop was used to pick a fresh colony of yeast. The colony was inoculated into 5 ml of appropriate medium and grown overnight at 30 °C with shaking at 200 rpm. The cell density of the overnight culture was measured using an Eppendorf Biophotometer plus. Overnight cultures were then diluted to OD_{600} 0.1 in 1 ml of the appropriate media. Cells were diluted to 1 x 10^7 cells/ml and were diluted 1000-fold over three serial dilutions. Each 1000-fold dilution of the sample was plated onto four different agar plates differing in concentration of $CuS0_4$. A 100 mM working stock of $CuS0_4$ was made. From this stock, 1 mM, 1.5 mM, 2 mM and 3 mM concentrations of $CuS0_4$ was added to 40 ml of agar media. Plates were dried and then incubated at 30 °C and checked after 48 and 72 hours. Following

incubation, visual analysis was performed to observe the differences in growth. Images were taken on a scanner (CANOscan 4000), 48 hours after plating.

2.9.7 GFP-ATG8 autophagy assay

A sterile inoculation loop was used to pick a fresh colony of yeast. The colony was inoculated into 5 ml of appropriate medium and grown overnight at 30 °C with shaking at 200 rpm. The cell density of the overnight culture was measured using an Eppendorf Biophometer plus. Cells were diluted to an OD_{600} of 0.1 in 5 ml of the appropriate fresh media. Cells were incubated at 30 °C shaking at 200 rpm for 24 hours. Following this, 1ml of culture was transferred to the nitrogen starvation media (Materials and Methods, Section 2.1.4) lacking ammonium sulphate to induce autophagy via nitrogen starvation and incubated at 30 °C with 200 rpm shaking for 6 hours. Total protein was extracted from cells pre- and post-induction of autophagy and subjected to western blotting (Materials and Methods, Section 2.8.5).

2.9.8 Chronological Ageing Assay

A sterile inoculation loop was used to pick a fresh colony of yeast. The colony was inoculated into 5 ml of appropriate medium and grown overnight at 30 °C with shaking at 200 rpm. The cell density of the overnight culture was measured using an Eppendorf Biophotometer plus. The overnight cultures were sub-cultured to a calculated OD_{600} of 0.1 in 10 ml of appropriate medium in 100 ml conical flasks. Samples were incubated at 30 °C with shaking at 200 rpm. After 24 hours of incubation, an aliquot of the culture was taken to calculate the colony forming units (Materials and Methods, Section 2.9.9) and for flow cytometry analysis to measure levels of propidium iodide (Materials and Methods, Section 2.9.12) and dihydroethidium fluorescence (Materials and Methods, Section 2.9.11). Once the aliquot of culture was taken, samples were immediately returned to the incubator to minimise sample

exposure time outside of the incubation parameters. Aliquots of cells were taken from the same culture sequentially at 24-hour intervals for 6 days and colony forming unit counts and flow cytometry analysis were undertaken. The final measurement was taken after 12 days of sample incubation.

2.9.9 Clonogenic Survival Assay of wild type cells overexpressing $RAS2^{S225A}$, $RAS2^{S225E}$ or a plasmid control

An aliquot of 10 µl of suspended cells was taken from the original culture and diluted in 990 µl of sterile water. The diluted sample was further diluted by a 1/100 dilution in PBS. The sample was then inserted into a CASY cell counter (Scharfe Systems) and the number of cells in a culture was calculated. Serial dilutions were performed to ensure that 300 cells of each sample were plated onto each agar plate, which, for 100 % viability, should lead to the growth of 300 colony forming units (CFU). Plates were incubated at 30 °C for 48 hours before counting to ensure that slow growing strains had sufficient time to grow. The percentage viability was determined by the dividing the number of observed CFU's by the number of expected CFU's and multiplied by 100.

2.9.10 Flow Cytometry

To detect the presence of fluorescence within yeast cells a BD FACSCalibur flow cytometer was used, and the BD FACStation data management system was used for acquisition and data analysis of samples. The system uses an air-cooled argon-ion laser exciting fluorophore. The FACS counted and analysed 10,000 cells per sample and the flow rate was set to ~60 µl/min. ~ 2 x 10^6 cells were diluted in 1 ml of 1 M PBS for FACS analysis.

2.9.11Flow cytometry to monitor DHE fluorescence to detect superoxide radicals

The dihydroethidium (DHE) dye (Invitrogen D23107) was used for the detection of superoxide radicals. The blue fluorescent DHE dye is oxidised by superoxide radicals to the red fluorescent form, hydroxyethidium. The 585 nm band pass filter (FL-2) placed in the light path before detection was used for red light detection. Approximately 2 x 106 cells were re-suspended in PBS containing 10µM DHE and incubated for 10-15 mins before FACS analysis.

2.9.12 Flow cytometry to detect Propidium Iodide uptake to assess necrosis

To check for the presence of necrotic cells in a population, 4 µl of propidium iodide was added 30 secs before being placed into the FACS. Propidium iodide (PI) accumulates in cells when the plasma membrane is compromised and intercalates into nucleic acids. PI can therefor only penetrate necrotic cells and is excluded by viable cells that have an intact plasma membrane. When PI is bound to nucleic acids, the fluorescent excitation maximum is 35 nm and the emission maximum is 617 nm. Propidium iodide (PI) binds to DNA by intercalating between the bases, with little or no sequence preference, and with a stoichiometry of one dye per 4–5 base pairs of DNAs. PI also binds to RNA, necessitating treatment with nucleases to distinguish between RNA and DNA staining. Once the dye is bound to nucleic acids, its fluorescence is enhanced 20- to 30-fold, the fluorescence excitation maximum is shifted ~30–40 nm to the red, and this is relatively low, PI exhibits a sufficiently large Stokes shift to allow simultaneous detection of nuclear DNA. A baseline was set using an unlabelled control.

2.10 Fluorescence Microscopy of yeast cells

2.10.1 Fluorescence Microscopy

For the visualisation of fluorescent cells, an Olympus 1X81 inverted microscope was used. The light source was provided by a Cool LED pE4000 illumination system. All images were captured using an Andor's Zyla 4.2 PLUS sCMOS camera. The acquisition software used to obtain images was Micro-Manger, version 1.4.22. A single drop of Olympus Immoil-F30CC immersion oil was applied to the surface of the cover slip and an Olympus 60 x objective lens (NA = 1.35) was used to locate cells within a sample. An Olympus 100 x objective lens (NA = 1.4) was used to visualize individual cells. Cells with GFP-tagged proteins were observable using the GFP channel with excitation/emission wavelengths of 488/512 nm. DIC images were acquired using a halogen light source with identical settings to GFP imaging. To ensure images were representative of the whole population each microscopy experiment was repeated in triplicate. For the analysis and processing of images the ImageJ FIJI software was used. The counting of cells for phenotype characterisation was conducted by eye from images generated from fluorescent microscopy.

2.10.2 Sample Preparation

A sterile inoculation loop was used to pick a fresh colony of yeast. The colony was inoculated into 5 ml of appropriate low fluorescence selective medium and grown overnight at 30 °C with shaking at 200 rpm. The optical density of the overnight culture was measured using an Eppendorf Biophotometer plus. For stationary phase microscopy analysis, overnight cultures were diluted to an OD_{600} of 0.1 in 5 ml of fresh media and grown for 24 hours. For the analysis of cells in logarithmic phase of cell growth, cells were sub-cultured and grown to OD_{600} 0.7. A 3 µl aliquot of the culture was placed on a microscope slide and covered with a 20 mm by 20

mm cover slip. A single drop of Olympus Immoil-F30CC immersion oil was added to the cover slip and examination under the microscope was carried out.

2.11 High Resolution Respirometry

The Oroboros O2K Oxygraph High Resolution Respirometer was used to determine the consumption of 0_2 from mitochondria in cell suspensions. The Datlab 4 software was used for the analysis and acquisition of data generated by the respirometer. The respirometer contained two chambers, each of which was maintained at 30 °C and held 2 ml of cells suspended in media without glucose. To calibrate the instrument, the medium from which the cells were grown in was used. An overnight liquid culture was diluted to a calculated OD_{600} of 0.1 and cells were analysed at 24 hours post inoculation. To ensure that an equal volume of cells was present in each chamber, cells were counted using a haemocytometer. A 1/80 dilution was performed, and a full haemocytometer grid of cells was counted to calculate the number of yeast cells present in 1 ml of culture. The samples were diluted to a cell density of 10^6 cells/ml into 3 ml of appropriate media. 2.5 ml of each diluted culture was inserted into one of the two chambers to ensure each chamber was full. The chamber stoppers were inserted into position and any residual liquid culture was aspirated away. The exact cell concentration was then entered into the Datlab4 software for an accurate oxygen flux/cell reading.

For the analysis of cells mitochondria, a series of drugs were introduced into the chamber using specifically engineered syringes, which target individual components of the electron transport chain. The following drugs: Triethiltyn bromide (TET) (Sigma-Aldrich), carbonylcyanidep-trifluoromethoxyphenylhydrazone (FCCP) (Fluka), and Antimycin A (AntA) (Sigma-Aldrich) were in added to each sample chamber. The sequence of drug addition was

as follows; a 0.2 mM final concentration TET was added to each chamber (8 µl from a 50 mM stock solution in DMSO), followed by 0.012 mM FCCP (2 µl of a 12 mM stock in ethanol) and finally 0.002 mM AntA (2 µl of a 2 mM stock solution in ethanol). To facilitate the detection of a full respiratory drug response, a 5-minute interval was left between the additions of each drug.

Chapter 3

Yeast as a model organism to study the effects of *RAS2*, *RAS2*^{S225A} or *RAS2*^{S225} overexpression

3.1 Introduction

Ras proteins are small GTPases that act as molecular switches within cells that link extracellular stimuli to intracellular effectors. Ras proteins play a conserved role in the control of both cell growth and proliferation [211]. As a result, mutations that induce the constitutive activation of Ras proteins are often associated with changes in cell behaviour that can lead to disease, such as human cancer [41]. The localisation of Ras proteins are reported to be predominantly to the inner cytoplasmic surface of the plasma membrane, but they can also be observed on endomembrane's, such as the endoplasmic reticulum, and the mitochondrial outer membrane [65][57][212].

In recent years, the localisation and signalling of Ras on the plasma membrane has been extensively studied. It has been shown that Ras undergoes a series of posttranslational modifications that dictate its subcellular localisation. Firstly, farnesylation of the cysteine on the C-terminal CAAX motif targets Ras to the cytosolic surface of the ER where the AAX is proteolytically cleaved and the c- terminus methylated [51][53]. In the majority of Ras proteins cysteine residues close to the CAAX motif are palmitoylated, facilitating the translocation of Ras from the ER to the plasma membrane [60]. Evidence exists to suggest that Ras proteins can undergo phosphorylation events which regulate its activity. Whistler and Rine identified Ser^{412} as an important phosphorylation site on the yeast Ras2 protein where substitution of serine with alanine at this residue lead to increased cAMP levels and elevated ration of Ras2-GTP compared to total Ras2 [74][213]. Surprisingly, the phosphorylation of Ras2p in *S. cerevisiae* has not been studied regarding its regulation of intracellular localisation, despite significant evidence existing linking Ras phosphorylation to its localisation in humans. For example, the phosphorylation by PKC of the $Serine^{181}$ residue

within K-Ras, promotes rapid dissociation of K-Ras from the inner leaflet of plasma membrane to other intracellular membranes, including the outer membrane of mitochondria [77] .

While phosphorylation is an important posttranslational modification, little is known on its effect on Ras2 protein activation and localisation. This study aims to further investigate whether Ras2p phosphorylation provides a mechanism that regulates Ras2p trafficking inside the cell.

In the laboratory of Dr Campbell Gourlay, previous investigations using data obtained from the PhosphoPep version 2.0 project www.phosphopep.org/index.php, produced experimental information regarding putative Ras2 phosphorylation sites that are affected by the deletion of *SSN3* and *SIT4* respectively. Interestingly, the phosphorylation sites that were predicted to be affected upon the deletion of either *SSN3* or *SIT4* were found to be identical and focussed upon the serine residue at position 225 of Ras2p. We therefor sought to investigate whether modification of Serine^{225} lead to any changes in Ras2 protein localisation or activity within the cell and whether this was accompanied by any phenotypes in cells expressing either *RAS2*^{S225A} or *RAS2*^{S225E}.

Figure 13. Sequence alignment of the yeast Ras2 and Ras1.

Interestingly, an independent group identified the Ser^{226} residue in Ras1 to be an important residue for Ras1 phosphorylation, as mutating this residue to an alanine drastically diminishes the level of Ras1 phosphorylation [214]. Upon sequence alignment of yeast Ras1 and Ras2 *(Figure 13)* we show little sequence similarity outside of the GTPase domain. However, the serine site position in both Ras1 and Ras2 is similar suggesting that serine residues located around this position may play a conserved regulatory role within Ras proteins.

3.2 Construction of the *RAS2* mutant alleles- site-directed mutagenesis substitution of the putative Ras2p phosphorylation site $Serine^{225}$ by Alanine or Glutamate

To investigate whether $Serine^{225}$ phosphorylation is important for the localisation of Ras2p, growth and viability a site directed mutagenesis approach was adopted. The wild type *RAS2* gene was mutated at $Serine^{225}$ where the serine was either substituted with alanine to produce a non-phosphoryatable residue or glutamate to produce phosphomimetic residue. Site-directed mutagenesis was previously undertaken by Eman Badr of the Gourlay Lab to replace $Serine^{225}$ in the Ras2p with alanine or glutamate in the gateway donor vector PDON221. To confirm the correct introduction of the necessary mutations, samples were sent off for DNA Sequencing as described in Materials and Methods, Section 2.7.15. Expression vectors were generated from the donor vector by use of the gateway LR clonase reaction as described in Materials and Methods**,** Section 2.7.14. N-terminal tagged GFP vectors for the expression of GFP-Ras2p, GFP-$Ras2p^{S225A}$ and GFP-$Ras2p^{S225E}$ were generated to investigate fluorescently tagged protein localisation. Vectors expressing untagged *RAS2, $RAS2^{S225A}$* and *$RAS2^{S225E}$* were also generated to investigate growth and viability of cells expressing these constructs.

3.3 Expression of *RAS2*, *RAS2^{S225A}* and *RAS2^{S225E}* alleles in *S. cerevisiae*

The levels of wild type and mutant Ras2p were determined by western blot analysis as described in Materials and Methods, Section 2.8. To examine whether the expression of the Ras2p changed during different phases of cell growth, samples were prepared from log and stationary cultures. To ensure uniform protein loading, the levels of 3-PhosphoGlycerate Kinase, Pgk1p, in each strain were examined as a control. After probing for the Pgk1p, the membrane was stained with coomassie brilliant blue as a further control for protein loading. To calculate the Ras2p band intensity relative to the Pgk1p loading control, ImageJ version 1.51n was used. Here the integrated intensity of the Ras2p band was calculated and divided by the integrated intensity of the Pgk1p band and normalised to the control strain.

Firstly, the levels of wild type and mutant Ras2p were analysed in a wild type background. As expected, exponentially growing cells expressing either the wild type or *RAS2* mutant alleles presented an increase in Ras2p expression when compared to the wild type control *(Figure 14/15)*. An increase in Ras2p expression was observed in cells overexpressing *RAS2^{S225A}* or *RAS2^{S225E}* when compared to the *RAS2* overexpression strain *(Figure 14/15)*. Furthermore, in cells overexpressing *RAS2^{S225A}* or *RAS2^{S225E}* an increase in protein degradation products was observed when compared to the wild type control and cells overexpressing *RAS2 (Figure 14)*.

As cells reached stationary phase of cell growth, 24 hours after inoculation, the levels of Ras2p in all overexpression strains were increased when compared to the wild type control *(Figure 16/17)*. An increase in Ras2p expression was observed in wild type cells overexpressing *RAS2^{S225A}* or *RAS2^{S225E}* when compared to the *RAS2* overexpression strain *(Figure 16/17)*. No significant difference in Ras2p degradation products was observed between wild type cells overexpressing *RAS2*, *RAS2^{S225A}* or *RAS2^{S225E} (Figure 16)*.

RAS2, *RAS2*^{S225A}, *RAS2*^{S225E} or an empty plasmid were expressed in a Δ*ras2* strain to examine the affects that the mutants of *RAS2* have on the levels of Ras2p produced in the absence of endogenous Ras2p. No Ras2p signal was detected in a Δ*ras2* strain expressing the empty plasmid backbone control, confirming the deletion of *RAS2* in this background *(Figure 18)*. No significant difference in the levels of Ras2p in strains were observed in cells overexpressing *RAS2*^{S225A} or *RAS2*^{S225E} when compared to the *RAS2* overexpression strain *(Figure 18/19)*.

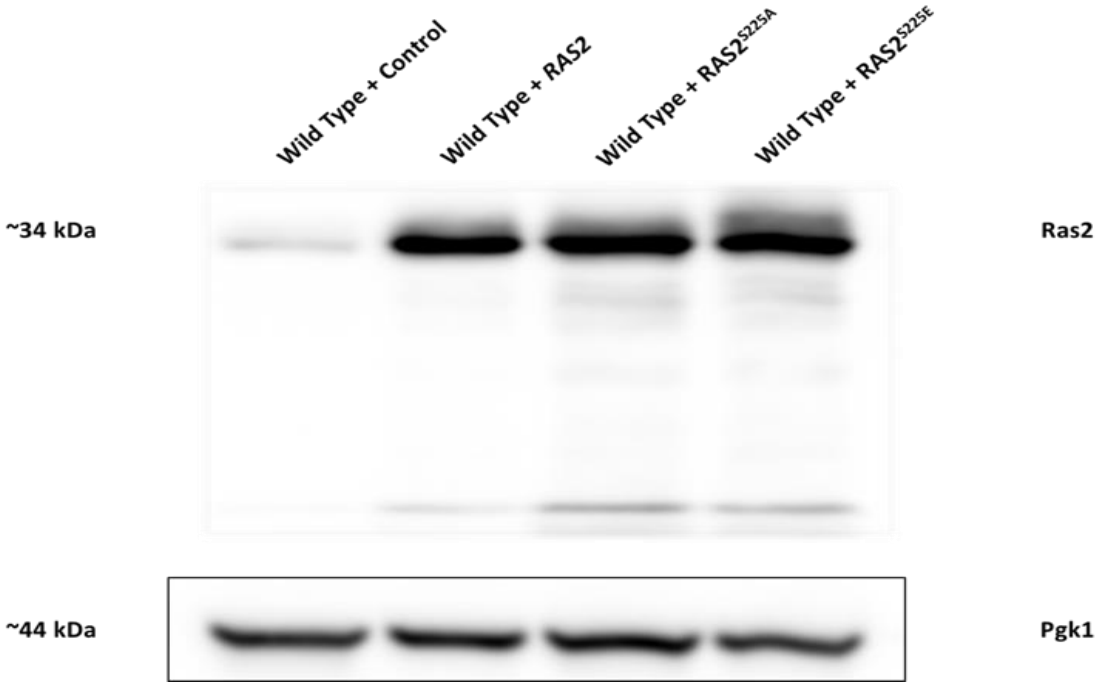

Figure 14. A western blot showing the detection of Ras2p in cells overexpressing RAS2, RAS2^{S225A}, RAS2^{S225E} or an empty plasmid control in a wild type background.
Cells were grown in SD –URA media and sampled during exponential phase of cell growth. To ensure uniform protein loading, the levels of Pgk1p were detected after probing for Ras2p. This experiment was repeated three times and a representative data set is shown.

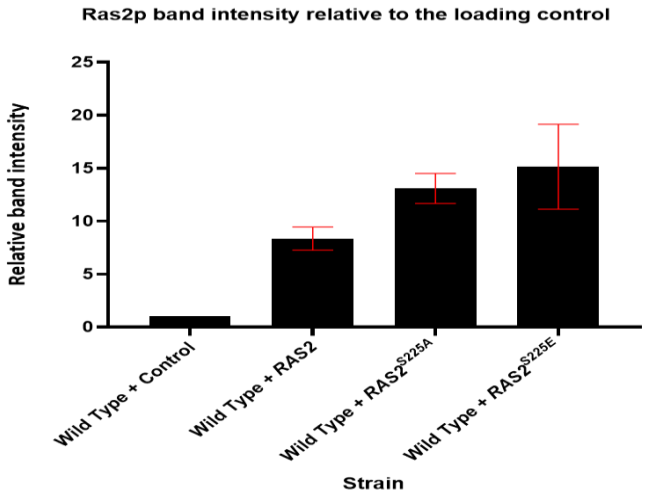

Figure 15. A bar chart representing the change in Ras2p band intensity relative to the Pgkp loading control of wild type cells overexpressing RAS2, RAS2^{S225A}, RAS2^{S225E} or empty plasmid control.

Cells were grown in –URA media and sampled during the exponential phase of growth. The data shown is an average of three biological repeats and the error bars represent the standard deviation.

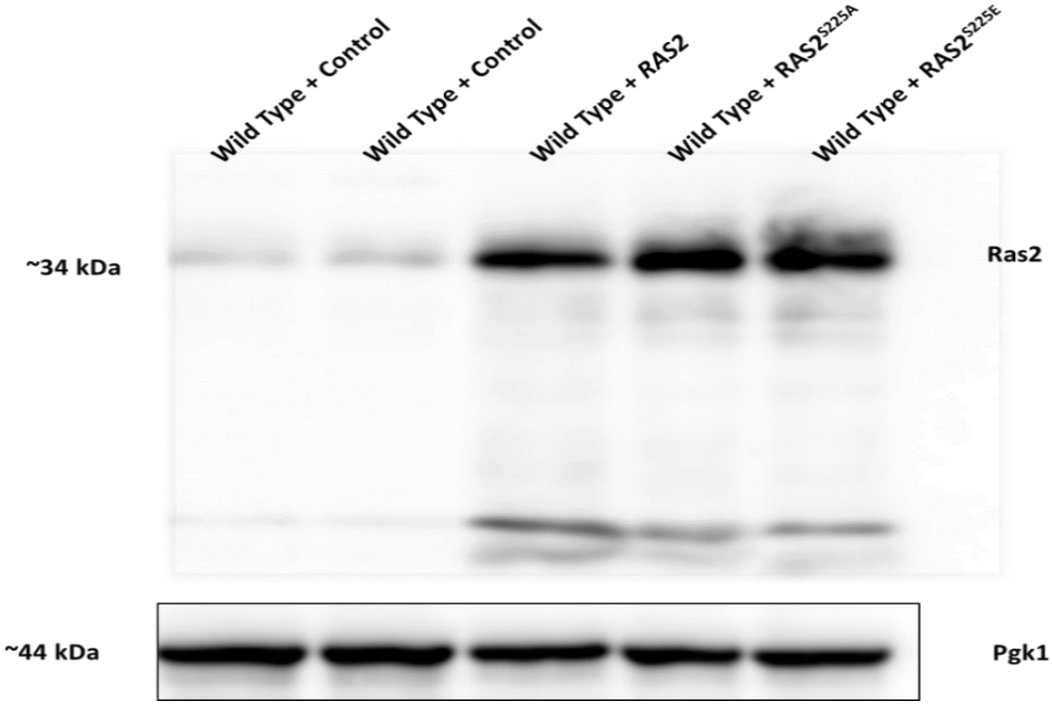

Figure 16. A western blot showing the detection of Ras2p in cells over expressing RAS2, RAS2^{S225A}, RAS2^{S225E} or an empty plasmid control in a wild type background.

Cells were grown in SD –URA media and sampled during stationary phase of growth. To ensure uniform protein loading, the levels of Pgk1p were detected after probing for Ras2p. This experiment was repeated three times and a representative data set is shown.

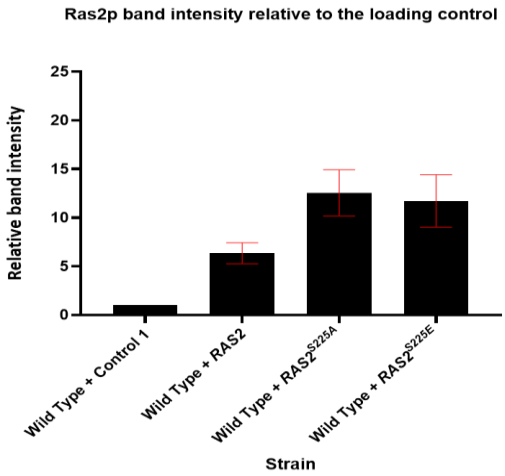

Figure 17. A bar chart representing the change in Ras2p band intensity relative to the Pgkp loading control of wild type cells overexpressing RAS2, RAS2^{S225A}, RAS2^{S225E} or an empty plasmid control.

Cells were grown in –URA media and sampled during stationary phase of growth. The data displayed is an average of three biological repeats and the error represent the standard deviation.

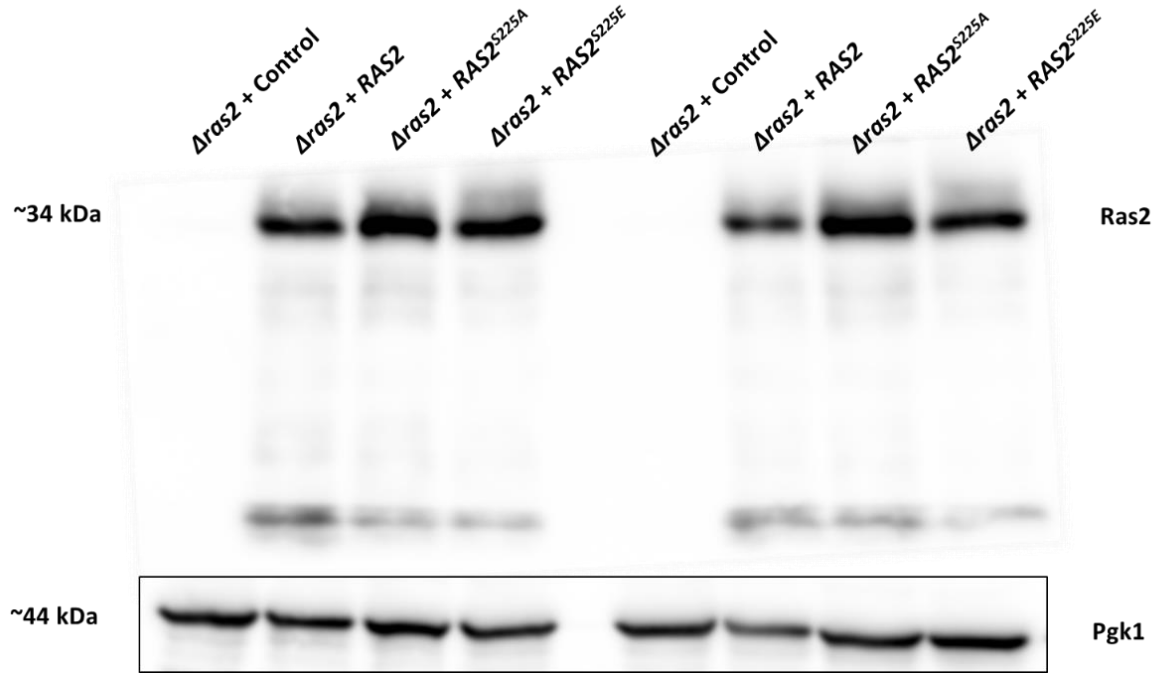

Figure 18. A western blot showing the detection of Ras2p in Δras2 cells over expressing RAS2, RAS2^{S225A}, RAS2^{S225E} or an empty plasmid control.

Cells were grown in SD –URA media and sampled during stationary phase of growth. To ensure uniform protein loading, the levels of Pgk1p were detected after probing for Ras2p. This experiment was repeated three times and a representative data set is shown.

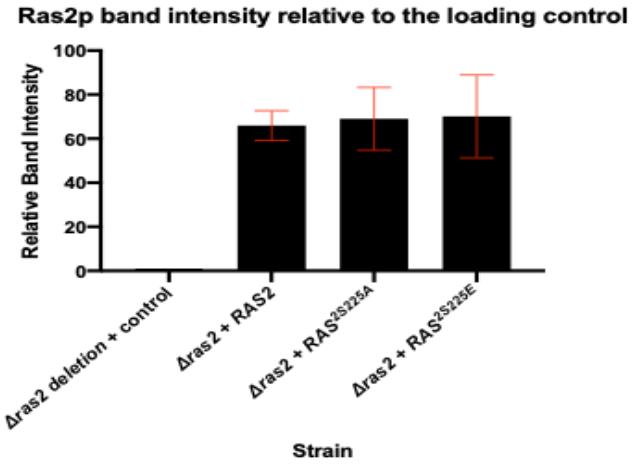

Figure 19. A bar chart representing the change in Ras2p band intensity relative to the Pgkp loading control of Δras2 cells overexpressing RAS2, RAS2^{S225A}, RAS2^{S225E} or an empty plasmid control.

Cells were grown in –URA media and sampled during stationary phase of growth. The data displayed is an average of three biological repeats and the error represent the standard deviation

3.4 Analysis of the effects of phosphorylation of Serine^{225} upon Ras2p localisation

3.4.1 Microscopic analysis of wild type cells expressing GFP-Ras2p, GFP-Ras2p^{S225A} or GFP-Ras2p^{S225E}

We sought to determine the localisation of N-terminally GFP-tagged Ras2p, Ras2p^{S225A} and Ras2p^{S225E} to determine whether disruption of this site of phosphorylation would affect localisation. An N-terminal GFP-tag was preferred over a C-terminal GFP-tag, as a C-terminal GFP-tag will be cleaved during Ras2 protein processing and furthermore interfere with the C-terminal CAAX motif and hinder Ras2p membrane targeting. The localisation of Ras2p was examined upon overexpression of the mutant constructs in both stationary and logarithmic phases of cell growth. Plasmids expressing either GFP-Ras2p, GFP-Ras2p^{S225A} or GFP-Ras2p^{S225E} were transformed into wild type cells and an expression vector containing only the

GFP label was used as a control. During logarithmic phase of cell growth, a widespread/diffused GFP signal was observed in wild type cells overexpressing GFP from the control plasmid. In wild type cells overexpressing either GFP-Ras2p, GFP-Ras2p^{S225A} or GFP-Ras2p^{S225E} a strong plasma membrane localisation of fluorescently labelled Ras2p was seen *(Figure 20)*.

During stationary phase of cell growth wild type cells overexpressing the control plasmid displayed widespread/diffused GFP signal throughout the cytoplasm of the cell *(Figure 20)*. In wild type cells overexpressing either GFP-Ras2p, GFP-Ras2p^{S225A} or GFP-Ras2p^{S225E} a predominant localisation of GFP-Ras2p was observed at the plasma membrane *(Figure 20)*. It was noted that these strains were also seen to localise GFP-Ras2p to intracellular foci which was not observed in the control strain. However, such an observation was noted infrequently. To quantify which was the predominant localisation of GFP-Ras2p, 100 cells for each strain were counted on three separate days and the number of cells displaying either plasma membrane, diffused/widespread and nuclear GFP-Ras2 localisation was calculated and represented as a percentage of the total number of cells counted. In both stationary and logarithmic phases of cell growth, wild type cells expressing the control plasmid displayed no nuclear or plasma membrane localisation of GFP *(Figure 21/22)*. Whereas 70-80 % of wild type cells expressing either GFP-Ras2p, GFP-Ras2p^{S225A} or GFP-Ras2p^{S225E} displayed a predominant localisation at the plasma membrane with a small population of cells displaying a widespread/diffused GFP signal. No Nuclear localisation of GFP-Ras2p, GFP-Ras2p^{S225A} or GFP-Ras2p^{S225E} was observed *(Figure 21/22)*. This data set suggest that GFP-Ras2p localises primarily to the plasma membrane in both log and stationary phase of growth regardless of the phosphorylation state of Serine^{225}.

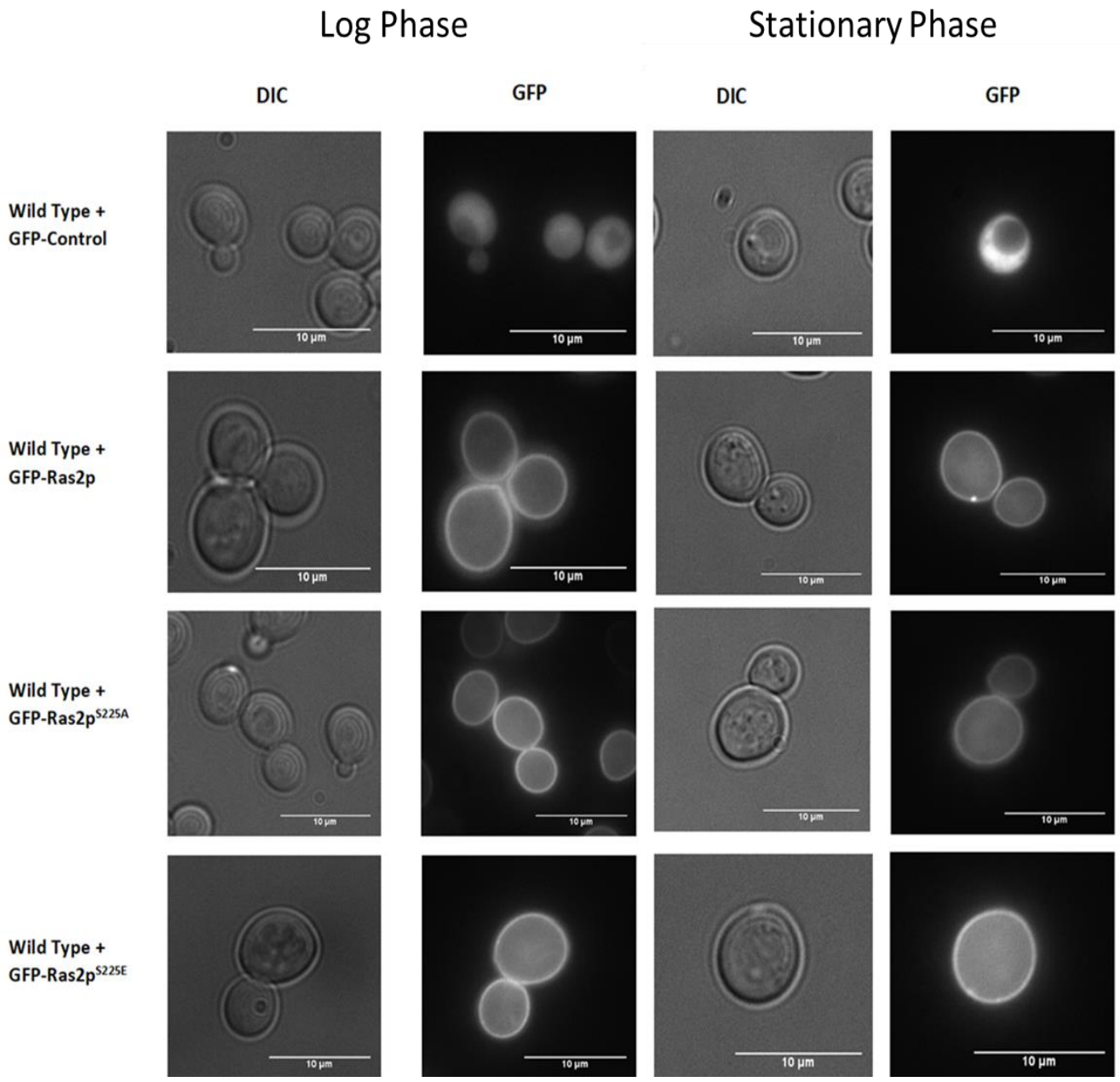

Figure 20. Images taken by fluorescent microscopy of wild type cells overexpressing either GFP-RAS2, GFP-RAS2^{S225A} or GFP-RAS2^{S225E} during logarithmic and stationary phase of cell growth.

The Fluorescent signal represents the presence of Ras2p within cells and a vector containing only the GFP probe was introduced into wild type cells as a control. Cells were cultured in SD – URA growth media. This experiment was repeated three times and a representative data set is shown. Scale bar – 10 µm

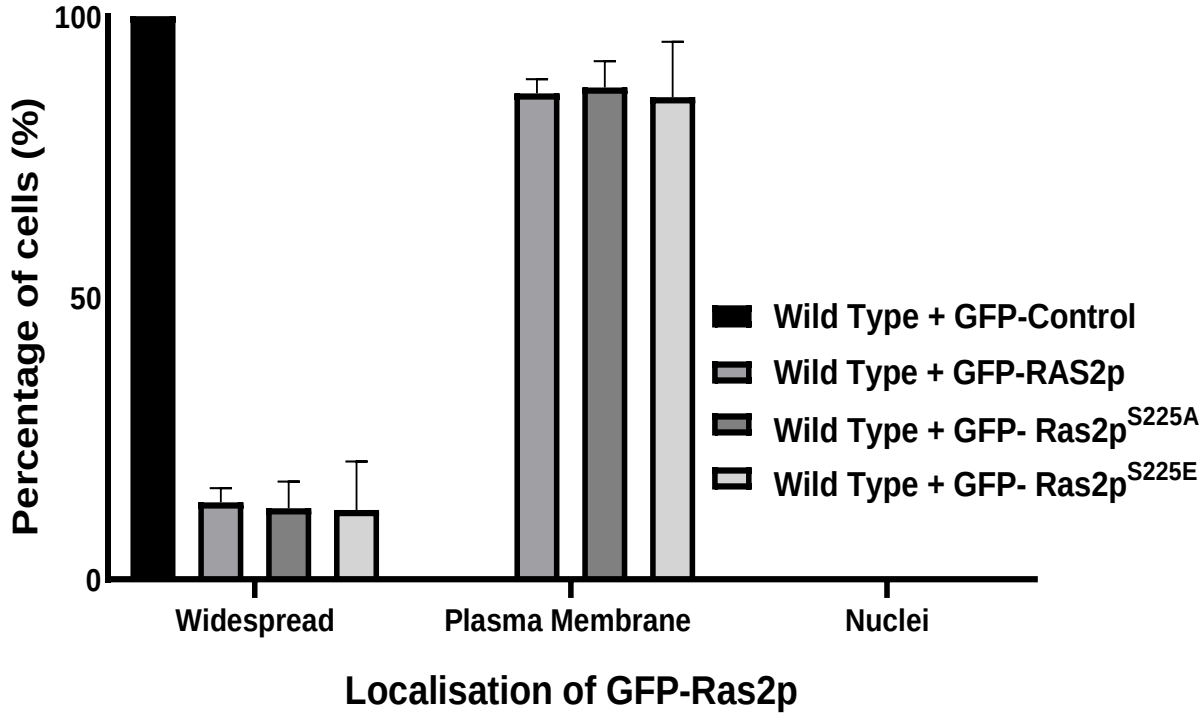

Figure 21. Graphical representation of the localisation of GFP-Ras2p in wild type cells expressing either GFP-RAS2, GFP-RAS2^{S225A} or GFP-RAS2^{S225E} during logarithmic phase of cell growth.

A vector containing only the GFP probe was used as a control. Cells were cultured in SD –URA growth media. To quantify the localisation of GFP-Ras2p, 100 cells for each strain were counted on three separate days with a total 300 cells being counted and the number of cells displaying the different phenotypes observed was calculated and represented as a percentage of the total number of cells counted. The data represents an average of three biological repeats and error bars represents the standard deviation.

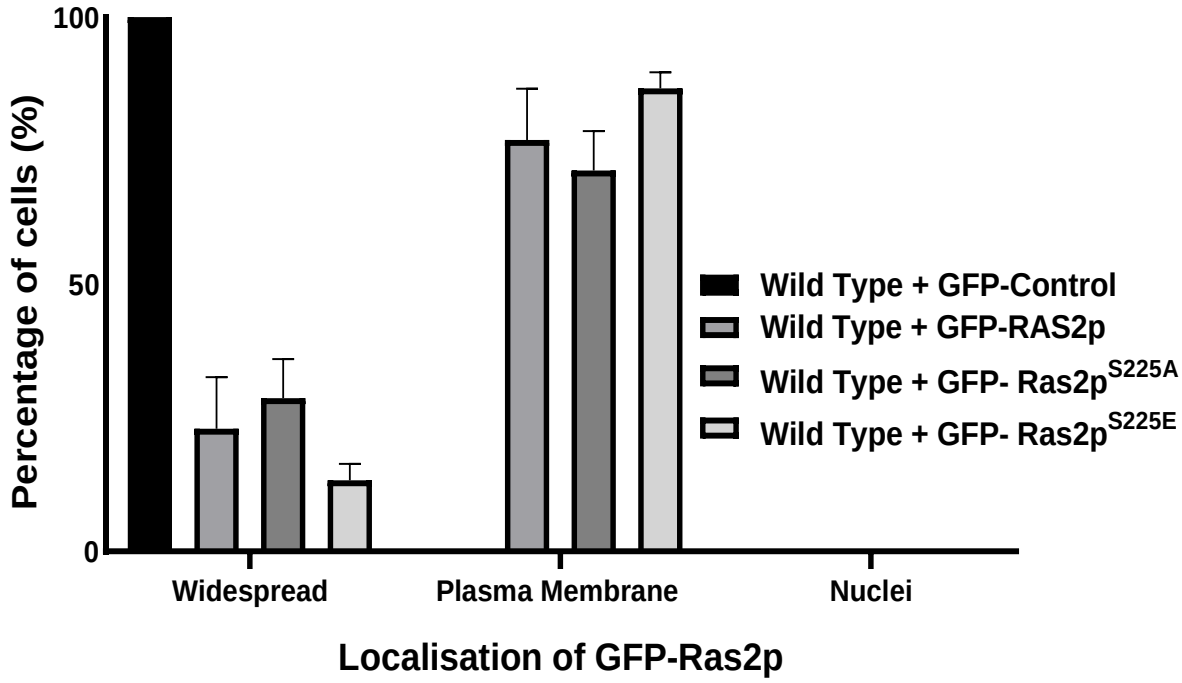

Figure 22. Graphical representation of the localisation of GFP-Ras2p in wild type cells expressing either GFP-RAS2, GFP-RAS2^{S225A} or GFP-RAS2^{S225E} during stationary phase of cell growth.

A vector containing only the GFP probe was used as a control. Cells were cultured in SD –URA growth media. To quantify the localisation of GFP-Ras2p 100 cells for each strain were counted on three separate days with a total 300 cells being counted and the number of cells displaying the different phenotypes observed was calculated and represented as a percentage of the total number of cells counted. The data represents an average of three biological repeats and error bars represents the standard deviation.

3.5 Analysis of the effects of phosphorylation of Serine^{225} upon the activation of Ras

3.5.1 Microscopic analysis of wild type cells expressing Ras2p, Ras2p^{S225A}, Ras2p^{S225E} co-expressed with an GFP-RBD probe

To investigate whether the modification of the Serine^{225} residue of Ras2p influences Ras activity a construct was introduced that expresses the Ras binding domain of human Raf1 fused to GFP [70]. The RBD domain binds to Ras proteins only in their GTP-bound state. The localisation of active-Ras proteins was analysed during the stationary and logarithmic phase

of growth. In these experiments a plasmid overexpressing Ras2p, Ras2p^{S225A} or Ras2p^{S225E} was introduced into wild type cells and their activity assessed by GFP-RBD localisation (*Figure 23*). In wild type actively growing yeast cells, the GFP-RBD signal is predominantly localised at both the plasma membrane and the nucleus as has previously been described [70]. During stationary phase, Ras activity is reduced as cells stop dividing and accordingly the probe was seen as a diffuse signal throughout the cell with a faint signal in the nucleus [70].

Interestingly, during logarithmic phase of growth wild type cells overexpressing either Ras2p^{S225A} or Ras2p^{S225E} showed very little plasma membrane or nuclear localisation of the GFP-RBD signal *(Figure 23/24)*. Instead the GFP-RBD probe was observed to accumulate at the nuclear envelope *(Figure 23/24)*. Such nuclear envelope localisation was never observed in either the control or Ras2p overexpression strains. This provides evidence that the modification of Serine^{225} leads to a change in the localisation of the active population of Ras when compared to the control and Ras2p overexpression strains during logarithmic growth. As the localisation of GTP-bound Ras2p dictates its interaction with its effector proteins and thus downstream signalling pathways, we hypothesize that the change in the localisation of the active Ras population observed in wild type cells overexpressing *RAS2^{S225A}* or *RAS2^{S225E}* may result in significant phenotypic changes when compared to the control and *RAS2* overexpression strains.

During stationary phase of cell growth, wild type cells expressing the control, or Ras2p overexpression plasmid presented an RBD-GFP probe signal that was predominantly seen as a diffused cytoplasmic signal with a faint nuclear signal *(Figure 23/25)*. In a small percentage of cells, we observed the RBD-probe signal manifesting in intracellular foci, which was not observed during logarithmic growth *(Figure 23)*.

Significant differences in RBD-GFP probe localisation was observed in wild type cells overexpressing Ras2p^{S225A} or Ras2p^{S225E} during stationary phase growth *(Figure 23/25)*. In wild type cells overexpressing either Ras2p^{S225A} or Ras2p^{S225E}, we observed nuclear envelope localisation of the RBD-probe, which again was not seen in the control or Ras2p overexpression strain *(Figure 23/25)*. An increase in the number of intracellular foci in these mutants was also observed when compared to the control strain *(Figure 25)*. Here we suggest that the modification of Ras2^{S225} leads to changes in active Ras localisation in both logarithmic and stationary phases of cell growth.

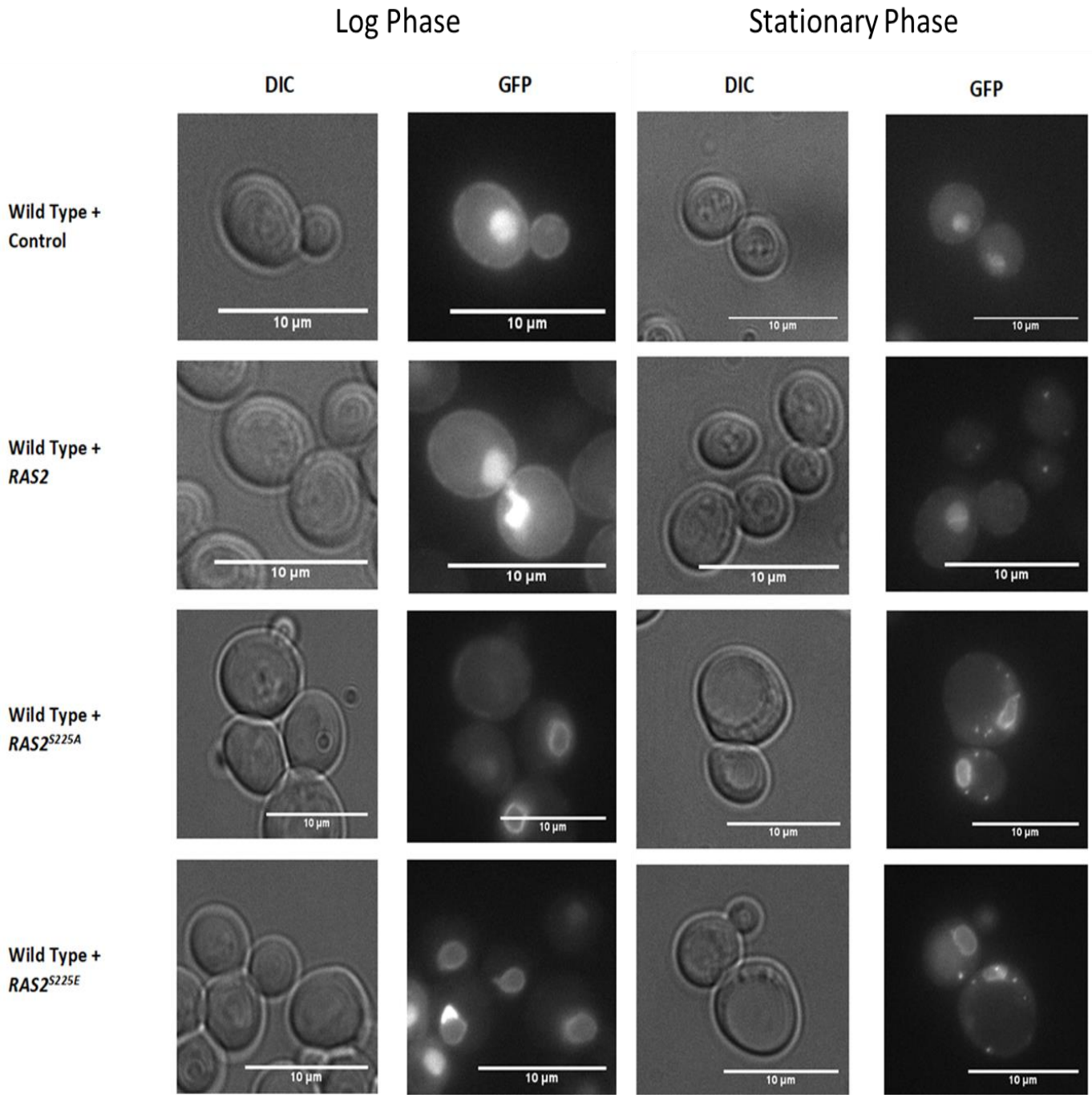

Figure 23. Fluorescence microscopy images of wild type strains overexpressing RAS2, $RAS2^{S225A}$, $RAS2^{S225E}$ or an empty plasmid backbone control using a GFP-RBD probe during logarithmic and stationary phase of growth.

Fluorescence signal represents the presence of active Ras within cells. Cells were cultured in SD –URA/-LEU growth media. This experiment was repeated three times and a representative data set is shown. Scale bar - 10 µm.

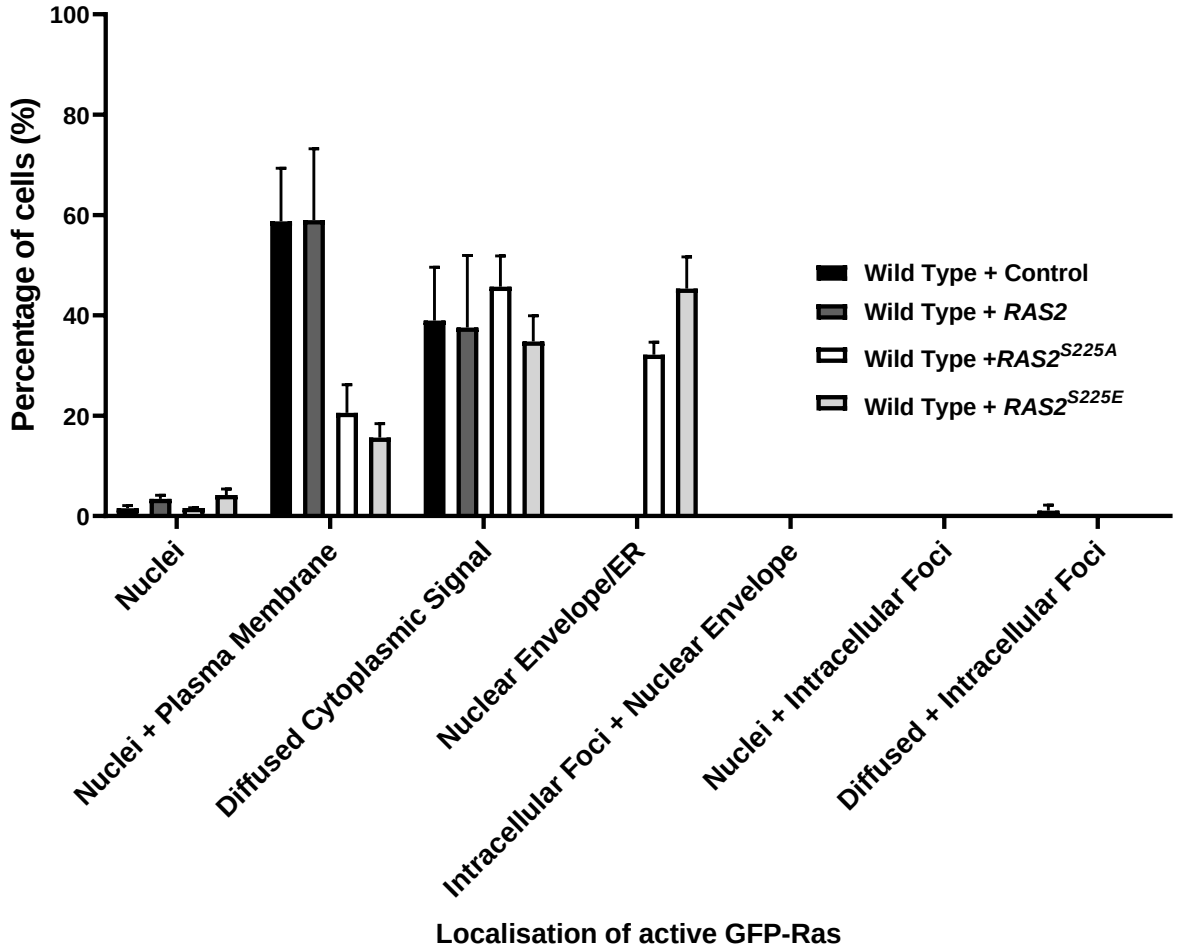

Figure 24. Graphical representation of the localisation of active-Ras in wild type cells expressing either RAS2, RAS2^{S225A}, RAS2^{S225E} or an empty plasmid control during logarithmic phase of cell growth. Cells were cultured in SD –URA/-LEU growth media.

To quantify the localisation of active Ras 100 cells for each strain were counted on three separate days with a total 300 cells being counted and the number of cells displaying the different phenotypes observed was calculated and represented as a percentage of the total number of cells counted. The data represents an average of three biological repeats and error bars represents the standard deviation.

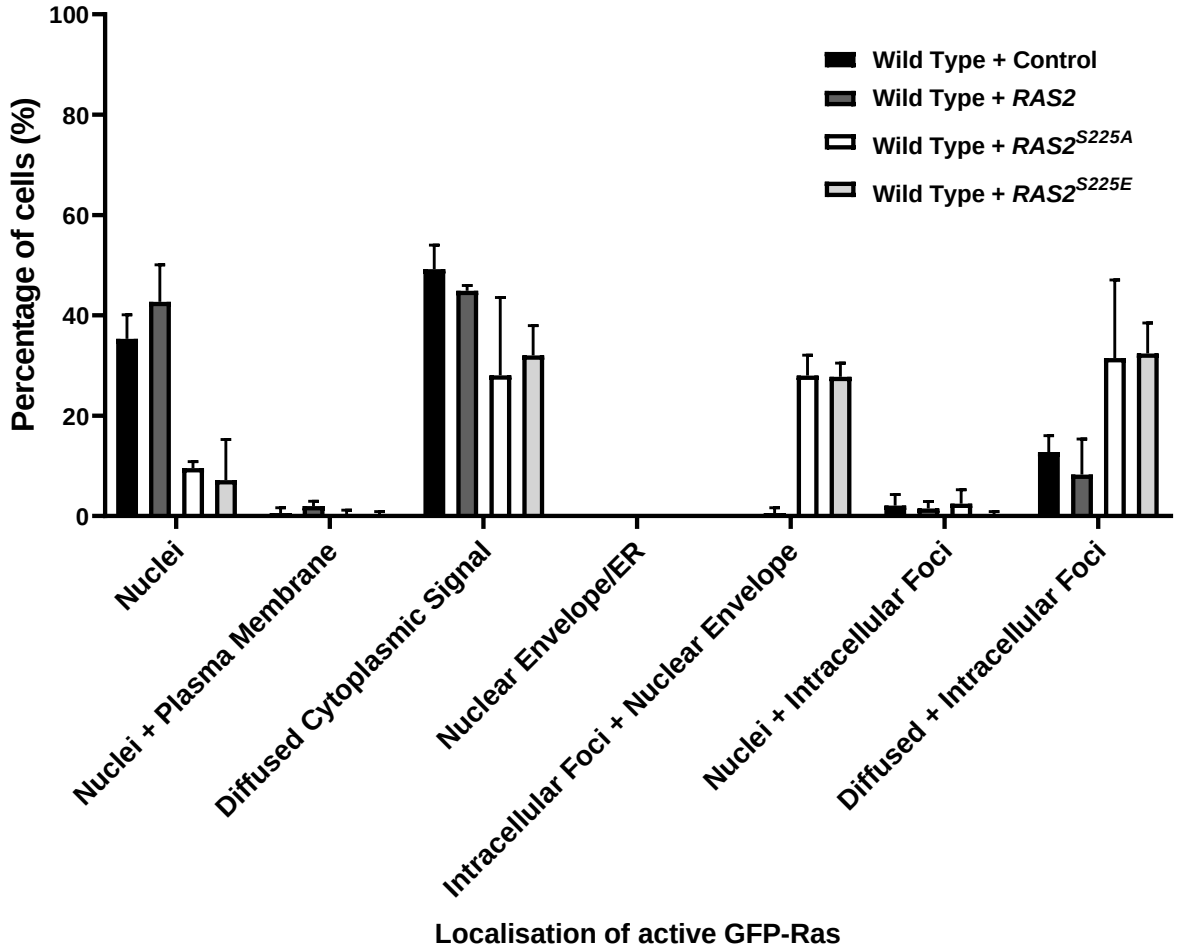

Figure 25. Graphical representation of the localisation of active-RAS in wild type cells expressing either RAS2, RAS2^{S225A}, RAS2^{S225E} or an empty plasmid control during stationary phase of cell growth.

Cells were cultured in SD –URA/-LEU growth media. To quantify the localisation of active Ras 100 cells for each strain were counted on three separate days with a total 300 cells being counted and the number of cells displaying the different phenotypes observed was calculated and represented as a percentage of the total number of cells counted. The data represents an average of three biological repeats and error bars represents the standard deviation.

3.6 Growth analysis of yeast cells overexpressing *RAS2*, *RAS2^{S225A}* or *RAS2^{S225E}*

To investigate the growth of yeast strains that overexpress the yeast *RAS2^{S225A} or RAS2^{S225E}* mutant alleles, growth and viability was compared to wild type cells overexpressing *RAS2* or an empty plasmid backbone control. The growth of *S. cerevisiae* in liquid culture is characterized into four distinct phases: lag, logarithmic (exponential), post-diauxic and stationary phase *(Figure 26)*. Each growth phase reflects the availability of nutrients and the adaption to changes in nutrient levels or exposure to stress.

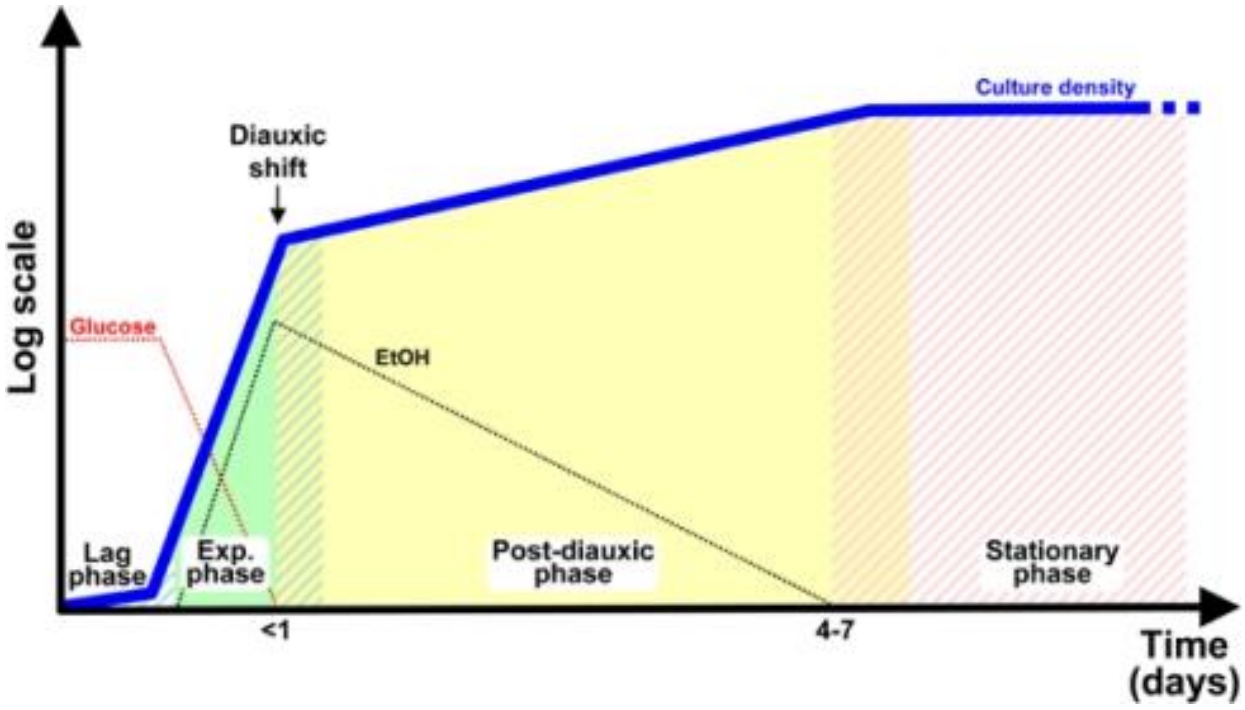

Figure 26. A diagram depicting the growth phases of S. cerevisiae cultivated in rich medium supplemented with glucose.
The optical density (OD) of yeast cells is measured at 600nm. The logarithmic (log) phase of growth represents fermentation of glucose. In log phase the presence of glucose suppresses mitochondrial respiratory function via the mechanism of glucose repression, and cells obtain their energy requirements from fermentative glycolysis resulting in the production of ethanol. The diauxic shift occurs when glucose levels become depleted and cells must shift their metabolism from fermentative growth to respiratory growth, and the aerobic utilisation of ethanol. The post-diauxic phase occurs when cells have fully shifted to respiratory growth and utilise oxidative phosphorylation to support cellular functions. Stationary phase represents a period of minimal growth because of nutrient depletion and high cell density. Solid colours indicate steady states, diagonal stripes transient states.

The lag phase represents the period during in which cells are adapting to new media addition or adaption to the environment and represents a period of minimal growth or time spent in the G_0 phase of the cell cycle. Cells transitioning into the exponential phase of growth represent actively proliferating cells which in our culture conditions cells preferentially use glucose to generate energy by fermentation and suppression of oxidative phosphorylation, the so called Crabtree effect [214].

The diauxic shifts represent a shift from glucose utilisation to the use of ethanol produced during fermentation and marks a period of glucose de-repression and upregulation of mitochondrial biogenesis to support the necessary oxidative phosphorylation. The stationary phase of cell growth represents a commitment to cell cycle exit and accumulation of storage carbohydrates [215]. The limited growth that can be detected during stationary phase requires a functional mitochondrial electron transport chain [215].

3.6.1 Overexpression of *RAS2^{S225A} or RAS2^{S225E} in* yeast cells leads to growth defects

The growth of *S. cerevisiae* can be influenced by several factors such as temperature, pH, and the availability of nutrients. To analyse the growth of yeast strains overexpressing *RAS2*, *RAS2^{S225A}*, *RAS2^{S225E}* or an empty plasmid control, a growth assay was performed as described in Materials and Methods, Section 2.9.1. The growth of both a wild type strain and a *Δras2* strain expressing the *RAS2* mutant alleles were analysed to determine whether the overexpression of either *RAS2^{S225A}* or *RAS2^{S225E}* affects cells in the presence of endogenous Ras2p.

In the presence of endogenous Ras2p the overexpression of either *RAS2*^{S225A} or *RAS2*^{S225E} led to a lower final OD, early transition into the post-diauxic phase of cell growth and extended lag phase when compared to the control strain *(Figure 27)*. Furthermore, In the presence of endogenous Ras2p the overexpression of *RAS2*^{S225A} or *RAS2*^{S225E} led to a decrease in the exponential growth rate when compared to the control strain *(Figure 28)*. The doubling times (growth rates) for a wild type control strain and a wild type strain overexpressing *RAS2* was approximately 180 minutes *(Figure 28)*. Wild type cells expressing either *RAS2*^{S225A} or *RAS2*^{S225E} displayed a significant increase in doubling time to approximately 200 minutes *(Figure 28)*.

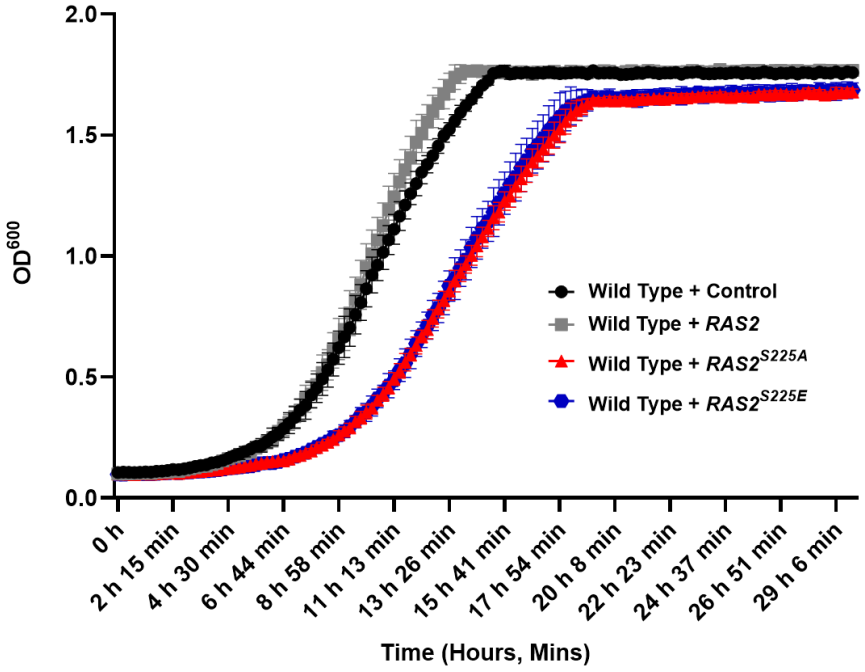

Figure 27. Growth analysis of S. cerevisiae wild type cells overexpressing RAS2, RAS2^{S225A}, RAS2^{S225E} or empty plasmid control.

The growth analysis was carried out in SD –URA media as described in Materials and Methods (Section 2.9.1). This data represents an average of three biological repeats and error bars represent the standard deviation.

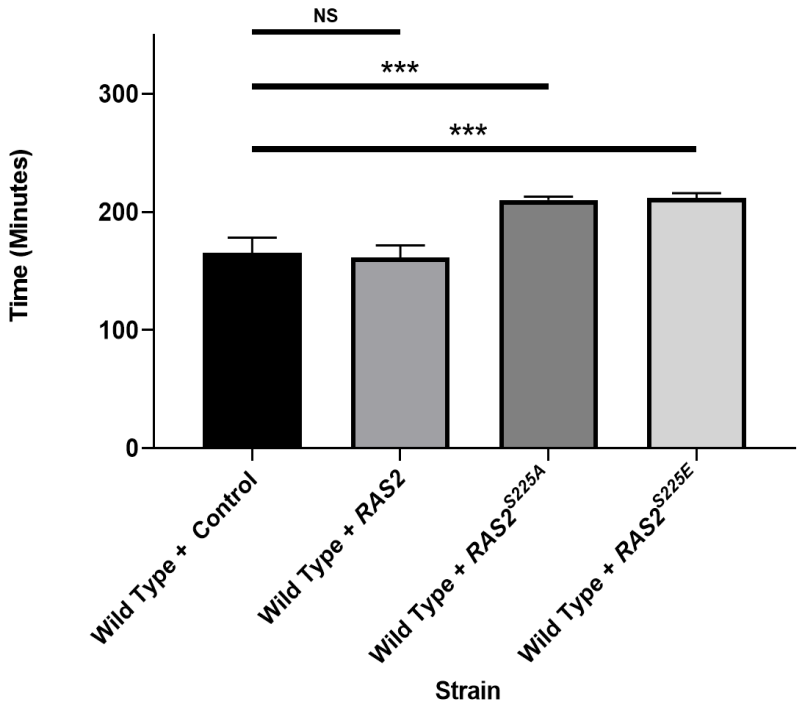

Figure 28. Growth rate analysis of S. cerevisiae wild type cells overexpressing RAS2 or RAS2^{S225A} or RAS2^{S225E}

*The growth rate analysis was carried out as described in Materials and Methods (Section 2.9.1). The data represents an average of three biological repeats and error bars represents the standard deviation. A One-way ANOVA using a Dunnetts multiple comparison test was used to determine statistical significance. Non-significant = NS, * = adjusted p-value ≤ 0.05 and *** = adjusted p value ≤ 0.001.*

The alleles *RAS2*, *RAS2*^{S225A} or *RAS2*^{S225E} were overexpressed in a Δ*ras2* strain to determine whether the expression of these alleles would result in a growth phenotype in the absence of endogenous Ras2p. The overexpression of either *RAS2*^{S225A} or *RAS2*^{S225E} *in a Δras2* background led a lower final OD, early transition into the post-diauxic phase of cell growth and extended lag phase when compared to the control strain *(Figure 29)*. Without the presence of endogenous Ras2p the overexpression of either *RAS2*^{S225A} or *RAS2*^{S225E} led to a decrease in the exponential growth rate when compared to the control strain *(Figure 30)*. The doubling times (growth rates) for a *Δras2* control strain and a *Δras2* strain overexpressing *RAS2* was approximately 180 minutes *(Figure 30)*. No significant difference in growth rate was observed

when *RAS2* or an empty plasmid control was overexpressed in either wild type cells or a *Δras2* background. *Δras2* cells overexpressing either *RAS2*^{S225A} or *RAS2*^{S225E} displayed a significant increase in doubling time when compared to the *Δras2* control and *RAS2* overexpression strain *(Figure 30)*. In wild type cells, the overexpression of either *RAS2*^{S225A} or *RAS2*^{S225E} presented a doubling time of 200 minutes *(Figure 29)*. In a *Δras2* background, the overexpression of *RAS2*^{S225E} presented a doubling time of also 200 minutes with a doubling of 190 minutes observed in the *RAS2*^{S225A} strain *(Figure 30)*. Suggesting that the growth defects caused by the overexpression of *RAS2*^{S225A} or *RAS2*^{S225E} are dominant as defects occur irrespective of whether endogenous Ras2p is present.

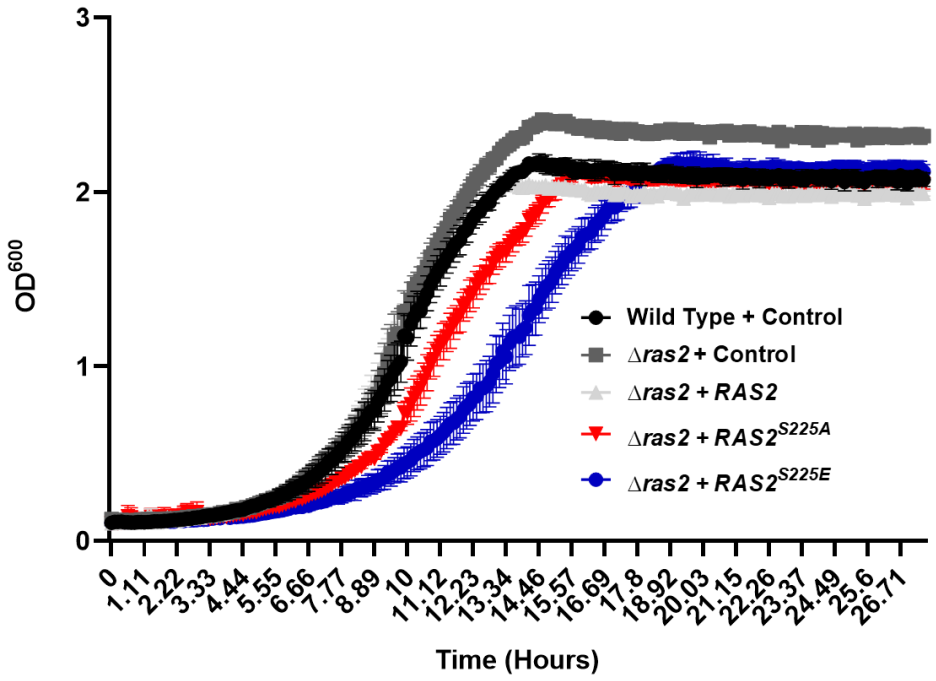

Figure 29. Growth rate analysis of a S. cerevisiae Δras2 strain overexpressing RAS2, RAS2^{S225A}, RAS2^{S225E} or an empty plasmid control.
The growth analysis was carried out in SD –URA media as described in Materials and Methods (Section 2.9.1). The data represents an average of three biological repeats and error bars represents the standard deviation.

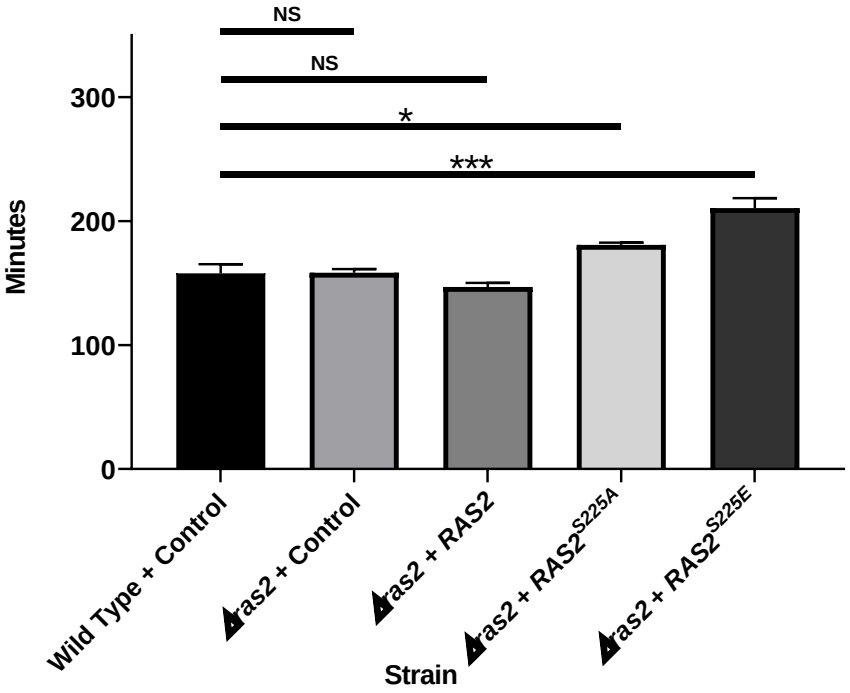

Figure 30. Growth rate analysis of S. cerevisiae Δras2 cells overexpressing RAS2, RAS2^{S225A}, RAS2^{S225E} or an empty plasmid control.

*The growth rate analysis was carried out as described in Materials and Methods (Section 2.9.1). The data represents an average of three biological repeats and error bars represents the standard deviation. A One-way ANOVA using a Tukey multiple comparison test was used to determine statistical significance. Non-significant = NS, * = adjusted p-value ≤ 0.05 and *** = adjusted p value ≤ 0.001.*

3.6.2 Overexpression of either *RAS2^{S225A}* or *RAS2^{S225E}* in yeast cells leads to decreased cell viability

To determine whether the overexpression of either *RAS2^{S225A}* or *RAS2^{S225E}* affects viability in both a wild type and *Δras2* background, a viability assay was conducted. An overnight culture was re-inoculated to 2 x 10^3 cells/ml and incubated for 24 hours. 200 µl (containing 300 cells) was plated onto selective, -URA agar plates. These were left to incubate at 30 °C for 36 hours and the colonies were then counted to allow quantification of colony forming units (CFUs). Viability of cells analysed from the inoculated culture represented the viability of cells, or cell death, during nutrient deprivation. Analysing viability of yeast cells under stresses such as nutrient deprivation can shed light on whether cells are functioning correctly. A stationary phase, after 24 hours of growth, wild type strain expressing a control plasmid, had approximately 40 % viability when grown in SD -URA medium.

The overexpression of *RAS2* in a wild type and *Δras2* background lead to an increase in cell viability when compared to the control strains *(Figure 31)*. In cells overexpressing the empty plasmid control the loss of *ras2* lead to no significant change in viability *(Figure 31)*. The overexpression of either *RAS2^{S225A}* or *RAS2^{S225E}* in both a wild type and *Δras2* background lead to a two-fold reduction in colony forming efficiency when compared to wild type and *Δras2* background control strains *(Figure 31)*. We can conclude that the overexpression of *RAS2*^{S225A} or *RAS2^{S225E}* leads to both perturbed growth and a reduction in viability when compared to the control strains in both a wild type and *Δras2* background.

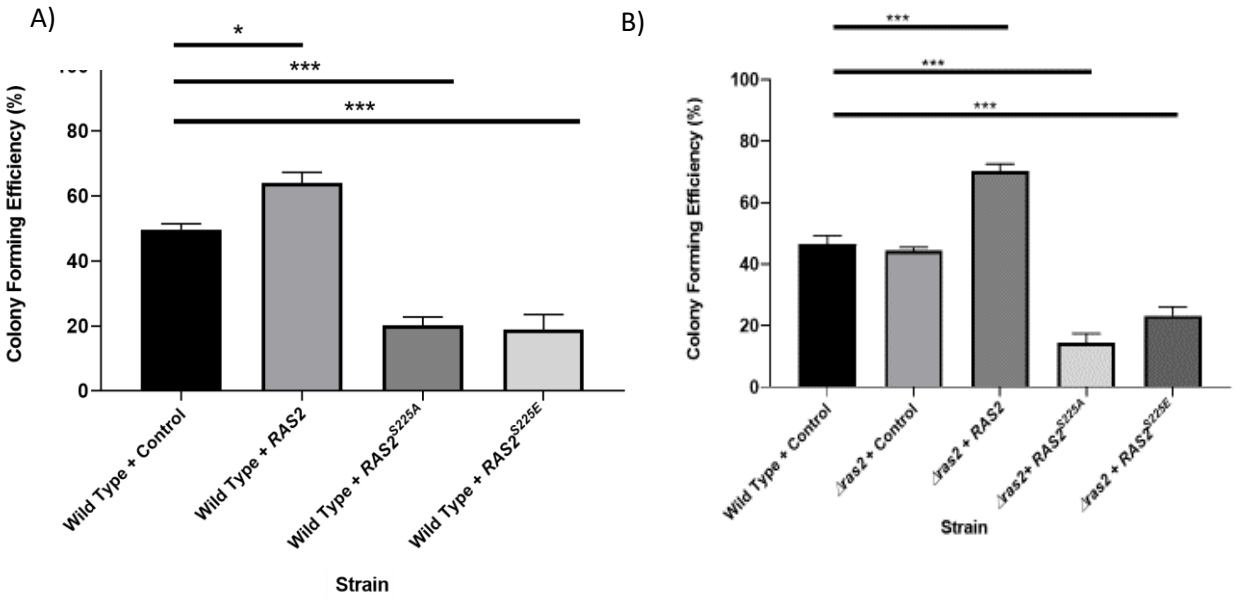

Figure 31. A colony forming efficiency assay of S. cerevisiae wild type or Δras2 cells overexpressing RAS2, RAS2^{S225A}, RAS2^{S225E}or an empty plasmid control grown in SD –URA media

*A) A colony forming efficiency assay of S. cerevisiae wild type cells overexpressing RAS2, RAS2^{S225A}, RAS2^{S225E}or an empty plasmid control grown in SD –URA media. A colony forming efficiency analysis was carried out as described in Materials and Methods (Section 2.9.3). A One-way ANOVA using a Dunnetts multiple comparison test was used to determine statistical significance. Non-significant = NS, * = adjusted p-value ≤ 0.05 and *** = adjusted p value ≤ 0.001. B) A colony forming efficiency assay of S. cerevisiae Δras2 cells overexpressing RAS2, RAS2^{S225A}, RAS2^{S225E}or an empty plasmid control, grown in SD –URA. The colony forming efficiency analysis was carried out as described in Materials and Methods (Section 2.9.3). A One-way ANOVA using a Tukey multiple comparison test was used to determine statistical significance. Non-significant = NS, * = adjusted p-value ≤ 0.05 and *** = adjusted p value ≤ 0.001.*

3.6.3 Overexpression of *RAS2^{S225A}* or *RAS2^{S225E}* in a yeast cells leads to a sensitivity to oxidative stress

Ras activity has been linked to cells ability to adapt to environmental stress [216]. We investigated the effect of oxidative stress on wild type cells expressing *RAS2*, *RAS2^{S225A}*, *RAS2^{S225E}* using a spotting assay as described in Materials and Methods, Section 2.9.5.

On the control plate a reduction in growth was observed in wild type cells overexpressing either *RAS2^{S225A}* or *RAS2^{S225}* when compared to the control strain *(Figure 32)*. This is

concordant with the phenotypes observed in the growth assay *(Figure 27)* and the viability assay *(Figure 31)*. Interestingly, the overexpression of *RAS2* in wild type cells led to an increase in growth when compared to the wild type control in all conditions investigated *(Figure 32)*. As the concentration of hydrogen peroxide increased, the growth of wild type cells overexpressing *RAS2*^{S225A} or *RAS2*^{S225E} decreased when compared to the wild type control and *RAS2* overexpression strains *(Figure 32)*. At a hydrogen peroxide concentration of 3 mM, we observe growth in both the control strain and the *RAS2* overexpression strain, but growth was absent in wild type cells expressing either *RAS2*^{S225A} or *RAS2*^{S225E} *(Figure 32)*. This suggests that the overexpression of either *RAS2*^{S225A} or *RAS2*^{S225E} leads to sensitivity to oxidative stress in wild type cells.

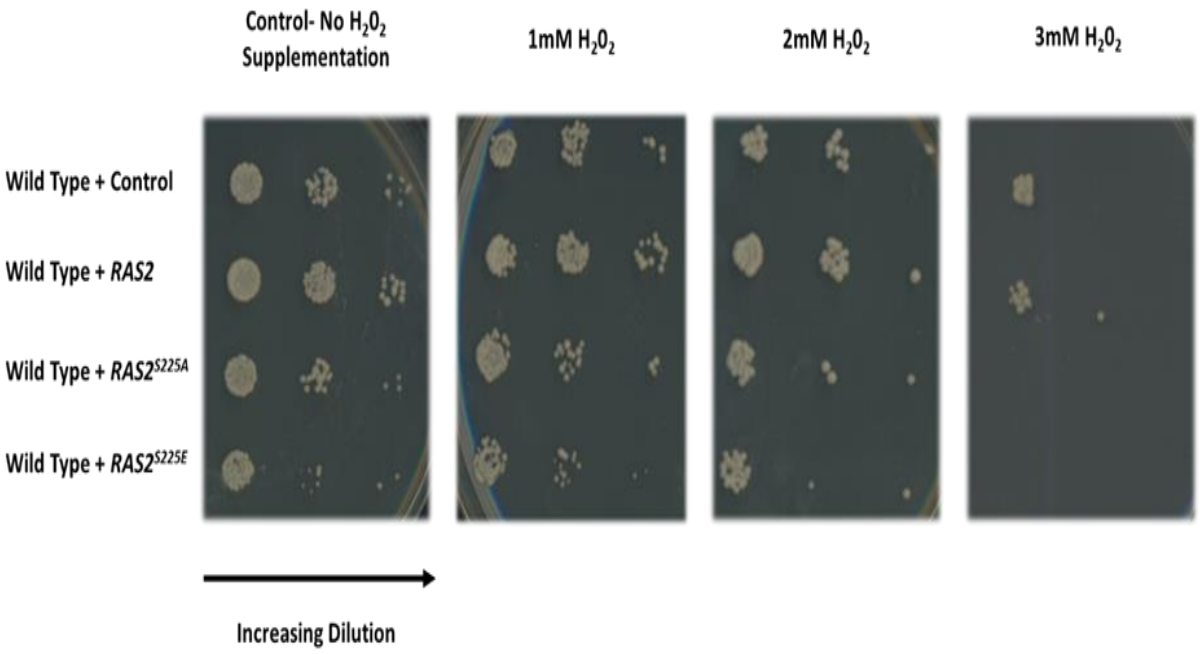

Figure 32. Spotting assay of wild type cells overexpressing RAS2, RAS2^{S225A,} RAS2^{S225E} or an empty plasmid control.
*Cells were serially diluted from 2*10^6/ml to 2*10^3/ml and plated onto SD -URA plates supplemented with increasing concentrations of hydrogen peroxide.*

To investigate whether the overexpression of either *RAS2*^{S225A} or *RAS2*^{S225E} in wild type cells leads to hydrogen peroxide sensitivity in liquid media, growth analysis was conducted when the media was supplement with 2 mM hydrogen peroxide. As previously observed, the expression of *RAS2*^{S225A} or *RAS2*^{S225E} in wild type cells leads to growth defects when grown in SD –URA media *(Figure 31)*. However wild type cells overexpressing either *RAS2*^{S225A} or *RAS2*^{S225E} and grown in 2 mM hydrogen peroxide, presented a further significant increase in lag time and a decrease in final OD reached when compared to cells expressing *RAS2*^{S225A} or *RAS2*^{S225E} grown without the presence of hydrogen peroxide *(Figure 33)*. Upon addition of hydrogen peroxide, we also observed a significant increase in doubling time when compared to wild type cells expressing *RAS2*^{S225A} or *RAS2*^{S225E} grown without the supplementation of hydrogen peroxide to the media *(Figure 34)*.

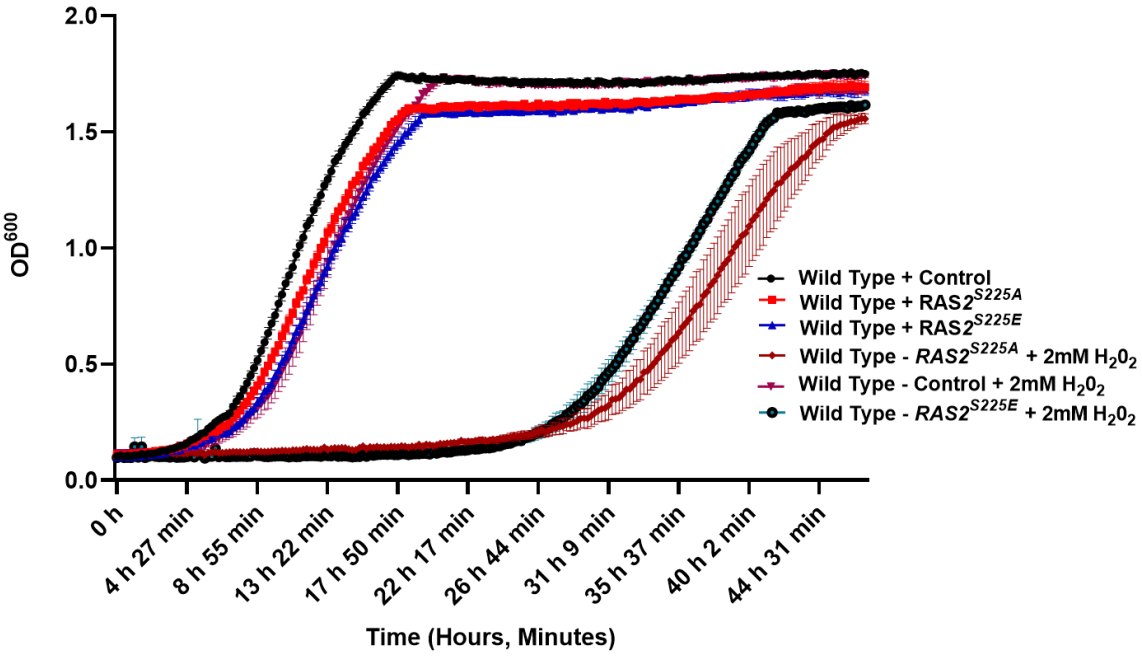

Figure 33. Growth analysis of S. cerevisiae wild type cells overexpressing RAS2, RAS2^{S225A}, RAS2^{S225E} or an empty plasmid control.

A growth analysis of wild type cells overexpressing RAS2, RAS2^{S225A}, RAS2^{S225E} or an empty plasmid control was carried out in SD –URA or SD-URA + 2mM H_2O_2 media as described in Materials and Methods (Section 2.9.1). This data represents an average of three biological repeats and error bars represent the standard deviation.

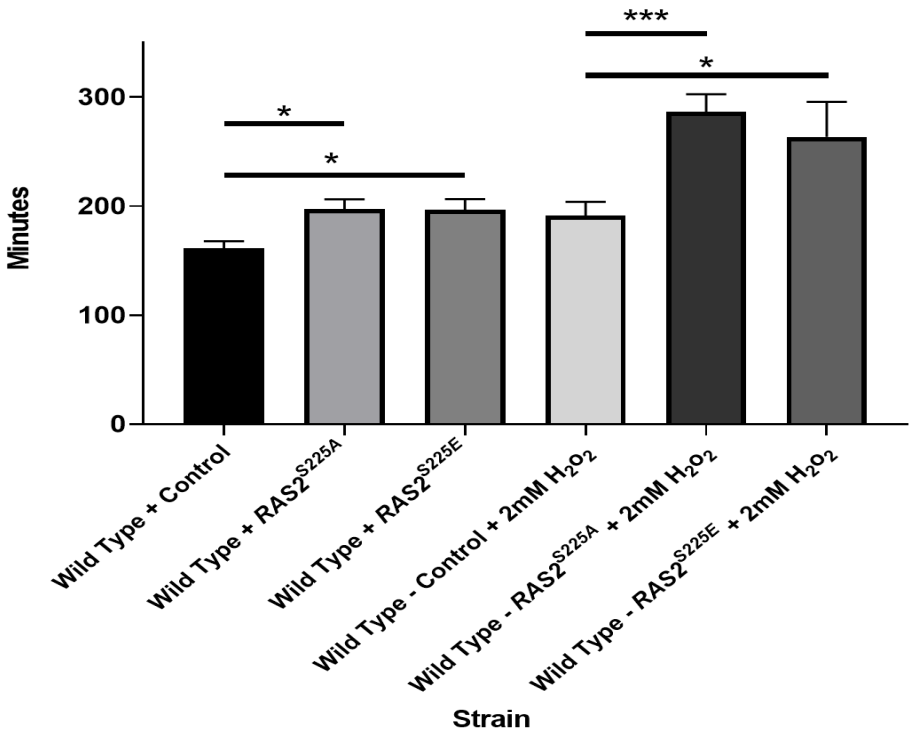

Figure 34. Growth rate analysis of wild type cells overexpressing RAS2, RAS2^{S225A}, RAS2^{S225E} or an empty plasmid control.

*A growth rate analysis of wild type cells overexpressing RAS2, RAS2^{S225A}, RAS2^{S225E} or an empty plasmid control grown in either SD –URA or SD –URA+ 2mM H_2O_2 was carried out as described in Materials and Methods (Section 2.9.1). The data represents an average of three biological repeats and error bars represents the standard deviation. A One-way ANOVA using a Tukey multiple comparison test was used to determine statistical significance. Non-significant = NS, * = adjusted p-value ≤ 0.05 and *** = adjusted p value ≤ 0.001.*

3.6.4 Overexpression of *RAS2^{S225A}* or *RAS2^{S225E}* in yeast cells leads to copper sensitivity

We have previously shown that the overexpression of either *RAS2^{S225A}* or *RAS2^{S225E}* in wild type cells leads to oxidative stress sensitivity. We sought to investigate whether the overexpression of either *RAS2^{S225A}* or *RAS2^{S225E}* in wild type cells resulted in other environmental stress sensitivities, such as heavy metal ion stress. Here we supplemented copper sulphate ($CuS0_4$) at varying concentrations to the growth media and investigated the effect of heavy metal ion stress on the growth of wild type cells overexpressing *RAS2*,

RAS2^{S225A}, *RAS2*^{S225E} or an empty plasmid control using a spotting assay as described in Materials and Methods, Section 2.9.6.

On the control plate a reduction in growth was observed in wild type cells overexpressing either *RAS2*^{S225A} or *RAS2*^{S225} when compared to the control strain *(Figure 35)*. As the concentration of $CuS0_4$ increased, the growth of wild type cells overexpressing *RAS2*^{S225A} or *RAS2*^{S225E} decreased when compared to the wild type control and *RAS2* overexpression strains *(Figure 35)*. At a $CuS0_4$ concentration of 3 mM, we observe growth in both the control strain and the *RAS2* overexpression strain, but no growth was observed in wild type cells expressing either *RAS2*^{S225A} or *RAS2*^{S225E} *(Figure 35)*. This suggests that the overexpression of either *RAS2*^{S225A} or *RAS2*^{S225E} leads to sensitivity to $CuS0_4$ in wild type cells.

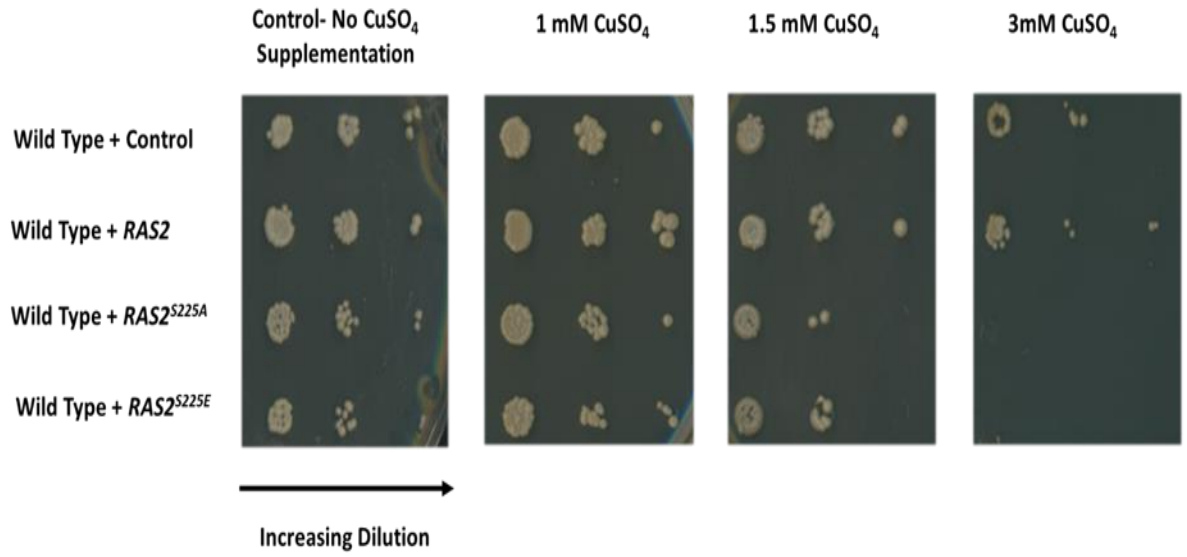

Figure 35. Spotting assay of wild type cells overexpressing RAS2, RAS2^{S225A,} RAS2^{S225E} or an empty plasmid control.
*Cells were serially diluted from 2*10^6/ml to 2*10^3/ml and plated onto SD -URA plates supplemented with increasing concentrations of copper sulphate. This experiment was completed three times and a representative result is shown.*

3.7 Chronological ageing analysis of *S. cerevisiae* cells overexpressing *RAS2^{S225A}*

3.7.1 Overexpression of *RAS2^{S225A}* in wild type cells reduces chronological life span

To further investigate the effects of the overexpression of the *RAS2^{S225A}* on both growth and viability a chronological ageing assay was conducted. Overnight cultures of wild type cells overexpressing the empty plasmid backbone control or *RAS2^{S225A}* mutant allele were grown and sub-cultured to a calculated OD_{600} of 0.1 in SD –URA media. After 24 hours of incubation, an aliquot of the culture was taken to calculate the colony forming units (Materials and Methods, Section 2.9.9) and for flow cytometry analysis to measure levels of propidium iodide (Materials and Methods, Section 2.9.12) and dihydroethidium fluorescence (Materials and Methods, Section 2.9.11) to assess necrosis and superoxide production respectively. Aliquots of cells were taken from the same culture sequentially at 24-hour intervals for 6 days and colony forming unit counts and flow cytometry analysis were undertaken. The final measurement was taken after 12 days of sample incubation.

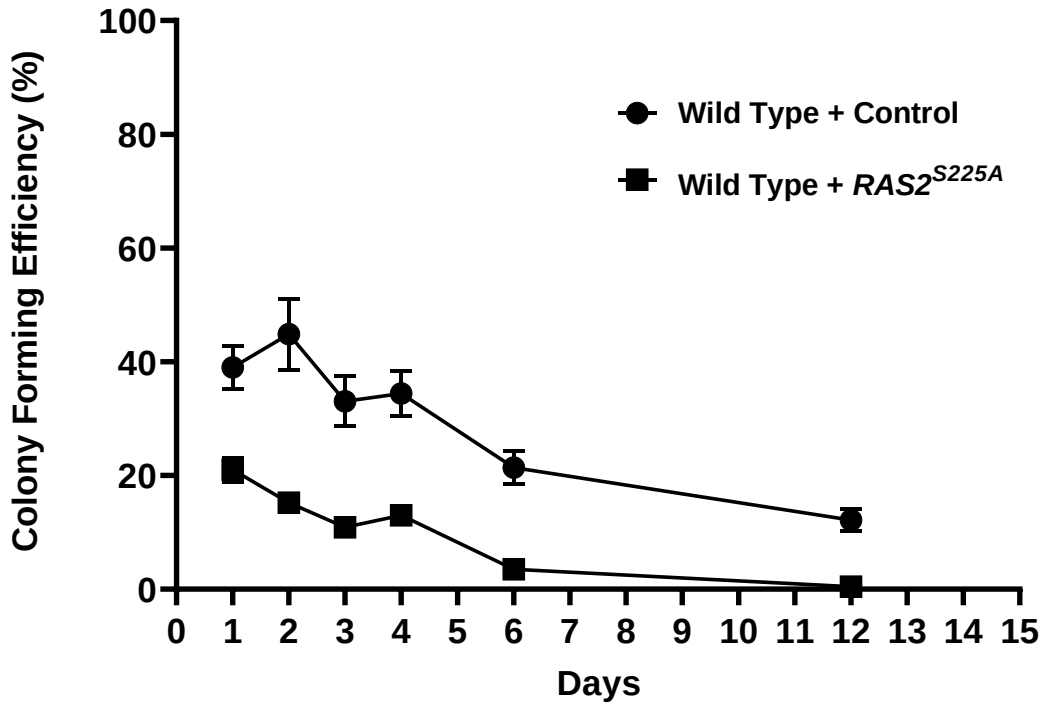

Figure 36. A chronological ageing assay of wild type cells over expressing RAS2^{S225A} or an empty plasmid control grown in SD –URA.
The chronological ageing assay was conducted as described in materials and method (Section 2.9.8). The data represents an average of three technical repeats and error bars represents the standard error of the mean.

After 24 hours of incubation the wild type control shows ~40 % viability compared to ~20 % in wild type cells overexpressing *RAS2^{S225A} (Figure 36)*. At day 2 we see an unexpected increase in viability in the wild type control but see a decrease in viability in cells overexpressing *RAS2^{S225A}*. Over time we observed an overall decrease in viability when compared to the first time point in both strains. At day 12, the *RAS2^{S225A}* mutant was unable to form viable colonies whereas the control strain had a colony forming efficiency of ~18 %. Thus, under the conditions used the overexpression of *RAS2^{S225A}* leads to a complete loss of viability after 12 days of incubation which was not observed in the wild type control *(Figure 36)*.

3.7.2 Flow cytometry to analyse the levels of ROS in wild type cells expressing *RAS2^{S225A}*

To investigate the levels of cell death in cells overexpressing *RAS2^{S225A}*, fluorescence-activated cell sorting (FACS) was utilised. This flow cytometry-based technique was used to determine whether the overexpression of *RAS2^{S225A}* results in an increase in ROS. Increased levels of ROS within cells is indicative of cell stress or programmed cell death [217][155][218]. The dye dihydroethidium (DHE) was used to analyse ROS levels within cells. DHE is oxidised by superoxide radicals ($O2^{\cdot -}$). The reaction between superoxide and DHE leads to a fluorescence output that can be detected using a flow cytometer. ROS accumulation was measured using flow cytometry as described in Materials and Methods, Sections 2.9.11. A marker (M1) was set to incorporate the standard peak for the comparison of samples to a control sample grown without any ROS indicator dye. The M1 marker was set at the same fluorescence intensity position on the x axis of all subsequent samples. The second marker (M2) was set to the right-hand side of the M1 marker and incorporated any peaks that represented an increase in fluorescence intensity. The control had no value for the M2 marker as there was no increase fluorescence detected.

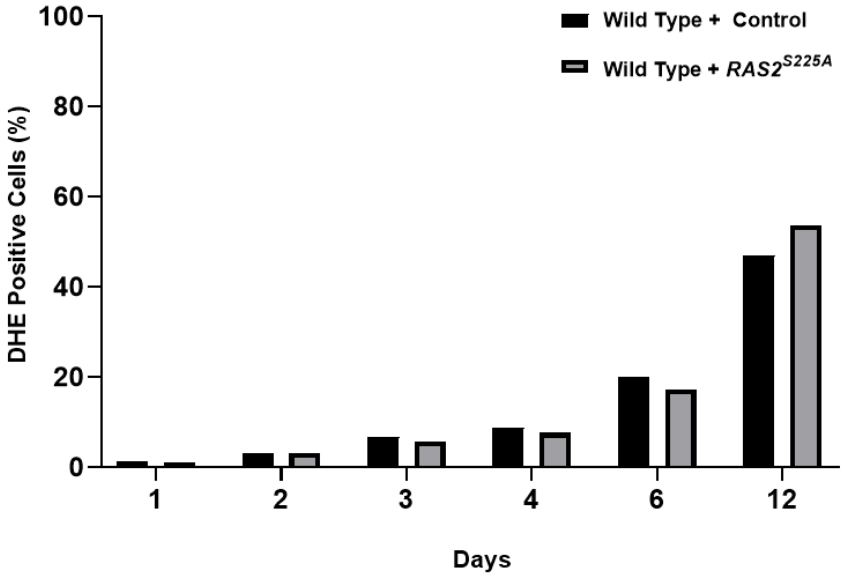

Figure 37. A bar chart presenting the percentage of DHE positive cells in wild type cells overexpressing RAS2^{S225A} or an empty plasmid control.
Strains were grown in SD-URA and measurements were taken over a 12-day period of continuous incubation. Cells were incubated with DHE in a 96 well plate for 15 minutes to measure superoxide production. The data displayed is an average of three biological repeats and error bars represent standard deviation

In both the wild type control and the *RAS2*^{S225A} strain there was a very low percentage of DHE positive cells after the first day of growth suggesting a small proportion of ROS producing cells *(Figure 37)*. Between days 2 to 6 there was an increase in the percentage of DHE positive in both strains. At day 6, the percentage of DHE positive cells rose to ~20% in both strains. At day 12 the percentage of DHE positive cells in the wild type control increased to 50 % and 55 % in wild type cells overexpressing *RAS2*^{S225A}*,* respectively *(Figure 37)*. This data set suggests that the overexpression of the *RAS2*^{S225A} mutant does not lead to a loss of viability that correlates with an increase in ROS production, a phenotype commonly linked to forms of cell death in yeast [217].

3.7.3 Flow Cytometry to analyse the levels of necrosis in wild type cells expressing *RAS2^{S225A}*

To investigate the levels of necrosis in the wild type control and wild type cells overexpressing *RAS2^{S225A}* propidium iodide was used. Propidium iodide (PI) intercalates into double stranded nucleic acids when the cell membrane is compromised. PI can therefore only penetrate necrotic cells and is excluded by viable cells and so its uptake is a useful marker of this mode of cell death. A marker (M1) was set to incorporate the standard peak for the comparison of samples to a control sample grown without any Propidium Iodide. The M1 marker was set at the same fluorescence intensity position on the x axis of all subsequent samples. The second marker (M2) was set to the right-hand side of the M1 marker and incorporated any peaks that represented an increase in fluorescence intensity. The control had no value for the M2 marker as there was no increase fluorescence detected.

In both the wild type control and wild type cells overexpressing *RAS2^{S225A}* the percentage of PI positive cells was negligible at day 1 *(Figure 38)*. Between days 1-4 there was a small increase in the percentage of PI positive cells from 1 to 10% in both strains. This was again expected, as the number of days of continuous growth increases the population of ageing cells in the culture will increase leading to an increase in cell death and hence an increase in the percentage of PI positive cells. At day 6 we observed a further increase in the percentage of PI positive cells in both strains, with the percentage of PI positive cells in the wild type control marginally exceeding that of the *RAS2^{S225A}* mutant strain. At day 12 a significant increase in PI positive cells is observed in the wild type control strain when compared to the *RAS2^{S225A}* strain. In the wild type control the percentage of PI positive cells reaches 50 % of the population with wild type cells overexpressing *RAS2^{S225A}* showing 40 % of the population

being PI positive *(Figure 38)*. This data suggests that the overexpression of *RAS2*^{S225A} in wild type cells does not lead to a loss of viability that can be explained by an increase in necrosis.

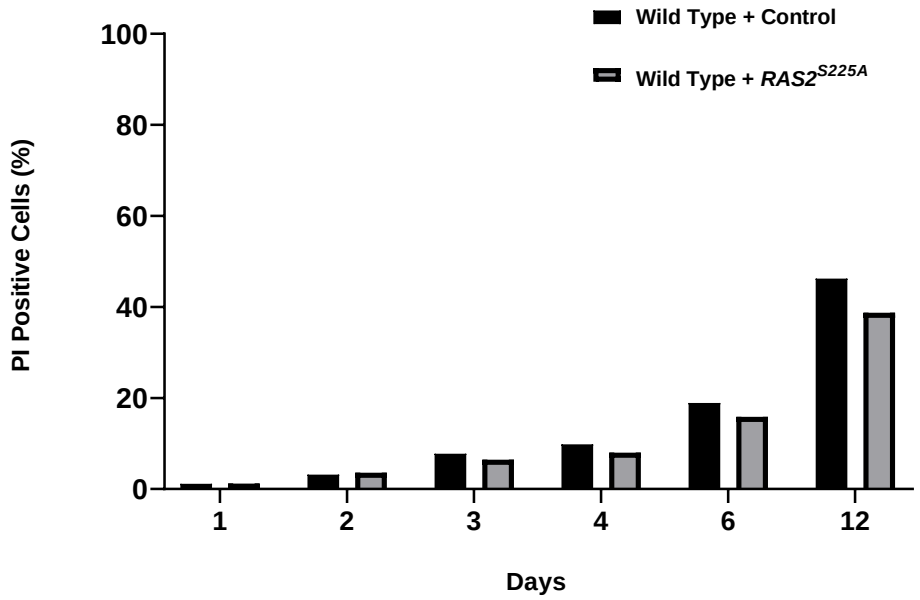

Figure 38. A bar chart presenting the percentage of PI positive cells in wild type cells overexpressing RAS2^{S225A} or an empty plasmid control.
Strains were grown in SD-URA and measurements were taken over a 12-day period of continuous incubation Cells were incubated with PI in a 96 well plate for 15 minutes to measure cell death. The data displayed is an average of three technical repeats and error bars represent standard deviation.

3.8 The overexpression of either *RAS2*^{S225A} or *RAS2*^{S225E} in wild type cells presents no significant abnormalities in cells ability to regulate autophagy

In *S. cerevisiae*, Ras proteins mediate autophagy through the activity of PKA [219][167]. The RAS/cAMP/PKA pathway has been shown to be highly interconnected with the TOR pathways which is also involved in the regulation of autophagy in yeast [219][167][166]. Both Tor and Ras often control overlapping effectors, including effectors involved in autophagy. We aim to investigate whether the overexpression of either *RAS2*, *RAS2*^{S225A} or *RAS2*^{S225E} in a *GFP-ATG8* strain leads to changes in cells ability to regulate autophagy. Here we analyse the autophagy-

related ubiquitin-like protein Atg8 as a tool for monitoring and quantifying autophagy upon the overexpression *RAS2, RAS2^{S225A}* or *RAS2^{S225E}* in yeast cells *(Figure 39)*.

Atg8 most commonly exists conjugated to the lipid phosphatidylethanolamine (PE). In *S. cerevisiae*, Atg8-PE conjugation is regulated by the nutritional status of the cells. During nutrient-rich conditions, Atg8 mainly exists in the unconjugated form but upon nitrogen starvation most of the Atg8 population conjugates to PE [220]. During nitrogen starvation Atg8-PE is recruited to the phagophore assembly site and localizes to both the inner and outer phagophore membranes, but is generally not detected on the surface of completed autophagosomes [220]. Upon autophagosome completion, Atg8-PE localised to the inner-autophagosome membrane is transported to the vacuole where it is degraded by vacuolar proteases as part of the autophagic body [220]. The population of Atg8 present on the outer membrane of the autophagosome is released via the deconjugation of the Atg8-PE by a Atg4-dependent cleave step [221]. GFP-Atg8 shows the same behaviour as Atg8, and autophagic flux can be followed by monitoring the vacuolar delivery and subsequent breakdown of GFP-Atg8. When autophagic flux is normal, GFP-Atg8 that is present inside the autophagosome is cleaved after the autophagic body membrane is lysed and the contents are exposed to the vascular hydrolases. The proteolysis of GFP-Atg8 liberates an intact GFP moiety, which accumulates in the vacuole as autophagy proceeds. The increase in free GFP levels can be detected and quantified by western blot analysis and correlated with the autophagic rate [222][223].

We transformed plasmids overexpressing either *RAS2*, *RAS2^{S225A}* or *RAS2^{S225E}* into a *GFP-ATG8* background to assess autophagic rate. An empty plasmid backbone was transformed into a *GFP-ATG8* background as a control. *ATG8–GFP* cells overexpressing either *RAS2*, *RAS2^{S225A}*,

RAS2^{S225E}, or an empty plasmid control were grown in SD-URA for 24 hours to stationary phase. Following this, 1ml of culture was transferred to nitrogen starvation media (Materials and Methods, Section 2.1.4) to induce autophagy, and incubated at 30 °C with 200 rpm shaking for 6 hours (Materials and Methods, Section 2.9.7). Total protein was extracted from cells pre- and post-induction of autophagy and subjected to western blotting (Materials and Methods Section 2.8). We did not observe any significant differences in autophagic flux in *GFP-ATG8* strains overexpressing *RAS2*, *RAS2*^{S225A} or *RAS2*^{S225E} when compared to the control *(Figure 39)*. In the absence of nitrogen starvation, no significant differences in the detection of GFP-ATG8 or GFP were observed between strains *(Figure 39)*. In the presence of nitrogen starvation, a significant increase in GFP detection was detected in all strains but no significant difference in free GFP detection was noted between strains *(Figure 39)*. As no significant differences in GFP liberation upon nitrogen starvation was observed when compared to the control strain, we propose that the overexpression of *RAS2*, *RAS2*^{S225A} or *RAS2*^{S225E} does not result in abnormalities in autophagic flux in wild type cells.

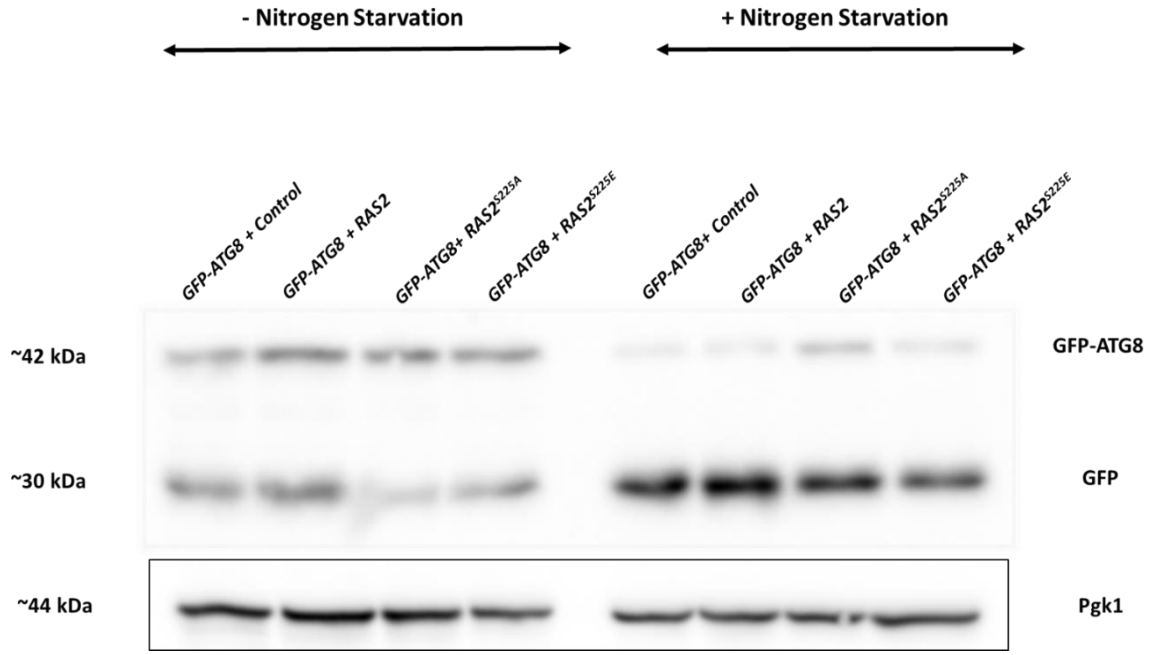

Figure 39. A western blot showing the detection of GFP in GFP-ATG8 cells overexpressing RAS2, RAS2^{S225A}, RAS2^{S225E} or an empty plasmid control.

Cells were grown in SD –URA media for 24 hours. 1ml of culture was transferred to nitrogen starvation media to induce autophagy via nitrogen starvation and incubated at 30°C with 200 RPM shaking for 6 hours. Total protein was extracted from cells pre- and post-induction of autophagy and subjected to western blotting. To ensure uniform protein loading, the levels of Pgk1p were detected after probing for Ras2p. This experiment was repeated three times and a representative data set is shown.

3.9 Analysis of the effects of the overexpression of *RAS2^{S225A}* or *RAS2^{S225E}* upon mitochondria morphology

3.9.1 Microscopic analysis of wild type cells overexpressing *RAS2^{S225A}*, *RAS2^{S225E}* or an empty plasmid control and co-expressed with a GFP-mitochondria probe

Ras activity has been linked to the regulation of mitochondrial function[224][218] [225]. To investigate the effect of the modification of Ras2^{S225} upon mitochondria morphology, wild type cells expressing either *RAS2^{S225A}*, *RAS2^{S225E}* or an empty plasmid control were transformed with a GFP-mitochondria probe. During stationary phase of growth, no significant differences in mitochondrial inheritance or morphology was observed in wild type cells overexpressing *RAS2^{S225A}* or *RAS2^{S225E}* when compared to the control strain *(Figure 40)*.

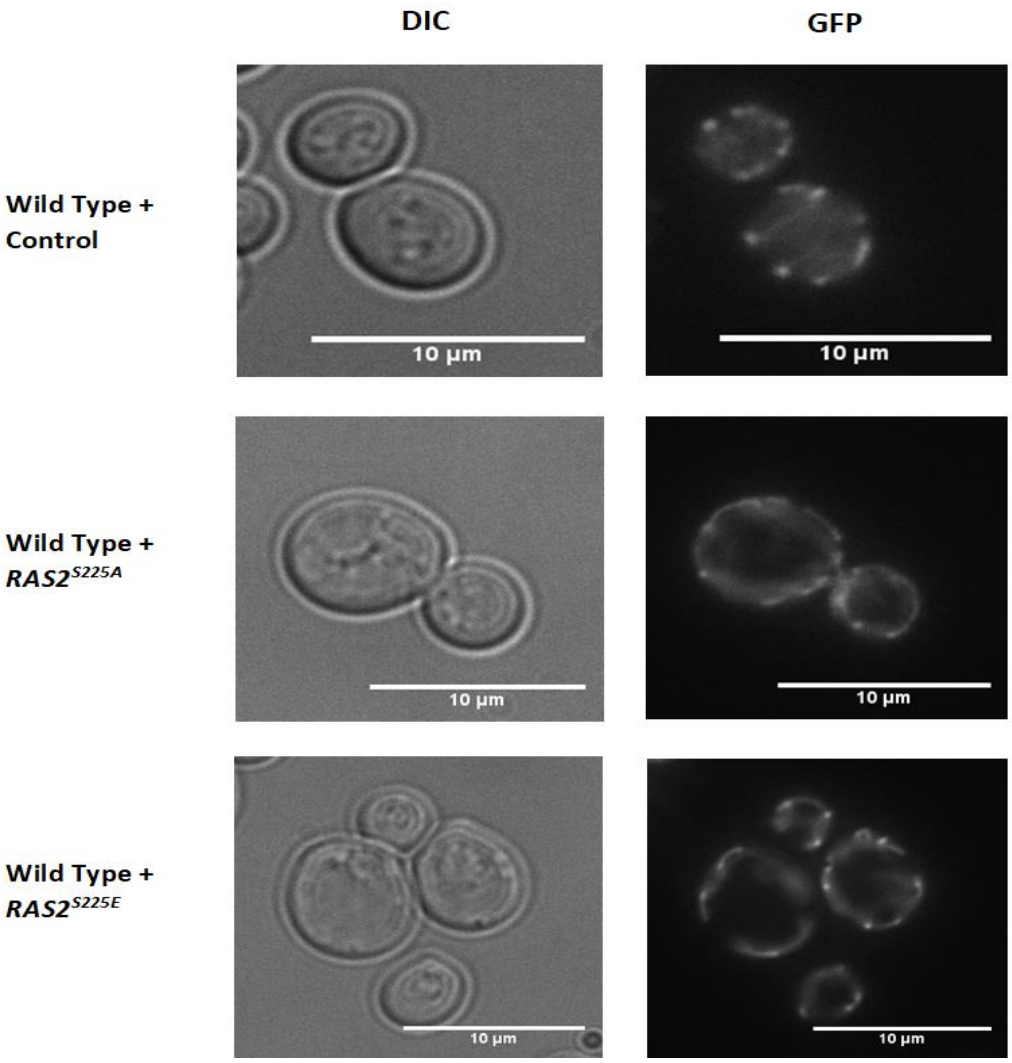

Figure 40. Images taken using fluorescence microscopy of wild type strains overexpressing $RAS2^{S225A}$, $RAS2^{S225E}$ or an empty plasmid control co-expressed with a GFP-mitochondria probe during stationary phase of growth.

Fluorescence signal represents the presence of mitochondria within cells. The GFP mitochondria probe contains the first 69 amino acids of subunit 9 of the F0 ATPase of Neurospora crassa [Su9(1–69)] which is a mitochondrial matrix targeting sequence and includes a processing site for the mitochondrial matrix processing peptidase (Westermann & Neupert 2000). Cells were cultured in SD –URA/-LEU growth media. This experiment was repeated three times and a representative data set is shown.

3.10 Respirometry to assess mitochondrial function in wild type cells overexpressing *RAS2^{S225A}* or *RAS2^{S225E}*

Our results indicate that the overexpression of either *RAS2^{S225A}* or *RAS2^{S225E}* in both a wild type and *Δras2* background can lead to a loss in viability that is not accompanied by an increase in either ROS accumulation or PI staining. One possibility is that cells overexpressing either *RAS2^{S225A}* or *RAS2^{S225E}* are in fact senescent or quiescent and that the loss of viability does not represent cell death, but rather an inability to divide. We noted no significant abnormalities in mitochondrial inheritance or morphology in cells overexpressing either *RAS2^{S225A}* or *RAS2^{S225E}*, however we did not investigate mitochondrial activity. To address this, we measured respiration within wild type cells overexpressing *RAS2^{S225A}* or *RAS2^{S225E}*.

A high-resolution respirometer was used to measure respiration by analysing the oxygen consumption of wild type cells overexpressing either *RAS2^{S225A}*, *RAS2^{S225E}* or an empty plasmid control. The oxygen consumption was measured as O_2 flow per cell *(Figure 41)*. The drugs Triethiltyn bromide (TET), Carbonylcyanide p-trifluoromethoxyphenylhydrazone (FCCP), and Antimycin A (AntA) were used to investigate the functioning of individual components of the mitochondrial respiratory chain.

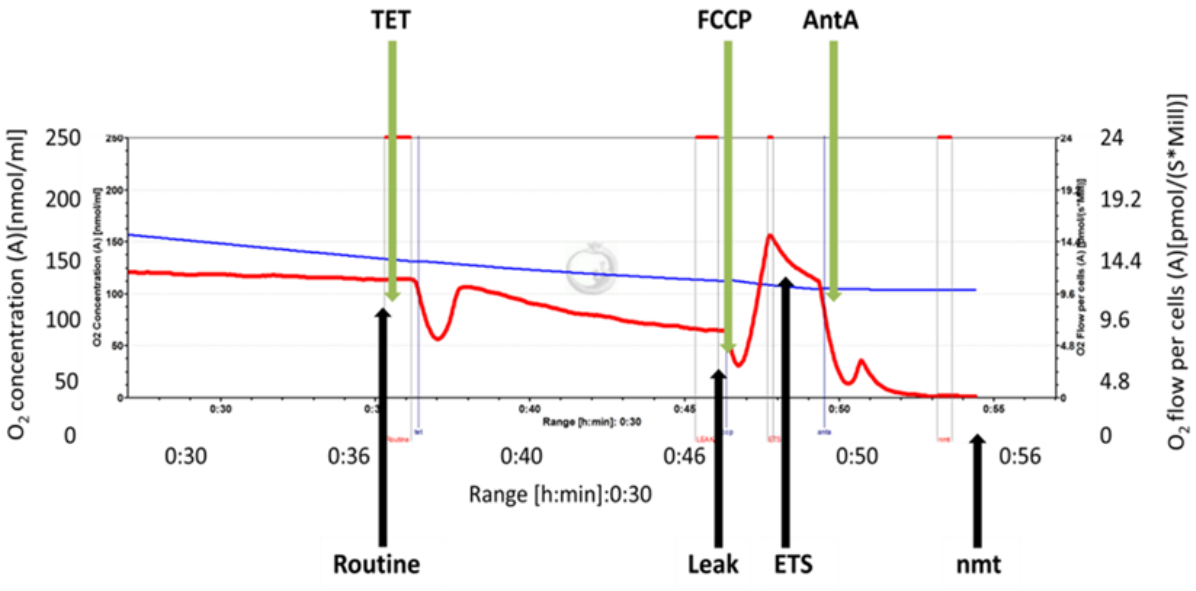

Figure 41. A typical respirometry profile generated from the Oroboros oxygraph-2k.
*The blue line shows oxygen concentration and the red line represents the oxygen flux per cell (pmol/s*Mill). The black arrows indicate the steady state oxygen flux (Routine), the induced mitochondrial resting state (Leak), the maximal capacity of the electron transport system (ETS) and the non-mitochondrial oxygen flux (nmt). For the analyses of individual components of the respiratory chain specific drugs were added to the chambers. The drug TET was used to induce leak respiration, FCCP was used to inhibit ATP synthase and therefore allow maximal electron transport through the ETS and AntA was used to inhibit the ETS.*

To measure 'Leak' respiration we used the drug TET, which inhibits ATP synthase complex V. ATP synthase produces energy in the form of ATP through the pumping of protons across the mitochondrial inner-membrane space (IMS) into the mitochondrial matrix. Inhibition of ATP synthase results in the accumulation of protons within the IMS, leading to an inhibition of the movement of electrons through the electron transport chain. The activity of ATP synthase therefore represents an integral control mechanism. Upon the addition of TET, any respiration that is detected when ATP synthase is inhibited does so because of protons moving freely across the IMM independently of the pump, and thus called leak respiration. If the leak respiration of a strain is higher than that of the control strain, we can conclude that

more respiration has been detected that is occurring independently of ATP synthase proton pumping activity and by association, ATP synthesis.

Mitochondrial membrane potential is a major regulator of electron passage, if the membrane potential is too high electrons cannot passage along the ETC as this requires proton pumping into the IMS, which becomes more difficult as the membrane potential is increased. The inhibition of ATP synthase stops election movement as the resulting affect is an increase in membrane potential. When a TET induced drop in respiration is not observed, it suggests that oxygen consumption and electron movement occurs independently of ATP synthase and therefor ATP is not synthesized as it requires the movement of protons through the pump; this is termed uncoupled respiration.

To measure the maximal capacity of the electron transport system (ETS) the drug FCCP was used. FCCP is a proton ionophore that forms pores in the IMM rendering it permeable and permitting the free flow of protons across it. The resulting effect if the disruption of the membrane potential provided by the proton gradient allowing the ETC to function at its maximal potential. As such, the higher the ETS detected, the higher the capacity of the ETC.

To measure the non-mitochondrial (nmt) origin of respiration the drug Antimycin A (AntA) was used. AntA inhibits cytochrome C reductase (complex III) through binding to the Qi site and preventing the transfer of electrons. Complex III is the third phase in the ETC and is oxidised at the Qi site, therefor inhibition of this site prevents re-oxidation by oxygen. As a result, any oxygen consumption detected after the addition of AntA is therefor of nmt origin.

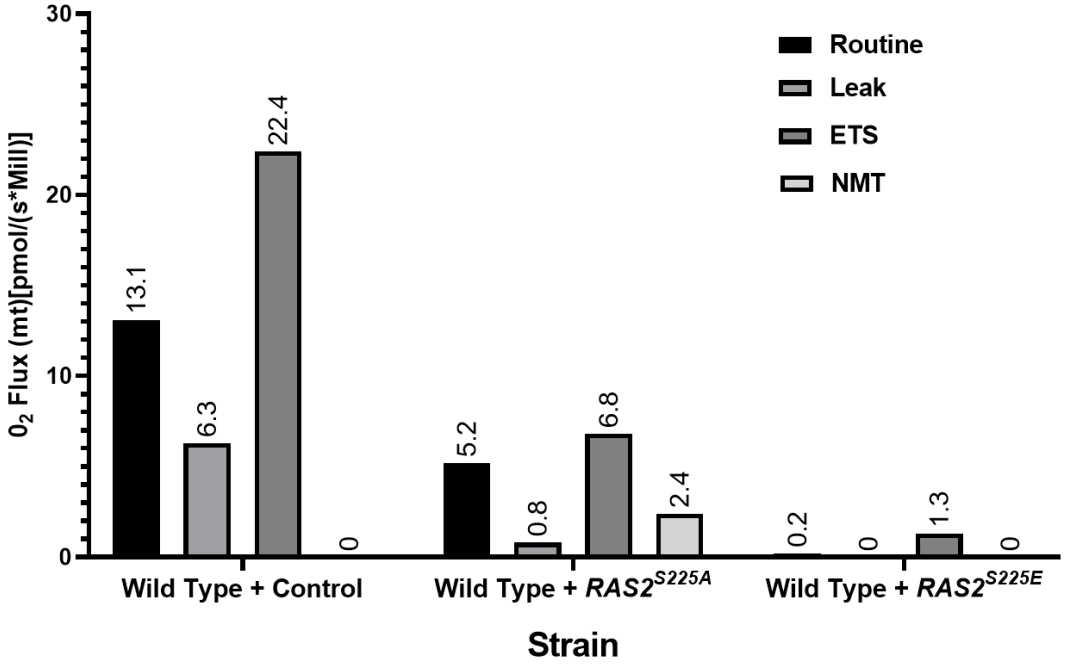

Figure 42. A bar chart showing the routine, leak, ETS and NMT O2 flux values for wild type cells overexpressing RAS2^{S225A}, RAS2^{S225E} or an empty plasmid backbone control.
The data shown represents one experiment.

A significant reduction in routine respiration was observed upon the overexpression *of RAS2^{S225A}* or *RAS2^{S225E}* in wild type cells when compared to the control strain *(Figure 42)*. The overexpression of *RAS2^{S225E}* presented the most notable reduction, with a routine respiration of 0.2 (mt)[pmol/(s*Mill)], compared to 13.1 (mt)[pmol/(s*Mill)] in the wild type control *(Figure 42)*. Our results indicate that the overexpression of either *RAS2^{S225A}* or *RAS2^{S225E}* in wild type cells results in a significant decrease in routine respiration when compared to the control strain. A significant decrease in leak respiration was also noted upon the overexpression of *RAS2^{S225A}* or *RAS2^{S225E}* when compared to the wild type control *(Figure 42)*. Interestingly, leak respiration was not detected in wild type cells overexpressing *RAS2^{S225E}*. As the leak respiration of strains overexpressing *RAS2^{S225A}* or *RAS2^{S225E}* is lower than that of the control strain, we can conclude that the respiration detected in these strains is not occurring independently of ATP synthase proton pumping activity.

A significant decrease was observed in the maximal capacity of the electron transport system (ETS) in wild type cells overexpressing *RAS2*^{S225A} or *RAS2*^{S225E} when compared to the wild type control, therefor suggesting that the overexpression of either *RAS2*^{S225A} or *RAS2*^{S225E} causes a reduction in the overall capacity of the ETS *(Figure 42)*.

Individual components of the ETC were further analysed to identify whether a component was affected by the overexpression of either *RAS2*^{S225A} or *RAS2*^{S225E}. This was completed by comparing the oxygen flux ratios between the Routine and ETS (R/E) and the Leak and ETS (L/E). The oxygen flux ratios from each strain were compared to the wild type expressing an empty plasmid backbone.

The ratio obtained from dividing the Routine respiration rate by the ETS respiration rate (R/E) defines how close to the maximal capacity the mitochondria are functioning during Routine respiration. The closer to 1 the R/E ratio is, the closer to maximum capacity the ETS is working in that strain. A higher R/E ratio could suggest more uncoupling of the ETC, an increase in ADP driven respiration or a limitation of the ETC components.

The ratio obtained from dividing the Leak respiration rate by the ETS respiration rate (L/E) was analysed to determine whether the ETC is uncoupled. The closer to 1 the L/E ratio is, the higher the levels of uncoupled respiration that are occurring independently of ATP synthase. Uncoupled respiration is not transformed into energy by phosphorylation of ADP.

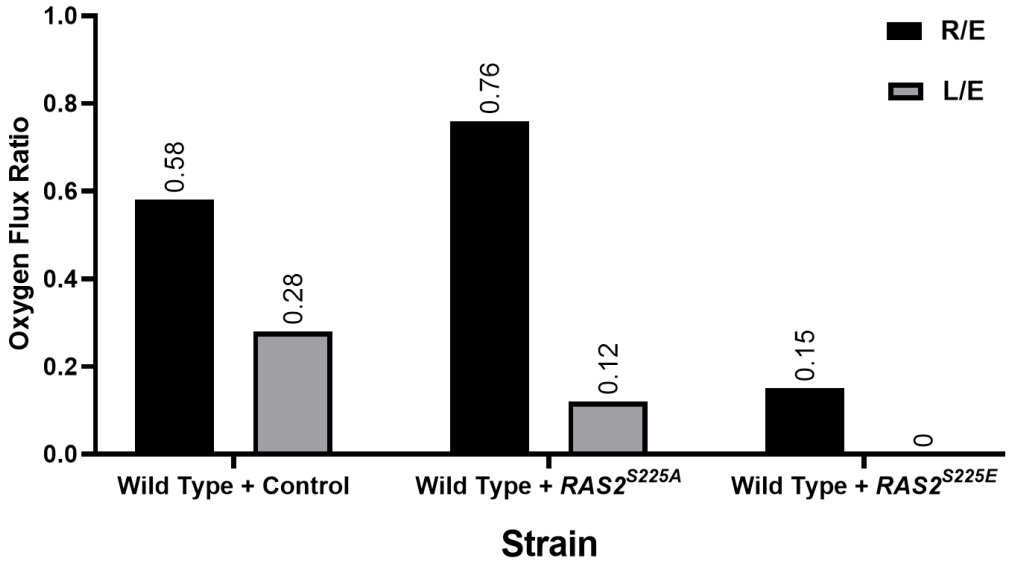

Figure 43. The oxygen flux ratios between the Routine and ETS (R/E) and the Leak and ETS (L/E) are shown for wild type cells overexpressing $RAS2^{S225A}$, $RAS2^{S225E}$ or an empty plasmid backbone control.

The data shown represents one experiment.

The increase in the R/E ratio observed in wild type cells overexpressing $RAS2^{S225A}$ suggests that the mitochondria in these cells are working closer to the maximal capacity when compared to the wild type control *(Figure 43)*. To determine whether the increase in R/E was due to uncoupled respiration, the ratio for L/E was analysed. The L/E ratio was decreased in wild type cells overexpressing $RAS2^{S225A}$, which suggests a decrease in uncoupled respiration, when compared to wild type control *(Figure 43)*. As the mitochondria in wild type cells overexpressing $RAS2^{S225A}$ are functioning close to their maximal capacity, we can conclude that wild type cells overexpressing $RAS2^{S225A}$ are neither necrotic nor apoptotic.

The decrease in the R/E ratio observed in wild type cells overexpressing $RAS2^{S225E}$ suggests that the mitochondria in these cells are not functioning close to the maximal capacity when compared to the wild type control *(Figure 43)*. To determine whether there is an increase in uncoupled respiration when compared to the control strain, the ratio for L/E was analysed. The L/E ratio was 0 in wild type cells overexpressing $RAS2^{S225E}$, which suggests there is no

uncoupled respiration present *(Figure 43)*. We suggest that the overexpression of *RAS2*^{S225E} in wild type cells results in severe mitochondrial dysfunction, as opposed to repression. From the data generated in this study, we see no evidence of cell death markers even when respiration is minimal. We therefor conclude that the overexpression of either *RAS2*^{S225A} or *RAS2*^{S225E} results in a deficit of growth resumption that accounts for the loss of viability observed.

3.11 Sequence alignment between Ras2 and human N-Ras suggests that Serine^{225} is conserved in human N-Ras at Serine^{173}

We have shown that the Serine^{225} residue of the Ras2 protein is important for growth, viability, and the localisation of Ras. We hypothesized that this residue may be conserved in higher eukaryotes. To address this, sequence alignment between the Ras2 protein and the human N-Ras protein was performed *(Figure 44)*. Remarkably, although significant sequence divergence between the yeast and human Ras proteins outside of the GTPase domain and C terminal CAAX box, we discovered that Ras2 Serine^{225} was conserved in human N-Ras at Serine^{173} *(Figure 44)*. The conservation of this serine residue in human Ras proteins may suggest an important role of this residue in higher eukaryotic systems. Plasmids overexpressing the wild type *NRAS* gene or plasmids containing the *NRAS* gene mutated at Serine^{S173}, where the serine was either substituted with alanine to produce a non-phosphoryatable residue or glutamate to produce phosphomimetic residue, were transformed into wild type cells and growth analysis was performed.

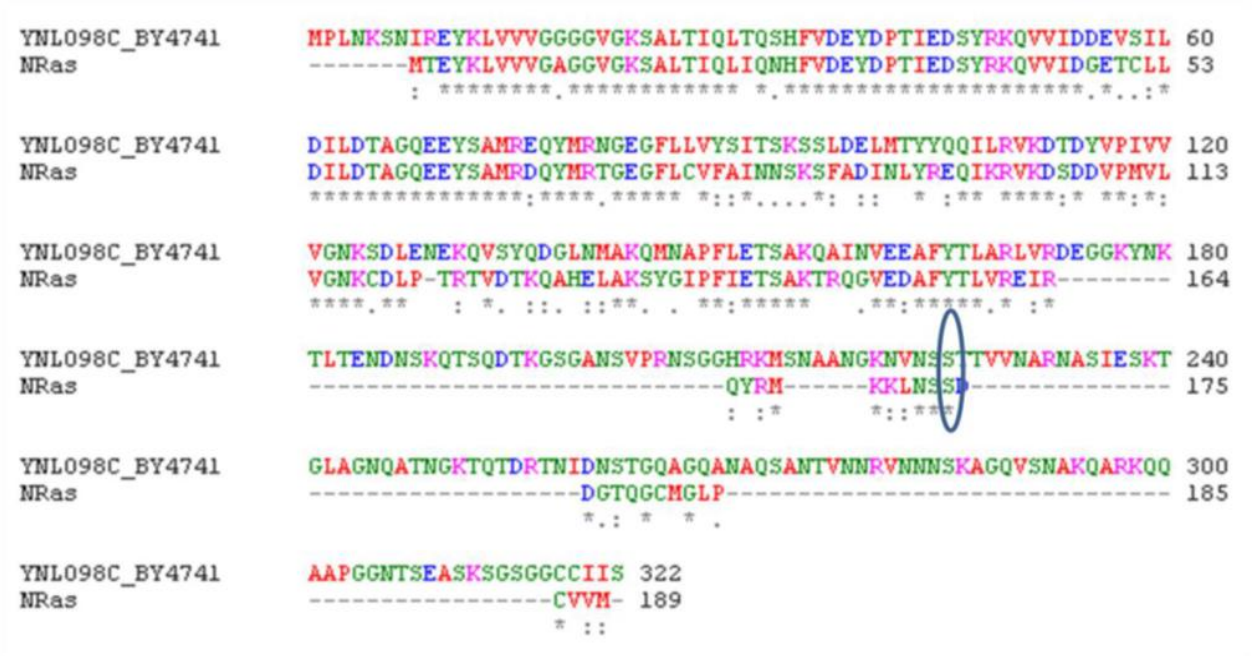

Figure 44. Sequence alignment of the Ras2 protein and human N-Ras shows that Serine^{225} of Ras2p (circled) is conserved in N-Ras at Serine^{173}.

3.11.1 The expression of *NRAS*, *NRAS*^{S173A} or *NRAS*^{S173E} induces growth defects in wild type cells

As sequence alignment revealed conservation of the yeast Ras2^{S225} phosphorylation site in the human Nras protein, constructs expressing human *NRAS* or human *NRAS* mutations at the equivalent phosphorylation site (Ser^{173}) were transformed into wild type cells. To analyse the growth of yeast strains overexpressing *NRAS*, *NRAS*^{S173A}, *NRAS*^{S173E} or an empty plasmid control, a growth assay was performed as described in Materials and Methods, Section 2.9.1. Overexpression of either *NRAS*, *NRAS*^{S173A} or *NRAS*^{S173E} in wild type cells resulted in severe growth defects when compared to the wild type control *(Figure 45)*. The expression of either wild-type or mutated human *NRAS* led to an increase in lag time, early transition to diauxic growth and overall lower final biomass when compared to the control strain *(Figure 45)*. The mutated forms of human *NRAS* were seen to perturb growth to a greater extent when

compared to the wild-type Human *NRAS* expressing strain. A significant increase in doubling time was observed upon the overexpression *NRAS*, *NRAS*^{S173A}, *NRAS*^{S173E} in wild type cells when compared to the control strain *(Figure 46)*.

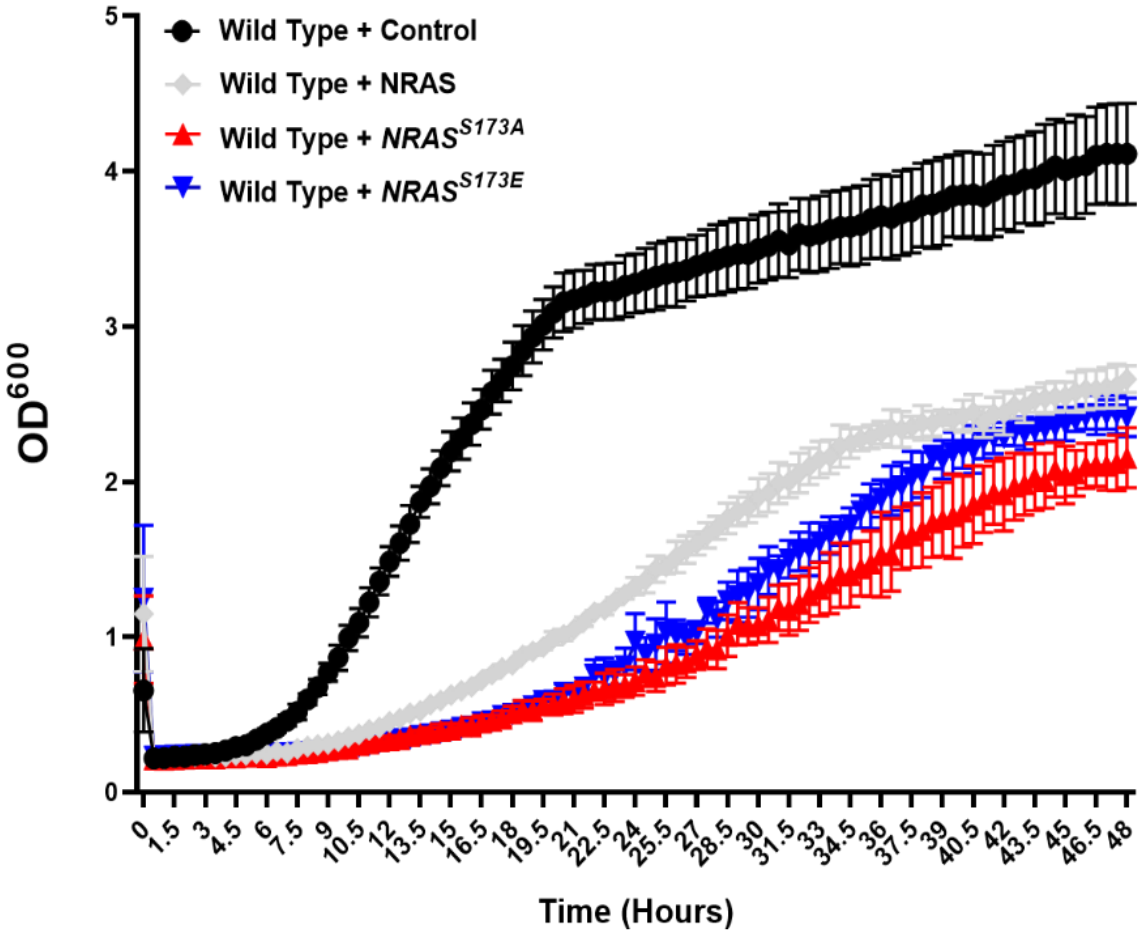

Figure 45. Growth analysis of S. cerevisiae wild type cells overexpressing RAS2, RAS2^{S225A}, RAS2^{S225E} or empty plasmid control.

The growth analysis was carried out in SD –URA media as described in Materials and Methods (Section 2.9.1). This data represents an average of three biological repeats and error bars represent the standard deviation.

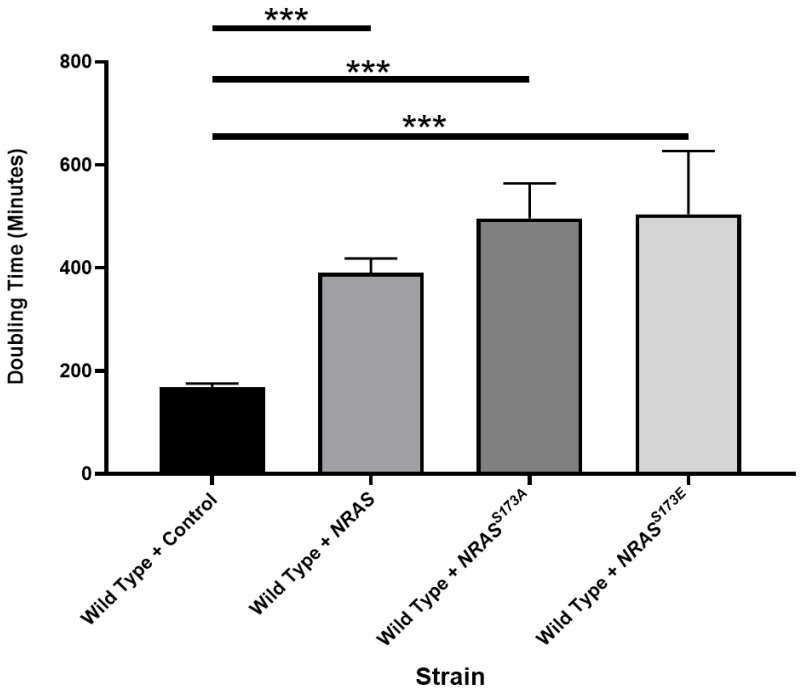

Figure 46. Growth rate analysis of S. cerevisiae wild type cells overexpressing RAS2 or RAS2^{S225A} or RAS2$^{S225E.}$

*The growth rate analysis was carried out as described in Materials and Methods (Section 2.9.1). The data represents an average of three biological repeats and error bars represents the standard deviation. A One-way ANOVA using a Dunnets multiple comparison test was used to determine statistical significance. Non-significant = NS, * = adjusted p-value ≤ 0.05 and *** = adjusted p value ≤ 0.001.*

3.11.2 Expression of *NRAS*, *NRAS*^{S173A} or *NRAS*^{S173E} in yeast cells leads to a reduction in viability

To determine whether the overexpression of either *NRAS*, *NRAS*^{S173A} or *NRAS*^{173E} led to changes in viability in wild type cells we performed a colony forming efficiency assay, as described in Materials and Methods, Section 2.9.3**.** The overexpression of either *NRAS*, *NRAS*^{S173A} or *NRAS*^{S173E} in wild type cells resulted in a significant reduction in viability when compared to the plasmid control in the wild type *(Figure 47)*. Our data suggests that the overexpression of Human *NRAS* in yeast cells leads to a significant decrease in viability

regardless of the status of Ser[173]. This data alone, therefor does not allow us to determine the significance of this residue without further studies.

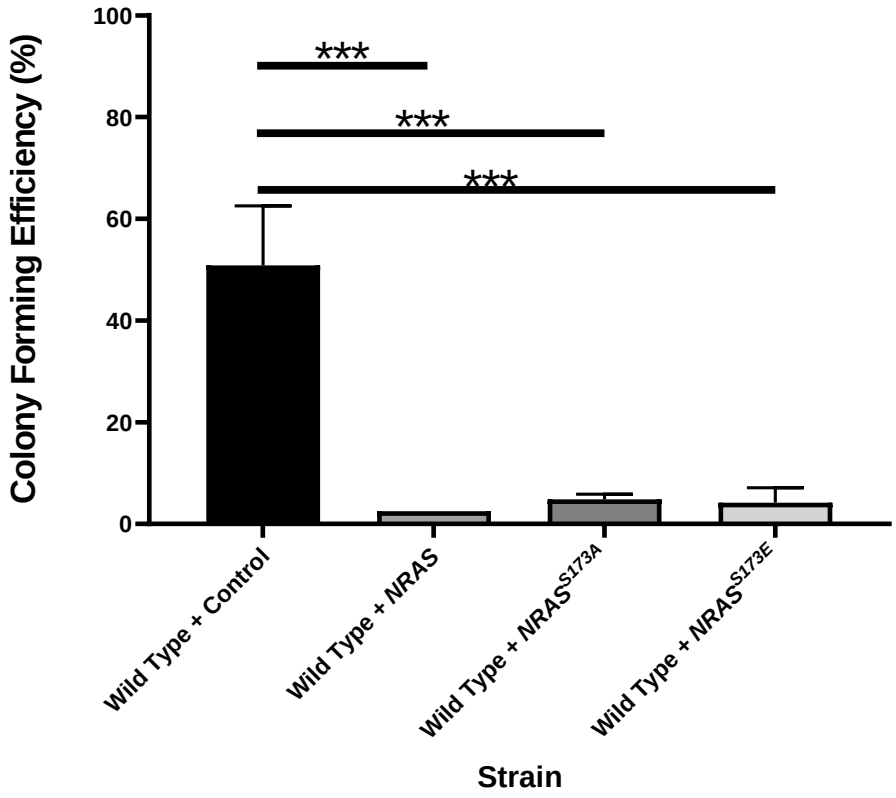

Figure 47. A colony forming efficiency assay of S. cerevisiae wild type cells overexpressing NRAS, NRAS^{S173A}, NRAS^{S173E} or an empty plasmid control grown in SD –URA media.

*A colony forming efficiency analysis was carried out as described in Materials and Methods (Section 2.9.3). This data represents three biological repeats and the error bars represent the standard deviation. A One-way ANOVA using a Dunnets multiple comparison test was used to determine statistical significance. Non-significant = NS, * = adjusted p-value ≤ 0.05 and *** = adjusted p value ≤ 0.001.*

3.12 Discussion of Results

Ras proteins are small GTPases that act as molecular switches within cells that link extracellular stimuli to intracellular effectors. Ras proteins play a conserved role in the control of both cell growth and proliferation [211]. As a result, mutations that induce the constitutive activation of Ras proteins are often associated with changes in cell behaviour that can lead to disease, such as human cancer [41]. The localisation of Ras proteins are reported to be predominantly to the inner cytoplasmic surface of the plasma membrane, but they can also be observed on endomembranes, such as the endoplasmic reticulum, and the mitochondrial outer membrane [65][57][212]. It has been shown that Ras undergoes a series of posttranslational modifications that dictate its subcellular localisation. Surprisingly, the phosphorylation of Ras2p in *S. cerevisiae* has not been studied in regards to its regulation of intracellular localisation, despite significant evidence existing linking phosphorylation to Ras localisation in humans [50][77]. While phosphorylation is an important posttranslational modification, little is known on its effect on Ras2 protein activation and localisation. Previous studies conducted by the Kent Fungal Lab, under the supervision of Dr Campbell Gourlay have identified the residue Ser^{225} of Ras2p as a potential phosphorylation site within the Ras2 protein of *S. cerevisiae*. The present study investigates further whether Ras2p phosphorylation provides a mechanism that regulates Ras2p trafficking inside the cell.

The data presented in this chapter suggests that the modification of the Ser^{225} residue of Ras2p is important for both localisation and activity of Ras proteins. We have shown that during both log and stationary phases of growth, the overexpression of either $RAS2^{S225A}$ or $RAS2^{S225E}$ in wild type cells results in significant changes in the localisation of active Ras populations when compared to the *RAS2* overexpression strain and wild type control. Actively

growing wild type cells localise GTP-bound Ras to the plasma membrane and nucleus. In wild type cells, such localisation results in the activation of the cAMP/PKA pathway, which signals to the cell to initiate both growth and proliferation. We suggest that during exponential growth, wild type cells overexpressing either *RAS2*^{S225A} or *RAS2*^{S225E} sequester active Ras to the nuclear envelope with reduced activity seen at the plasma membrane and nucleus. We hypothesize that the miss-localisation and inappropriate activation of Ras at the nuclear envelope results in aberrant activation of the cAMP/PKA pathway.

Upon nutrient depletion, GTP-bound Ras populations present a widespread/diffused signal with a faint nuclear localisation within wild type cells. Interestingly, we show that the overexpression of *RAS2*^{S225A} or *RAS2*^{S225E} presents a nuclear envelope localisation of GTP-bound Ras which was not observed in either the control or *RAS2* overexpression strains. We suggest that the overexpression of *RAS2*^{S225A} or *RAS2*^{S225E} leads to the miss localisation of active Ras to the nuclear envelope and an inappropriate activity during nutrient depletion, a time in which Ras activity should be minimal. We hypothesize that the resulting localisation of GTP-bound Ras caused by the overexpression of *RAS2*^{S225A} or *RAS2*^{S225E}, results in the inappropriate activation of PKA during a period of growth where its activity should be reduced.

The localisation of GFP-Ras2p, GFP-Ras2p^{S225A} or GFP-Ras2p^{S225E} was investigated using fluorescent microscopy. Surprisingly, no significant changes in the localisation of fluorescently labelled Ras2p was observed between wild type cells overexpressing *RAS2*, *RAS2*^{S225A} or *RAS2*^{S225E}. The predominant localisation of GFP-Ras2p was observed at the plasma membrane in both stationary and exponential phase of cell growth. As previously mentioned, the overexpression of *RAS2*^{S225A} or *RAS2*^{S225E} resulted in significant differences in the localisation

of active Ras population when compared to the control and *RAS2* overexpression strain. Therefor it was surprising that the overexpression of the mutant *RAS2* alleles failed to result in changes in GFP-Ras2p localisation. As the RBD domain binds to Ras proteins only in their GTP-bound state and does not differentiate between Ras1 and Ras2, we hypothesize that the modification of Ser^{225} results in the miss localisation of both Ras proteins when only in their GTP-bound state.

In the current study, the localisation of both active Ras and GFP-Ras2p was investigated exclusively in wild type cells. For future investigations, we believe it would be useful to study the localisation of active Ras populations and GFP-Ras2p in a *Δras2* background. Such investigations will reveal the effects of the overexpression of either *RAS2*, $RAS2^{S225A}$ or $RAS2^{S225E}$ on the localisation of active Ras populations in the absence of endogenous wild-type Ras2p. Similarly, we would like to investigate the localisation of GFP-Ras2p, GFP-$Ras2p^{S225A}$ or GFP-$Ras2p^{S225E}$ in a *Δras2* background to identify whether the presence of endogenous wild type Ras2p affects the localisation of GFP-Ras2p, GFP-$Ras2p^{S225A}$ or GFP-$Ras2p^{S225E}$.

Western blot analysis confirmed that Ras2, $Ras2p^{S225A}$ and $Ras2p^{S225E}$ are being overexpressed in both a wild type and Δ*ras2* background. The overexpression of $RAS2^{S225A}$ or $RAS2^{S225E}$ in wild type cells during exponential phase of cell growth led to an increase in Ras2p protein expression when compared to the control and *RAS2* overexpression strain. We hypothesize that this could be the result of an increase in the stability of the Ras2 protein, although it is not known whether this is due to an increase in mRNA levels, translation, or the stability of the protein itself. The overexpression of either $RAS2^{S225A}$ or $RAS2^{S225E}$ in a wild type background led to an increase Ras2p expression during stationary phase when compared to

the control and *RAS2* strain. Suggesting a putative role of Ser^{225} in the regulation of Ras2 protein expression or protein stability.

The overexpression of $RAS2^{S225A}$ or $RAS2^{S225E}$ resulted in significant growth defects when compared to the empty plasmid control in both wild type and *Δras2* backgrounds. Our findings show that $Ras2^{S225}$ is important for Ras function and furthermore that the growth defects induced by the overexpression of $RAS2^{S225A}$ or $RAS2^{S225E}$ are in fact dominant as growth defects manifest irrespective of whether endogenous Ras2p is present. Furthermore, we have identified the importance of $Ras2^{S225}$ in the maintenance of chronological lifespan. We show that the overexpression of $RAS2^{S225A}$ in wild type cells leads to a significant decrease in chronological life span when compared to the wild type, providing further evidence that the Ser^{225} residue is important for Ras function.

As Ras2p is involved in the regulation of antioxidant defences, we investigated whether the substitution of Ser^{225} of yeast Ras2 with glutamate or alanine led to changes in the cells ability to tolerate the addition of hydrogen peroxide to both liquid and solid media. The addition of H_2O_2 to liquid media resulted in significant growth defects in cells overexpressing *RAS2* mutant alleles when compared to the control strain. This effect was also recapitulated on solid media, with an increased sensitivity to peroxide observed in wild type cells overexpressing $RAS2^{S225A}$ or $RAS2^{S225E}$ when compared to the control strain. The inability of wild type cells overexpressing $RAS2^{S225A}$ or $RAS2^{S225E}$ to recover from this stress response is an indication that overexpression of either $RAS2^{S225A}$ or $RAS2^{S225E}$ alters the signalling properties of Ras and leads to a suppression of the oxidative stress response.

To investigate whether perturbed growth was accompanied by changes in culture viability a colony forming efficiency assay was performed. The expression of $RAS2^{S225A}$ or $RAS2^{S225E}$ in

both a wild type and *Δras2* background leads to a significant reduction in viability when compared to the control strain. The expression of *RAS2* did not appear to reduce viability in the *Δras2* background but interestingly increased viability when expressed in wild type cells. This reduction in viability only observed in cells overexpressing $RAS2^{S225A}$ or $RAS2^{S225E}$ suggests that the Ser^{225} of Ras2 is important for Ras function.

The findings within this chapter suggest that the modification of ser^{225} residue of Ras2 leads to growth defects, changes in the oxidative stress response and leads to a reduction in viability in wild type cells. We therefore investigate whether the overexpression of either $RAS2^{S225A}$ in a wild type background leads to an increase in markers of cell death, such as ROS. Increased levels of ROS within cells is indicative of cell stress or programmed cell death [217][155][218]. Using FACS analysis with the dye dihydroethidium (DHE) we measured ROS levels in cells overexpressing $RAS2^{S225A}$. Interestingly our data indicated the overexpression of $RAS2^{S225A}$ presented no significant increase in the percentage of DHE positive cells when compared to the wild type control. This data set suggests that the overexpression of the $RAS2^{S225A}$ mutant does not lead to a loss of viability that correlates with an increase in ROS production, a phenotype commonly linked to forms of cell death in yeast [217].

With no significant elevation in cellular ROS levels in strains assayed, we performed a FACS analysis using the dye propidium iodide to determine whether wild type cells overexpressing $RAS2^{S225A}$ showed increased levels of necrosis when compared to the wild type control. Our data suggests that the overexpression of $RAS2^{S225A}$ presented no significant increase in the percentage of necrotic cells when compared to the wild type control. This data suggests that the overexpression of $RAS2^{S225A}$ in wild type cells does not lead to a loss of viability that can be explained by an increase in necrosis.

In *S. cerevisiae*, Ras proteins mediate autophagy through the activity of PKA [219][167]. The RAS/cAMP/PKA pathway has been shown to be highly interconnected with the TOR pathways which is also involved in the regulation of autophagy in yeast [219][167][166]. Both Tor and Ras often control overlapping effectors, including effectors involved in autophagy. We investigated whether the overexpression of either *RAS2*, *RAS2*^{S225A} or *RAS2*^{S225E} led to changes in cells ability to regulate autophagy. We observed no significant differences in autophagic flux upon the overexpression of *RAS2*^{S225A} or *RAS2*^{S225E} when compared to the control strain, indicating that the overexpression of either *RAS2*^{S225A} or *RAS2*^{S225E} does not result in autophagic flux abnormalities.

We show that the expression of *RAS2*^{S225A} or *RAS2*^{S225E}, in both a wild type and *Δras2* background results in a loss of viability but is not accompanied by elevated DHE or PI staining. An explanation is that cells expressing the mutant *RAS2* alleles are in fact senescent or quiescent and that the loss of viability does not represent cell death, but rather an inability to divide. To address this, we investigated levels of respiration within wild type cells overexpressing *RAS2*^{S225A} or *RAS2*^{S225E}. We can confirm that wild type cells overexpressing *RAS2*^{S225A} or *RAS2*^{S225E} are respiring suggesting these cells are not dead but have an inability to divide.

The findings in this chapter clearly suggest an important role of the Ser^{225} residue of Ras2 for both protein localisation and function. We hypothesized that this residue may be conserved in higher eukaryotes. To address this, sequence alignment between the Ras2 protein and the human N-Ras protein was performed. Interestingly, although significant sequence divergence between the yeast and human Ras proteins outside of the GTPase domain and C terminal CAAX box, we discovered that Ras2 Serine^{S225} was conserved in human N-Ras at Serine^{173}. As

sequence alignment revealed conservation of the yeast Ras2^{S225} phosphorylation site in the human Nras protein, constructs expressing human *NRAS* or human *NRAS* mutations at the equivalent phosphorylation site (Ser^{173}) were transformed into wild type cells. Growth analysis revealed that the overexpression of either *NRAS*, *NRAS^{S173A}* or *NRAS^{S173E}* in wild type cells resulted in severe growth defects and reduced viability when compared to the wild type control. However, it appears that the overexpression of human *NRAS* in the yeast system is inherently toxic and therefor the importance of the *NRAS^{S173}* is unknown and requires further investigation.

In this study we observed a loss in viability upon the overexpression of *RAS2^{S225A}* or *RAS2^{S225E}* that cannot be explained by cell death. We therefor propose that the loss of viability observed in these cells is not attributable to cell death but rather a cessation of cell growth. Future investigations will focus on determining the nature of the growth arrest driven by the miss localisation of active Ras and to determine under which conditions cells can re-engage in the cell cycle.

Chapter 4

Probing the Ras/cAMP/PKA pathway

4.1 Introduction

The Ras/cAMP/PKA pathway in *S. cerevisiae* plays a major role in the control of growth and metabolism in response to nutrients. The main positive regulator of the pathway is Cdc25, which in response to nutrients, activates the redundant small GTPases Ras1 and Ras2 [78]. GTP-bound Ras activates adenylate cyclase, stimulating the production of cAMP. An increase in cAMP results in the activation of Protein Kinase A (PKA) via the dissociation of the PKA regulatory subunit Bcy1 from the PKA catalytic subunit(s) encoded by *TPK1*, *TPK2* and *TPK3* [81][192]. Upon activation, PKA controls a number of essential cellular and physiological processes such as growth, resting state, glycogen and trehalose content, carbohydrate and nitrogen metabolism, stress tolerance and the expression of genes that are controlled by STRE-boxes in their promotors [226][154][216].

The production of cAMP plays an integral role in the transmission and coordination of nutrient signals into the cell. Extracellular glucose levels in the growth medium are coupled to intracellular cAMP concentrations that regulate appropriate responses [227][228]. Control of cAMP levels is essential for yeast cell adaption, for example the regulation has been shown to mediate glycogen storage, oxidative metabolism, response to heat shock as well as a commitment to cell death [228][229][230][147]. Ras activity and cAMP levels are also tightly linked to growth, for example the expression of ribosomal protein genes is increased upon cAMP elevation to support cell division [119]. The production of intracellular cAMP is tightly regulated through feedback loops and the action of the phosphodiesterases, which catalyse the degradation of cAMP [86][85]. *S. cerevisiae* contains two cAMP phosphodiesterases, *PDE1* and *PDE2*, which encode a low-affinity (Pde1) and a high-affinity cAMP phosphodiesterase (Pde2) [86][85]. Pde2 is an Mg2+ requiring, zinc-binding enzyme which controls the basal

cAMP levels in the cell and thereby protects it from changes in the extracellular environment [88].

Mutations that inhibit the production of cAMP, such as seen in *Δcdc25* mutants, prevent progression through the cell cycle check point in late G1 called start, rendering cells arrested in G1 in a manner closely resembling the cell cycle arrest promoted by nutrient depletion [231][232]. While mutations that activate the Ras/cAMP pathway, such as activating mutations in the *RAS2* gene and *BCY1* mutations appear to present the opposite phenotype. Wild type cells perform G1 arrest in response to nutrient depletion [233], where cells carrying activating mutations in the Ras/cAMP pathway fail to accumulate as G1-arrested cells upon nutrient deprived conditions [115]. Cells with constitutive Ras/cAMP signalling, such as the ras^{val19} mutant, fail to adapt to nutrient depletion and rapidly lose viability [98].

We have shown that the overexpression of $RAS2^{S225A}$ or $RAS2^{S225E}$ in wild type cells lead to growth defects, reduced viability, sensitivity to both reactive oxygen species and copper and reduced respiration. We show that the overexpression of $RAS2^{S225A}$ or $RAS2^{S225E}$ results in the miss localisation of active Ras populations to the nuclear envelope during both log and stationary phases of growth. We hypothesize that such defects are a result of an early transition into a post-diauxic growth because of the miss localisation of active Ras populations to nuclear envelope. Previous studies have established a correlation between post-translational processing of Ras, its membrane localization, and its biological activity [234][235][61]. In *S. cerevisiae*, Ras proteins are localised predominantly in the cell in a membrane compartment, as are other components of the signal transduction pathway with which Ras interacts, including adenylyl cyclase and Cdc25 [236][237]. Mutation of the site of farnesylation in Ras blocks all post-translational processing, abolishes its biological activity,

and renders the protein predominantly cytoplasmic [78]. This has prompted models suggesting that post-translational modification of Ras is essential for its biological activity because it allows co-localization of Ras with other components of the signal transduction apparatus.

As the predominant plasma membrane localisation of active Ras during log phase growth was not observed in cells overexpressing either *RAS2*^{S225A} or *RAS2*^{S225E}, we sought to investigate whether the premature transition into reduced growth was induced through aberrant Ras/cAMP signalling. To address this, *RAS2*^{S225A} or *RAS2*^{S225E} mutant alleles were overexpressed in strains lacking different components of the RAS/cAMP/PKA pathway and growth and viability were conducted.

4.2 Growth analysis of the overexpression of *RAS2^{S225A}* or *RAS2^{S225E}* in a *Δpde2* background

Pde2 is a high-affinity cAMP phosphodiesterase which catalyses the degradation of cAMP [86]. The deletion of *PDE2* leads to an elevation in intracellular cAMP, resulting in the over activation of PKA [238][165]. To investigate whether an increase in activation of the Ras/cAMP/PKA pathway in cells overexpressing *RAS2^{S225A}* or *RAS2^{S225E}* resulted in further changes in growth and viability, we overexpressed either *RAS2^{S225A}* or *RAS2^{S225E}* in a *Δpde2* background and conducted both growth and viability assays.

4.2.1 Over expression of *RAS2^{S225A}* or *RAS2^{S225E}* in a *Δpde2* background leads to growth defects

The growth of cells overexpressing *RAS2^{S225A}*, *RAS2^{S225E}* or containing an empty plasmid control in a *Δpde2* background was analysed using the growth assay described in Materials and Methods, Section 2.9.1. The growth of *Δpde2* strains was compared to a wild type strain expressing an empty plasmid control. The overexpression of *RAS2^{S225A}* or *RAS2^{S225E}* in a *Δpde2* background lead to a significant increase in lag time and reached a lower final biomass when compared to the control strain in both the wild type and *pde2* deletion background *(Figure 48)*. When compared to the wild type control, *Δpde2* strains expressing an empty plasmid control displayed an early transition into the post-diauxic phase of cell growth and reached a lower final biomass after 24 hours of growth *(Figure 48)*. When compared to the overexpression of either *RAS2^{S225A}* or *RAS2^{S225E}* in a wild type background *(Figure 28)*, a significant increase in lag time and decrease in overall biomass was observed after 24 hours of growth when either *RAS2^{S225A}* or *RAS2^{S225E}* was overexpressed in a *Δpde2* background *(Figure 48)*.

No significant difference in growth rates was observed between wild type cells or *Δpde2* cells expressing an empty plasmid control *(Figure 49)*. Although, a significant decrease in growth rate was observed in strains overexpressing *RAS2*^{S225A} or *RAS2*^{S225E} in a *pde2* deletion background when compared the wild type and *Δpde2* control strain *(Figure 49)*. When compared to the growth rate of wild type cells overexpressing either *RAS2*^{S225A} or *RAS2*^{S225E} *(Figure 29)*, we observed a 60-minute decrease in growth rate when overexpressing *RAS2*^{S225A} or *RAS2*^{S225E} in a *Δpde2* background. Our results imply that a loss in the ability to control the activation of the Ras/cAMP/PKA results in a further loss in fitness upon the overexpression of either *RAS2*^{S225A} or *RAS2*^{S225E}, as supported by previous published observations, Leadsham et al 2010 [224].

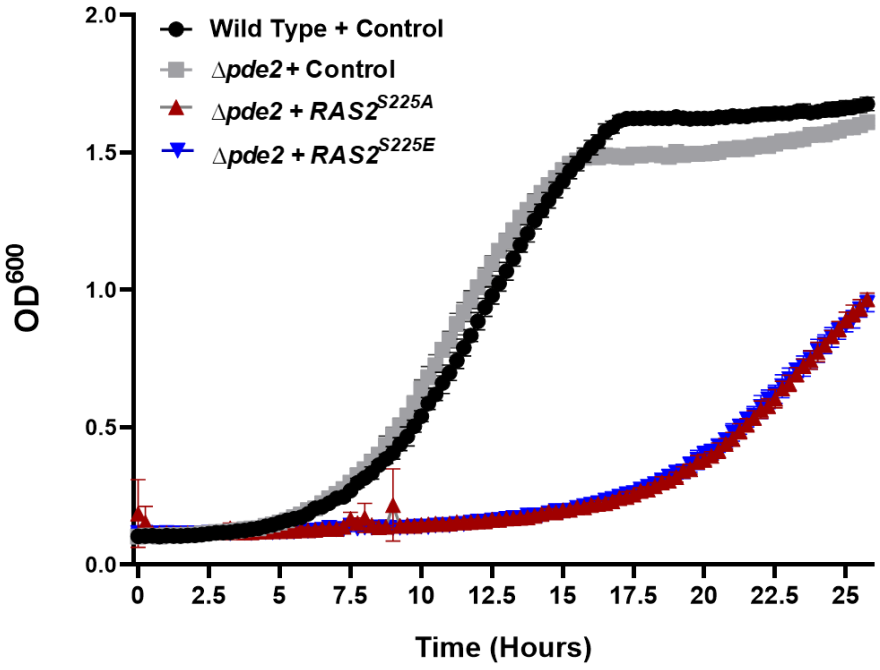

Figure 48. Growth analysis of cells overexpressing RAS2^{S225A}, RAS2^{S225E} or empty plasmid control in Δpde2 background.

Wild type cells expressing an empty plasmid control was assayed as an additional control. The growth analysis was carried out in SD –URA media as described in Materials and Methods (Section 2.9.1). The experiment was repeated three times and representative data set is shown. This data represents an average of three technical repeats and error bars represent the standard deviation.

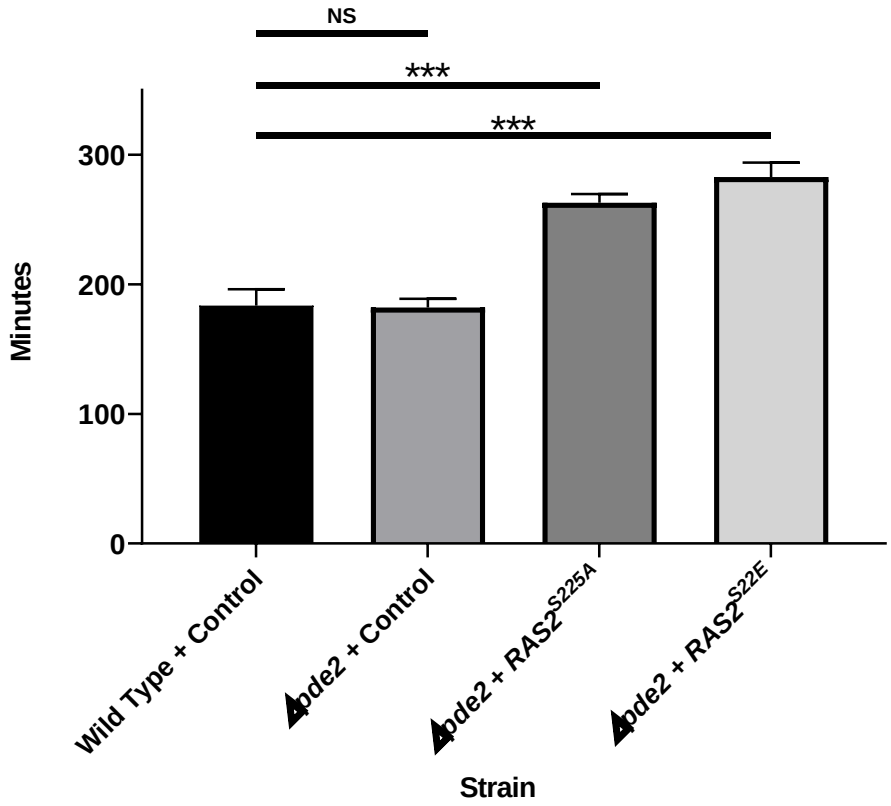

Figure 49. Growth rate analysis of cells overexpressing RAS2^{S225A}, RAS2^{S225E} or an empty plasmid backbone control in Δpde2 background.

*Wild type cells expressing an empty plasmid control was assayed as an additional control. The growth rate analysis was carried out as described in Materials and Methods (Section 2.9.1). The experiment was repeated three times and representative data set is shown. The data represents an average of three technical repeats and error bars represents the standard deviation. A One-way ANOVA using a Dunnets multiple comparison test was used to determine statistical significance. Non-significant = NS, * = adjusted p-value ≤ 0.05 and *** = adjusted p value ≤ 0.001.*

4.2.2 The Overexpression of either *RAS2^{S225A}* or *RAS2^{S225E}* in a *Δpde2* background leads to a further decrease in viability when compared to the overexpression of *RAS2* mutants in wild type cells

To determine whether the overexpression of either *RAS2^{S225A}* or *RAS2^{S225E}* in a *Δpde2* background lead to a reduction in viability, a viability assay was conducted as described in Materials and Methods, Section 2.9.3. The viability of cells overexpressing *RAS2^{S225A}* or

RAS2^{S225E} in a *Δpde2* background was compared to wild type cells expressing the *RAS2*^{S225A} or *RAS2*^{S225E} to attest whether the deletion of *pde2* further attenuated viability.

An overnight culture was re-inoculated to 2 x 10^3 cells/ml and incubated for 24 hours. 300 cells were plated onto selective, -URA agar plates. These were left to incubate at 30 °C for 36 hours and the colonies were then counted to allow quantification of colony forming units (CFUs). Viability of cells analysed from the inoculated culture represented the viability of cells, or cell death, during nutrient deprivation.

A wild type strain expressing a control plasmid grown for 24 hours, had approximately 40 % viability when grown on SD -URA medium. The expression of an empty plasmid control in a *Δpde2* background lead to no significant change in viability when compared to the wild type control strain *(Figure 50)*. The overexpression of *RAS2*^{S225A} or *RAS2*^{S225E} in a *Δpde2* background presented a significant reduction in viability when compared to the wild type and *Δpde2* control strains *(Figure 50)*. Upon the deletion of *PDE2*, cells overexpressing either *RAS2*^{S225A} or *RAS2*^{S225E} presented a significant decrease in viability when compared to wild type cells overexpressing *RAS2*^{S225A} or *RAS2*^{S225E} *(Figure 50)*. Indicating that the deletion of *pde2* in wild type cells overexpressing *RAS2*^{S225A} or *RAS2*^{S225E} further attenuates viability.

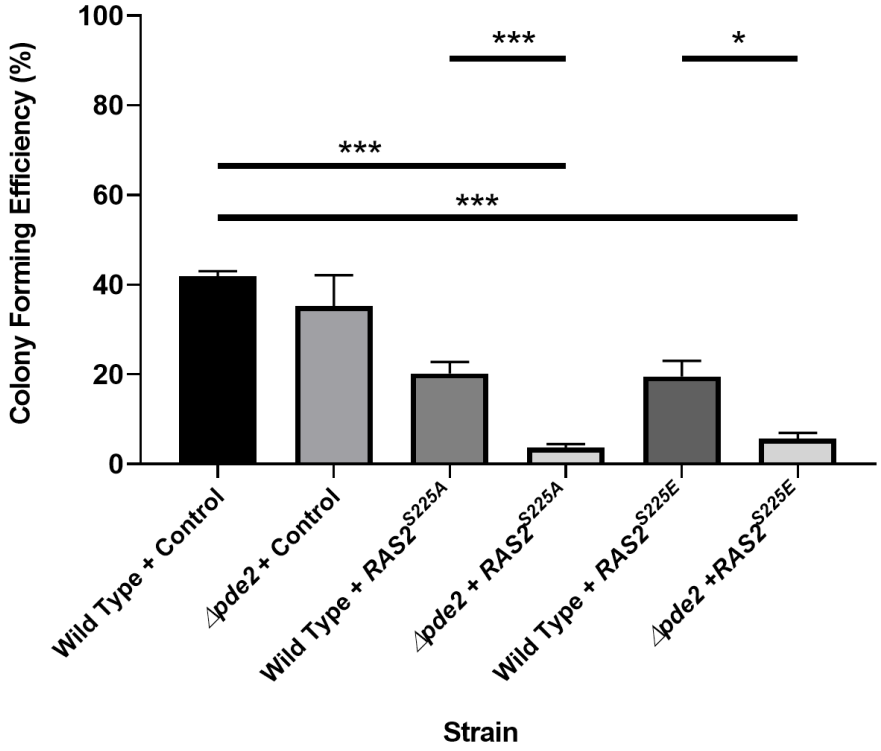

Figure 50. A colony forming efficiency assay of S. cerevisiae wild type and Δpde2 cells overexpressing RAS2^{S225A}, RAS2^{S225E}or an empty plasmid control, grown in SD –URA.
*The colony forming efficiency analysis was carried out as described in Materials and Methods (Section 2.9.3). The data presented is the average of three biological repeats and error bars represent standard deviation. A One-way ANOVA using a Tukey multiple comparison test was used to determine statistical significance. Non-significant = NS, * = adjusted p-value ≤ 0.05 and *** = adjusted p value ≤ 0.001.*

4.3 Growth analysis of wild type cells co-expressing *PDE2* and the *RAS2* mutant alleles

4.3.1 The co-expression of *PDE2* in wild type cells overexpressing *RAS2^{S225E}* rescues growth defects

We have previously observed that the overexpression of either *RAS2^{S225A}* or *RAS2^{S225E}* in a *Δpde2* background further attenuates growth and viability when compared to the overexpression of *RAS2^{S225A}* or *RAS2^{S225E}* in wild type cells. We hypothesize that such observations are a result of an elevation in the activity of the Ras/cAMP/PKA pathway which

is further increased due to the cells inability to degrade cAMP in the absence of *PDE2*. We investigate whether reducing the activation of the Ras/cAMP/PKA through the overexpression of *PDE2*, will lead to differences in growth and viability in cells overexpressing either $RAS2^{S225A}$ or $RAS2^{S225E}$ mutant alleles. To analyse the growth of wild type cells co-expressing *PDE2* with $RAS2^{S225A}$, $RAS2^{S225E}$ or an empty plasmid backbone, a growth assay was performed as described in Materials and Methods, Section 2.9.1. The growth of these strains was compared to a wild type strain expressing an empty plasmid control.

All strains overexpressing *PDE2* presented an early transition into post diauxic growth and reached a lower final biomass after 24 hours of growth when compared to the wild type control *(Figure 51)*. Interestingly, the overexpression of *PDE2* in wild type cells overexpressing $RAS2^{S225E}$ lead to no observable growth defects when compared to wild type cells co-expressing *PDE2* with the empty plasmid control. Wild type cells co-expressing *PDE2* with $RAS2^{S225A}$ presented significant growth defects when compared to the wild type cells co-expressing *PDE2* with the empty plasmid control *(Figure 51)*.

A decreased growth rate when compared to the wild type control was observed in all *PDE2* overexpression strains. An increase in growth rate was observed when *PDE2* was co-expressed with $RAS2^{S225E}$ when compared to the *PDE2* overexpression control strain *(Figure 52)*. However, no significant differences in growth rate were observed when *PDE2* was co-expressed with $RAS2^{S225A}$ in wild type cells when compared to the *PDE2* overexpression control strain *(Figure 52)*. Our data indicates that the overexpression of *PDE2* in wild type cells overexpressing either $RAS2^{S225A}$ or $RAS2^{S225E}$ results in a rescue of the growth rate defects.

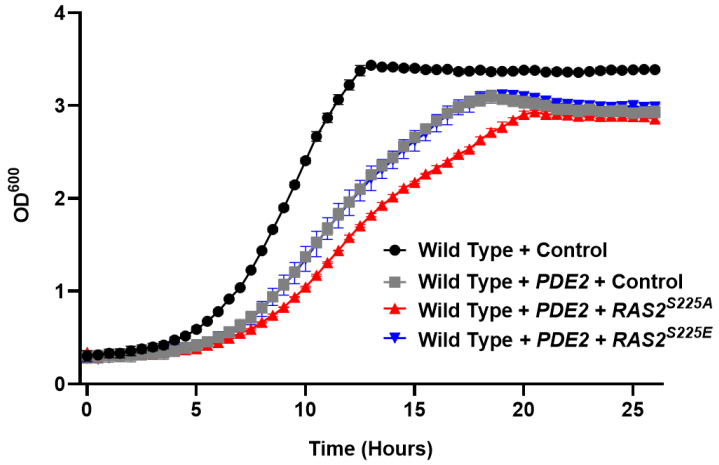

Figure 51. Growth analysis of wild type cells co-expressing PDE2 with either RAS2^{S225A}, RAS2^{S225E} or empty plasmid control.

Wild type cells expressing an empty plasmid control was assayed as an additional control. The growth analysis was carried out in SD -URA/-LEU media as described in Materials and Methods (Section 2.9.1). The experiment was repeated three times and representative data set is shown. This data represents an average of three technical repeats and error bars represent the standard deviation.

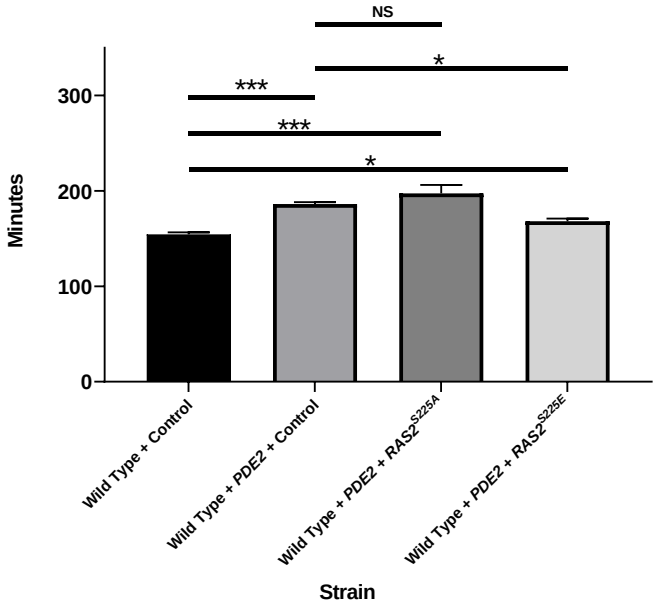

Figure 52. Growth rate analysis of wild type cells overexpressing RAS2^{S225A}, RAS2^{S225E} or an empty plasmid backbone co-expressed with PDE2.

*Wild type cells expressing an empty plasmid control was assayed as an additional control. The growth rate analysis was carried out as described in Materials and Methods (Section 2.9.1). The experiment was repeated three times and representative data set is shown. The data represents an average of three technical repeats and error bars represents the standard deviation. A One-way ANOVA using a Tukey multiple comparison test was used to determine statistical significance. Non-significant = NS, * = adjusted p-value ≤ 0.05 and *** = adjusted p value ≤ 0.001.*

4.3.2 The expression of *PDE2* in wild type cells overexpressing $RAS2^{S225A}$ or $RAS2^{S225E}$ rescues viability

To determine whether the overexpression of *PDE2* in wild type cells overexpressing $RAS2^{S225A}$, $RAS2^{S225E}$ or an empty plasmid control resulted in a change in viability, a viability assay was conducted as described in Materials and Methods, Section 2.9.3.

The viability of wild type cells overexpressing $RAS2^{S225A}$ or $RAS2^{S225E}$ and *PDE2* was compared to wild type cells expressing the *RAS2* mutant alleles without *PDE2* overexpression. When compared to the wild type control, no significant differences in viability was observed when *PDE2* was overexpressed in wild type cells overexpressing $RAS2^{S225A}$ or $RAS2^{S225E}$ *(Figure 53)*. Suggesting that overexpression of *PDE2* rescues viability when co-expressed with either $RAS2^{S225A}$ or $RAS2^{S225E}$. In wild type cells overexpressing $RAS2^{S225A}$ or $RAS2^{S225E}$ only, the percentage of viable cells was significantly lower than when *PDE2* was co-overexpressed with $RAS2^{S225A}$ or $RAS2^{S225E}$ *(Figure 53)*.

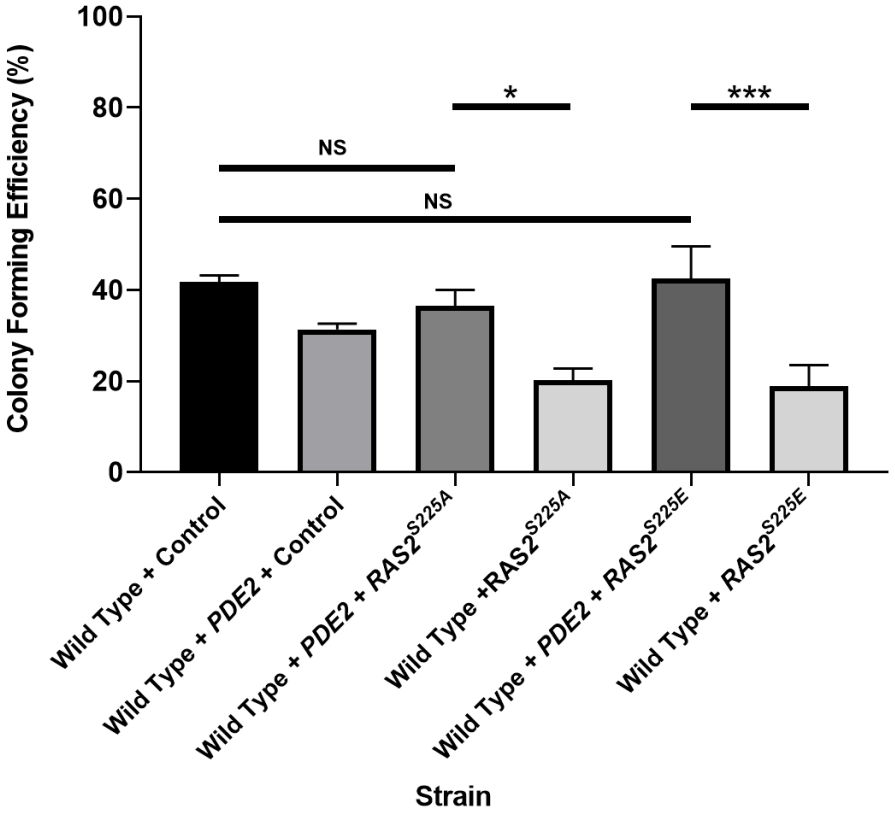

Figure 53. A colony forming efficiency assay of wild type cells overexpressing RAS2^{S225A}, RAS2^{S225E} or an empty plasmid backbone co-expressed with PDE2.

*Cells were grown in SD-URA/-LEU or -URA. The colony forming efficiency analysis was carried out as described in Materials and Methods (Section 2.9.3). The data presented is the average of three biological repeats and error bars represent standard deviation. A One-way ANOVA using a Tukey multiple comparison test was used to determine statistical significance. Non-significant = NS, * = adjusted p-value ≤ 0.05 and *** = adjusted p value ≤ 0.001.*

4.4 Growth analysis of the effects of the deletion of *TPK1*, *TPK2* or *TPK3* on wild type cells overexpressing *RAS2*^{S225A} or *RAS2*^{S225E}

4.4.1 Deletion of *TPK2 or TPK3* reduces growth defects in cells overexpressing *RAS2*^{S225A} or *RAS2*^{S225E}

PKA is a heterotetramer comprised of two regulatory subunits and two catalytic subunits [239]. In *S. cerevisiae, BCY1* encodes the regulatory subunit and the catalytic subunits are encoded by *TPK1*, *TPK2* and *TPK3*. [81][78]. The binding of two cAMP molecules to each regulatory subunit in the holoenzyme triggers the release of the catalytic subunits and their activation. The PKA subunits Tpk1, 2 and 3 share overlapping functions but also have been shown to be involved in the regulation of several separable processes. Tpk1 has been identified to play a role in the branched chain amino acid biosynthesis pathway, mitochondrial DNA stability and mitochondrial iron homeostasis [82]. Whereas Tpk2 has been shown to impact iron uptake, trehalase synthesis and water homeostasis [82][83]. However, constitutive PKA activity can prove deleterious, with the overexpression of *TPK3* shown to inhibit growth [84].

We have previously shown that the viability of wild type cells overexpressing either *RAS2*^{S225A} or *RAS2*^{S225E} can be significantly altered though either the deletion or overexpression of *PDE2*. Our results indicate that the overexpression of *RAS2* mutant alleles results in an inability of cells to appropriately regulate the Ras/cAMP/PKA pathway. We sort to investigate whether the deletion of one or more of the TPK subunits in strains overexpressing *RAS2*^{S225A} or *RAS2*^{S225E} results in any significant changes in growth and viability.

To analyse the growth of cells overexpressing *RAS2*^{S225A}, *RAS2*^{S225E} or an empty plasmid backbone control in a *Δtpk1, Δtpk2 or Δtpk3* background, a growth assay was performed as

described in Materials and Methods, Section 2.9.1. The growth of *Δtpk1, Δtpk2 or Δtpk3* strains was compared to a wild type strain containing an empty plasmid *(Figure 54)*.

The overexpression of either *RAS2*^{S225A} or *RAS2*^{S225E} in a *Δtpk1, Δtpk2 or Δtpk3* background presented an early transition into post diauxic growth and reached a lower final biomass after 24 hours of growth when compared to all strains expressing an empty plasmid control *(Figure 54)*. Strains expressing either *RAS2*^{S225A} or *RAS2*^{S225E} in a *Δtpk1* background presented the most severe growth defects when compared to control strains *(Figure 54)*. When compared to the overexpression of *RAS2*^{S225A} or *RAS2*^{S225E} in wild type cells, the expression of *RAS2* mutant alleles in a *Δtpk2 or Δtpk3* background presented a reduction in the severity of the growth defects *(Figure 54)*. In both a *Δtpk2 or Δtpk3* background, the overexpression of either *RAS2*^{S225A} or *RAS2*^{S225E} displayed no significant changes in growth rate when compared to the wild type control *(Figure 55)*. Whereas expression in a *Δtpk1* background led to a decrease in growth rate when compared to the wild type control strain *(Figure 55)*. This data suggests that the loss of either *TPK2* or *TPK3* in cells overexpressing *RAS2*^{S225A} or *RAS2*^{S225E} leads to a rescue of growth rate defects, indicating an involvement of the function of Tpk2 and Tpk3 in

the toxic effects on growth rate induced by the overexpression of either *RAS2*^{S225A} or *RAS2*^{S225E}.

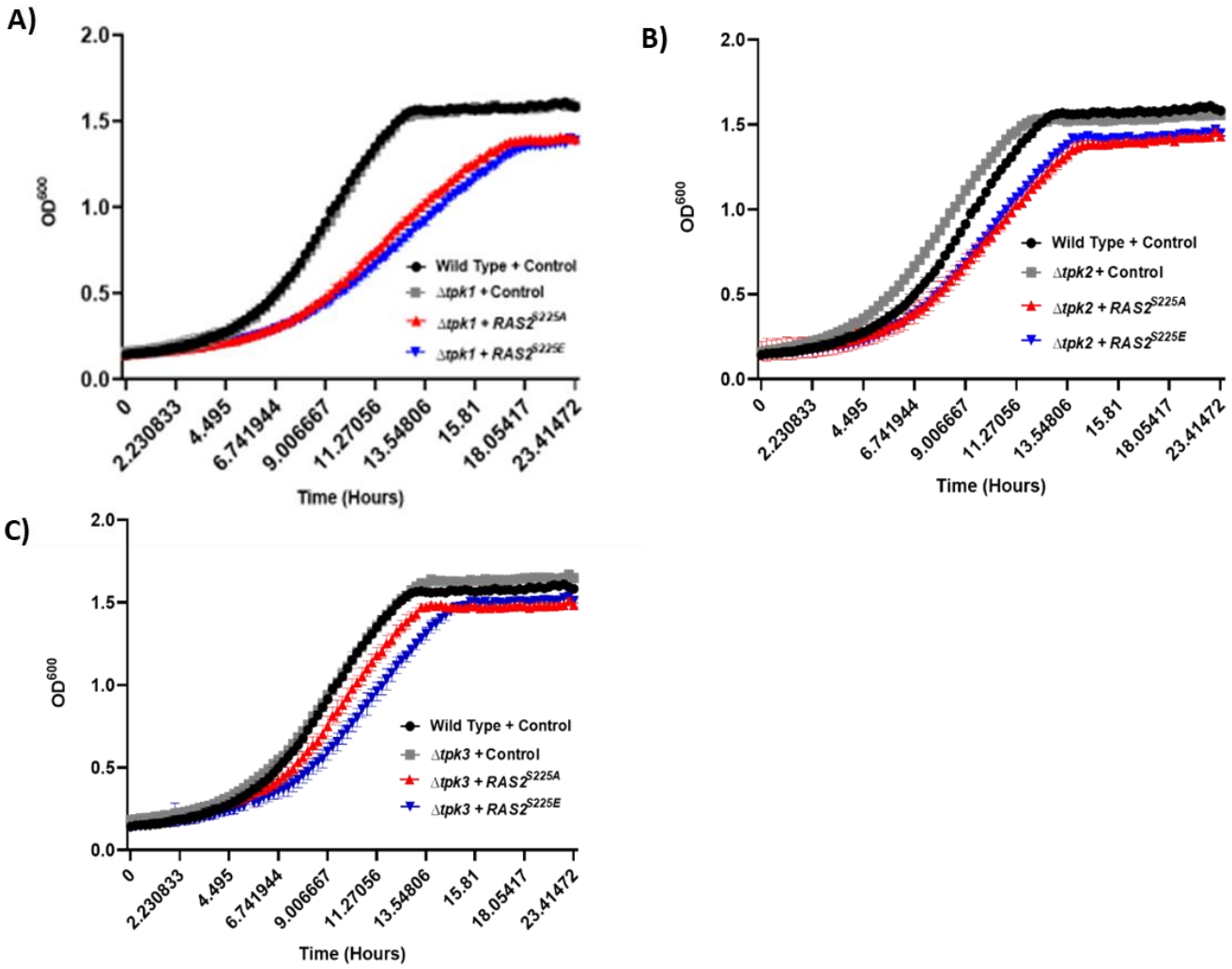

Figure 54. Growth analysis of cells overexpressing RAS2^{S225A}, RAS2^{S225E} or empty plasmid control in Δtpk1 (A), Δtpk2 (B) or Δtpk3 (C)

Wild type cells expressing an empty plasmid control was assayed as an additional control. The growth analysis was carried out in SD –URA media as described in Materials and Methods (Section 2.9.1). The experiment was repeated three times and representative data set is shown. This data represents an average of three technical repeats and error bars represent the standard deviation.

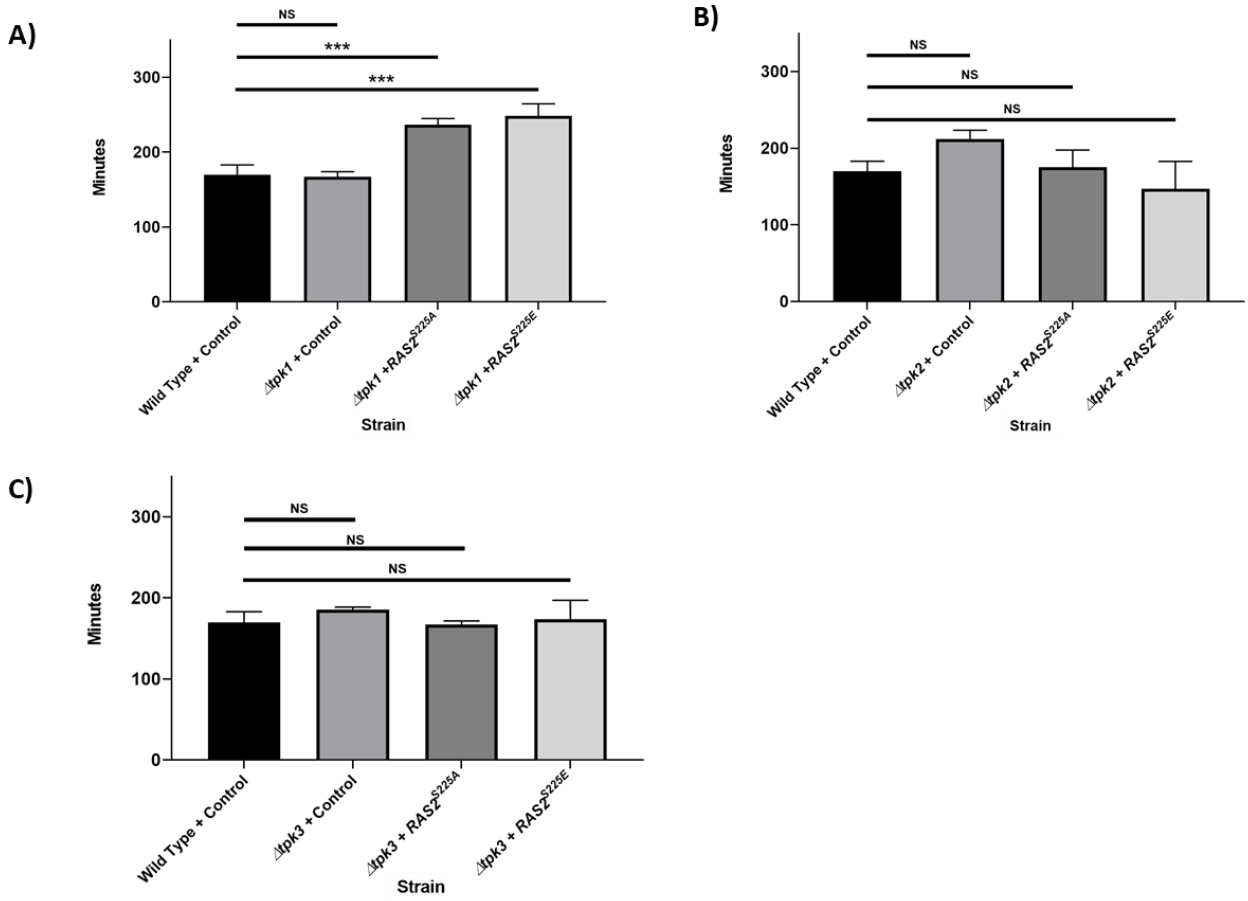

Figure 55. Growth rate analysis of wild type cells overexpressing RAS2^{S225A}, RAS2^{S225E} or an empty plasmid backbone in Δtpk1 (A), Δtpke2 (B) or Δtpk3 background (C).

*Wild type cells expressing an empty plasmid control was assayed as an additional control. The growth rate analysis was carried out as described in Materials and Methods (Section 2.9.1). The experiment was repeated three times and representative data set is shown. The data represents an average of three technical repeats and error bars represents the standard deviation. A One-way ANOVA using a Dunnetts multiple comparison test was used to determine statistical significance. Non-significant = NS, * = adjusted p-value ≤ 0.05 and *** = adjusted p value ≤ 0.001.*

4.4.2 Analysis of viability in *Δtpk1, Δtpk2* or *Δtpk3* cells overexpressing *RAS2^{S225A}* or *RAS2^{S225E}*

To determine whether the overexpression of either *RAS2^{S225A}* or *RAS2^{S225E}* in a *Δtpk1, Δtpk2 or Δtpk3* background led to changes in viability, a viability assay was conducted as described in Materials and Methods, Section 2.9.3. The viability of cells overexpressing *RAS2^{S225A}* or *RAS2^{S225E}* in a *tpk1, tpk2 or tpk3* single deletion background was compared to wild type or *tpk1-3* deletion strains expressing an empty plasmid control. The viability of wild type cells overexpressing *RAS2^{S225A}* or *RAS2^{S225E}* was also compared to the viability observed upon the overexpression of *RAS2^{S225A}* or *RAS2^{S225E}* in a *tpk1, tpk2 or tpk3* single deletion background.

An overnight culture was re-inoculated to 2 x 10^3 cells/ml and incubated for 24 hours. 300 cells were plated onto selective, -URA agar plates. These were left to incubate at 30 °C for 36 hours and the colonies were then counted to allow quantification of colony forming units (CFUs). Viability of cells analysed from the inoculated culture represented the viability of cells, or cell death, during nutrient deprivation. After 24 hours of growth, a wild type strain expressing a control plasmid, had approximately 40 % viability when grown on SD -URA medium.

Upon the deletion of *tpk1* in all strains, a reduction in viability was observed when compared to the wild type control *(Figure 56)*. *Δtpk1* cells expressing an empty plasmid control presented a significant decrease in viability when compared to the wild type control, suggesting a putative function of Tpk1 in the maintenance of viability under the growth conditions used. Interestingly, the expression of *RAS2^{S225A}* in a *Δtpk1* background lead to an increase in viability when compared to *Δtpk1* cells expressing an empty plasmid control *(Figure 56)*. However, no significant change in viability was observed when compared to wild

type cells overexpressing *RAS2*^{S225A} *(Figure 56)*. No significant changes in viability was observed when *RAS2*^{S225E} was expressed in a *Δtpk1* background when compared to the *Δtpk1* control strain *(Figure 56)*. A decrease in viability was seen in cells overexpressing *RAS2*^{S225E} in a *Δtpk1* background when compared to wild type strains overexpressing *RAS2*^{S225E} *(Figure 56)*. Our data suggests that Tpk1p and the Ras2p^{S225A} mutants are acting within different pathways, as loss of *TPK1* leads to a loss in viability which can be improved upon the overexpression of *RAS2*^{S225A}. However, the loss of *TPK1* increases the toxic effects on viability upon the overexpression of *RAS2*^{S225E} when compared to the expression of *RAS2*^{S225E} in wild type cells but not when compared to the *Δtpk1* control, providing further evidence to suggest that Tpk1 and *RAS2* mutant alleles are functioning independently. This observation aligns with the data shown in *Figure 54*, suggesting that the toxic effects induced by the overexpression of *RAS2*^{S225A} or *RAS2*^{S225E} are not mediated through Tpk1.

Upon the overexpression of *RAS2*^{S225A} or *RAS2*^{S225E} in a *Δtpk2* background a decrease in viability was observed when compared to the wild type control and the *Δtpk2* control strain *(Figure 56)*. Interestingly, an increase in viability is observed in *Δtpk2* cells expressing an empty plasmid control when compared to the wild type control suggesting that *TPK2* has a putative function in reducing viability during the post diauxic shift under the growth conditions used *(Figure 56)*. The overexpression of *RAS2*^{S225A} or *RAS2*^{S225E} in a *Δtpk2* background results in no further decrease in viability when compared to the overexpression of *RAS2*^{S225A} or *RAS2*^{S225E} in a wild type background *(Figure 56)*. We therefore propose that the loss in viability induced by the overexpression of *RAS2* mutant alleles in cells does not depend on Tpk2 alone. Therefor the role of Tpk2 in exponential growth is separable from the observed loss of viability during stationary phase growth.

Upon the overexpression of *RAS2*^{S225A} or *RAS2*^{S225E} in *Δtpk3* cells a significant decrease in viability is observed when compared to the wild type and *Δtpk3* control strains *(Figure 56)*. No significant difference in viability was observed between the wild type and *Δtpk3* control strain *(Figure 56)*. Indicating the deletion of *tpk3* does not play an important function in maintenance of cell viability under the conditions used. Our data suggests that the deletion of *tpk3* in cells overexpressing *RAS2*^{S225A} or *RAS2*^{S225E} does not rescue viability to wild type levels. However, a significant decrease in viability was observed upon the deletion of *tpk3* in cells overexpressing *RAS2*^{S225E} when compared to wild type cells overexpressing either *RAS2*^{S225E}. However, no significant difference in viability was observed between the overexpression of *RAS2*^{S225A} in a *Δtpk3* or wild type background. Our data indicates that the loss of *tpk3* in cells overexpressing *RAS2*^{S225E} results in a further attenuation of viability. However, the loss of *tpk3* in cells overexpressing *RAS2*^{S225A} does not present any changes in viability when compared to expression of *RAS2*^{S225A} in wild type cells. Overall, we show the loss viability observed upon expression of the RAS mutant alleles used here cannot be attributed to the activity of any single PKA subunit.

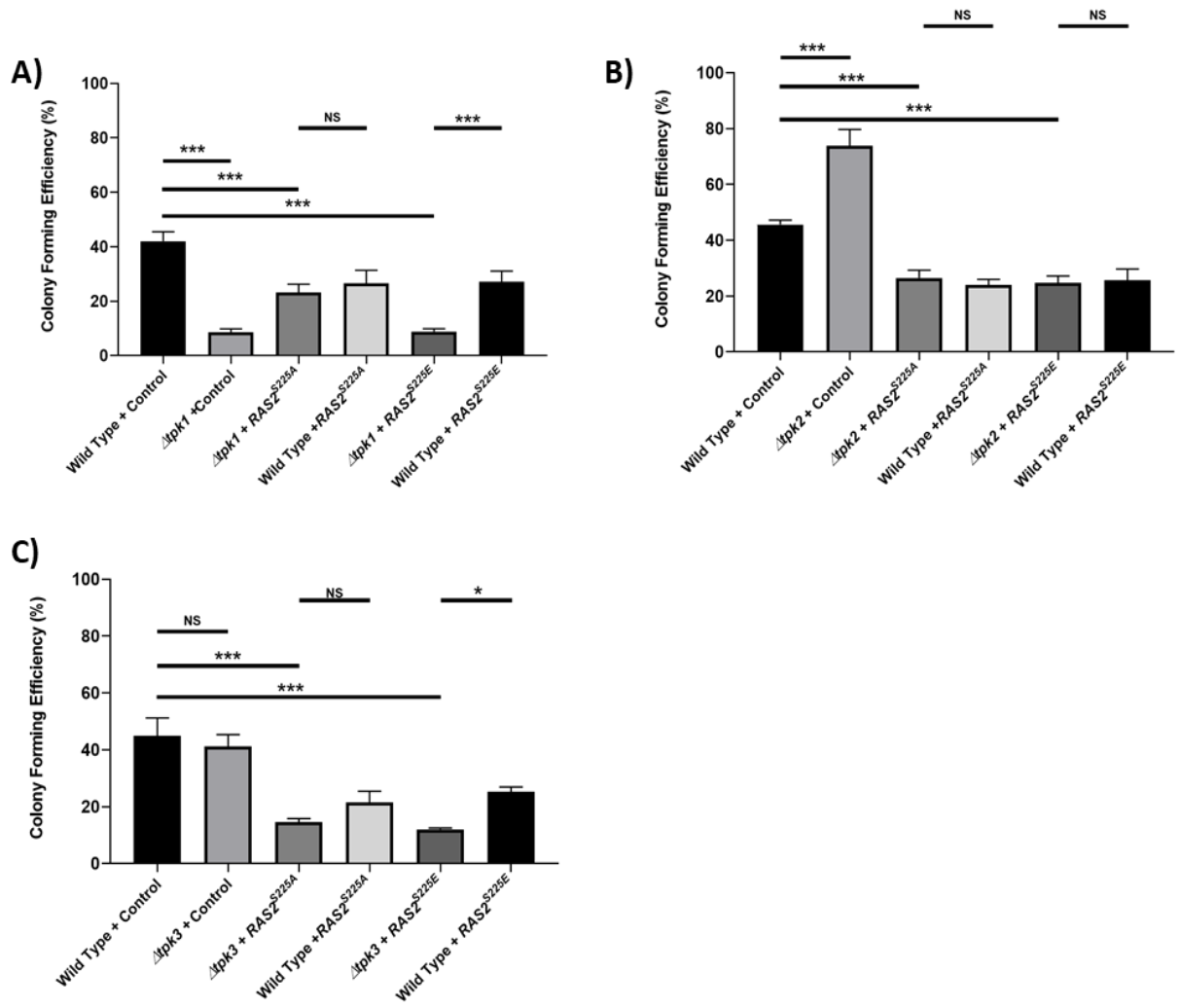

Figure 56. A colony forming efficiency assay of S. cerevisiae wild type, Δtpk1 (A), Δtpk2 (B) or Δtpk3 (C) cells overexpressing RAS2^{S225A}, RAS2^{S225E}or an empty plasmid control, grown in SD –URA.

*The colony forming efficiency analysis was carried out as described in Materials and Methods (Section 2.9.3). The data presented is the average of three biological repeats and error bars represent standard deviation. A One-way ANOVA using a Tukey multiple comparison test was used to determine statistical significance. Non-significant = NS, * = adjusted p-value ≤ 0.05 and *** = adjusted p value ≤ 0.001*

4.5 Growth analysis of the double deletion of *tpk1/tpk2*, *tpk3/tpk2* or *tpk1/tpk3* on wild type cells overexpressing *RAS2* mutant alleles

4.5.1 Overexpression of *RAS2* mutant alleles in tpk*1-3* double deletion backgrounds leads to no rescue of growth defects

The deletion of *TPK1*, *TPK2* or *TPK3* in cells overexpressing $RAS2^{S225A}$ or $RAS2^{S225E}$ failed to result in a complete rescue of viability or growth. We hypothesized that the double deletion of different Tpk subunits in cells overexpressing the *RAS2* mutant alleles may result in a full restoration of viability to that of the wild type control.

To analyse the growth of cells overexpressing $RAS2^{S225A}$, $RAS2^{S225E}$ or an empty plasmid backbone control in a *Δtpk1/ Δtpk2, Δtpk2/ Δtpk3 or Δtpk1/ Δtpk3* background, a growth assay was performed as described in Materials and Methods, Section 2.9.1. The growth of mutant strains was compared to a wild type strain expressing an empty plasmid control.

The overexpression of $RAS2^{S225A}$ or $RAS2^{S225E}$ in all backgrounds presented an early transition into post diauxic growth and reached a lower final biomass after 24 hours of growth when compared to all strains expressing an empty plasmid control *(Figure 57)*. When compared to the overexpression of $RAS2^{S225A}$ or $RAS2^{S225E}$ in wild type cells, the expression of *RAS2* mutant alleles in a *Δtpk1/ Δtpk2* background presented a reduction in the severity of the growth defects previously observed when expressed in wild type cells *(Figure 57)*. Strains expressing $RAS2^{S225A}$ or $RAS2^{S225E}$ in a *Δtpk3/ Δtpk2* background presented the most severe growth defects when compared to control strains (Figure 57). We observed a marginal decrease in growth rate when $RAS2^{S225A}$ was overexpressed in a *tpk1/tpk2* when compared to the wild type control *(Figure 58)*. No significant changes in growth rate were observed upon the overexpression of $RAS2^{S225A}$ or $RAS2^{S225E}$ in a *Δtpk1/ Δtpk3* background when compared to the

wild type control *(Figure 58)*. However, a significant decrease in growth rate was observed upon the overexpression of *RAS2*^{S225A} or *RAS2*^{S225E} in *Δtpk2/ Δtpk3* background when compared to the wild type control *(Figure 58)*. We suggest that the overlapping functions of either Tpk1 and Tpk2 or Tpk1 and Tpk3 is either responsible for the reduced growth rate or that the combined loss of these subunits can compensate for the toxic effects of the overexpression of *RAS2*^{S225A} or *RAS2*^{S225E} in wild type cells.

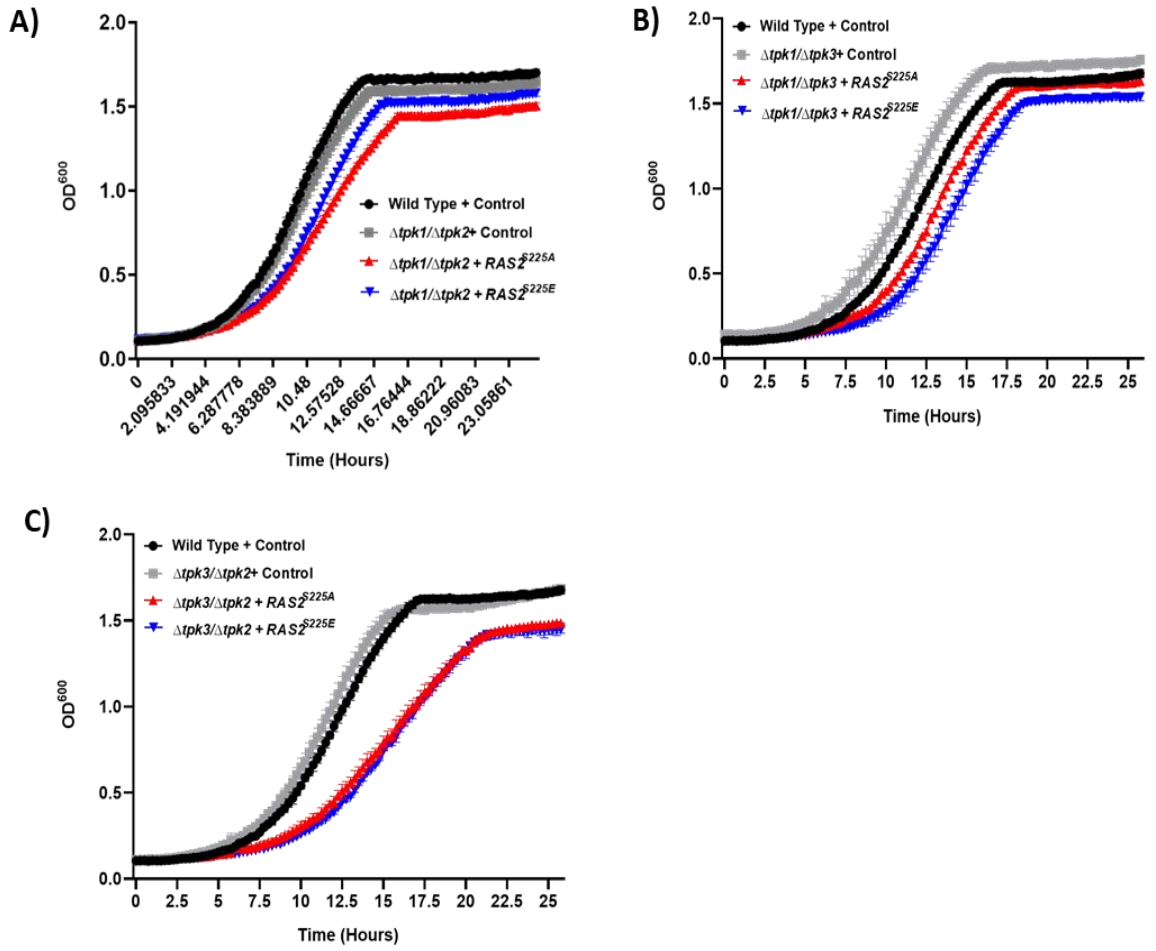

Figure 57. Growth analysis of cells overexpressing RAS2^{S225A}, RAS2^{S225E} or empty plasmid control in a Δtpk1/ Δtpk2 (A), Δtpk1/ Δtpk3 (B), or Δtpk1/ Δtpk3 (C).
Wild type cells expressing an empty plasmid control was assayed as an additional control. The growth analysis was carried out in SD –URA media as described in Materials and Methods (Section 2.9.1). The experiment was repeated three times and representative data set is shown. This data represents an average of three technical repeats and error bars represent the standard deviation.

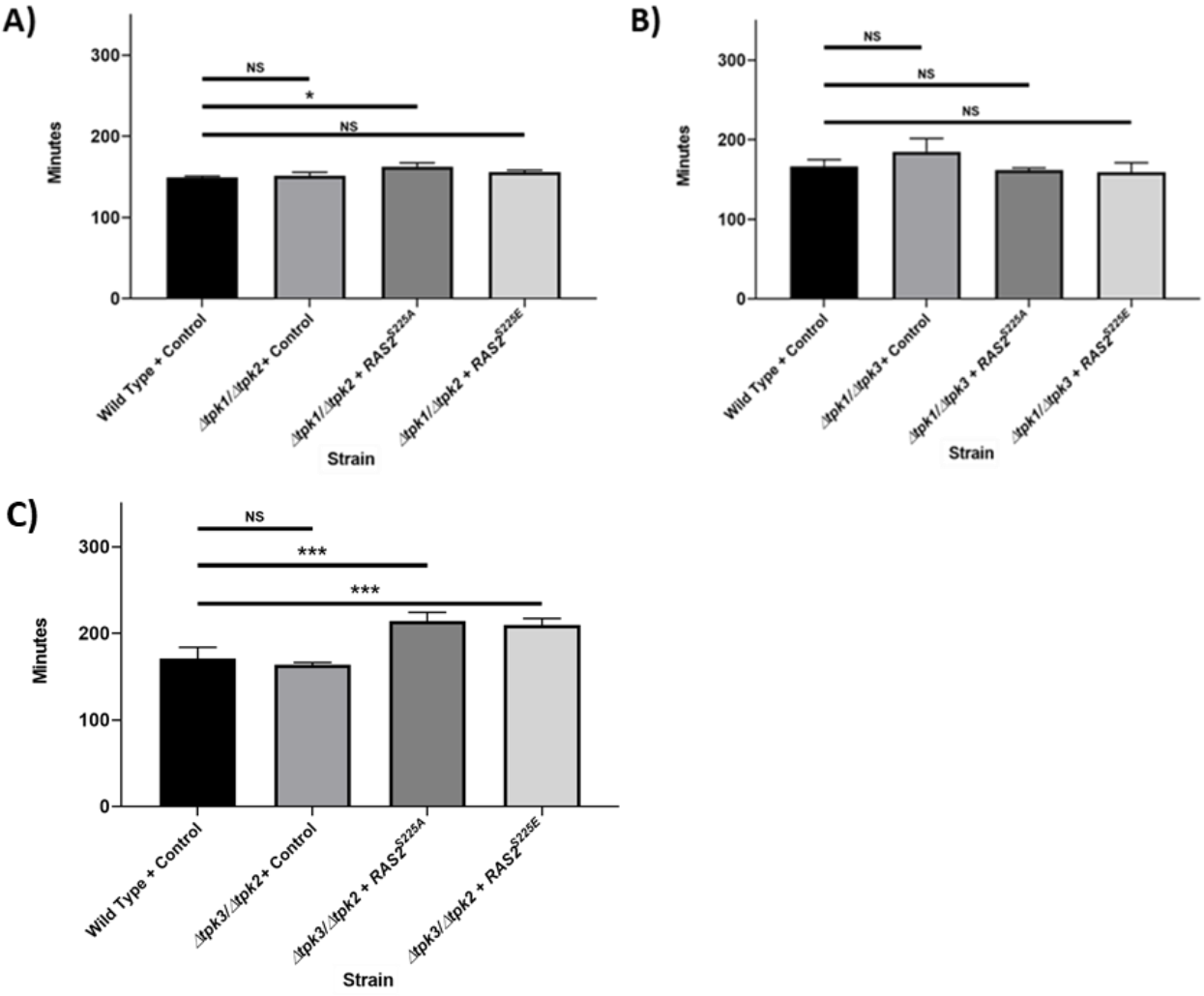

Figure 58. Growth rate analysis of yeast cells overexpressing RAS2^{S225A}, RAS2^{S225E} or an empty plasmid backbone in a Δtpk1/ Δtpk2 (A), Δtpk1/ Δtpk3 (B) or Δtpk1/ Δtpk3 (C) background.

*Wild type cells expressing an empty plasmid control was assayed as an additional control. The growth rate analysis was carried out as described in Materials and Methods (Section 2.9.1). The experiment was repeated three times and representative data set is shown. The data represents an average of three technical repeats and error bars represents the standard deviation. A One-way ANOVA using a Dunnets multiple comparison test was used to determine statistical significance. Non-significant = NS, * = adjusted p-value ≤ 0.05 and *** = adjusted p value ≤ 0.001.*

4.5.2 Analysis of viability in cells overexpressing *RAS2^{S225A}* or *RAS2^{S225E}* in a *Δtpk1/ Δtpk2, Δtpk1/ Δtpk3 or Δtpk1/ Δtpk3* background

As the overexpression of either *RAS2^{S225A}* or *RAS2^{S225E}* in a *Δtpk1, Δtpk2 or Δtpk3* background did not result in a full rescue of viability to wild type levels, the *RAS2* mutant alleles were expressed in backgrounds containing the double deletion of the genes encoding the Tpk subunits to investigate whether the combination of Tpk subunit deletions restored viability in wild type cells overexpressing the *RAS2* mutant alleles. To determine whether the overexpression of either *RAS2^{S225A}* or *RAS2^{S225E}* in a *Δtpk1/ Δtpk2, Δtpk1/ Δtpk3 or Δtpk1/ Δtpk3* background lead to a change in viability, a viability assay was conducted as described in Materials and Methods, Section 2.9.3. The viability of cells overexpressing *RAS2^{S225A}* or *RAS2^{S225E}* in Tpk subunit double deletion strains was compared to wild type and *tpk1-3* double deletion strains expressing an empty plasmid as a control.

Cells overexpressing an empty plasmid control in a *Δtpk1/ Δtpk2* background presented no significant changes in viability when compared to the wild type control *(Figure 59*). The overexpression of *RAS2^{S225A}* or *RAS2^{S225E}* in a *Δtpk1/ Δtpk2* background showed a decrease in viability when compared to the wild type and *Δtpk1/ Δtpk2* control *(Figure 59)*. However, no significant change in viability was observed when compared to wild type cells overexpressing *RAS2* mutant alleles. Our data suggests that deletion of both Tpk1 and Tpk2 in wild type cells expressing the mutant *RAS2* alleles does not result in the rescue of viability to wild type levels. This suggests that the toxicity observed through either the overexpression of *RAS2^{S225A}* or *RAS2^{S225E}* is not mediated through the combined functions of Tpk1 and Tpk2.

Cells expressing the control plasmid in a *Δtpk1/ Δtpk3* background showed a significant reduction in viability when compared to the wild type control with cells eliciting less than 5%

viability *(Figure 59)*. This result suggests a putative role for both subunits in the maintenance of viability in stationary phase of growth under the conditions used. The expression of either *RAS2*^{S225A} or *RAS2*^{S225E} in a *Δtpk1/ Δtpk3* background did not lead to the formation of viable colonies, thus indicating that the deletion of both *Δtpk1* and *Δtpk3* in wild type cells overexpressing *RAS2*^{S225A} or *RAS2*^{S225E} prevents the formation of viable colonies *(Figure 59)*.

Upon the expression of an empty plasmid in a *Δtpk3/ Δtpk2* background, a small decrease in viability is observed when compared to the wild type control *(Figure 59)*. Upon the expression of either *RAS2*^{S225A} or *RAS2*^{S225E} mutant alleles in a *Δtpk3/ Δtpk2* background, we see a significant decrease in viability when compared to the *Δtpk3/ Δtpk2* control strain *(Figures 59)*. When compared to wild type cells expressing either *RAS2*^{S225A} or *RAS2*^{S225E}, the deletion of *Δtpk3/ Δtpk2* in these strains leads to a further decrease in viability *(Figure 59)*. Suggesting that the deletion of both tpk3 and tpk2 is important for the maintenance of viability in wild type cells overexpressing *RAS2*^{S225A} or *RAS2*^{S225E} mutant alleles.

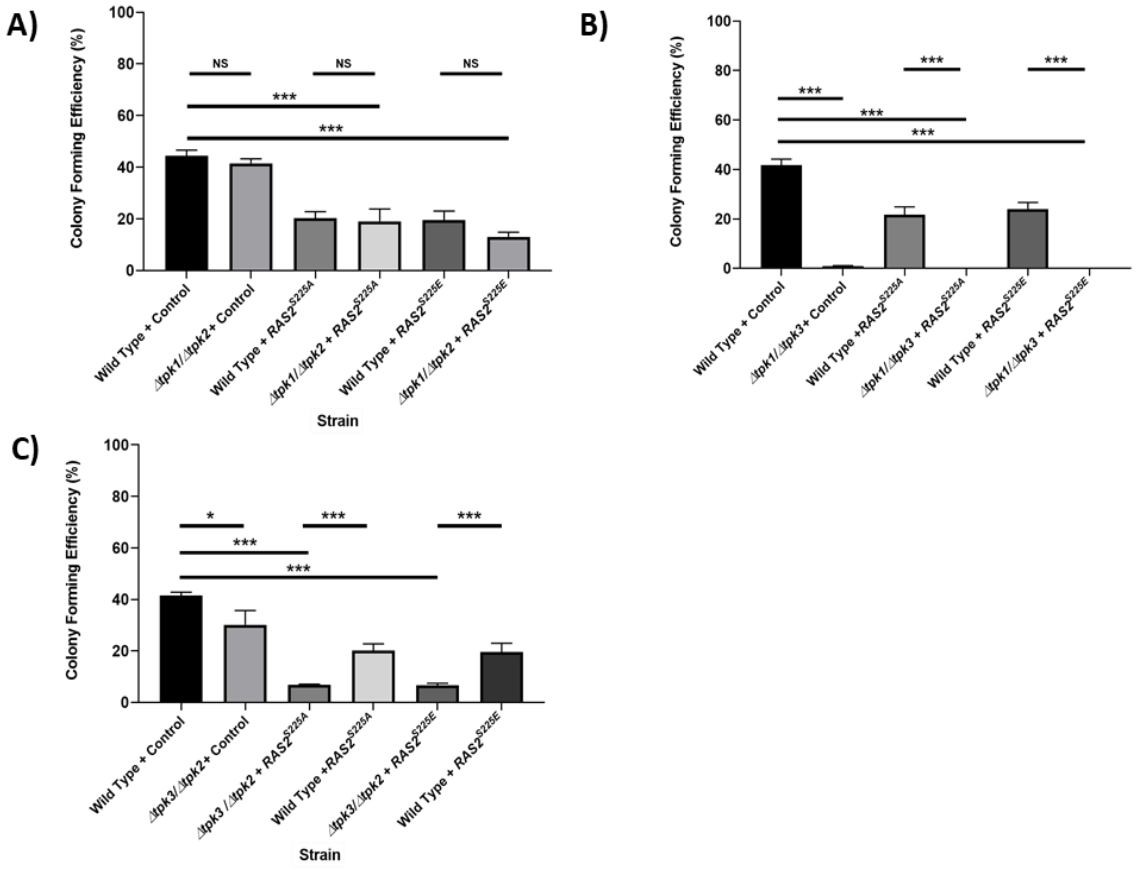

Figure 59. A colony forming efficiency assay of wild type, Δtpk1/ Δtpk2 (A), Δtpk1/ Δtpk3 (B) or Δtpk3/ Δtpk2 (C) cells overexpressing $RAS2^{S225A}$, $RAS2^{S225E}$or an empty plasmid control, grown in SD –URA.

*The colony forming efficiency analysis was carried out as described in Materials and Methods (Section 2.9.3). The data presented is the average of three biological repeats and error bars represent standard deviation. A One-way ANOVA using a Tukey multiple comparison test was used to determine statistical significance. Non-significant = NS, * = adjusted p-value ≤ 0.05 and *** = adjusted p value ≤ 0.001.*

4.6 Microscopic analysis of GFP-Tpk1p, GFP-Tpk2p or GFP-Tpk3p cells overexpressing *RAS2^{S225A}*, *RAS2^{S225E}* or an empty plasmid control

In the mammalian system, PKA anchor proteins (AKAPs) localise PKA holoenzymes to distinct subcellular localisations. Such targeting facilitates the spatio-temporal control of PKA signalling in order to phosphorylate specific localized effectors [240]. Considering the wide variety of PKA-controlled targets in *S. cerevisiae*, it is therefore not surprising that subcellular localisation of PKA subunits, as in multicellular organisms, occurs in the yeast system.

In *S. cerevisiae*, wild type cells grown on glucose localise Byc1 almost exclusively in the nucleus during exponential growth, while in stationary phase Bcy1 is distributed in both nuclear and cytoplasmic compartments [241]. In wild type yeast growing on glucose, GFP-Tpk1, GFP-Tpk2 and GFP-Tpk3 present a predominated localisation in the nucleus [242][241]. GFP-Tpk2 presents the strongest nuclear localisation with GFP-Tpk1 and GFP-Tpk3 showing a more even distribution over both the nuclear and cytoplasmic compartments. It was shown by Portela et al (2009), that wild type yeast cells grown to stationary phase showed a pronounced decrease in nuclear accumulation of all PKA subunits with GFP-Tpk2 and GFP-Tpk3 concentrated in extra-nuclear foci [242]. As it has been shown that PKA subunit localisation has been correlated to intracellular cAMP levels we sought to investigate whether the overexpression of $RAS2^{S225A}$ or $RAS2^{S225E}$ in wild type cells resulted in changes to the localisation of GFP-Tpk1, GFP-Tpk2 or GFP-Tpk3.

To attest whether the overexpression of $RAS2^{S225A}$ or $RAS2^{S225E}$ influenced the localisation of either GFP-Tpk1, GFP-Tpk2 or GFP-Tpk3, fluorescent microscopy was conducted as described in Methods and Materials (Section 2.10). The localisation of fluorescently labelled Tpk subunits was examined during both stationary and exponential phases of cell growth *(Figure 60)*. An empty plasmid control was introduced to all fluorescently tagged strains as a control.

In wild type cells grown on glucose, GFP-Tpk1 is reported to be mainly accumulated in the nucleus during exponential growth [242][241]. Our findings are concordant with literature and show that a GFP-Tpk1 strain expressing an empty plasmid control also presents a predominant nuclear localisation *(4.14A)*. Such localisation of GFP-Tpk1 was also observed in cells overexpressing either $RAS2^{S225A}$ or $RAS2^{S225E}$ *(Figure 60/61)*. No significant changes in the percentage of cells presenting nuclear localisation was observed upon the overexpression of

either *RAS2*^{S225A} or *RAS2*^{S225E} in a GFP-Tpk1 background when compared to the control strain *(Figure 60/61)*. Our results suggest that the overexpression of either *RAS2*^{S225A} or *RAS2*^{S225E} does not affect GFP-Tpk1p localisation during exponential growth.

It has been shown that during stationary phase growth, a pronounced decrease in nuclear accumulation of all PKA subunit is observed. Our results are not in keeping with such an observation as the localisation of GFP-Tpk1 still presented a predominant nuclear localisation with no significant loss of nuclear accumulation of GFP-Tpk1 observed between log and stationary phases of growth in all strains *(Figure 60/61)*. Portela et al (2009), assayed cells after 7 days of growth, whereas in this study our definition of stationary phase is growth after 24 hours. One explanation is that the 6-day time difference between the experiments conducted in this study and those conducted by Portela et al (2009), is the cause in the differences in localisation observed. The predominant localisation of GFP-Tpk1 in all strains assayed is a nuclear localisation with no significant differences in the percentage of cells presenting a nuclear localisation of GFP-Tpk1 observed upon the overexpression of *RAS2* mutant alleles when compared to the control *(Figure 60/61)*. Our results indicate that the overexpression of either *RAS2*^{S225A} or *RAS2*^{S225E} does not affect GFP-Tpk1 localisation during stationary phase growth.

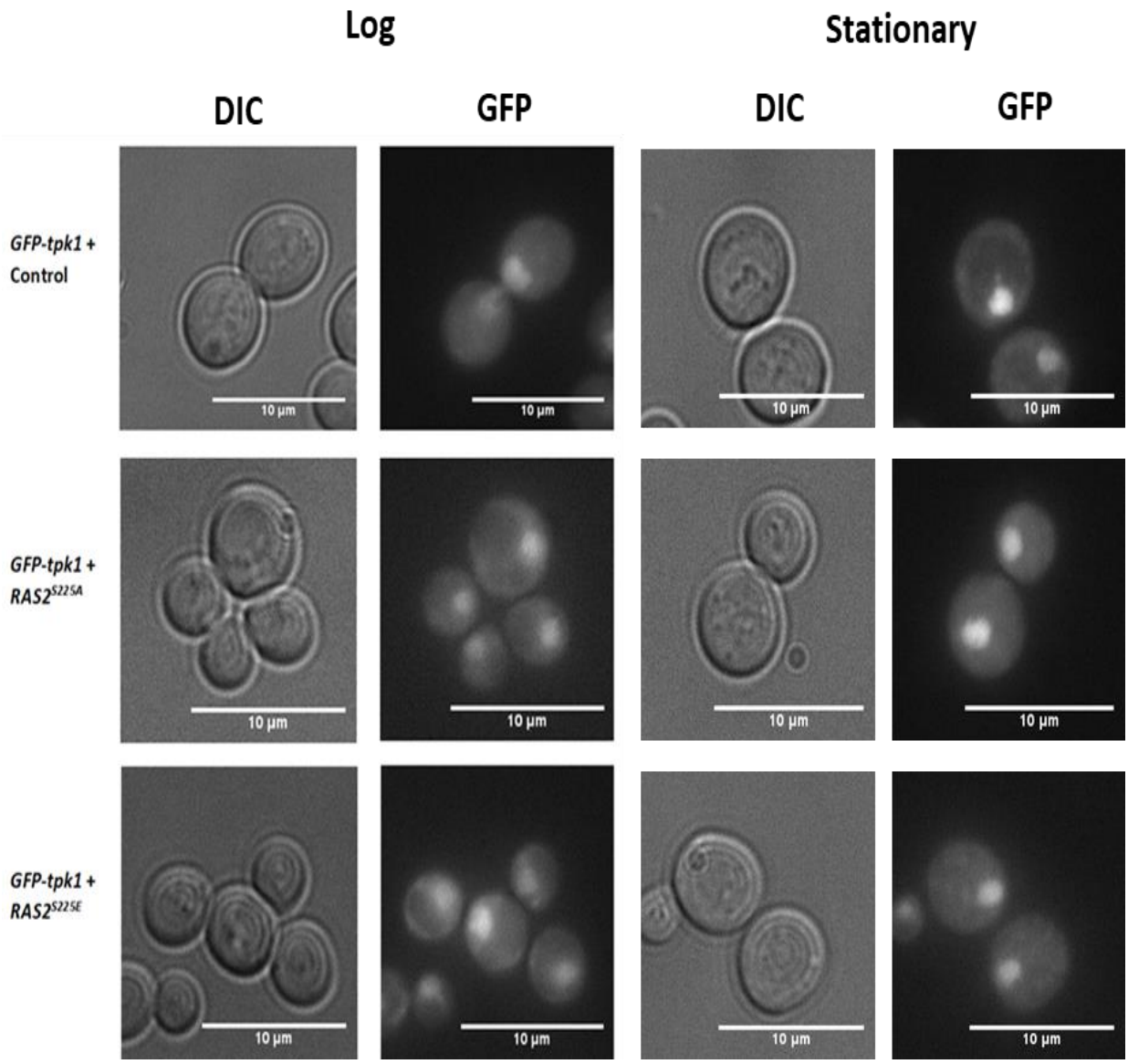

Figure 60. Images taken by fluorescent microscopy of GFP-Tpk1p cells overexpressing either RAS2^{S225A}, RAS2^{S225E} or an empty plasmid vector control during exponential and stationary phase of cell growth.

The fluorescent signal represents the presence of GFP-Tpk1 within cells. Cells were cultured in SD – URA growth media. This experiment was repeated three times and a representative data set is shown. Scale bar = 10 µm

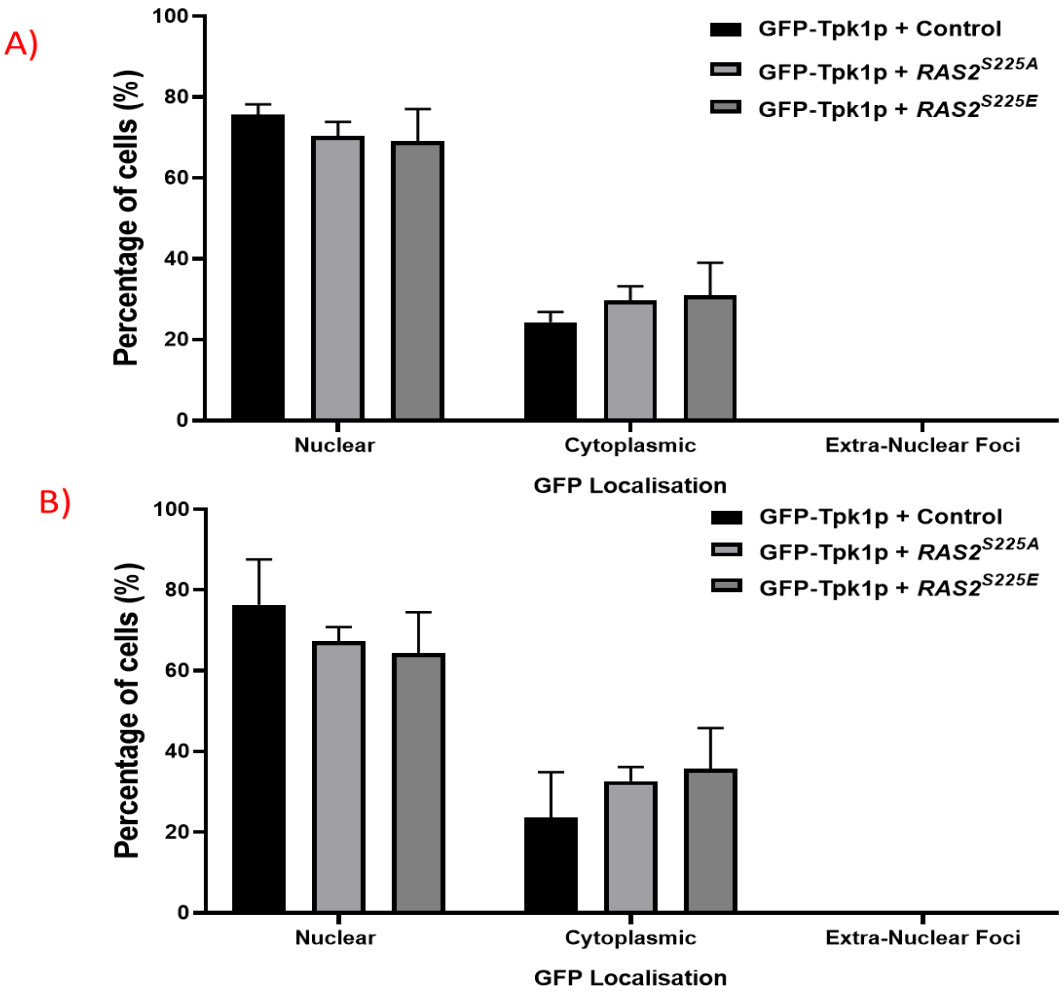

Figure 61. Graphical representation of the localisation of GFP-Tpk1p in cells expressing either RAS2^{S225A,} RAS2^{S225E} or an empty plasmid control during the logarithmic (A) or stationary (B) phase of cell growth.

Cells were cultured in SD –URA growth media. To quantify the localisation of GFP-Tpk1, 100 cells for each strain were counted on three separate days with a total 300 cells being counted and the number of cells displaying the different phenotypes observed was calculated and represented as a percentage of the total number of cells counted. The data represents an average of three biological repeats and error bars represents the standard deviation.

In wild type cells, GFP-Tpk2 is localised in the nucleus during logarithmic growth. Our data reflects current literature and presents GFP-Tpk2 localised to the nucleus in the GFP-Tpk2p control strain during log phase growth *(Figure 62/63)*. We observed no significant change in GFP-Tpk2 localisation in cells expressing *RAS2^{S225A}* or *RAS2^{S225E}* when compared to the control,

suggesting that expression of either *RAS2*^{S225A} or *RAS2*^{S225E} does not affect GFP-Tpk2p localisation in actively growing cells *(Figure 62/63)*.

It has been reported that during stationary phase of growth in wild type cells, GFP-Tpk2 presents a pronounced reduction in nuclear accumulation and GFP-Tpk2 localises to extra-nuclear foci. In this study we see a predominant nuclear localisation of GFP-Tpk2 in all strains examined *(Figure 62/63)*, however we infrequently noted the presence of extra-nuclear foci. No significant difference in the percentage of cells presenting nuclear localisation of GFP-Tpk2 or the percentage extra-nuclear foci was observed upon the overexpression of either *RAS2*^{S225A} or *RAS2*^{S225E} in a GFP-Tpk2 background when compared to the control strain (*Figure 62/63)*. We therefore propose that the overexpression of *RAS2*^{S225A} or *RAS2*^{S225E} does not affect GFP-Tpk2p localisation in stationary phase cells.

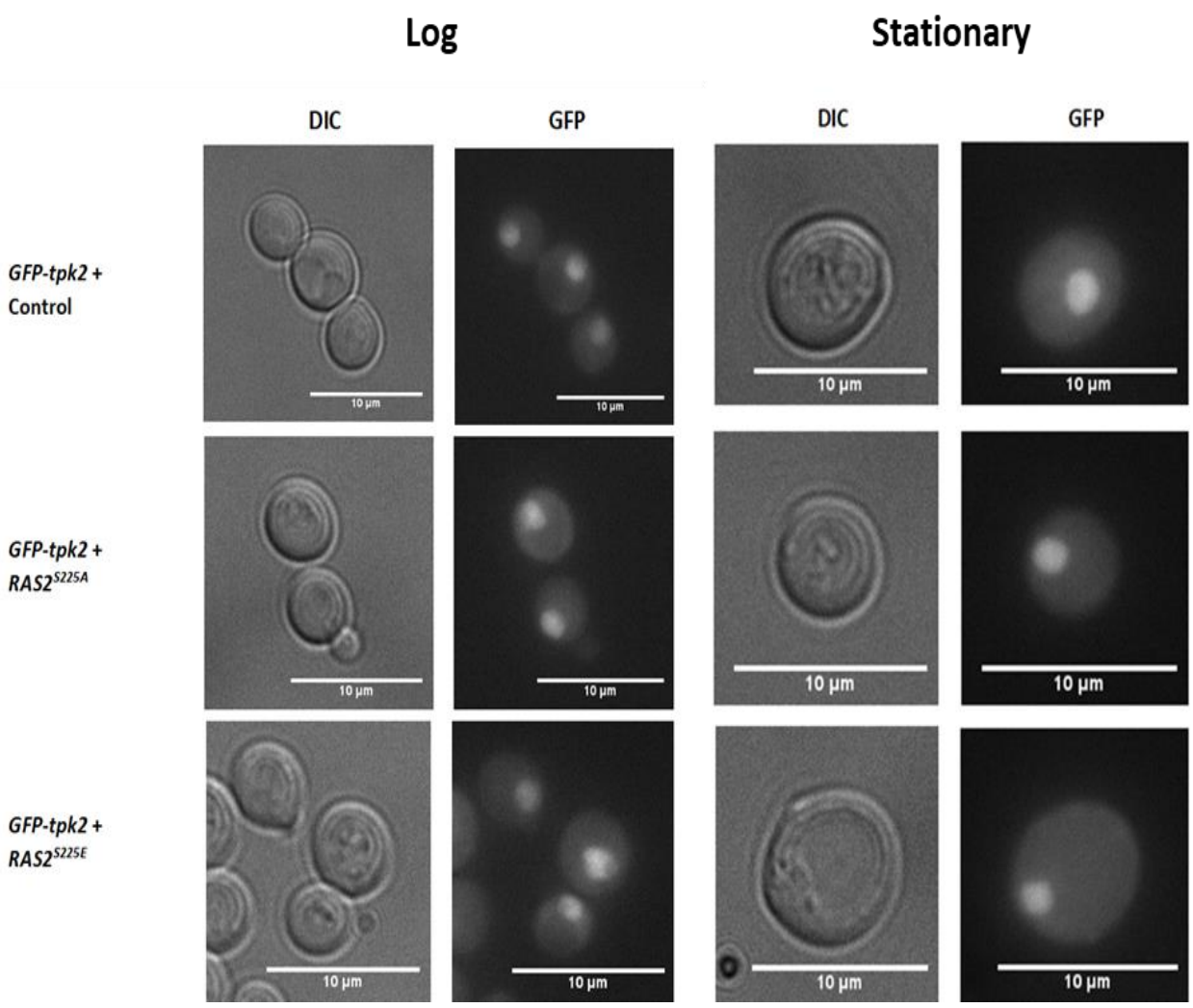

Figure 62. Images taken by fluorescent microscopy of GFP-Tpk2p cells overexpressing either $RAS2^{S225A}$, $RAS2^{S225E}$ or an empty plasmid vector control during exponential and stationary phase of cell growth.

The fluorescent signal represents the presence of GFP-Tpk2p within cells. Cells were cultured in SD – URA growth media. This experiment was repeated three times and a representative data set is shown.

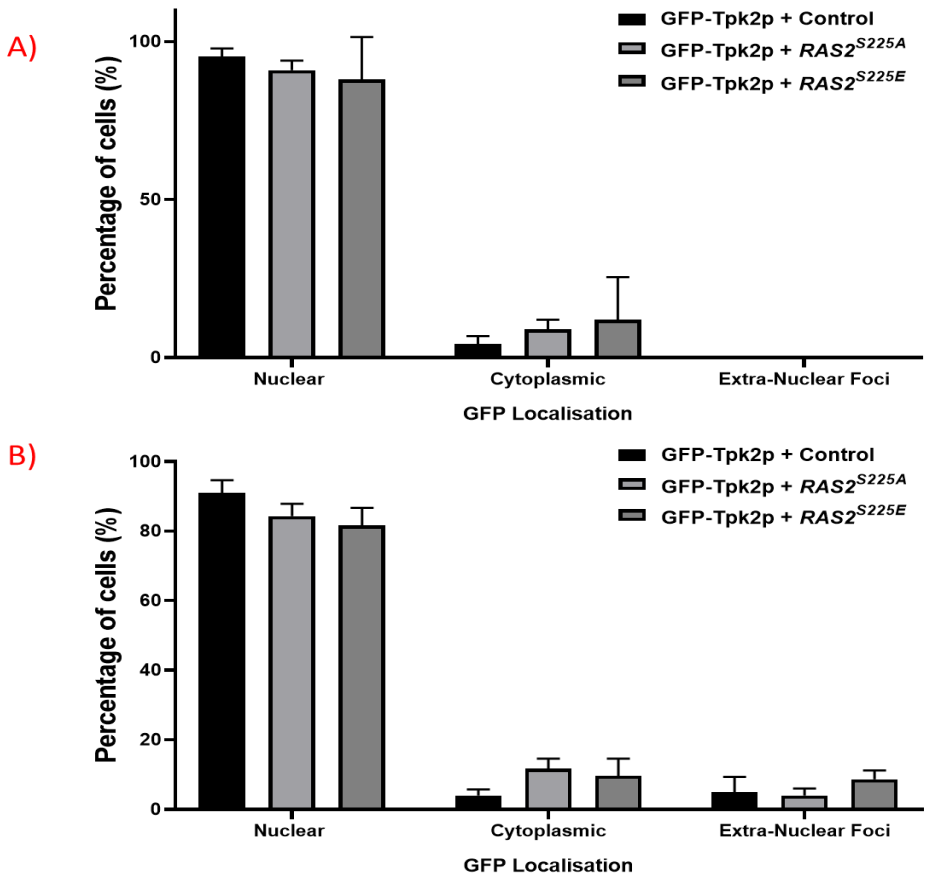

Figure 63. Graphical representation of the localisation of GFP-Tpk2p in cells expressing either RAS2^{S225A,} RAS2^{S225E} or an empty plasmid control during the logarithmic (A) or stationary (B) phase of cell growth.

Cells were cultured in SD –URA growth media. To quantify the localisation of GFP-Tpk2, 100 cells for each strain were counted on three separate days with a total 300 cells being counted and the number of cells displaying the different phenotypes observed was calculated and represented as a percentage of the total number of cells counted. The data represents an average three biological repeats and error bars represents the standard deviation.

In wild type yeast cells grown on glucose, GFP-Tpk3 accumulates in the nucleus during exponential growth and sequesters in extra-nuclear foci in stationary phase. During exponential growth, a predominant nuclear localisation of GFP-Tpk3 was observed in all strains examined with no difference in GFP-Tpk3p localisation upon the overexpression of *RAS2^{S225A}* or *RAS2^{S225E}* when compared to the control strain *(Figure 64/65)*. We therefor

propose that the overexpression of either *RAS2*^{S225A} or *RAS2*^{S225E} does not lead to changes in GFP-Tpk3 localisation during exponential growth.

During stationary phase, all strains examined show a pronounced reduction in the percentage of cells with a nuclear localisation of GFP-Tpk3 and an increase in GFP-Tpk3 localising to the cytoplasmic compartment was observed *(Figure 64/65)*. GFP-Tpk3 was seen to localise to extra-nuclear foci but again this was noted infrequently *(Figure 64/65)*. The predominant localisation of GFP-Tpk3 in all strains was cytoplasmic with no significant differences in GFP-Tpk3 localisation observed upon the overexpression of *RAS2*^{S225A} or *RAS2*^{S225E} when compared to control strain noted *(4.18B)*. We propose that the overexpression of *RAS2*^{S225A} or *RAS2*^{S225E} does not result in the miss localisation of Tpk subunits in either exponential or stationary growth.

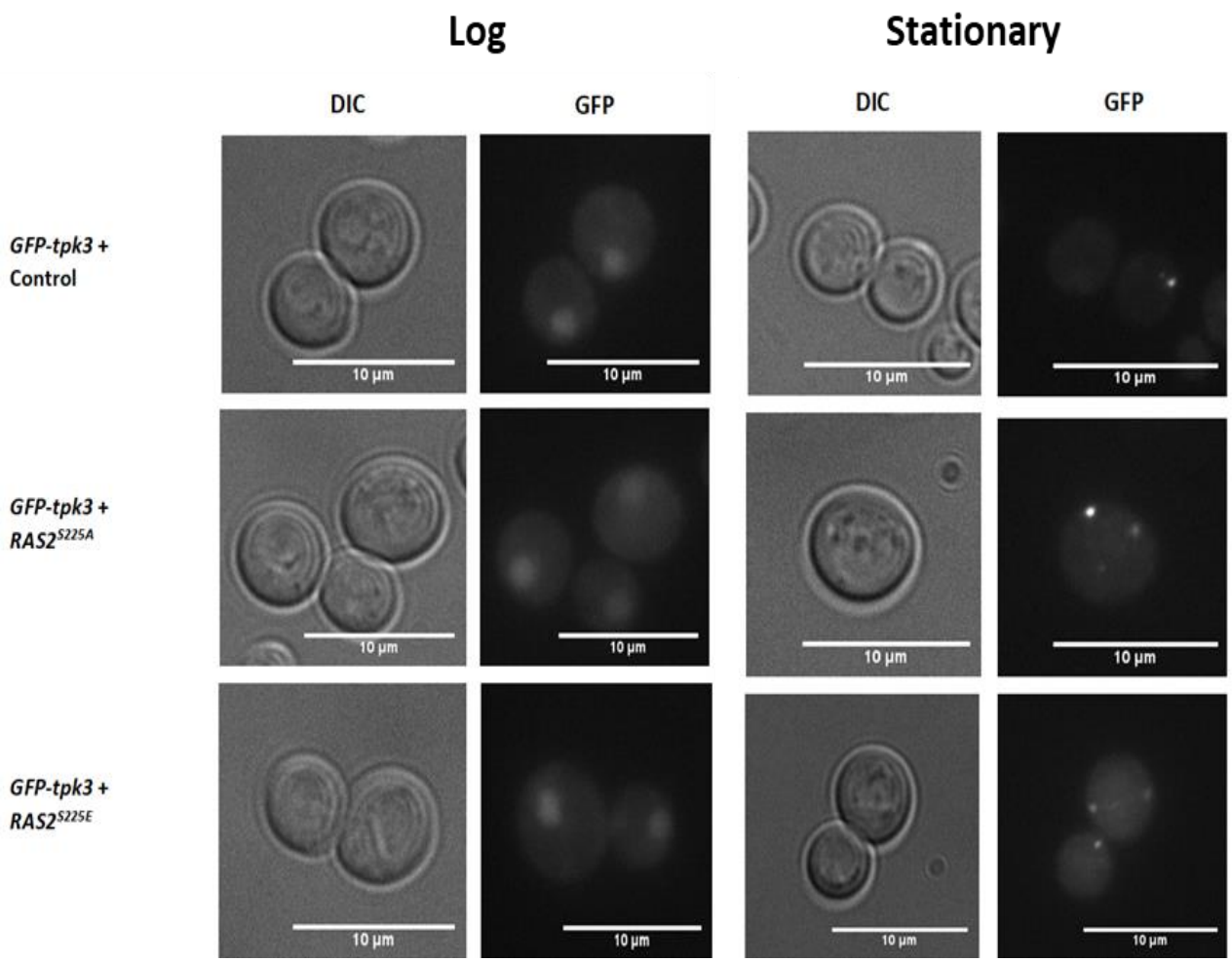

Figure 64. Images taken by fluorescent microscopy of GFP-Tpk3p cells overexpressing either $RAS2^{S225A}$, $RAS2^{S225E}$ or an empty plasmid vector control during exponential and stationary phase of cell growth.

The fluorescent signal represents the presence of GFP-Tpk3p within cells. Cells were cultured in SD – URA growth media. This experiment was repeated three times and a representative data set is shown.

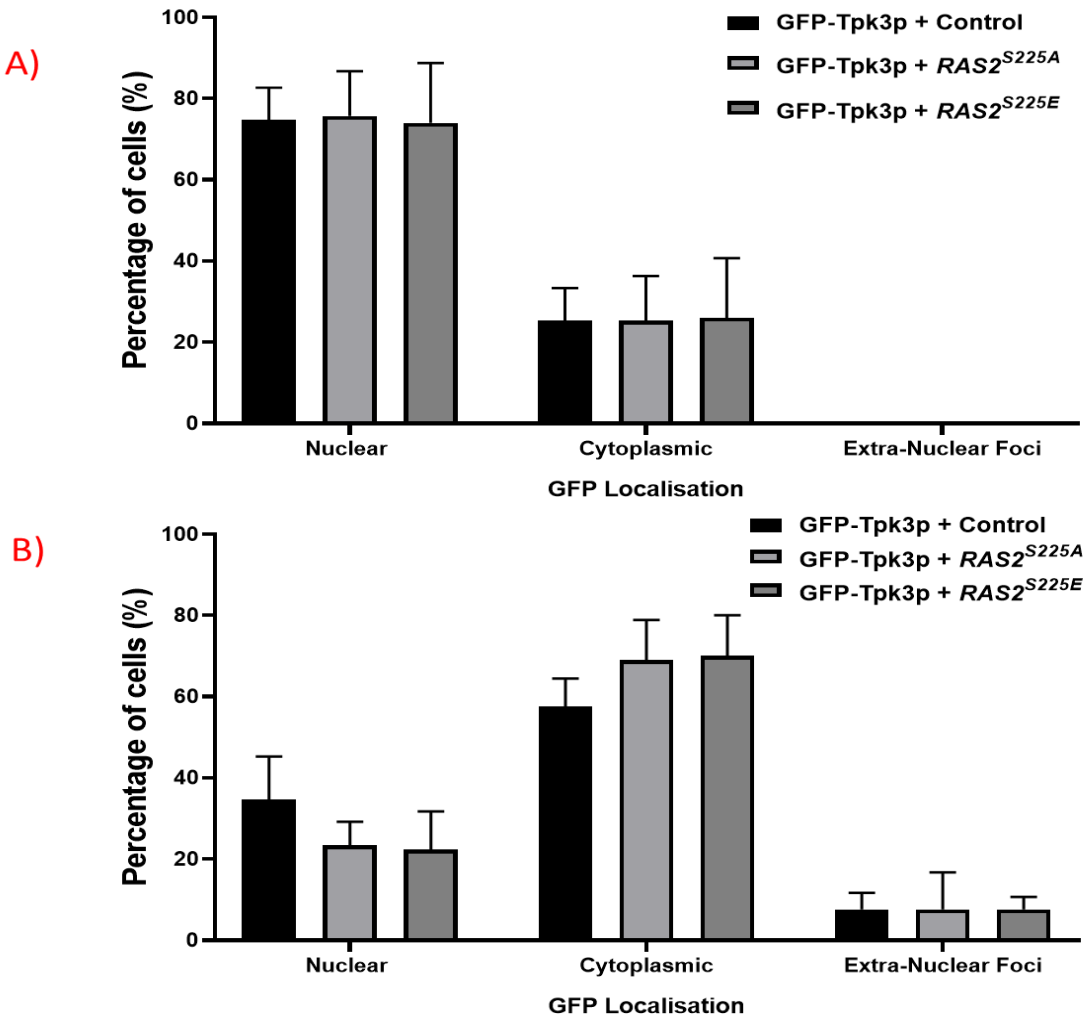

Figure 65. Graphical representation of the localisation of GFP-Tpk3p in cells expressing either RAS2^{S225A,} RAS2^{S225E} or an empty plasmid control during the logarithmic (A) or stationary (B) phase of cell growth.

Cells were cultured in SD –URA growth media. To quantify the localisation of GFP-Tpk3, 100 cells for each strain were counted on three separate days with a total 300 cells being counted and the number of cells displaying the different phenotypes observed was calculated and represented as a percentage of the total number of cells counted. The data represents an average three biological repeats and error bars represents the standard deviation.

4.7 Discussion

S. cerevisiae tolerates diverse environmental conditions through the coordinated regulation of growth, cell cycle progression and metabolic activities. The Ras/cAMP pathway is fundamental for the regulation and integration of these processes [147][136][243][216]. The reprogramming of cell metabolism at the diauxic shift, as well as adaptions during both the post-diauxic phase and entry into stationary phase, are negatively regulated by the Ras/cAMP/PKA pathway [216][154][244][153]. Therefore, mutations that activate the Ras/cAMP pathway, such as activating mutations in the *RAS2* gene and *BCY1* mutations fail to undergo correct diauxic reprogramming during nutrient depletion [233][115]. Cells with elevated cAMP levels rapidly lose viability in stationary phase as they fail to activate gene expression programmes that facilitate storage of carbohydrates, oxidative phosphorylation and upregulation of stress response mechanisms [233][115]. Conversely, cells with lower cAMP/PKA activity, such as seen in *Δcdc25* mutants, exhibit physiological changes associated with nutrient limitation, including G_1 cell cycle arrest, accumulation of storage carbohydrates and increased resistance towards heat and depleted oxidative stress responses [231][232].

We have previously shown that the overexpression of $RAS2^{S225A}$ or $RAS2^{S225E}$ in wild type cells results in the miss localisation of active Ras populations to the nuclear envelope, resulting in significant defects in both growth and viability. We hypothesize that such defects are a result of the dysregulation of the cell cycle . We sought to investigate whether cessation of growth was caused through the aberrant signalling of Ras/cAMP/PKA pathway. To address this, $RAS2^{S225A}$ or $RAS2^{S225E}$ mutant alleles were overexpressed in strains lacking different components of the Ras/cAMP/PKA pathway.

The loss of *PDE2* in cells overexpressing *RAS2*^{S225A} or *RAS2*^{S225E} resulted in a further attenuation of viability and growth defects when compared to the overexpression of *RAS2* mutant alleles in wild type cells. Our results imply that a loss in the ability to control intracellular cAMP levels and Ras/cAMP/PKA pathway activation, results in a further loss in fitness upon the overexpression of either *RAS2*^{S225A} or *RAS2*^{S225E}, as supported by previous published observations, Leadsham et al 2010 [224]. We hypothesize that such observations can be explained through an elevation in intracellular cAMP levels and increased activity of the Ras/cAMP/PKA pathway, which is further increased due to the cells inability to degrade cAMP in the absence of *PDE2*. To reduce the levels of intracellular cAMP and Ras/cAMP/PKA activation in wild type cells overexpressing *RAS2*^{S225A} or *RAS2*^{S225E} we co-expressed *PDE2* and performed both a growth and viability assay. The overexpression of *PDE2* in cells expressing either *RAS2*^{S225A} or *RAS2*^{S225E} resulted in a complete rescue of viability and growth rate to that of wild type levels. We suggest that the growth and viability defects observed are a result of increased levels of cAMP, and thus activation of PKA, which can be repressed via reducing cAMP levels via the co-expression of *PDE2.*

We hypothesize that the overexpression of either *RAS2*^{S225A} or *RAS2*^{S225E} in wild type cells results in an increase in the activation of the Ras/cAMP/PKA pathway. We therefore sought to investigate whether the deletion of the genes encoding downstream targets of cAMP, such as the PKA catalytic subunits *TPK1*, *TPK2* and *TPK3* in wild cells overexpressing *RAS2*^{S225A} or *RAS2*^{S225E} resulted in changes in growth and viability in a manner analogous to the deletion or overexpression of *PDE2.* Our results suggest that *TPK1* is epistatic with the expression of the *RAS2*^{S225A} mutant allele with respect to viability. We conclude this as expression of *RAS2*^{S225A} rescues viability defects upon loss of *TPK1* in wild type cells. Tpk2 function is responsible for the reduction in viability observed in the wild type but is not involved in the

loss of viability observed upon the overexpression of either *RAS2*^{S225A} or *RAS2*^{S225E} in wild type cells. We propose that Tpk3 contributes to the maintenance of viability in cells overexpressing *RAS2*^{S225A} or *RAS2*^{S225E} as loss of Tpk3 results in a further loss in viability. We suggest that the loss in viability upon the overexpression of *RAS2* mutant alleles cannot be attributed to the activity of any single Tpk, as the deletion of single Tpk subunits does not rescue the viability phenotype. We therefor investigated the effect of deleting combinations of the Tpk subunits in wild type cells overexpressing *RAS2*^{S225A} or *RAS2*^{S225E}. We suggest that the overlapping functions of either Tpk1 and Tpk2 or Tpk1 and Tpk3 is either responsible for the reduced growth rate or that the combined loss of these subunits can compensate for the toxic effects of the overexpression of *RAS2*^{S225A} or *RAS2*^{S225E} in wild type cells.

We conclude that the deletion of PKA subunits in wild type cells overexpressing *RAS2*^{S225A} or *RAS2*^{S225E} has pronounced effects on the growth rate but not viability. A possible explanation is that all three subunits contribute to the loss of viability, but the more likely explanation is that the complexity of PKA function means that the deletion of multiple subunits results in pleiotropic effects and the loss of viability observed upon the combined deletion of Tpk subunits are additive to the toxic effects of the overexpression *RAS2*^{S225A} or *RAS2*^{S225E}*.* The single or double deletion of the genes encoding the downstream targets of cAMP, such as the PKA catalytic subunits *TPK1*, *TPK2* and *TPK3* in wild cells overexpressing *RAS2*^{S225A} or *RAS2*^{S225E} did not result in changes in growth and viability analogous to the overexpression of *PDE2.* This observation does not wholly support our hypothesis that the effects of *RAS2*^{S225A} or *RAS2*^{S225E} overexpression are mediated via the PKA pathway. But as the overexpression of *PDE2* was sufficient to rescue viability in wild type cells overexpressing *RAS2* mutant alleles, we propose that the reduced growth phenotype is mediated by the dysregulated activation of PKA. However, the genetic approach of deleting Tpk subunits could not dissect the control of PKA

on the slow growth phenotype observed. We propose the following model *(Figure 66)* to explain the control of PKA on the phenotypes observed upon the overexpression of *RAS2*^{S225A} or *RAS2*^{S225E} in wild type cells. Further investigations will focus on whether there any environmental conditions, such as growth in nutrient rich media, which rescue cells overexpressing *RAS2* mutant alleles to resume normal growth.

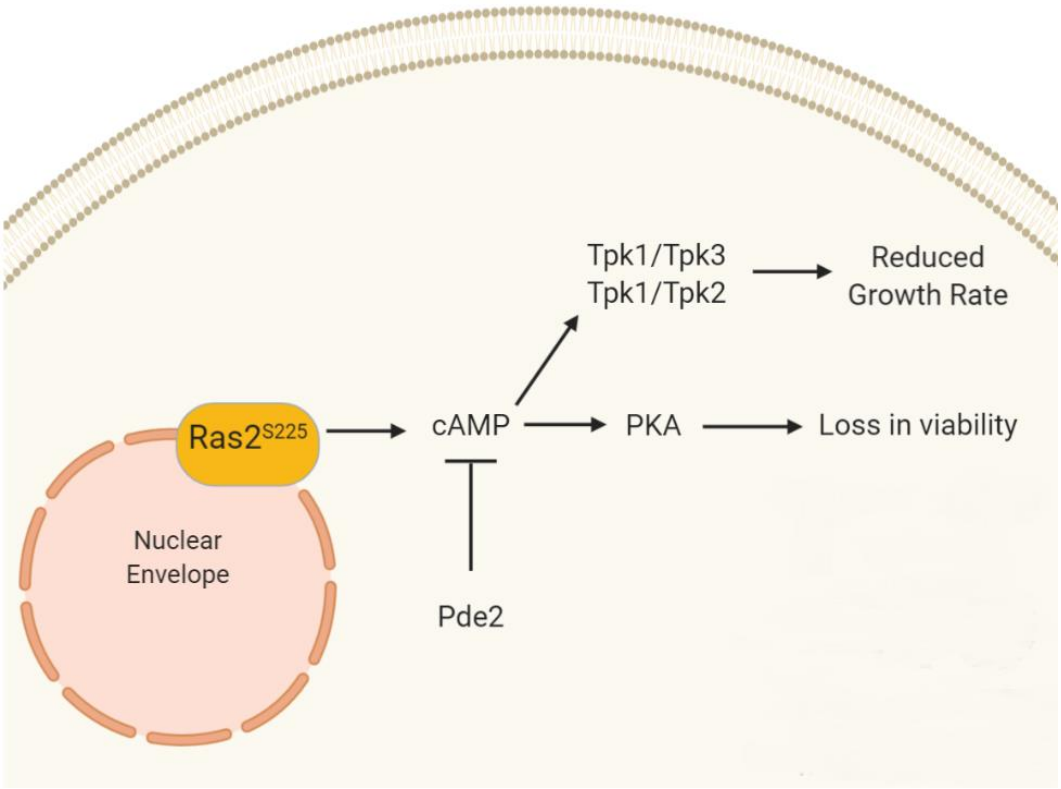

Figure 66. A schematic demonstrating how the miss localisation of Ras2p^{S225} to the nuclear envelope effects PKA activity.

The modification of RAS2^{S225} results in the miss localisation of active-Ras to the nuclear envelope during both log and stationary phase of growth. Miss localization of Ras to the nuclear envelope leads to an increased activation of PKA. The redundant functions of Tpk1 and Tpk2 or Tpk1 and Tpk3 are responsible for the reduction in growth rate defects and increased PKA activity drives a loss in viability that is attributed to a state of cell cycle dysregulation. Viability can be rescue upon the overexpression of PDE2 demonstrating that viability defects are dependent on PKA activity.

Chapter 5

The role of nutrient availability in the growth of *Ras2*^{225} mutant strains

5.1 Introduction

In previous chapters we show that the overexpression of either *RAS2*^{S225A} or *RAS2*^{S225E} leads to Ras miss localisation and activation at the nuclear envelope. Such localisation results in growth defects and a loss of viability that we propose is attributable to a dysregulation of the cell cycle. We established that the slow growth phenotype observed is linked to elevated PKA activity, as overexpression of *PDE2* in strains overexpressing *RAS2*^{S225A} or *RAS2*^{S225E} rescued viability.

Investigations thus far involved the culturing of cells in minimal media to allow for the selection of plasmids used in this study. We consistently observed that overnight cultures of wild type cells exhibited a viability between 40-50 % suggesting that the media used is limiting. However, overexpression of *RAS2* led to an increase in viability in minimal media, suggesting that the media itself may not be limiting. It may be the case that the wild type strain used in this study is unable to access or forage for certain metabolites, leading to reduced viability, which can be corrected upon the overexpression of *RAS2*. This finding suggests an interplay between Ras activity, utilisation of available nutrition and cell fate. We sought to investigate whether changing the nutritional composition of growth media would enable cells overexpressing *RAS2* mutant alleles to resume growth in a manner analogous to the co-expression with *PDE2.*

In this chapter we focus on the effects of di/tri-peptide availability and uptake on cell fate within the context of Ras activation. Peptides are composed of sequences of amino acids and once catabolized provide the essential building blocks required for protein synthesis. In addition, certain peptides and amino acids can be utilized as a nitrogen source and can act as signalling molecules that alter cell behaviour. For example, the branched-chain amino acid

leucine, has been shown to control TORC1 activity [171][172]. TORC1 senses and responds to nutrients to promote cell growth and the inhibition of catabolic processes, such as autophagy. Branched-chain amino acids such as leucine function by affecting the 'nucleotide binding status of the Exit from G_0 Complex' (EGOC) GTPase subunits Gtr1 and Gtr2 in *Saccharomyces cerevisiae,* promoting growth[173][174].

In mammals, amino acids exert a major role on the regulation of protein synthesis through the control of the kinases mTOR and Gcn2 [172][177]. The regulation of Gcn2 activity by amino acid availability relies on the capacity of Gcn2 to sense the increased levels of uncharged tRNAs upon amino acid scarcity [177]. Upon low levels of essential amino acids, Gcn2 phosphorylates the α-subunit of eukaryotic initiation factor 2 alpha (eIF2α), resulting in the inhibition of protein synthesis. [178].

Due to the multifaceted role of amino acids and peptides in biological systems, it is therefore not surprising that microbes have evolved a multitude of mechanisms to facilitate peptide and amino acid uptake. The study of such mechanisms has been extensively examined in yeast, with amino acid uptake mechanisms presenting high conservation in mammals.

Saccharomyces cerevisiae has two distinct peptide transport mechanisms, a di-/tripeptides (the PTR system) and a tetra-/pentapeptides (the OPT) transport system [245][246][180]. The PTR family of peptide transporters transport a number of substrates, including amino acids, nitrates and di/tri-peptides [179]. *PTR2* encodes an integral membrane protein (Ptr2p) involved in the physical translocation of peptides across the plasma membrane by the means of proton-motive force [180]. The transporter is specific for di-/tripeptides, with a preference for peptides containing hydrophobic amino acids. In *S. cerevisiae* the regulation of *PTR2* expression is strongly affected by the composition of the extracellular environment.

In the absence of the preferred nitrogen sources *PTR2* expression is induced [181] [182].The import of di/tripeptides composed of basic or bulky hydrophobic N-terminal residues increases *PTR2* expression via reducing cellular levels of Cup9p, the homeodomain-containing transcriptional repressor of *PTR2*. Specific di/tri-peptides function as both as ligands and regulators of the E3 ubiquitin ligase Ubr1p. Ubr1p mediates the Cup9p degradation system that is governed by the identity of N-terminal amino acids [183][184]. Most di/tripeptides are too small to be degraded by the proteasome and are assimilated as nutrients by intracellular peptidases. However, di/tripeptides with basic (Type 1: His, Lys, or Arg) and bulky (Type 2: Ile, Trp, Leu, Tyr, or Phe) N-terminal residues can compete with larger protein substrates and bind at the Type 1 and Type 2 Ubr1p substrate-binding sites. Once bound, Ubr1p-mediated degradation of Cup9p is allosterically activated via the release of the Ubr1p auto inhibitory domain, revealing a substrate-binding domain that binds an internal degron in Cup9p [185]. Relief of Cup9p repression of *PTR2* results in enhanced *PTR2* expression. A positive regulatory feedback loop is created where di/tripeptide uptake perpetuates Ubr1p-mediated Cup9p degradation, upregulating *PTR2* expression and thus increased di/tripeptide uptake.

Although Ptr2p is the major transporter of di/tripeptides in *S. cerevisiae*, di/tripeptides can also be imported with a low efficacy by Dal5p, whose primary function is the import of nitrogen sources, such as allantoate and ureidosuccinate [186]. As aforementioned, the peptide transporters Opt1 and Opt2, which have partially overlapping functions, import peptides of 4–5 residues. In addition, Opt1 is a high affinity importer of glutathione, a “noncanonical” tripeptide [187]. In the same way as the Ptr2 transporter of di/tripeptides, the expression of *OTP2* is down-regulated by Cup9p, whereas the expression of *OPT1* is independent of Cup9p [187]. In addition to *PTR2* and *OPT2*, the N-end rule pathway also controls the expression of *DAL5*, but in a manner contrary to that of the other two

transporters: whereas Cup9p is a transcriptional repressor of *PTR2* and *OPT2*, Cup9p up-regulates the expression of *DAL5* [179][187].

In this chapter we investigate how the availability and uptake of di/tripeptides interplays with entry and restore growth in cells overexpressing *RAS2*^{S225A} or *RAS2*^{S225E} mutant alleles grown in -URA

5.2 Growth on nutrient rich media rescues viability in wild type cells overexpressing *RAS2^{S225A}* or *RAS2^{S225E}*

In Chapter 3, we show that the viability of wild type cells overexpressing either *RAS2^{S225A}* or *RAS2^{S225E}* is significantly reduced after 24 hours of growth in minimal media. We sought to investigate whether growth on nutrient rich media, such as YPD, rescued viability in cells overexpressing *RAS2^{S225A}* or *RAS2^{S225E}*. To address this, a colony forming efficiency assay was performed. An overnight culture was re-inoculated to 2 x 10^3 cells/ml and incubated for 24 hours. 300 cells were plated onto either selective -URA agar plates or YPD agar plates. These were left to incubate at 30 °C for 36 hours and the colonies were then counted to allow quantification of colony forming units (CFUs).

All strains re-plated onto YPD media presented a significant increase in viability when compared to strains grown on SD –URA *(Figure 67)*. When compared to wild type cells overexpressing *RAS2^{S225A}* or *RAS2^{S225E}* grown on SD-URA, the re-plating of *RAS2^{S225A}* or *RAS2^{S225E}* strains onto nutrient rich agar resulted in a significant increase in colony forming efficiency *(Figure 67)*. No significant differences in viability were observed between wild type cells overexpressing *RAS2^{S225A}*, *RAS2^{S225E}* or an empty plasmid control when grown on YPD *(Figure 67)*. This data indicates that overexpression of either *RAS2^{S225A}* or *RAS2^{S225E}* in wild type cells does not lead to cell death but rather a cessation of proliferation. Cells were able to re-proliferate upon re-plating on nutrient rich agar, providing further evidence to suggest that overexpression of *RAS2^{S225A}* or *RAS2^{S225E}* leads to a cessation of growth as opposed to cell death in the yeast system.

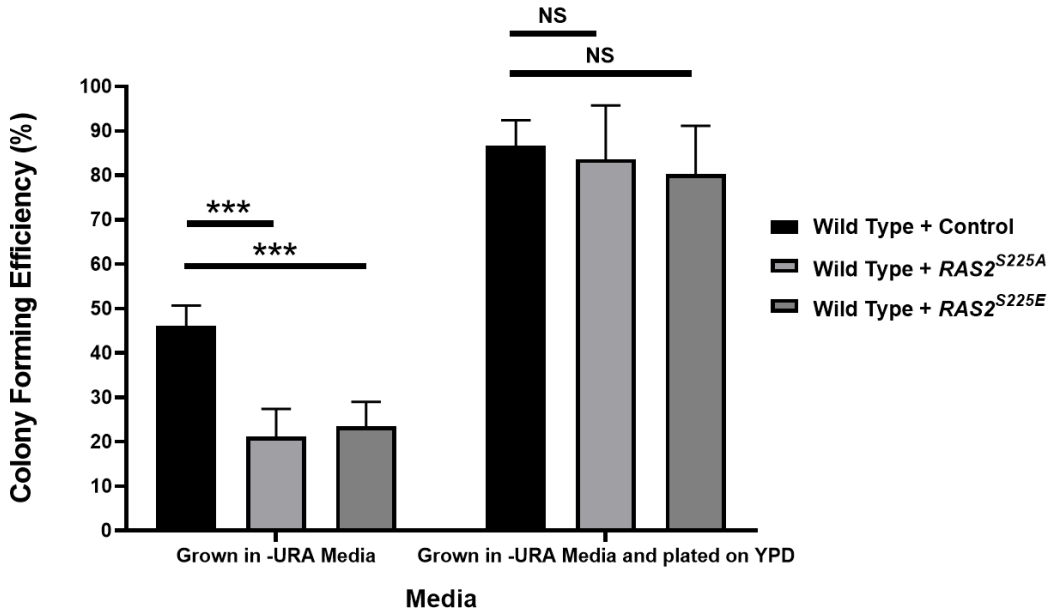

Figure 67. A colony forming efficiency assay of S. cerevisiae wild type cells overexpressing $RAS2^{S225A}$, $RAS2^{S225E}$or an empty plasmid control grown in SD –URA media and plated on either SD-URA or YPD.

*A colony forming efficiency analysis was carried out as described in Materials and Methods (Section 2.9.3). A One-way ANOVA using a Tukey multiple comparison test was used to determine statistical significance. Non-significant = NS, * = adjusted p-value ≤ 0.05 and *** = adjusted p value ≤ 0.001*

5.3 Determination of the component of YPD that allows $RAS2^{S225A}$ or $RAS2^{S225E}$ to escape growth cessation

5.3.1 Supplementation of Yeast Extract to minimal media rescues viability in wild type cells expressing $RAS2^{S225A}$ or $RAS2^{S225E}$

In order to determine which component of the nutrient rich media results in the exit from the reduced growth phenotype observed in cells overexpressing $RAS2^{S225A}$ or $RAS2^{S225E}$, YPD was broken down into its constituent parts and these were individually added to the SD –URA agar at the same concentration as seen in YPD. A colony forming efficiency assay was performed as described in Materials and Methods Section 2.9.3, and after 24 hours of incubation in SD –URA media cells were plated onto either SD-URA or SD –URA + Yeast Extract solid media and the colony forming efficiency for each condition was calculated.

Upon growth on SD-URA media supplemented with yeast extract, a significant increase in viability was observed in all strains when compared to strains grown on SD-URA *(Figure 68)*. Again, no significant changes in viability were observed in wild type cells overexpressing *RAS2*^{S225A} or *RAS2*^{S225E} alleles compared to the wild type control grown in SD –URA plus yeast extract *(Figure 68)*. We therefor suggest that the supplementation of yeast extract to SD-URA media rescues viability in wild type cells overexpressing *RAS2*^{S225A} or *RAS2*^{S225E} mutant alleles enabling cells to resume normal growth.

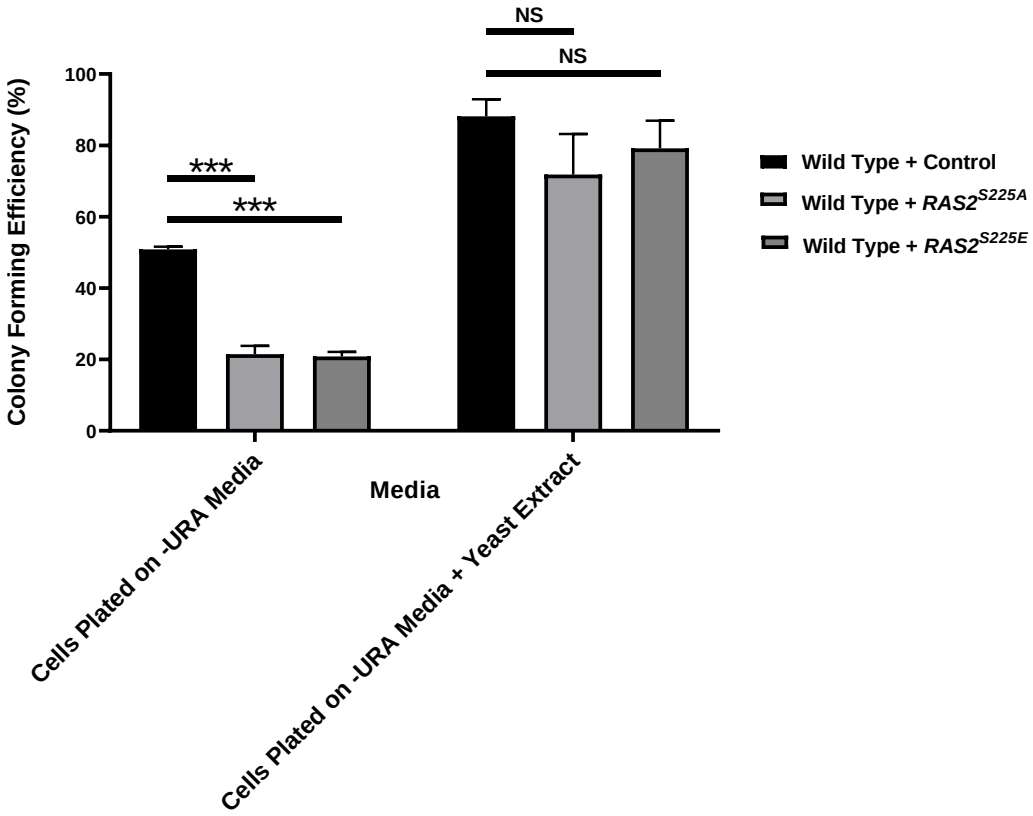

Figure 68. A colony forming efficiency assay of S. cerevisiae wild type cells overexpressing RAS2^{S225A}, RAS2^{S225E}or an empty plasmid control grown in SD –URA media and plated on either SD-URA or SD-URA + Yeast Extract.

*A colony forming efficiency analysis was carried out as described in Materials and Methods (Section 2.9.3). A One-way ANOVA using a Tukey multiple comparison test was used to determine statistical significance. Non-significant = NS, * = adjusted p-value ≤ 0.05 and *** = adjusted p value ≤ 0.001*

5.3.2 Increasing the glucose concentration in the growth media does not rescue viability in wild type cells overexpressing *RAS2*^{S225A} or *RAS2*^{S225E}

It has previously been established that the addition of glucose to nutrient starved cultures provides the stimulus for cells to exit a quiescent state and re-proliferate [247] [149][226][150]. To attest whether increasing the glucose concentration in the growth media would result in an increase in viability in cells overexpressing either *RAS2*^{S225A} or *RAS2*^{S225E} in a manner resembling that of the re-plating of cells on YPD, a colony forming efficiency assay was conducted**.** After 24 hours of growth in SD –URA, cells were plated on either SD-URA (2 % glucose) or SD-URA (4 % glucose). We observed no significant difference in colony forming efficiency in the wild type control when re-plated on SD-URA containing 4 % glucose *(Figure 69)*. No rescue in the viability to that of the wild type control was observed in *RAS2*^{S225A} or *RAS2*^{S225E} mutants when plated on media containing 4 % glucose *(Figure 69)*. We therefor conclude that increasing the availability of glucose in the growth media does not rescue viability in a manner resembling that of growth on YPD. We therefor conclude that the resumption of normal growth observed in cells overexpressing *RAS2*^{S225A} or *RAS2*^{S225E} is not glucose dependent.

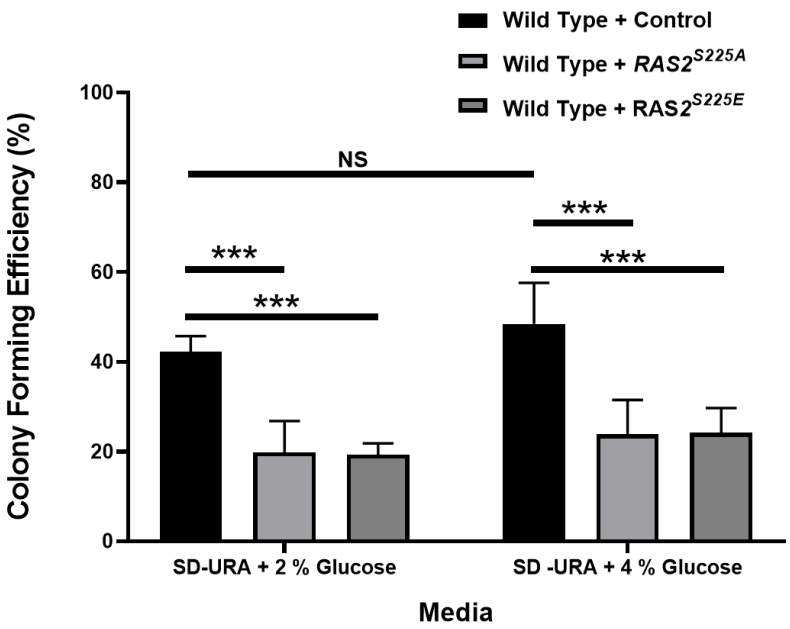

Figure 69. A colony forming efficiency assay of S. cerevisiae wild type cells overexpressing RAS2^{S225A}, RAS2^{S225E}or an empty plasmid control grown in SD –URA media and plated on either SD-URA (2 % glucose) or SD-URA (4 % glucose).
*A colony forming efficiency analysis was carried out as described in Materials and Methods (Section 2.9.3). A One-way ANOVA using a Tukey multiple comparison test was used to determine statistical significance. Non-significant = NS, * = adjusted p-value ≤ 0.05 and *** = adjusted p value ≤ 0.001*

5.3.3 Supplementation of Peptone to minimal media increases viability of wild type cells overexpressing *RAS2*^{S225A} or *RAS2*^{S225E}

As we have observed that the supplementation of yeast extract to SD-URA was sufficient to rescue the toxic effects on viability of expressing either *RAS2*^{S225A} or *RAS2*^{S255E} in wild type cells. We sort to investigate whether the supplementation of peptone, at the same concentration seen in YPD, to SD-URA media allow cells overexpressing *RAS2* mutant alleles to re-engage the cell cycle. To address this question, a colony forming efficiency assay was conducted as previously described and cells were plated on either SD-URA or SD-URA supplemented with peptone.

Upon growth on SD-URA media supplemented with peptone, a significant increase in viability was observed in all strains when compared to growth on SD-URA *(Figure 70)*. Again, no significant changes in viability were observed in wild type cells overexpressing *RAS2*^{S225A} or *RAS2*^{S225E} mutant alleles when compared to the wild type control grown in SD –URA with the supplementation of peptone *(Figure 70)*. We therefor propose that the supplementation of peptone to SD-URA media rescues viability in wild type cells overexpressing *RAS2*^{S225A} or *RAS2*^{S225E} and enables cells escape growth cessation.

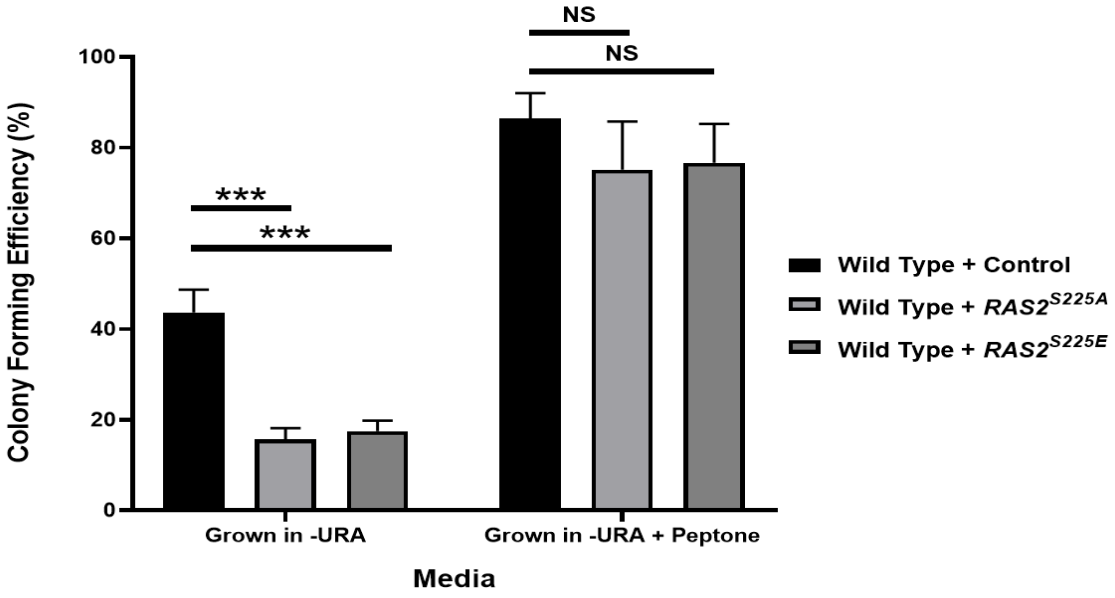

Figure 70. A colony forming efficiency assay of S. cerevisiae wild type cells overexpressing RAS2^{S225A}, RAS2^{S225E}or an empty plasmid control grown in SD –URA media and plated on either SD-URA or SD-URA + Peptone.

*A colony forming efficiency analysis was carried out as described in Materials and Methods (Section 2.9.3). A One-way ANOVA using a Tukey multiple comparison test was used to determine statistical significance. Non-significant = NS, * = adjusted p-value ≤ 0.05 and *** = adjusted p value ≤ 0.001*

5.4 Supplementation of Peptone to minimal media increases chronological life span of wild type cells overexpressing *RAS2*^{S225A}

We have previously shown that the overexpression of *RAS2*^{S225A} in wild type cells lead to a decrease in chronological life span. As the supplementation of peptone to the growth media was shown to rescue viability in wild type cells overexpressing R*AS2*^{S225A}, we sought to investigate whether supplementation of peptone to SD-URA media, at the same concentration found in YPD, would lead to an increase in the chronological lifespan of cells overexpressing *RAS2*^{S225A}. To test this hypothesis, a chronological life span assay was conducted as described in Materials and Methods, Section 2.9.8. Cells were grown in and then plated on SD-URA media or grown in SD-URA + Peptone and then plated on media containing SD-URA + Peptone.

All strains grown in the presence of peptone presented a significant increase in chronological lifespan when compared to strains grown without peptone supplementation *(Figure 71)*. On day 1, the wild type control strain grown in the presence of peptone presented a significant increase in viability when compared to the control strain grown in SD-URA only *(Figure 71)*. At day 12, the wild type control grown with peptone supplementation showed ~40 % of the culture still being able to form viable colonies compared to only ~20 % in the wild type control grown without peptone *(Figure 71)*.

Wild type cells overexpressing *RAS2*^{S225A} grown in SD-URA + peptone, presented a significant increase in viability after day 1 when compared to the *RAS2*^{S225A} mutant grown in –URA media *(Figure 71)*. After day 12, wild type cells overexpressing *RAS2*^{S225A} were unable to form viable colonies, however when grown in media supplemented with peptone, ~20 % of cells were able to form viable colonies *(Figure 71)*. We therefor propose that peptone supplementation

increases chronological lifespan in all strains and reduces the detrimental effects of the overexpression of *RAS2*^{S225A} on chronological lifespan in wild type cells.

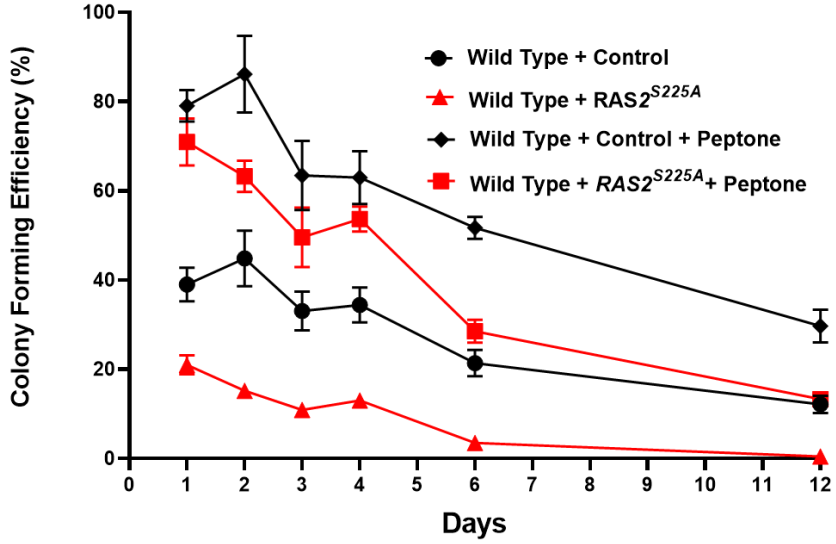

Figure 71. A chronological ageing assay of wild type cells over expressing RAS2^{S225A} or an empty plasmid control grown in SD –URA and plated on SD-URA or grown in SD-URA + Peptone and plated on SD-URA + Peptone.

The chronological ageing assay was conducted as describe in materials and method (Section 2.9.8). The data represents an average of three biological repeats and error bars represents the standard error of the mean.

5.5 Supplementation of peptone to minimal media protects cells from necrosis

We have shown that the supplementation of peptone to SD –URA increases the chronological lifespan of all strains examined. We aimed to attest whether an increase in chronological lifespan was coupled with a decrease in cell death. To address this question, fluorescence-activated cell sorting (FACS) was employed to analyse the levels of cell death markers in wild type cells overexpressing *RAS2*^{S225A} or an empty plasmid control when grown in either SD –URA or SD –URA + peptone. To investigate the levels of necrosis in the wild type control and wild type cells overexpressing *RAS2*^{S225A} propidium iodide was used.

The supplementation of peptone to SD –URA significantly decreased the percentage of PI positive cells in all strains *(Figure 72)*. No significant difference in the percentage of PI positive cells between wild type and the *RAS2*^{S225A} overexpression strain were observed after 12 days *(Figures 5.6B)*. On day 12, cells grown without peptone supplementation presented ~40% of the cells being PI positive, whereas cells grown in the presence of peptone presented less than 2 % of the population being PI positive *(Figure 72)*. After 12 days of growth in peptone supplemented media, no significant elevation in cell death was observed *(Figure 72)*. We therefor conclude that peptone addition protects all strains examined from necrosis and that necrosis cannot explain the loss of viability observed in wild type or *RAS2*^{S225A} expressing cells during the chronological lifespan assay. However, we conclude that necrosis does account for a significant proportion of dead cells after day 6 of the chronological ageing assay and that this is prevented by peptone supplementation to the media.

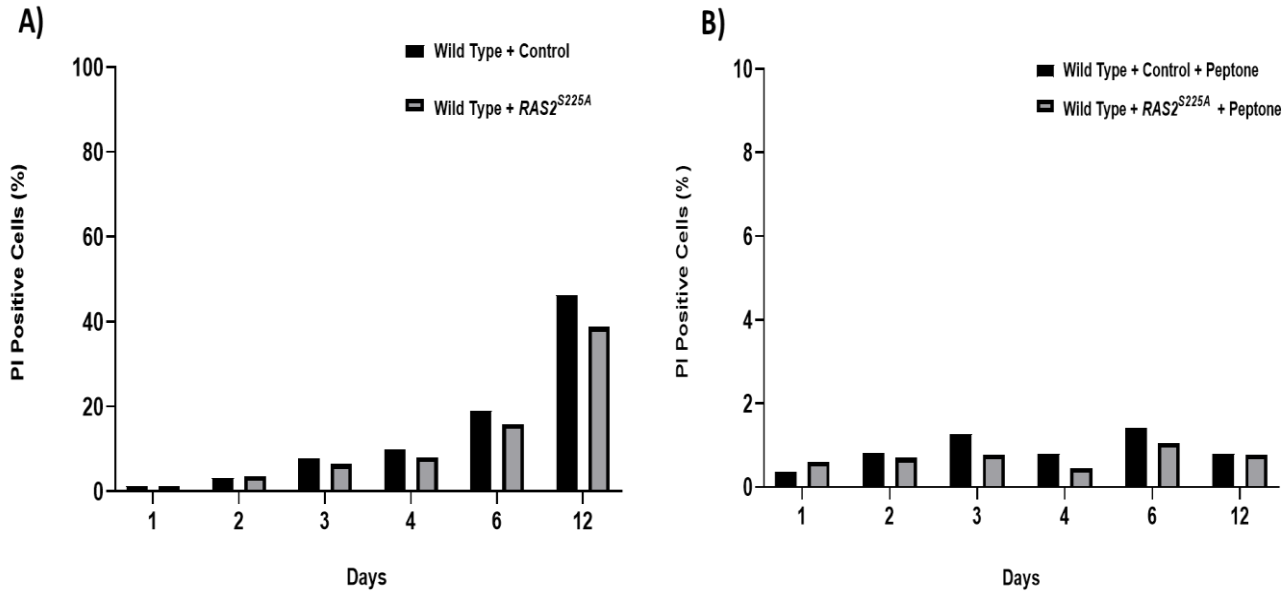

Figure 72. A bar chart presenting the percentage of PI positive cells in wild type cells overexpressing RAS2^{S225A} or an empty plasmid control grown in -URA (A) or -URA + Peptone (B)

(A) A bar chart presenting the percentage of PI positive cells in wild type cells overexpressing RAS2^{S225A} or an empty plasmid control. Strains were grown in SD-URA and measurements were taken over a 12-day period of continuous incubation. Cells were incubated with PI in a 96 well plate for 15 minutes to measure cell death. The data displayed is an average of three biological repeats. (B) A bar chart presenting the percentage of PI positive cells in wild type cells overexpressing RAS2^{S225A} or an empty plasmid control. Strains were grown in SD-URA + Peptone and measurements were taken over a 12-day period of continuous incubation. Cells were incubated with PI in a 96 well plate for 15 minutes to measure cell death. The data displayed is an average of three biological repeats and error represent standard deviation.

5.6 Supplementation of peptone to minimal media retards ROS accumulation in cells

The supplementation of peptone to the growth media increased the chronological life span of all strains examined and reduced the levels of necrosis within the population. We therefor sort to attest whether the supplementation of peptone reduced the accumulation of ROS, a marker attributed to cell death, in all strains examined. To investigate the levels of cell death in cells overexpressing *RAS2^{S225A}* or an empty plasmid control, fluorescence-activated cell sorting (FACS) was utilised. This flow cytometry-based technique was used to determine

whether the overexpression of *RAS2*^{S225A} results in an increase in ROS. The dye dihydroethidium (DHE) was used to analyse superoxide levels within cells. During the first six days of incubation, the addition of peptone to the growth media reduced the percentage of DHE positive cells in all strains examined when compared to cells grown in SD –URA (Figure 73). Between days 1 and 4 in strains grown in the presence of peptone, less than 1 % of the cell population tested positive for elevated DHE *(Figure 73)*. However, at day 12, the supplementation of peptone did not reduce the percentage of DHE positive cells when compared to the strains grown in SD –URA only *(Figure 73)*. We propose that the addition of peptone to the growth media protects all strains examined from ROS accumulation during the first 6 days of incubation. We suggest that ROS accumulation cannot explain the loss in viability of cells until the last two time points of the chronological ageing assay, where elevated ROS contributes significantly.

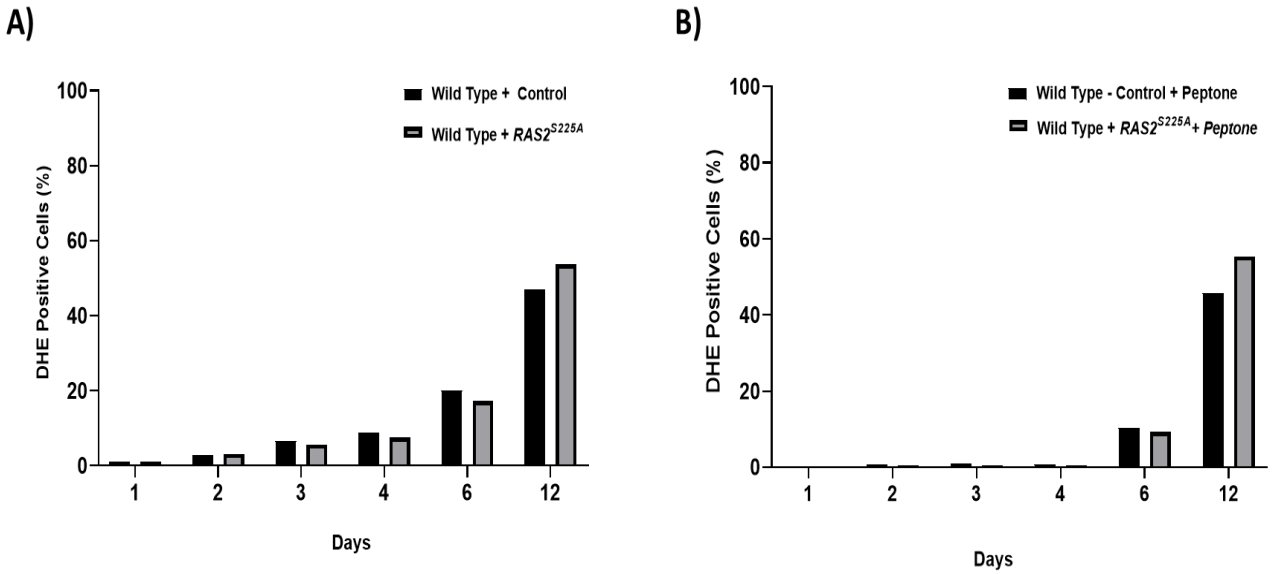

Figure 73. A bar chart presenting the percentage of DHE positive cells in wild type cells overexpressing RAS2^{S225A} or an empty plasmid control grown in -URA (A) or -URA + Peptone (B)

A) A bar chart presenting the percentage of DHE positive cells in wild type cells overexpressing RAS2^{S225A} or an empty plasmid control. Strains were grown in SD-URA and measurements were taken over a 12-day period of continuous incubation. Cells were incubated with DHE in a 96 well plate for 15 minutes to measure superoxide production. The data displayed is an average of three biological repeats. (B) A bar chart presenting the percentage of DHE positive cells in wild type cells overexpressing RAS2^{S225A} or an empty plasmid control. Strains were grown in SD-URA + peptone and measurements were taken over a 12-day period of continuous incubation. Cells were incubated with DHE in a 96 well plate for 15 minutes to measure superoxide production. The data displayed is an average of three biological repeats and error bars represent standard deviation.

5.7 Supplementation of Peptone to minimal media protects cells from oxidative stress

We have previously shown that the overexpression of either *RAS2*^{S225A} or *RAS2*^{S225E} in wild type cells leads to an increase in hydrogen peroxide sensitivity when compared to the wild type control and *RAS2* overexpression strain. We have shown that the supplementation of peptone to minimal media resulted in increased chronological life span and overall decrease in cell death and stress in all strains examined. We sought to investigate whether the supplementation of peptone to SD –URA media containing different concentrations of

hydrogen peroxide would rescue the hydrogen peroxide sensitivity previously observed upon the overexpression of *RAS2*^{S225A} or *RAS2*^{S225E} in wild type cells. To investigate the effect of oxidative stress on wild type cells expressing *RAS2*, *RAS2*^{S225A}, *RAS2*^{S225E} or an empty plasmid control, a blotting assay was conducted as described in Materials and Methods, Section 2.9.5.

On the SD -URA control plate, which did not contain H_2O_2 or peptone, a reduction in growth can be observed in cells expressing *RAS2*^{S225A} or *RAS2*^{S225E} when compared to the control strain *(Figure 74)*. Upon the supplementation of peptone to the control plate, the reduced growth observed in cells overexpressing *RAS2*^{S225A} or *RAS2*^{S225E} is rescued *(Figure 74)*. In the absence of peptone, as the concentration of hydrogen peroxide is increased, the growth of the wild type cells overexpressing *RAS2*^{S225A} or *RAS2*^{S225E} decreases *(Figure 74)*. At a hydrogen peroxide concentration of 3 mM, we observed growth in both the control strain and the *RAS2* overexpression strain, but growth was absent in wild type cells overexpressing either *RAS2*^{S225A} or *RAS2*^{S225E} *(Figure 74)*. However, in the presence of peptone, all strains assayed grew on all concentrations of hydrogen peroxide *(Figure 74)*. As the concentration of hydrogen peroxide was increased, we observed no significant decrease in growth across all strains (Figure 74). We therefor propose that peptone supplementation is protective against

peroxide stress in wild type cells overexpressing *RAS2*, *RAS2*^{S225A}, *RAS2*^{S225E} or an empty plasmid control.

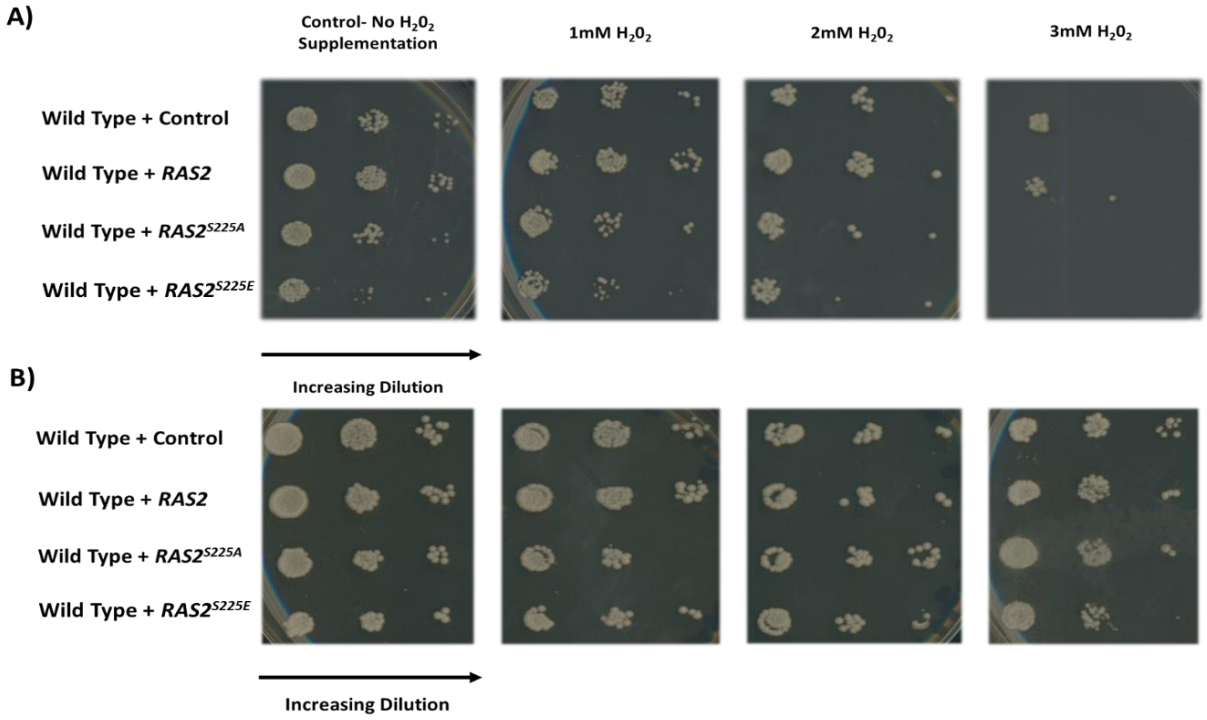

Figure 74. Spotting assay of wild type cells overexpressing RAS2, RAS2^{S225A,} RAS2^{S225E} or an empty plasmid control grown on -URA (A) or -URA + Peptone (B) in the presence of hydrogen peroxide.

*(A) Spotting assay of wild type cells overexpressing RAS2, RAS2^{S225A,} RAS2^{S225E} or an empty plasmid control. Cells were serially diluted from 2*10^6/ml to 2*10^3/ml and plated onto SD -URA plates supplemented with increasing concentrations of hydrogen peroxide. (B) Spotting assay of wild type cells overexpressing RAS2, RAS2^{S225A,} RAS2^{S225E} or an empty plasmid control. Cells were serially diluted from 2*10^6/ml to 2*10^3/ml and plated onto SD -URA plates containing peptone and supplemented with increasing concentrations of hydrogen peroxide.*

5.8 Leucine supplementation does not rescue viability in wild type cells overexpressing *RAS2*^{S225A} or *RAS2*^{S225E}

Certain peptides and amino acids can be utilized as a nitrogen source and can act as signalling molecules that alter cell behaviour. For example, the branched-chain amino acid leucine, has been shown to control TORC1 activity [171][172]. TORC1 senses and responds to nutrients to promote cell growth and the inhibition of catabolic processes, such as autophagy. Branched-

chain amino acids such as leucine function by affecting the 'nucleotide binding status of the Exit from G_0 Complex' (EGOC) GTPase subunits Gtr1 and Gtr2 in *Saccharomyces cerevisiae* [173][174].

We hypothesize that growth on YPD and supplementation of either yeast extract or peptone to SD –URA media increases the concentration of amino acids within the media. As leucine concentrations have been positively correlated with cell growth, we investigated whether increasing the concentration of leucine in the media rescues viability in wild type cells overexpressing $RAS2^{S225A}$ or $RAS2^{S225E}$. A colony forming efficiency assay was conducted as previously described in methods and materials, Section 2.9.3. Cells were plated on either SD-URA or SD-URA supplemented with 150 µg/ml of leucine. The normal levels of leucine required in the medium for the growth of *S. cerevisiae* are 30 µg/ml. A synthetic complete (SC) URA drop out mixture of amino acids from Formedium however contains 380 µg/ml leucine. We increased the levels of leucine further by adding an additional 150 µg/ml of leucine to the SD –URA media and investigated whether additional leucine supplementation resulted in pronounced changes in viability of wild type cells overexpressing $RAS2^{S225A}$ or $RAS2^{S225E}$ *(Figure 75)*.

We observed no significant difference in colony forming efficiency in the wild type control when re-plated on SD-URA supplemented with 150 µg/ml of leucine (Figure 75). No rescue in the viability to that of the wild type control was observed in $RAS2^{S225A}$ or $RAS2^{S225E}$ mutants when plated on media containing additional leucine (Figure 75). We therefor conclude that increasing the availability of leucine in the growth media does not rescue viability in a manner resembling that of growth on YPD. We therefor conclude that the exit from growth cessation observed in cells overexpressing $RAS2^{S225A}$ or $RAS2^{S225E}$ is not leucine dependent.

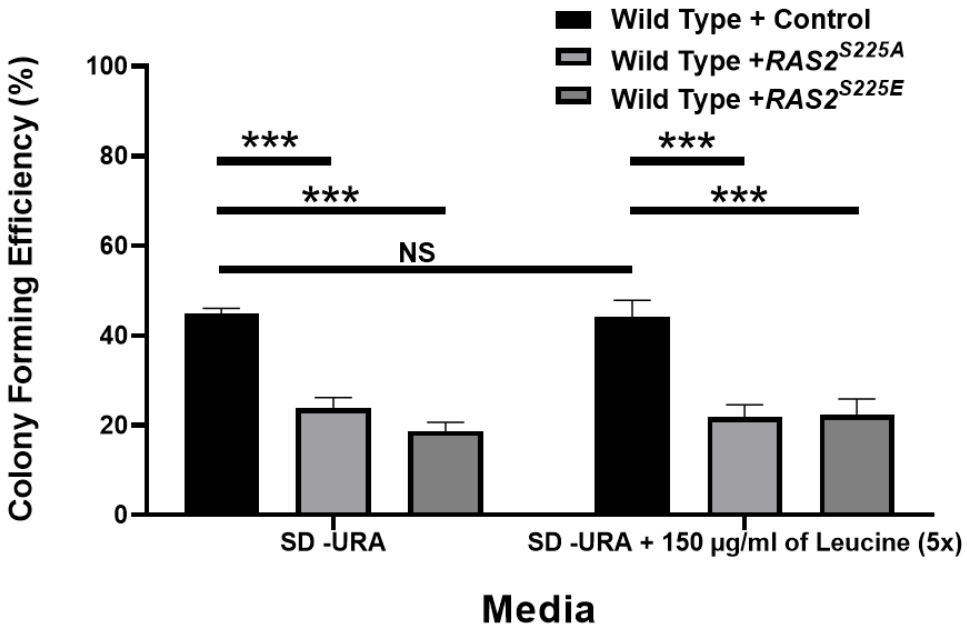

Figure 75. A colony forming efficiency assay of S. cerevisiae wild type cells overexpressing RAS2^{S225A}, RAS2^{S225E}or an empty plasmid control grown in SD –URA media and plated on either SD-URA or SD-URA + 150 µg/ml of leucine.

*A colony forming efficiency analysis was carried out as described in Materials and Methods (Section 2.9.3). A One-way ANOVA using a Tukey multiple comparison test was used to determine statistical significance. Non-significant = NS, * = adjusted p-value ≤ 0.05 and *** = adjusted p value ≤ 0.001*

5.9 Deletion of the di/tri-peptide transporter *PTR2* does not further attenuate viability in wild type cells overexpressing *RAS2*^{S225A}or *RAS2*^{S225E} mutant alleles

We suggest that the supplementation of either yeast extract or peptone to minimal media is sufficient to allow wild type cells expressing *RAS2*^{S225A} or *RAS2*^{S225E} to re-engage the cell cycle. We hypothesized that both peptone and yeast extract may share a common metabolite(s) to which the increase in the viability observed can be attributed to.

Peptone is produced by the enzymatic digest of proteins, producing water-soluble, protein hydrolysates of non-chemically defined nature, containing peptides, amino acids, and

inorganic salts, but devoid of lipids and sugars. Whereas yeast extract consists of the intracellular content of yeast cells upon removal of the cell wall. Upon the analysis of the two ingredients, we observed that both ingredients provide a source of di/tripeptides to the cells. We hypothesized that the increase in viability observed in wild type cells overexpressing the *RAS2*^{S225A} or *RAS2*^{S225E} mutant alleles upon the supplementation of either yeast extract or peptone to the media is a result of elevated intracellular levels of di/tri-peptides within cells.

In *S. cerevisiae*, the uptake of di/tripeptides is predominantly performed by the transmembrane peptide transporter Ptr2p. We hypothesized that the deletion of *PTR2* in wild type cells overexpressing *RAS2*^{S225A} or *RAS2*^{S225E} would further attenuate viability. To attest this hypothesis, plasmids overexpressing *RAS2*^{S225A}, *RAS2*^{S225E} or an empty plasmid control were introduced into a *Δptr2* background and a colony forming efficiency assay was performed as described in Materials and Methods, Section 2.9.3. The deletion of *PTR2* in wild type cells expressing the empty plasmid control presented no significant changes in viability when compared to the wild type control *(Figure 76)*. In wild type strains expressing either *RAS2*^{S225A} or *RAS2*^{S225E} the deletion of *PTR2* resulted in ~20 % of cells within the population being able to form colony forming units *(Figure 76)*, presenting no difference in viability when compared wild type cells overexpressing *RAS2*^{S225A} or *RAS2*^{S225E} mutant alleles *(Figure 76)*. We therefor propose that the deletion of *PTR2* does not further attenuate viability in wild type cells expressing either *RAS2*^{S225A} or *RAS2*^{S225E}.

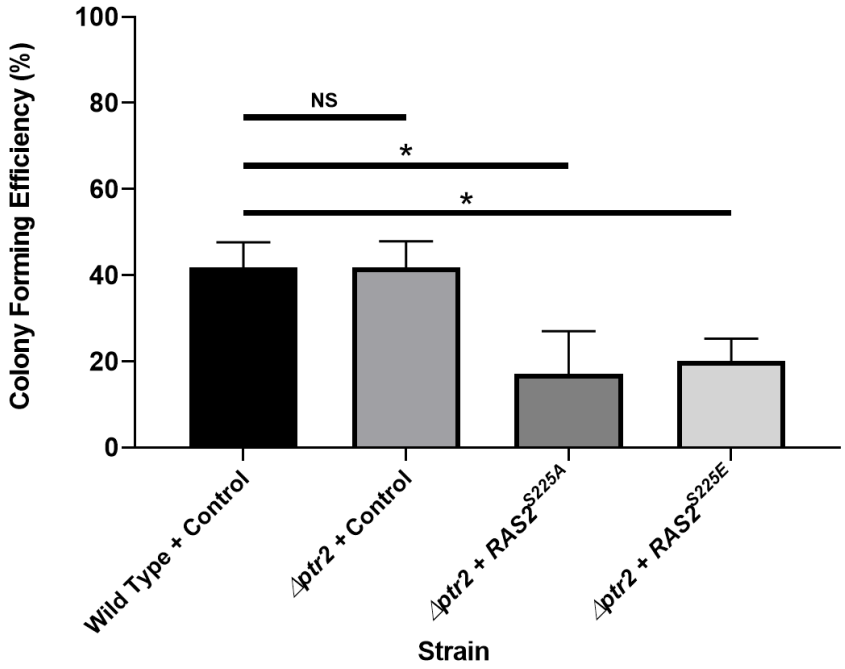

Figure 76. A colony forming efficiency assay of S. cerevisiae wild type or Δptr2 cells overexpressing RAS2^{S225A}, RAS2^{S225E}or an empty plasmid control grown in SD –URA media.
*A colony forming efficiency analysis was carried out as described in Materials and Methods (Section 2.9.3). A One-way ANOVA using a Dunnetts multiple comparison test was used to determine statistical significance. Non-significant = NS, * = adjusted p-value ≤ 0.05 and *** = adjusted p value ≤ 0.001*

5.10 Deletion of *CUP9* in wild type cells overexpressing *RAS2^{S225A}* or *RAS2^{S225E}* rescues growth defects

Expression of the *PTR2* peptide transporter is induced by dipeptides with destabilizing N-terminal residues. These dipeptides bind to Ubr1p, the ubiquitin ligase of the N-end rule pathway, and allosterically accelerate the Ubr1-dependent degradation of Cup9p, a transcriptional repressor of *PTR2*. Ubr1p targets Cup9p through its internal degron [185]. We have previously shown that deletion of *PTR2* presented no significant changes in viability in wild type cells overexpressing *RAS2^{S225A}* or *RAS2^{S225E}* mutant alleles. We hypothesized that increasing *PTR2* expression and thus increasing di/tri-peptide transport in wild type cells

overexpressing either *RAS2*^{S225A} or *RAS2*^{S225E} may enhance viability. To increase *PTR2* expression, we deleted the gene encoding for the transcriptional repressor of *PTR2*, *CUP9*. Plasmids encoding either *RAS2*^{S225A} or *RAS2*^{S225E} or an empty plasmid control were introduced into a *Δcup9* background and a growth analysis was conducted as described in Materials and Methods, Section 2.9.1.

*W*e observed no significant growth defects in *Δcup9* strains overexpressing *RAS2*^{S225A} or *RAS2*^{S225E} mutant alleles when compared to the wild type control *(Figure 77)* with no significant differences in growth rate observed *(Figure 78)*. Deletion of *CUP9* in wild type cells rescues the growth defects previously observed when overexpressing *RAS2*^{S225A} or *RAS2*^{S225E} in wild type cells.

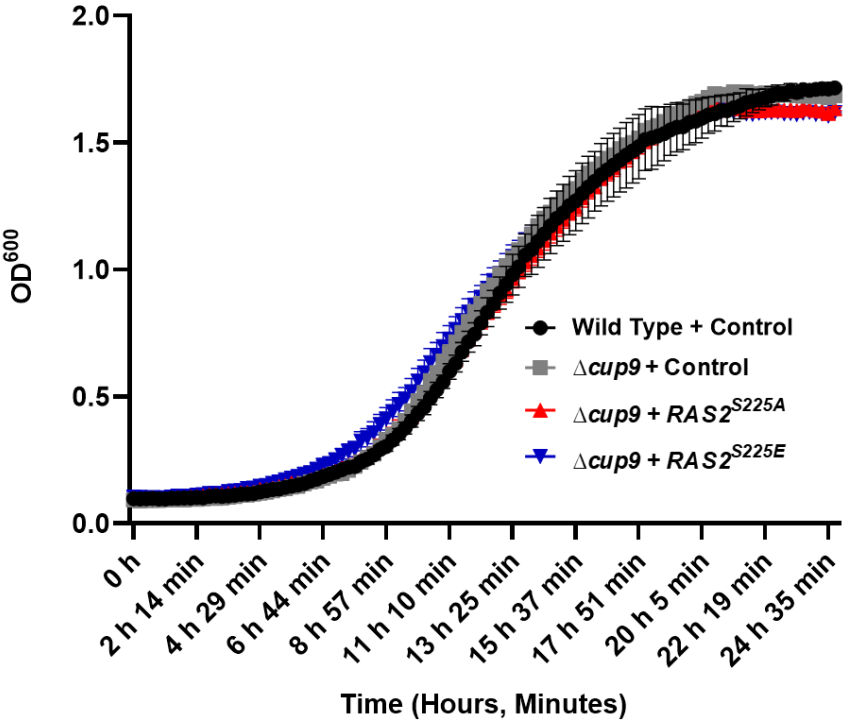

Figure 77. Growth analysis of S. cerevisiae wild type and Δcup9 cells overexpressing RAS2^{S225A}, RAS2^{S225E} or empty plasmid control.

The growth analysis was carried out in SD –URA media as described in Materials and Methods (Section 2.9.1). This data represents an average of three biological repeats and error bars represent the standard deviation.

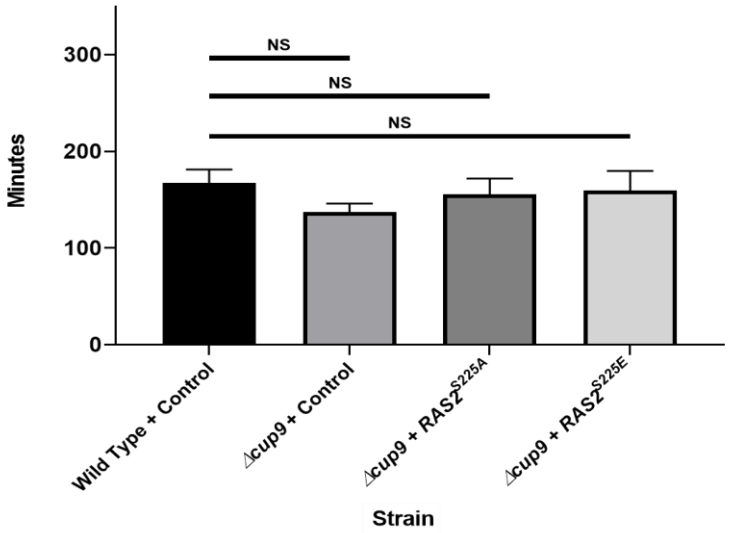

Figure 78. Growth rate analysis of S. cerevisiae wild type or Δcup9 cells overexpressing RAS2^{S225A}, RAS2^{S225E} or an empty plasmid control.

*The growth rate analysis was carried out as described in Materials and Methods (Section 2.9.1). The data represents an average of three biological repeats and error bars represents the standard deviation. A One-way ANOVA using a Dunnets multiple comparison test was used to determine statistical significance. Non-significant = NS, * = adjusted p-value ≤ 0.05 and *** = adjusted p value ≤ 0.001.*

5.11 Deletion of *CUP9* in wild type cells expressing *RAS2* mutant alleles rescues viability

To determine whether the overexpression of either *RAS2*^{S225A} or *RAS2*^{S225E} affects viability in a *Δcup9* background, a viability assay was conducted as described in Materials and Methods, Section 2.9.3 The deletion of *CUP9* in wild type cells expressing a plasmid control presented no significant change in viability when compared to the wild type control *(Figure 79)*. Interestingly, the overexpression of *RAS2*^{S225E} in a *Δcup9* background lead to a significant increase in viability when compared to the wild type control *(Figure 79)*. Furthermore, the overexpression of *RAS2*^{S225A} in a *Δcup9* background lead to no significant changes in viability when compared to the wild type control *(Figure 79)*. Our data suggests that the deletion of *CUP9* in wild type cells overexpressing *RAS2*^{S225A} or *RAS2*^{S225E} prevents the toxic gain of function of the overexpression of either *RAS2*^{S225A} or *RAS2*^{S225E} in wild type cells and prevents cells from disengaging the cell cycle.

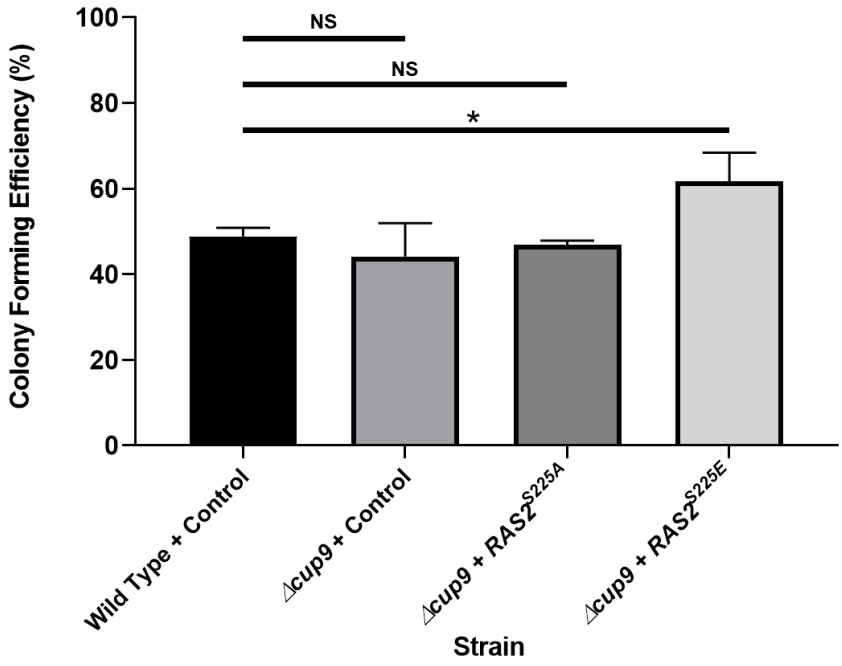

Figure 79. A colony forming efficiency assay of S. cerevisiae wild type or Δcup9 cells overexpressing RAS2^{S225A}, RAS2^{S225E}or an empty plasmid control grown in SD –URA media.
*A colony forming efficiency analysis was carried out as described in Materials and Methods (Section 2.9.3). The data represents an average of three biological repeats and error bars represents the standard deviation. A One-way ANOVA using a Dunnetts multiple comparison test was used to determine statistical significance. Non-significant = NS, * = adjusted p-value ≤ 0.05 and *** = adjusted p value ≤ 0.001.*

5.12 Deletion of *UBR1* does not further attenuate viability in wild type cells overexpressing *RAS2^{S225A}* or *RAS2^{S225E}*

We have previously shown that the deletion of *CUP9* rescues the growth defects induced by the overexpression of either *RAS2^{S225A}* or *RAS2^{S225E}* in wild type cells. We hypothesize that deletion of *CUP9*, increases *PTR2* expression thus increasing the transportation of di-tripeptides into the cell and restoring viability. As Ubr1p degrades cellular Cup9p, we hypothesize that the deletion of *UBR1* in wild type cells will increase the levels of cellular Cup9p and thus decrease the expression of *PTR2* which may further decrease viability in wild type cells overexpressing either *RAS2^{S225A}* or *RAS2^{S225E}*. To attest this hypothesis, plasmids

encoding *RAS2*^{S225A}, *RAS2*^{S25E} or an empty plasmid control were introduced into a *Δubr1* strain and a colony forming efficiency assay was conducted as described in Materials and Methods, Section 2.9.3).

The expression of an empty plasmid control in a *Δubr1* background lead to no significant changes in viability when compared to the wild type control *(Figure 80)*. The overexpression of either *RAS2*^{S225A} or *RAS2*^{S225E} in a *UBR1* deletion strain lead to a decrease in viability when compared to the control strains *(Figure 80*). The viability of *Δubr1* strains expressing either *RAS2*^{S225A} or *RAS2*^{S225E} was ~20%, which mirrors that seen in wild type cells overexpressing the *RAS2*^{S225A}or *RAS2*^{S225E} mutant alleles *(Figure 30)*. We therefor propose that the deletion of *UBR1* in wild type cells overexpressing *RAS2*^{S225A} or *RAS2*^{S225E} does not lead to a further attenuation of viability.

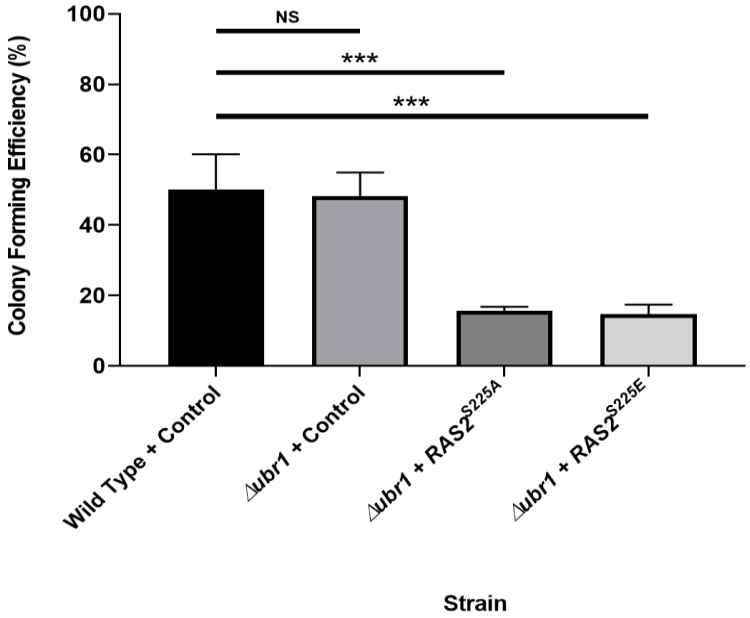

Figure 80. A colony forming efficiency assay of S. cerevisiae wild type or Δubr1 cells overexpressing RAS2^{S225A}, RAS2^{S225E}or an empty plasmid control grown in SD –URA media.
*A colony forming efficiency analysis was carried out as described in Materials and Methods (Section 2.9.3). The data represents an average of three biological repeats and error bars represents the standard deviation. A One-way ANOVA using a Dunnetts multiple comparison test was used to determine statistical significance. Non-significant = NS, * = adjusted p-value ≤ 0.05 and *** = adjusted p value ≤ 0.001.*

5.13 The effects of di-peptide supplementation on the viability of wild type cells overexpressing the *RAS2* mutant alleles

We have shown that the deletion *of CUP9* in wild type cells overexpressing either *RAS2*^{S225A} or *RAS2*^{S225E} rescues both growth and viability. We hypothesize that the deletion of *CUP9*, relieves *PTR2* from repression and increases its expression. We propose that increased *PTR2* expression will lead to elevate di/tri-peptide uptake into cells which may result in the rescue of the growth defects observed in wild type cells overexpressing *RAS2*^{S225A} or *RAS2*^{S225E}.

It has been previously revealed that the regulation of *PTR2* expression in *S. cerevisiae* is also influenced by the extracellular environment. In particular di/tri-peptides have been identified to induce *PTR2* expression [185][182][179]. Furthermore, the import of di/tri-peptides comprised of basic or bulky hydrophobic N-terminal residues have also been shown to increase *PTR2* expression via the reduction of cellular levels of the *PTR2* repressor Cup9p [185].

In order to increase *PTR2* expression without the deletion of its repressor *CUP9* in wild type cells overexpressing *RAS2*^{S225A}, we proposed to utilize the positive regulatory feedback loop mediated by di/tri-peptide uptake by the supplementation of peptides containing bulky and basic N-terminal residues to the –URA growth media. We hypothesize that the supplementation of these specific di/tripeptides will upregulate *PTR2* expression and thus increase di/tri-peptide uptake and enable wild type cells overexpressing *RAS2*^{S225A} to exit growth cessation. To attest this hypothesis, a colony forming efficiency assay was performed as described in (Materials and Methods, Section 2.9.4) and after 24 hours of incubation in SD –URA media, cells were plated onto either SD-URA or SD –URA with the addition of a specific

di-peptide at a 1 mM concentration. After 36 hours of incubation the colony forming efficiency for each condition was calculated.

Surprisingly, no significant difference in viability was observed in all strains grown in the presence of any of the supplemented di-peptides *(Figure 81)*. No increase in viability to that of the wild type was observed in the *RAS2*^{S225A} mutant upon supplementation of any of the di/tripeptides to the minimal media *(Figure 81)*. We therefor conclude that the presence of either Leu-Leu, Ala-Leu, Tyro-Ala or His-Leu at a 1 mM concentration does increase viability in wild type cells overexpressing *RAS2*^{S225A} in the conditions used.

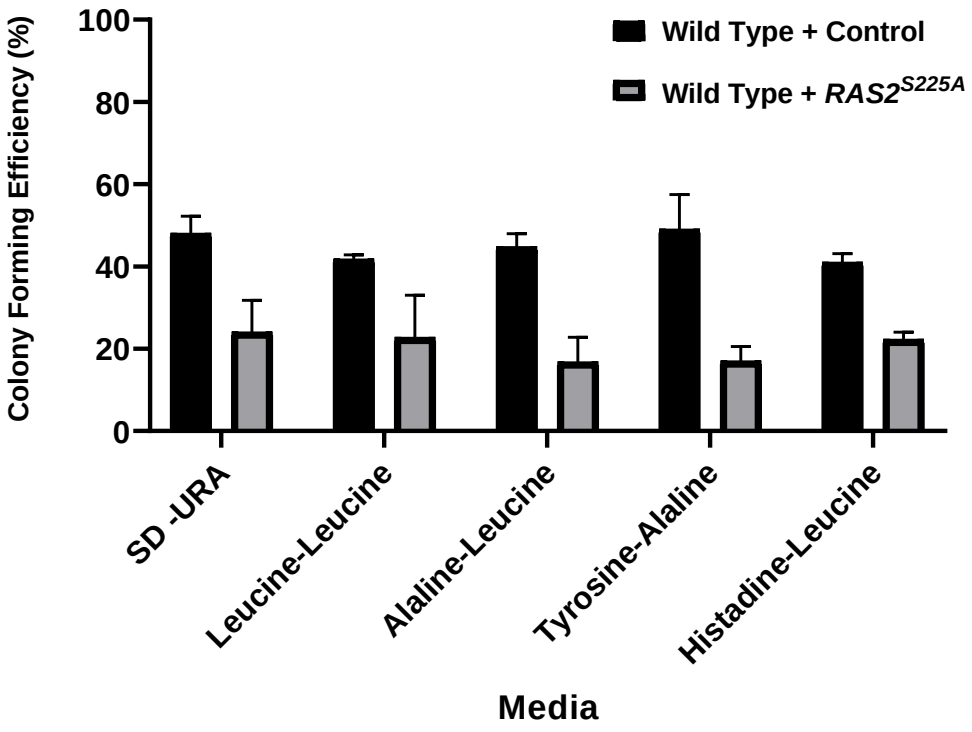

Figure 81. A colony forming efficiency assay of S. cerevisiae wild type cells overexpressing RAS2^{S225A} or an empty plasmid control grown in SD –URA media and plated on SD-URA supplemented with a di-peptide at a 1 mM concentration.

A colony forming efficiency analysis was carried out as described in Materials and Methods (Section 2.9.4). The data represents an average of three biological repeats and error bars represents the standard deviation.

The supplementation of either Leucine-Leucine, Alaline-Leucine, Tyrosine-Alaline or Histadine-Leucine dipeptides to the growth media at a 1 mM concentration did not rescue viability in wild type cells overexpressing *RAS2*^{S225A}. We hypothesized that combining all the previously examined dipeptides together in the growth media may present changes in viability of the *RAS2*^{S225A} mutant, which were not observed previously when dipeptides were supplemented to the growth media singularly. To attest this hypothesis, a colony forming efficiency assay was conducted as previously described in Materials and Methods, Section 2.9.4. Cells were plated onto SD –URA media containing the following dipeptides at a 1 mM concentration, Leucine-Leucine, Alaline-Leucine, Tyrosine-Alaline and Histadine-Leucine. The supplementation of the dipeptide mix did not result in a rescue of viability in wild type cells overexpressing *RAS2*^{S225A} when compared to the wild type control *(Figure 82)*. We conclude that the supplementation of the dipeptides examined in this study, either added singularly or combined together, failed to produce any significant changes in the viability of either the wild type control or the *RAS2*^{S225A} mutant when compared to cells grown on SD-URA media.

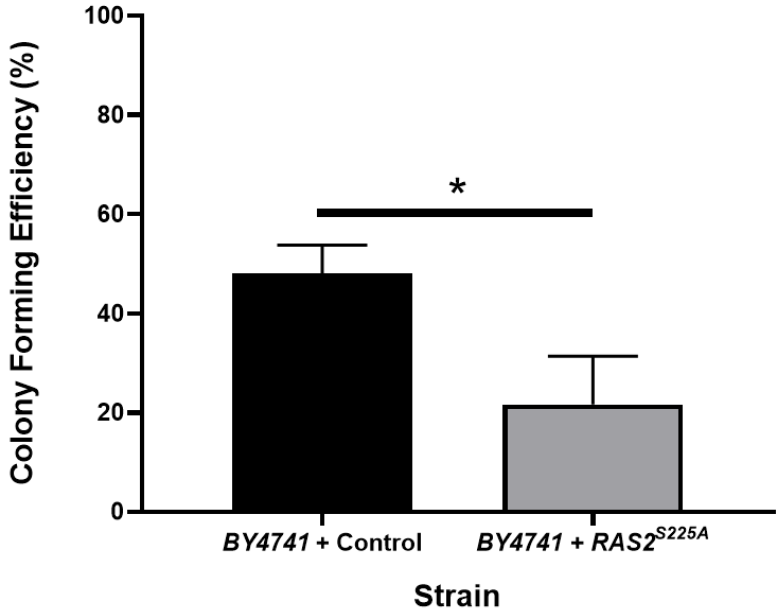

Figure 82. A colony forming efficiency assay of S. cerevisiae wild type cells overexpressing RAS2^{S225A} or an empty plasmid control grown in SD –URA media and plated on SD-URA supplemented with the di-peptides; Leucine-Leucine, Alaline-Leucine, Tyrosine-Alaline and Histadine-Leucine at a 1 mM concentration.

*A colony forming efficiency analysis was carried out as described in Materials and Methods (Section 2.9.1). The data represents an average of three biological repeats and error bars represents the standard deviation. A One-way ANOVA using a Dunnetts multiple comparison test was used to determine statistical significance. Non-significant = NS, * = adjusted p-value ≤ 0.05 and *** = adjusted p value ≤ 0.001.*

5.14 Discussion

In previous chapters we suggest that the overexpression of either *RAS2*^{S225A} or *RAS2*^{S225E} leads to the miss localisation of active Ras to the nuclear envelope. Such localisation results in growth defects and a loss of viability that we believe to be attributable to deregulation in the cell cycle. We established that the slow growth phenotype observed is linked to elevated PKA activity, as overexpression of *PDE2* in strains overexpressing *RAS2*^{S225A} or *RAS2*^{S225E} rescued viability. We sought to investigate whether changing the nutrition availability would enable cells overexpressing *RAS2* mutant alleles to restore growth and viability in manner analogous to the co-expression with *PDE2.*

We show that the growth of wild type cells overexpressing *RAS2*^{S225A} or *RAS2*^{S225E} on nutrient rich media, such as YPD, rescued viability. We therefore propose that the overexpression of either *RAS2*^{S225A} or *RAS2*^{S225E} in wild type cells does not lead to cell death but rather a cessation of proliferation, as cells were able to re-proliferate upon re-plating on nutrient rich agar. This provides further evidence to suggest that the overexpression of *RAS2*^{S225A} or *RAS2*^{S225E} leads to a cessation of growth in the yeast system opposed to cell death. To determine which component of the nutrient rich media results in the reengaging of the cell cycle, YPD was broken down into its constituent parts and these were individually added to the SD –URA agar at the same concentration as seen in YPD. Viability assays were conducted and the supplementation of both yeast extract or peptone to SD –URA media resulted in a rescue of viability in wild type cells overexpressing *RAS2*^{S225A} or *RAS2*^{S225E}. Interestingly, increasing the availability of either glucose or leucine to cells overexpressing *RAS2*^{S225A} or *RAS2*^{S225E} did not lead to any changes in viability. This indicates that the nature of the slow growth phenotype seen upon overexpression of *RAS2* mutant alleles is not mediated through glucose and leucine levels.

The effects of peptone supplementation were investigated further with regards to its effect on chronological life span, cell death and oxidative stress sensitivity. In wild type cells overexpressing *RAS2*^{S225A} or *RAS2*^{S225A}, the supplementation of peptone increased the chronological life span of cells and decreased the levels of both necrosis and ROS in the cell population.

We show that the supplementation of either yeast extract or peptone to minimal media is sufficient to allow wild type cells expressing *RAS2*^{S225A} or *RAS2*^{S225E} to restore growth. We hypothesized that both peptone and yeast extract may share a common metabolite(s) to

which the increase in the viability observed can be attributed to. Upon the analysis of the two ingredients, we observed that both ingredients provide a source of di/tripeptides to the cells. We hypothesized that the increase in viability observed in wild type cells overexpressing the *RAS2*^{S225A} or *RAS2*^{S225E} mutant alleles upon the supplementation of either yeast extract or peptone to the media is a result of elevated intracellular levels of di/tri-peptides within cells.

In *S. cerevisiae*, the uptake of di/tripeptides is predominantly performed by the transmembrane peptide transporter Ptr2p. To reduce the intracellular levels of di/tripeptides, *PTR2* was deleted in cells overexpressing *RAS2* mutant alleles. Surprisingly, the deletion of *PTR2* presents no significant changes in viability. However, the deletion of *CUP9*, the transcriptional repressor of *PTR2*, rescued both growth and viability defects. We propose that the deletion of *CUP9* increases *PTR2* expression, increases peptide uptake and allowing cells to reengage in the cell cycle. This data indicates an interplay between Ras activity, utilisation of available nutrition and cell fate.

To further investigate the effects of di/tri-peptide uptake on the viability of cells overexpressing either *RAS2*^{S225A} *or RAS2*^{S225E}, the dipeptides; Leu-Leu, Ala-Leu, Tyro-Ala or His-Leu were supplemented to the growth media and viability assays conducted. However, no significant effects on cell viability were observed upon the addition of any of the di-peptides. We then hypothesised that the rescue of viability observed in cells overexpressing *RAS2*^{S225A} or *RAS2*^{S225E} may not be mediated by a single di-peptide but rather a combination. To attest this the dipeptides previously examined were added together in the growth media and viability assays were conducted. However, no change in viability was recorded in wild type cells overexpressing *RAS2* mutant alleles. We therefor propose that the rescue in viability

observed from growth on YPD, supplementation of either peptone or yeast and deletion of *CUP9* is not wholly attributable to an increase in di/tripeptide uptake.

Although unlikely, it is possible that the growth of wild type cells in nutrient rich media may result in a reduction of plasmid copy number. In this scenario, a reduction in copy number of either the plasmids expressing $RAS2^{S225A}$ or $RAS2^{S225E}$ in wild type cells could explain the increase in viability observed when grown in YPD media when compared to cells grown in SD –URA media. This is an important considerations and further investigations must be conducted to address this question. In the next chapter we investigate the global effects of the overexpression of either $RAS2^{S225A}$ or $RAS2^{S225E}$ in wild type cells via genome-wide transcriptome analysis.

Chapter 6

Transcriptome analysis of *RAS2*^{S225A} or *RAS2*^{S225E} overexpressing cells

6.1 Introduction

Quiescence in yeast cells is defined as a temporary non-proliferating cellular state. In *S. cerevisiae*, quiescent cells display a number of specific characteristics that differentiate them from proliferating cells: the overall transcription rate is substantially reduced [215]; the rate of overall protein synthesis is reduced to approximately 0.3 % of that observed in exponential cultures [248]; the expression of specific gene sets is severely downregulated e.g. genes encoding ribosomal proteins[249]; and chromosomes are condensed [250].

In previous chapters we suggest that the overexpression of either *RAS2*^{S225A} or *RAS2*^{S225E} in wild type cells leads to growth defects and a loss of viability that we propose to be attributable to a dysregulation in the cell cycle. We suggest that the slow growth phenotype is mediated through the Ras/cAMP/PKA pathway as suppression of this pathway, through the overexpression of *PDE2*, leads to a complete rescue of viability and growth. In addition, we show that increasing the nutrient availability to cells overexpressing *RAS2* mutant alleles, either through growth on nutrient rich media or through deletion of *CUP9*, also results in a rescue of the loss of viability phenotype. We therefore sought to investigate the gene expression patterns that govern the reduced growth phenotype observed using an RNA sequencing approach.

6.2 Illumina library preparation and RNA sequencing

After 24 hours of growth, total RNA was extracted in biological triplicate from wild type cells overexpressing *RAS2*^{S225A}, *RAS2*^{S225E} or containing an empty plasmid using the E.Z.N.A.™ Yeast RNA Kit as detailed in Materials and Methods, Section 2.7.4. After extraction, RNA purity was estimated using a NanoDrop ND-1000 spectrophotometer and sent to the Centre for Genome

Enabled Biology and Medicine (Aberdeen, UK) for library preparation and sequencing. Sequencing was performed on the Illumina NextSeq500 platform, producing 75bp single end reads.

Prior to library preparation the quality and quantification of RNA samples were evaluated with TapeStation (Agilent) and Qubit (Thermal Fisher) by Dr Jin Pu from the Centre for Genome Enabled Biology and Medicine (Aberdeen, UK). The samples with the minimum RIN of 8.0 were proceeded. The mRNA-Seq libraries were prepared using TruSeq™ Stranded mRNA Sample Preparation Kit (Ilumina) according to the manufacturer's instructions. Briefly, Poly-A RNA were purified from 500ng of total RNA with 1ul (1:100) ERCC spike (Thermal Fisher) as an internal control using RNA purification oligo(dT) beads, fragmented and retrotranscribed using random primers. Complementary-DNAs were end-repaired, and 3-adenylated, indexed adapters were then ligated. 15 cycles of PCR amplification were performed, and the PCR products were cleaned up with AMPure beads (Beckman Coulter). Libraries were validated for quality on Agilent DNA1000 Kit and quantified with the qPCR NGS Library Quantification kit (Roche). The final libraries were equimolar pooling and sequenced using the High Output 1X75 kit on the Illumina NextSeq 500 platform producing 75 bp single end reads. For each library a depth 20-30M reads were generated.

6.3 Quality control analysis of RNA-Seq reads

The analysis of RNA–Seq samples was performed using the Galaxy web platform (www.usegalaxy.org) [202]. The quality of the RNA sequencing reads was checked using the FASTQC v0.11.5 plug-in, using the default settings [203]. The FastQC plug-in provides a simplistic platform to perform quality control checks on raw sequencing data sourced from high throughput sequencing pipelines. FastQC delivers visual readouts of the quality of raw

sequencing data, providing information on basic statistics including the average sequence length, number of sequences and the number of poor-quality sequences. Importantly, FastQC produces a Phred score for each sample, providing information on the probability of a base being erroneous and provides an adapter content score, indicating the level of adapter contamination within the reads.

After the completion of the FastQC analysis, the information obtained was used to determine whether any trimming of the sequencing was necessary before deeper analysis. All samples with low quality ends (Phred score < 20) and adapter sequences were trimmed using the TrimGalore v0.4.3 plug-in [204]. After trimming, 98.8% of initial reads remained and FastQC v0.11.5 [203] was run again to confirm the quality. There were no Poly-A reads (more than 90% of the bases equal A), ambiguous reads (containing N) or low-quality reads (more than 50% of the bases with a Phred score < 20). After processing, the mean Phred score per read was 37.

6.4 FastQC output

6.4.1 Basic Statistics

The basic statistics output generated from the FastQC analysis indicated that there were no sequences flagged as poor quality after trimming across all samples (Table 6.1). The sequence length of the reads after trimming was between 40-52 bases and the average sequencing depth was 34 M across all samples with an average GC % of 41.

Table 13. Basic statistics output from FastQC analysis of the RNA sequencing reads generated from RNA isolated from wild type cells overexpressing RAS2^{S225A} (replicate 1). *This table is representative of all the samples.*

Basic Statistics

Measure	Value
Filename	Trim Galore_ on data 67_ trimmed reads.gz
File type	Conventional base calls
Encoding	Sanger / Illumina 1.9
Total Sequences	34051638
Sequences flagged as poor quality	0
Sequence length	40-52
%GC	41

6.4.2 Phred Score

A Phred quality score is a measure of the quality of identification of the nucleobases generated by automated DNA sequencing [251]. The Phred scores provides an insight into the probability that a base within a sequencing read has been wrongly assigned, thereby providing an estimation of the quality of the sequencing reaction, and hence resulting reads.

A phred score resides on a logarithmic scale ranging from 1-40 where the higher the Phred score the lower the probability of the base being erroneous. A nucleotide base Phred score of 30 indicates a 1 in 1000 probability that the base was assigned incorrectly during the sequencing reaction. This translates to an accuracy of 99.9 % and therefore reads with a Phred score greater than 30 are considered good quality reads and progressed to next-generation sequencing applications such as RNA-Seq [251]. For the 9 samples investigated in this study, all samples produced Phred scores greater than 30, with the average Phred score being 35 *(Figure 83)*

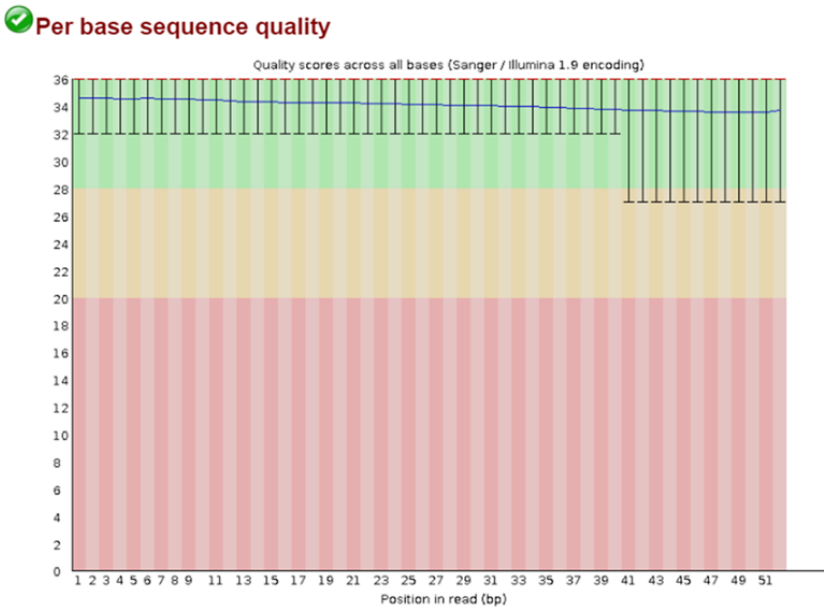

Figure 83. The average Phred score for each base across the length of the sequencing read. *This read was generated from the RNA isolated from wild type cells overexpressing RAS2^{S225A} (replicate 1). This graph is representative of all samples investigated.*

6.4.3 N content

The N content indicates the number of ambiguous reads within a sample, i.e. the number of reads containing at least one base which was not assigned and hence denoted as N. There were no ambiguous reads in any of the 9 samples under investigation *(Figure 84)*

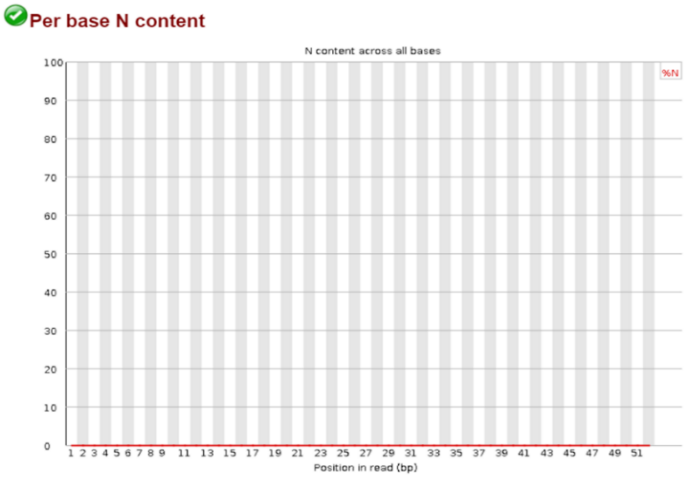

Figure 84. N content across all bases within the reads from RNA isolated from wild type cells overexpressing RAS2^{S225A} (Sample 1).
This graph is representative of all samples.

6.4.4 Adapter Content

The adapter content value provides a quantification of any contamination in reads caused by the presence of sequences originating from the library preparation. Contaminations caused by the presence of adapter sequences can result in alignment errors when aligning the reads to a reference genome since the adaptor sequences will not appear in the genome. Therefor trimming of reads is necessary to remove any adaptor sequences which could influence downstream applications. Post trimming, no adaptor sequences were detected in reads from all samples *(Figure 85)*.

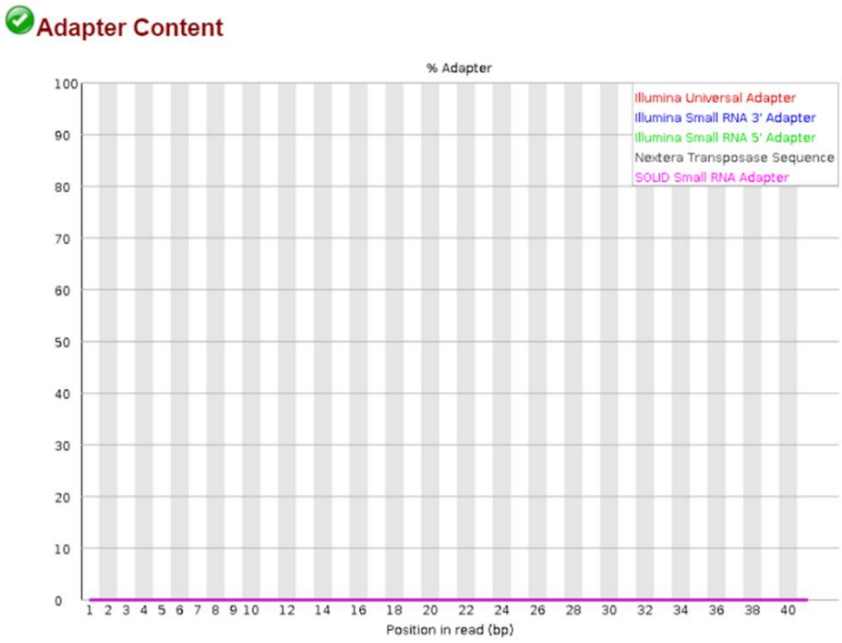

Figure 85. Adaptor content across bases within the reads of RNA isolated from wild type cells overexpressing RAS2^{S225A} (sample 1).
This graph is representative of all samples.

6.5 Principle Component Analysis

A principle component analysis (PCA) is a statistical procedure used for the exploration of large data sets. PCA is a valuable method for the visualisation of large data sets and is used to determine the degree of similarity between biological replicates, and how different they are to samples from other conditions. PCA was conducted within the DESeq2 package as part of the differential gene expression analysis [207].

The PCA reduces the dimensionality of the data sets by determining directions along which the most variation occurs thus simplifying very large data sets while retaining as much information as possible [252]. Within a PCA, the first principle component (PC1), is the direction along which most of variation occurs and the second principal component (PC2) covers as much of the remaining variation as possible [252]. Samples are plotted on a PCA graph based on the two principle components. Samples displaying clear clustering, indicates similarity between samples and large degrees of separation between samples indicates a low level of similarity.

In this study, biological replicates of the RNA sequenced from wild type cells overexpressing either *RAS2*^{S225A}, *RAS2*^{S225E} or an empty plasmid control cluster well along both the PC1 and PC2 axis, indicating that within the biological repeats there is a high degree of similarity *(Figure 86)*. There is also a significant degree of separation between the clusters of the biological repeats suggesting differential gene expression between strains *(Figure 86)*.

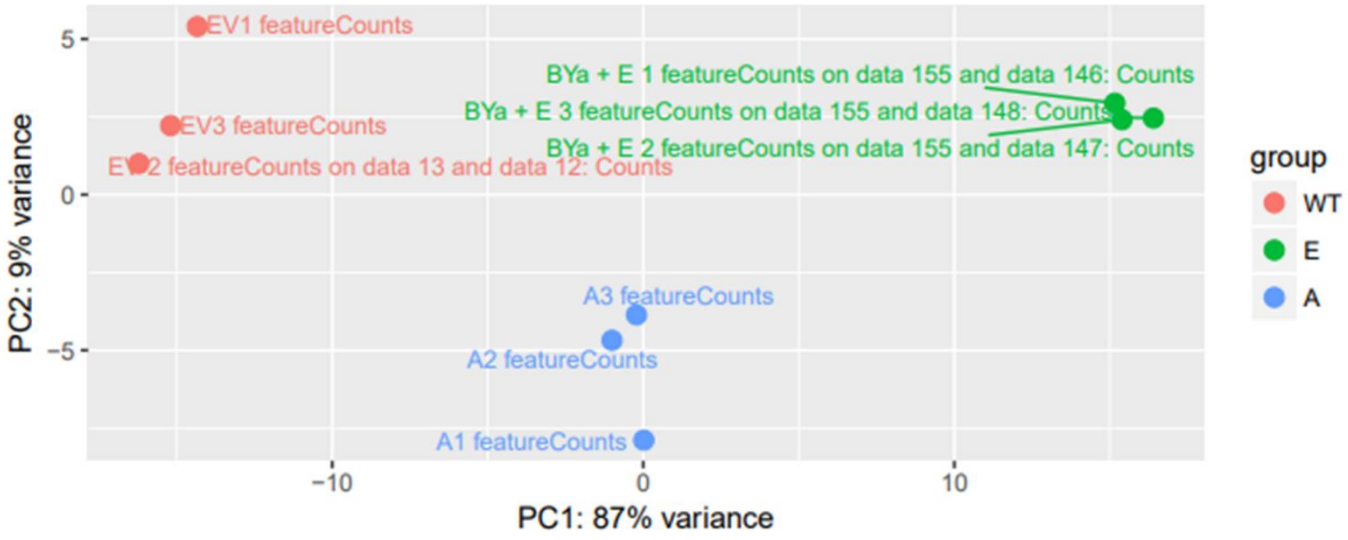

Figure 86. Principle component analysis of the RNA-Seq data obtained from wild type cells overexpressing RAS2^{S225A}, RAS2^{S225E} or an empty plasmid control.

6.6 Analysis of RNA-Seq reads using the Galaxy online platform

Processed reads were aligned with the reference *S. cerevisiae* genome S288C version R64-2-1_20150113 (SacCer3) using HISAT2 v2.1.0 with single-end reads and reverse strand settings, with all other settings set to default [205]. After the completion of the alignment, the number of mapped reads which overlapped CSD features in the genome, using the S288C version R64-2-1_20150113_features gtf annotation file, were determined using the featureCounts plug-in v1.6.3 with default settings [206]. Reads aligning to multiple positions or overlapping more than one gene were discarded, counting only reads aligning unambiguously to a single gene. Differential gene expression analysis between RNA extracted from wild type cells overexpressing *RAS2*^{S225A}, *RAS2*^{S225E} or an empty plasmid control were performed using DESeq2 v1.18.1 using default settings [207].

Using DESeq2, the expression levels of each gene in wild type cells overexpressing either

RAS2^{S225A} or *RAS2*^{S225E} was compared to samples generated from wild type cells overexpressing an empty plasmid control. The overexpression of either *RAS2*^{S225A} or *RAS2*^{S225E} led to a global response resulting in the significant differential expression of genes when compared to the wild type control. The overexpression of *RAS2*^{S225A} lead to the differential gene expression (false-discovery-rate adjusted p-value (q) ≤ 0.05) of 4133 genes, with roughly equal numbers of genes up- and downregulated (2054 up and 2079 down) *(Figure 87)*. 58 genes were strongly (log2 fold change >2) upregulated and 23 were strongly (log2 fold change <-1.5) downregulated. The overexpression of *RAS2*^{S225E} lead to the differential gene expression (false-discovery-rate adjusted p-value (q) ≤ 0.05) of 5202 genes, with 2543 upregulated and 2659 down downregulated *(Figure 88)*. 281 genes were strongly (log2 fold change >2) upregulated and 644 genes were strongly (log2 fold change <-1.5) downregulated. To identify the cellular pathways which these differentially expressed genes are within we conducted Gene Set Enrichment Analysis (GSEA; Broad Institute) [208]. The GSEA is a computational method which determines whether a prior defined gene set data presents statistically significant, concordant differences between two biological states.

To conduct a GSEA analysis, a list of significantly (q ≤ 0.05) differentially expressed genes, ranked from the most upregulated to the most downregulated were uploaded into the GSEA database and compared to a gene set data base (S288C version R64-2-1_20150113_features gtf annotation file). GSEA functions to identify whether the members of each gene set are randomly distributed within the ranked gene list or significantly overrepresented (enriched) at either end of the gene list. Gene sets are ranked using a normalised enrichment score (NES). A positive normalised enrichment score indicates that genes within a specific a gene set are located at the top of the ranked gene list whereas a negative normalised enrichment score indicates that genes within a specific gene set are located at the bottom of the ranked

gene list. From this information we can predict which biological processes or pathways are up- or downregulated between strains. The GSEA is a powerful form of analysis as an increase in the expression of 15 % of all genes associated with a pathway may have more effect than a single gene that has say a 10-fold increase in expression. The GSEA output provides enrichment profiles showing correlations with numerous overlapping gene sets, we were able to visualise networks of similar gene sets using the cytoscape 3.7.1 EnrichmentMap plug-in [253] *(Figure 87)*.

6.7. GSEA analysis of cellular processes differentially regulated by the overexpression of *RAS2^{S225A}*

Interestingly, the overexpression of *RAS2^{S225A}* in wild type cells induced a significant upregulation in pathways involved in ribosomal biogenesis, transcription, translation, glucose transport and central metabolism *(Figure 87)*. Such an observation was surprising as the pathways upregulated recapitulate those observed from exponentially growing cells [248][249][226][226].

However, such an observation can be explained upon the analysis of the pathways downregulated by the overexpression of *RAS2^{S225A}*. We observed a significant downregulation in cytoskeletal, microtubule and kinetochore dynamics and nuclear and cell division; chromosome condensation and segregation, cell cycle phase transition, mitosis and transcription factors associated with cell cycle phase progression *(Figure 87)*. The resulting effect of the downregulation of the pathways are indicative of a cessation of proliferation. It may be the case that a loss of co-ordination between cytoplasmic and nuclear machinery occurs upon the overexpression of *RAS2^{S225A}* in that cells are primed for cell division but possess an inability to divide.

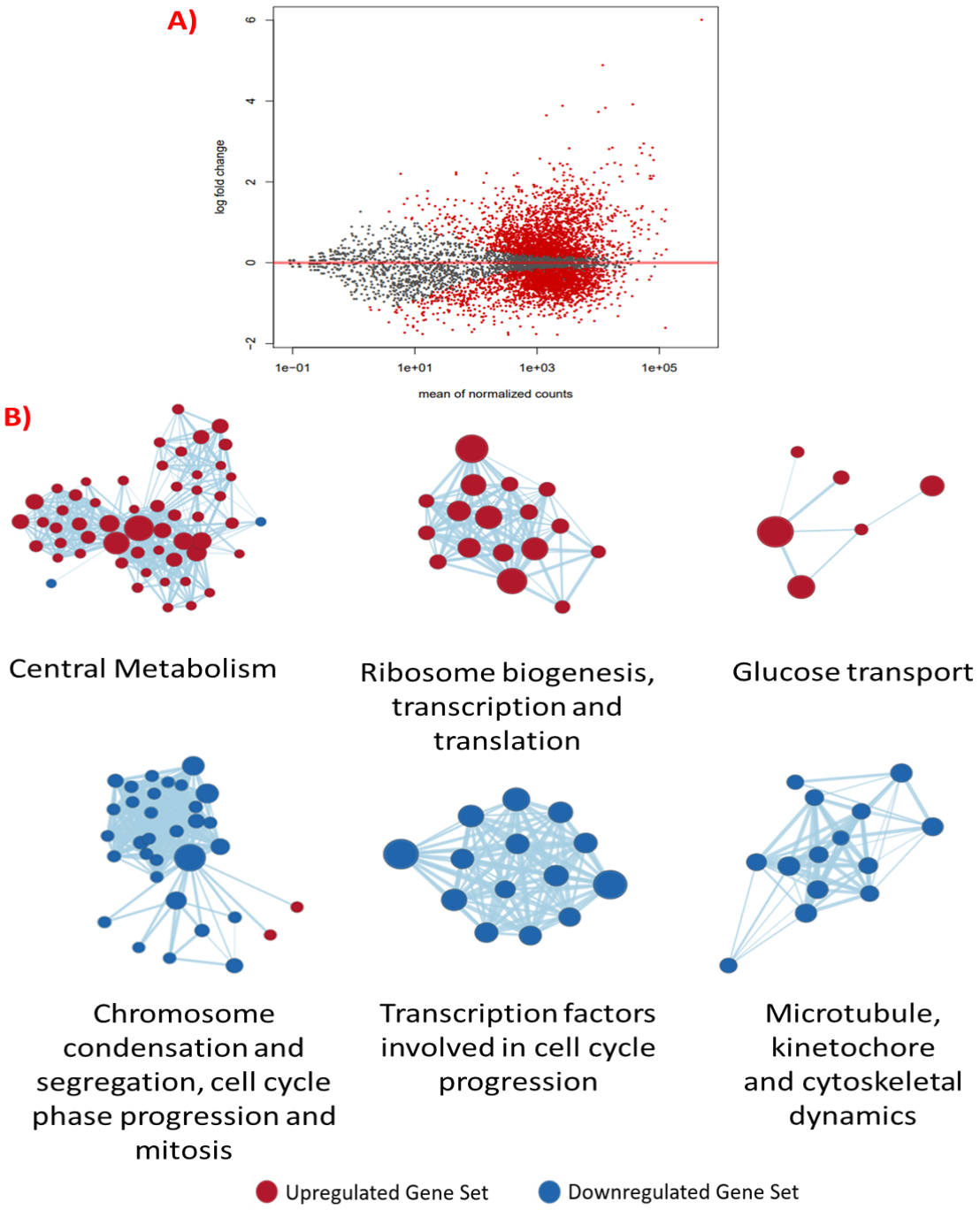

Figure 87. Global gene expression changes in wild type cells overexpressing RAS2^{S225A} when compared to a wild type control.

(A) DESeq2 was used to compare gene expression in wild type cells overexpressing RAS2^{S225A} to a wild type control and a volcano plot was generated of the log_2 fold change against mean of normalised counts for each gene; red dots = significantly differentially expressed ($q \leq 0.05$) genes, grey dots = not significant. In total there were 4133 significantly differentially expressed genes. Normalised counts are the number of reads a gene has and therefor the higher the mean of normalised count, the greater the expression of that gene. (B) Gene set cluster map created using the cytoscape plug in showing the most upregulated and downregulated gene

sets as determined by GSEA analysis along with their cellular functions. Each circle represents a gene set and the lines between them corresponds to how much they overlap, the thicker the line the greater the genes they have in common.

6.7. GSEA analysis of cellular processes differentially regulated by the overexpression of *RAS2^{S225E}*

GSEA analysis revealed that the overexpression of *RAS2^{S225E}* in wild type cells elicits a similar pattern in the cellular pathways upregulated to that observed upon the overexpression of *RAS2^{S225A}*. We observed an upregulation in pathways involved in ribosomal biogenesis, transcription, translation, glucose transport and central metabolism *(Figure 88)*. All of which can be attributed to an actively growing population of cells. The pathways downregulated mimicked those seen upon overexpression of *RAS2^{S225A}* with chromosome condensation and segregation, cell cycle phase transition, mitosis and transcription factors associated with cell cycle phase progression and chromatin remodelling all downregulated *(Figure 88)*. This data suggests that both *RAS2^{S225E}* and *RAS2^{S225A}* lead to similar changes in the regulation of cell processes that may explain why cells enter a quiescent state.

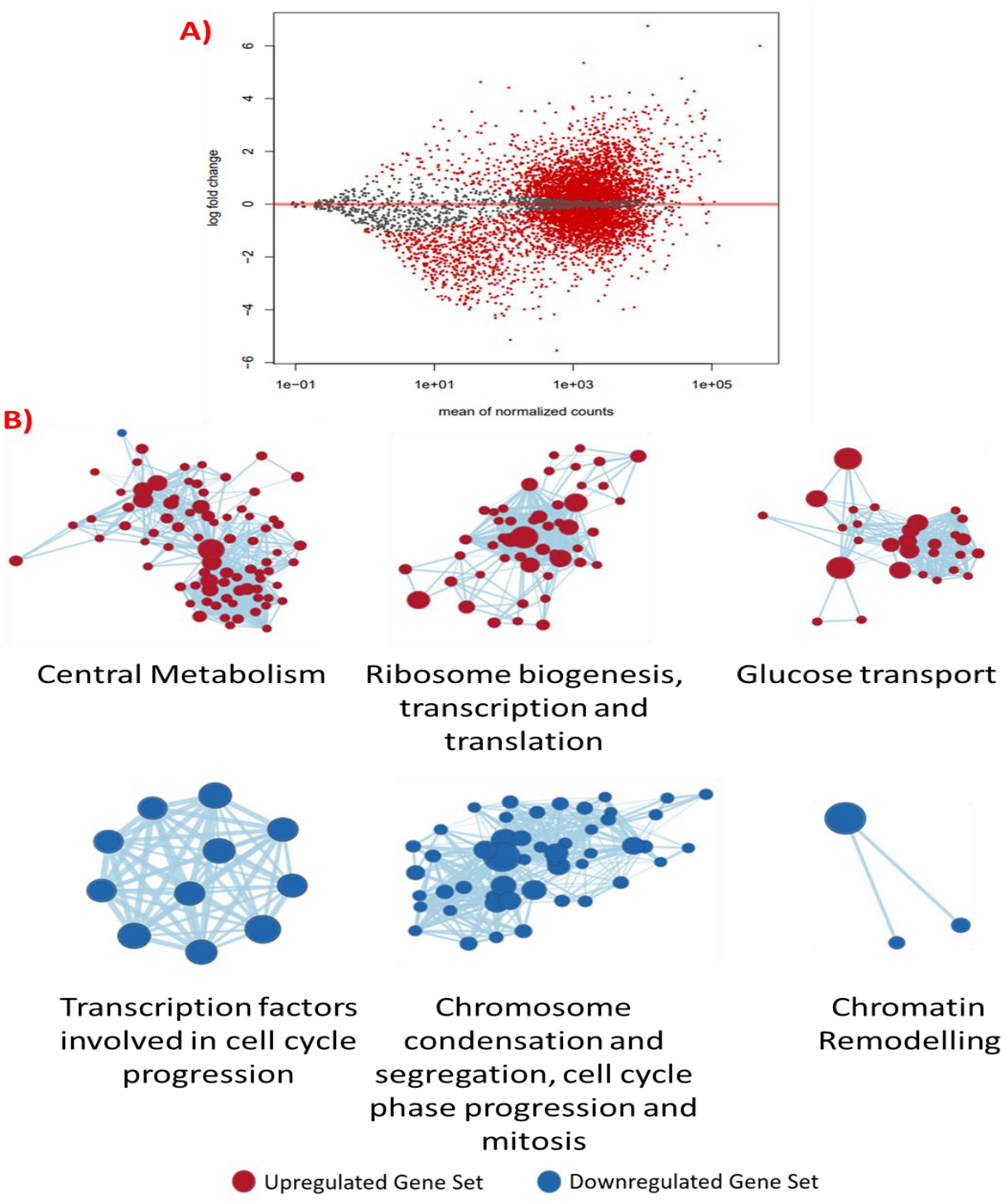

Figure 88. Global gene expression changes in wild type cells overexpressing RAS2^{S225E} when compared to a wild type control.

(A) DESeq2 was used to compare gene expression in wild type cells overexpressing RAS2^{S225E} to a wild type control and a volcano plot was generated of the log_2 fold change against mean of normalised counts for each gene; red dots = significantly differentially expressed ($q \leq 0.05$) genes, grey dots = not significant. In total there were 5202 significantly differentially expressed genes. Normalised counts are the number of reads a gene has and therefor the higher the mean of normalised count, the greater the expression of that gene. (B) Gene set cluster map generated by cytoscape showing the most upregulated and downregulated gene sets as

determined by GSEA analysis along with their cellular functions. Each circle represents a gene set and the lines between them corresponds to how much they overlap, the thicker the line the greater the genes they have in common.

6.8 Further analysis of the gene sets enriched upon overexpression of *RAS2*^{S225A} in wild type cells

Following GSEA analysis we sought to visualise networks of similar gene sets using the cytoscape plug in *(Figure 89)*. We sought to identify which processes within these gene set networks were up- or downregulated. To achieve this, we used the normalised enrichment score (NES) to identify which processes and to what extent genes in these pathways were either up- or downregulated when compared to the wild type control. Upon the overexpression of *RAS2*^{S225A} in wild type cells we observed an increase in ribosomal biogenesis, transcription, and translation. Here we observed that gene sets involved in; cytoplasmic translation (NES = 2.29), cytosolic ribosome (NES = 2.29), ribosome biogenesis (NES = 2.07), translation elongation (NES = 2.43), preribosome (NES = 2.19) and ribosome assembly (NES = 2.18) were all significantly upregulated *(Figure 89)*. A full list of the genes within the gene set networks that regulate the processes detailed below can be found in the appendix.

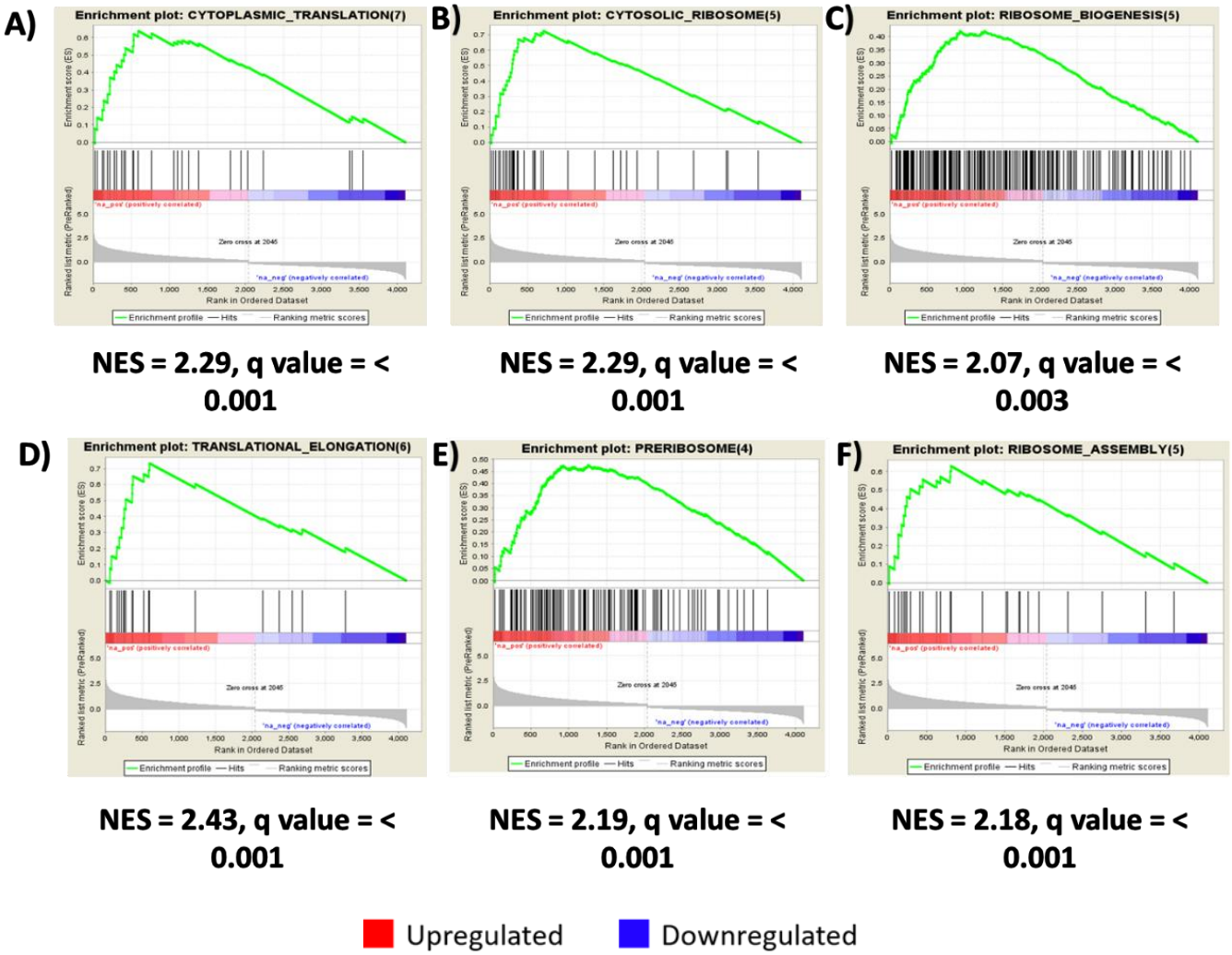

Figure 89. Gene sets shown to be upregulated upon the overexpression of RAS2^{S225A} when compared to the wild type control. (A), cytosolic ribosomes (B), ribosome biogenesis (6) , translation elongation (D) , preribosome (E) and ribosome assembly (F).

Vertical black lines represent individual genes in the significantly differentially expressed ranked gene list from upregulated (left) to downregulated (right). An increase in the enrichment score is seen if there are many genes towards the beginning of the ranked list (upregulated) in the gene set. When the green line climbs rapidly and peaks near the start of the graph (as shown here) it can be concluded that that gene set is overall upregulated. NES = normalised enrichment score, positive NES shows enrichment in the upregulated group of genes.

The gene sets significantly downregulated upon the overexpression of *RAS2*^{S225A}, indicated by a negative normalised enrichment score (NES), included condensation of chromosomes (NES = - 2.22), kinetochore dynamics (NES = -2.31), sister chromatid segregation (NES = -2.08), regulation of mitotic metaphase anaphase transition (NES = -2.08), the U2 spliceosome complex (NES = -2.33) and microtubule based processes (NES = -1.93) (Figure 90). A list of the genes within the gene set networks that regulate the processes detailed below can be found in the appendix.

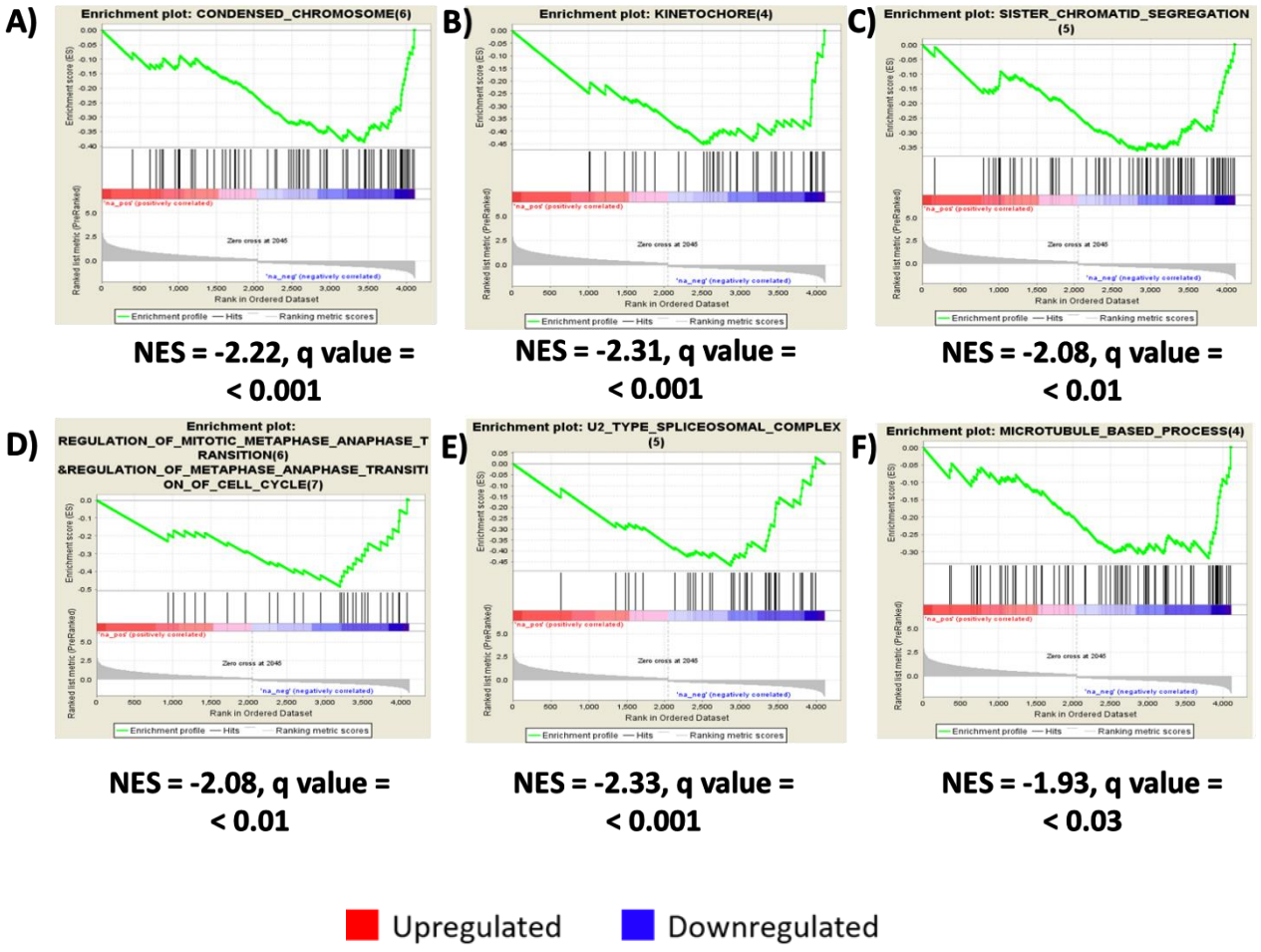

Figure 90. Gene sets shown to be downregulated upon the overexpression of RAS2^{S225A} when compared to the wild type control. Chromosome condensation (A), kinetochore and microtububle based processes (B), sister chromatid segregation (C) , the regulation of mitotic-metaphase-anaphase transition (D) , U2 Type splicesomal complex (E) and microtubule based processes (F).

Vertical black lines represent individual genes in the significantly differentially expressed ranked gene list from upregulated (left) to downregulated (right). An increase in the enrichment score is seen if there are many genes towards the beginning of the ranked list (upregulated) in the gene set. When the green line climbs rapidly and peaks near the start of the graph (as shown here) it can be concluded that that gene set is overall upregulated. NES = normalised enrichment score, positive NES shows enrichment in the upregulated group of genes.

6.9 Further analysis of the gene sets enriched upon overexpression of *RAS2^{S225E}* in wild type cells

Upon the overexpression of *RAS2^{S225E}* in wild type cells we observed a similar gene enrichment profile when compared to the *RAS2^{S225A}* mutant. Here we observed gene sets involved in cytoplasmic translation (NES = 2.41), cytosolic ribosomes (NES = 2.67), ribosome biogenesis (NES = 2.76), translation elongation (NES = 2.53), preribosome (NES = 2.89) and ribosome assembly (NES = 2.58) were all significantly upregulated (Figure 91). When compared wild type cells overexpressing *RAS2^{S225A}*, the normalised enrichment score for each of the above processes is higher in cells overexpressing *RAS2^{S225E}*. A list of the genes within the gene set networks that regulate the processes detailed below can be found in the appendix.

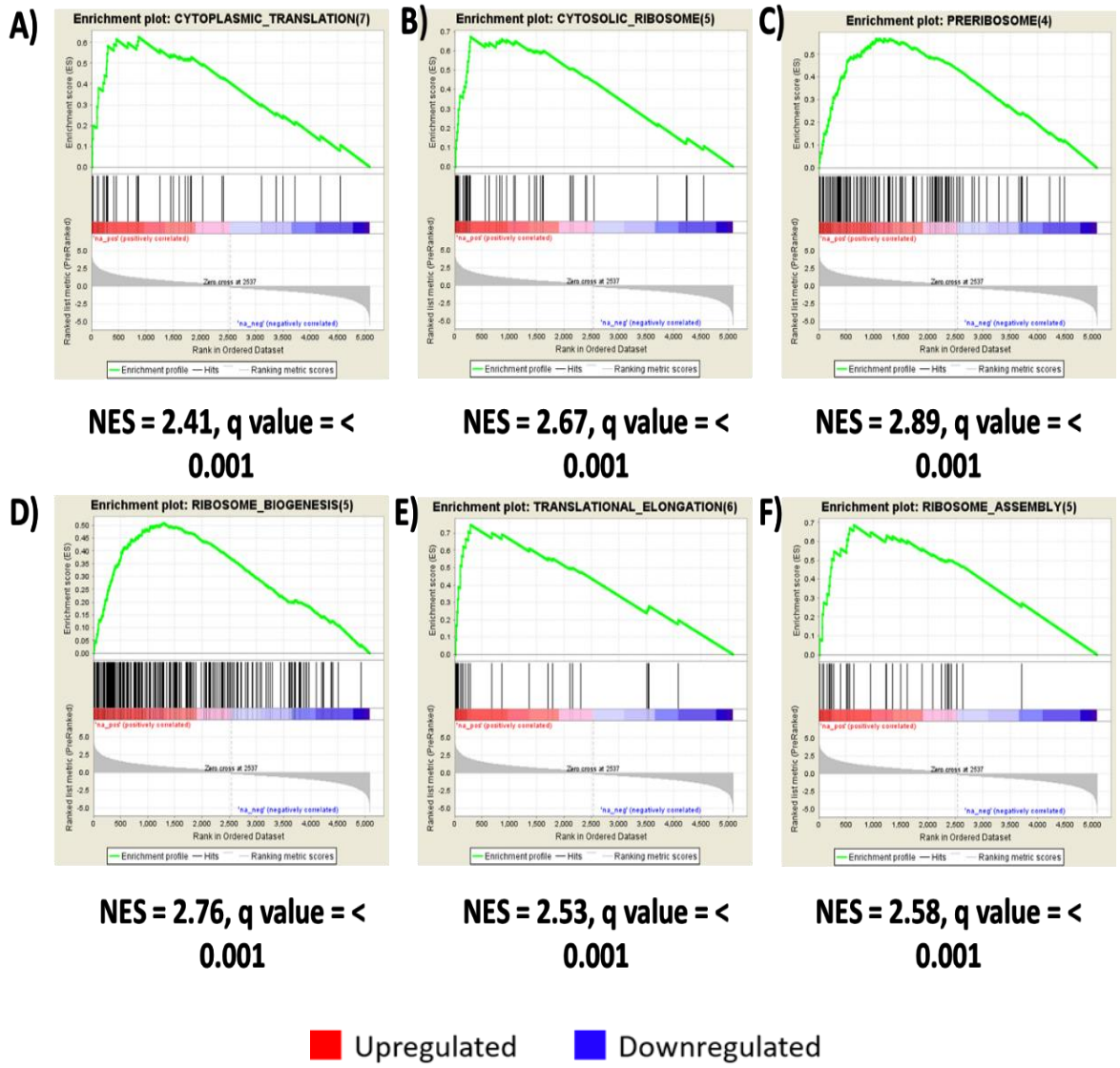

Figure 91. Gene sets shown to be upregulated upon the overexpression of RAS2^{S225E} when compared to the wild type control. Cytoplasmic translation (A), cytosolic ribosomes (B), preribosome (C), ribosome biogenesis (D), translation elongation (E), and ribosome assembly (F).

Vertical black lines represent individual genes in the significantly differentially expressed ranked gene list from upregulated (left) to downregulated (right). An increase in the enrichment score is seen if there are many genes towards the beginning of the ranked list (upregulated) in the gene set. When the green line climbs rapidly and peaks near the start of the graph (as shown here) it can be concluded that that gene set is overall upregulated. NES = normalised enrichment score, positive NES shows enrichment in the upregulated group of genes.

The gene sets significantly downregulated upon the overexpression of *RAS2*^{S225E}, indicated by a negative normalised enrichment score (NES), included; condensation of chromosomes (NES = - 2.55), nuclear division (NES = -1.84), sister chromatid segregation (NES = -2.19), organelle fission (NES = -1.90), chromosome segregation (NES = -2.30) and microtubule based processes (NES = -2.16) (Figure 92).

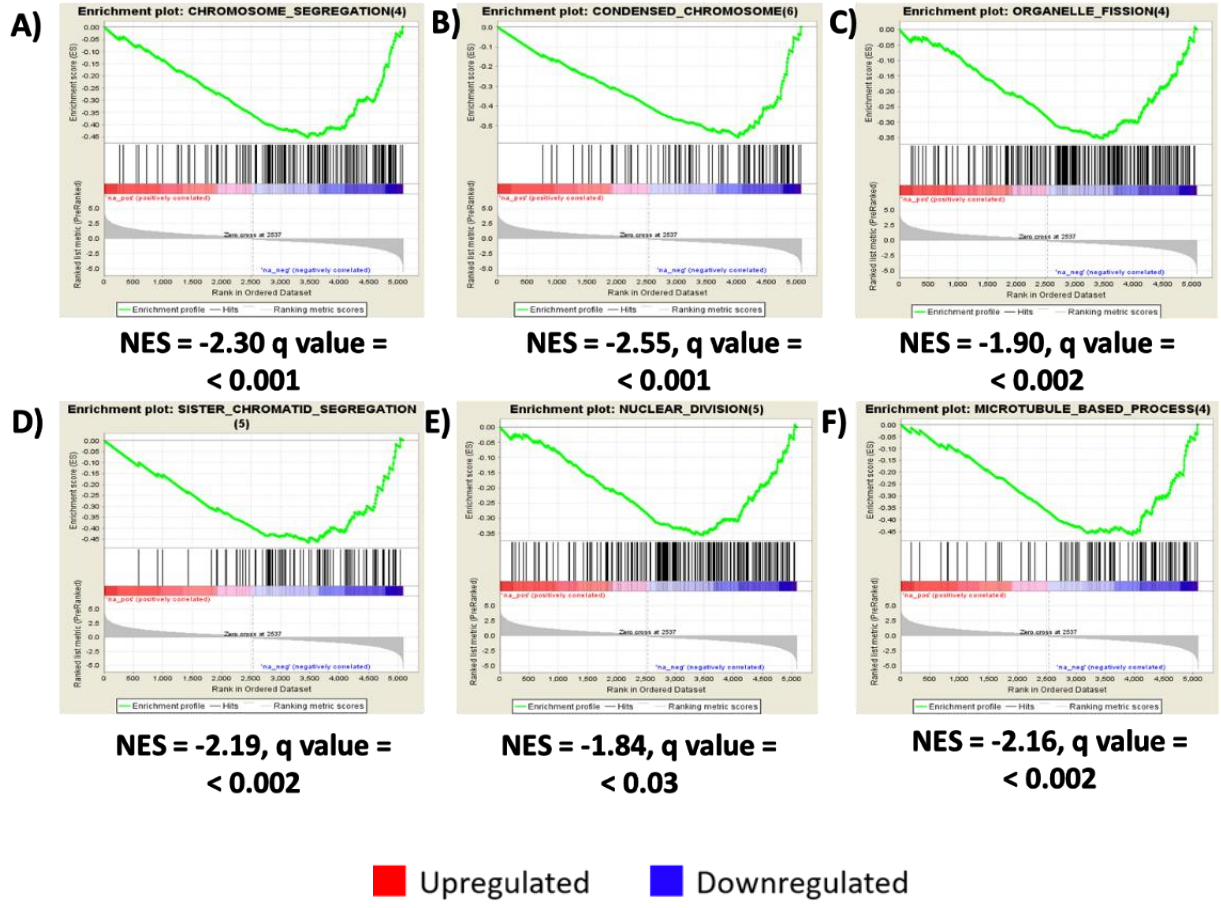

Figure 92. Gene sets shown to be downregulated upon the overexpression of RAS2^{S225E} when compared to the wild type control. Chromosome segregation (A) , chromosome condensation (B) , organelle fission (C) , sister chromatid segregation (D) , nuclear division (E) and microtubule based processes (D).

Vertical black lines represent individual genes in the significantly differentially expressed ranked gene list from upregulated (left) to downregulated (right). An increase in the enrichment score is seen if there are many genes towards the beginning of the ranked list (upregulated) in the gene set. When the green line climbs rapidly and peaks near the start of the graph (as shown here) it can be concluded that that gene set is overall upregulated. NES = normalised enrichment score, positive NES shows enrichment in the upregulated group of genes.

6.10 Discussion

In previous chapters we suggest that the overexpression of either *RAS2*^{S225A} or *RAS2*^{S225E} in wild type cells leads to growth defects and a loss of viability that we propose to be attributable to a dysregulation of the cell cycle. We propose that the slow growth phenotype is mediated through the Ras/cAMP/PKA pathway and that nutrient availability, or indeed the cells ability to acquire nutrition, appears to play an important role.

Through genome-wide transcriptome analysis of wild type cells overexpressing either *RAS2*^{S225A} or *RAS2*^{S225E} we sought to investigate the gene expression patterns that may govern the slower growth phenotype. Of particular interest was to ascertain whether mutant Ras2 expression led to changes in gene expression patterns that might be regarded as hallmarks of cell quiescence. Quiescence in yeast cells is typically defined as a temporary non-proliferating cellular state characterised by reduced protein synthesis and chromosome condensation. In addition, a number of phenotypes have been described within quiescent yeast cells such as fragmented mitochondria, presence of actin bodies, chromosome condensation, formation of P-bodies, stress granules and proteasome storage granules and nuclear localisation of heat-shock proteins [254]. Crucially however, quiescent cells are capable of responding to environmental signals such as the presence of carbon and quickly re-engage the cell cycle [109].

Upon the transition of cells into the quiescent state, the coordinated downregulation of ribosome synthesis contributes to a dramatic ~300-fold reduction in protein synthesis rates [255][256]. Ribosomal protein synthesis represents 15 % of total translation and ribosome RNA transcription represents 60 % of the total transcription. It is therefore not surprising that the first global downregulation of genes upon transition into quiescence is the shutdown of

the transcription of genes encoding for the proteins in both subunits of the ribosome [255]. As protein synthesis requires a significant amount of energy such down regulation may be crucial for the survival of non-dividing or quiescent cell populations.

Unexpectedly, the overexpression of either *RAS2*^{S225A} or *RAS2*^{S225E} in wild type cells resulted in a significant upregulation of transcription, translation, and ribosomal biogenesis. Such an observation was unexpected as the pathways upregulated recapitulate those observed within exponentially growing cells. We suggest that the overexpression of *RAS2*^{S225A} in wild type cells results in a transition into a quiescence like phenotype. However, quiescence is not hallmarked by an upregulation in either transcriptional or translational machinery [215][151][254]. So, does the expression of *RAS2*^{S225A} or *RAS2*^{S225E} lead to quiescence at all?

The cell-based assays conducted in this study show that overexpression of *RAS2*^{S225A} or *RAS2*^{S225A} leads to both a significant reduction in viability and a reduced level of respiration. This is not concordant with the status of an actively growing population. However, upon analysis of the pathways downregulated upon the overexpression of these *RAS2* alleles we observe the downregulation of processes that govern cell division such as chromosome condensation and segregation, cell cycle phase transition, mitosis and transcription factors associated with cell cycle phase progression. The resulting effect of the downregulation of the pathways represent the fact that these cells are not engaged in the cell cycle and may provide an explanation for the loss in viability observed. But can a reduction in these pathways explain the inability of cells to resume normal growth upon exposure to fresh growth media?

We hypothesize that the upregulation of transcription, translation and ribosomal biogenesis may be a result of increased PKA activity, as cells with enhanced PKA functions fail to undergo transcriptional reprogramming upon entry in diauxic growth [257]. However, constitutive PKA

activity is usually correlated with a significant loss of viability that is attributed to cell death, as in seen cells expressing the *ras*^{val19} mutant [98]. The overexpression of either *RAS2*^{S225A} or *RAS2*^{S225E} also results in a loss of viability but which is accompanied by cell death. We therefore propose that the overexpression of either *RAS2*^{S225A} or *RAS2*^{S225E} in wild type cells leads to an unreported slow growth phenotype that is characterized by an upregulation of transcriptional and translational machinery and a downregulation of nuclear and cellular division.

Chapter 7
Final Discussion

Ras proteins are small GTPases that act as molecular switches within cells that link extracellular stimuli to intracellular effectors. Ras proteins play a conserved role in the control of both cell growth and proliferation [211]. As a result, mutations that induce the constitutive activation of Ras proteins are often associated with changes in cell behaviour that can lead to disease, such as human cancer [41]. The localisation of Ras proteins are reported to be predominantly to the inner cytoplasmic surface of the plasma membrane, but they can also be observed on endomembrane's, such as the endoplasmic reticulum, and the mitochondrial outer membrane [65][57][212].

In recent years, the localisation and signalling of Ras on the plasma membrane has been extensively studied. It has been revealed that Ras undergoes a series of posttranslational modifications that dictate its subcellular localisation. Evidence exists to suggest that Ras proteins can undergo phosphorylation events which regulate its activity. Whistler and Rine identified Ser^{412} as an important phosphorylation site on the yeast Ras2 protein where substitution of serine with alanine at this residue lead to increased cAMP levels and elevated ration of Ras2-GTP compared to total Ras2 [74][213]. Surprisingly, the phosphorylation of Ras2p in *S. cerevisiae* has not been studied in regards to its regulation of intracellular localisation, despite significant evidence existing linking Ras phosphorylation to its localisation in humans [77]. This study aims to further investigate whether Ras2p phosphorylation provides a mechanism that regulates Ras2p trafficking inside the cell.

7.1 Modification of the Ser^{225} residue of Ras2p is important for localisation, activity, and function of Ras proteins

The data presented in this thesis suggests that the modification of the Ser^{225} residue of Ras2p is important for both localisation and activity of Ras proteins. We have shown that during both log and stationary phases of growth, the overexpression of either *RAS2*^{S225A} or *RAS2*^{S225E} in wild type cells results in significant changes in the localisation of active Ras populations. Actively growing wild type cells localise GTP-bound Ras to the plasma membrane and nucleus. In wild type cells, such localisation results in the activation of the cAMP/PKA pathway, which signals to the cell to initiate both growth and proliferation. We suggest that during exponential growth, wild type cells overexpressing either *RAS2*^{S225A} or *RAS2*^{S225E} sequester active Ras to the nuclear envelope with reduced activity seen at the plasma membrane and nucleus. Furthermore, we suggest that the overexpression of *RAS2*^{S225A} or *RAS2*^{S225E} also leads to the miss localisation of active Ras to the nuclear envelope and an inappropriate activity during stationary phase of growth. This finding therefor highlights the important role of Ras2 protein phosphorylation on both the modulation of protein activity and localisation.

The findings within this thesis propose that the modification of Ras2^{S225} is also important for Ras protein function. As modification of Ras2^{S225} leads to growth defects, changes in the oxidative stress response and leads to a reduction in viability in wild type cells. We show that the reduction of viability observed upon the overexpression of *RAS2* mutant alleles does not represent cell death but rather an inability to divide. We therefor propose that the overexpression of *RAS2* mutant alleles leads to a cessation of growth in wild type cells. Looked at together, we clearly suggest a novel role of the Ser^{225} residue of Ras2p for the localisation of GTP-bound Ras and propose a link between subcellular localisation of active Ras and growth cessation. Such findings provide important insights on how targeting phosphorylation

sites, such as Ras2^{S225}, can be exploited to prevent growth in cells where uncontrolled proliferation leads to disease.

7.2 Overexpression of *RAS2^{S225A}* or *RAS2^{S225E}* results in aberrant Ras/cAMP/PKA signalling and entry into state of reduced growth

We suggest that the overexpression of either *RAS2^{S225A}* or *RAS2^{S225E}* leads to the miss localisation of active Ras to the nuclear envelope. Such localisation results in growth defects and a loss of viability that we believe to be attributable to a dysregulation in the cell cycle. We sought to investigate whether the dysregulation of the cell cycle was caused through the aberrant signalling of Ras/cAMP/PKA pathway. We established that the slow growth phenotype observed is linked to elevated PKA activity, as overexpression of *PDE2* in strains overexpressing *RAS2^{S225A}* or *RAS2^{S225E}* rescued viability. This observation was interesting as we initially hypothesized that the slow growth phenotype was a result of decreased PKA signalling. As mutations that inhibit the production of cAMP and thus reduce PKA activation, prevent progression through the cell cycle check point and render cells arrested in G1. Such a scenario would provide an explanation for the reduced growth phenotype observed upon overexpression of *RAS2* mutant alleles [231][232]. Typically, mutations that activate the Ras/cAMP/PKA pathway, such as activating mutations in the *RAS2* gene and *BCY1* mutations fail to accumulate as G1-arrested cells upon nutrient deprived conditions resulting in a decrease in viability that is strongly correlated to cell death [115]. Whereas, we show that overexpression of *RAS2^{S225A}* or *RAS2^{S225E}* leads to enhanced PKA activity resulting in a reduction of viability that is not attributable to cell death but rather to a cessation of growth. We believe the answer lies within the localisation of active Ras, overexpression of *RAS2* mutant alleles sequesters active Ras to the nuclear envelope as opposed to the inner leaflet

of the plasma membrane. We hypothesize that Ras signalling from the nuclear envelope to PKA may result in the activation of effectors that elicit a change in gene expression that promotes a loss in co-ordination of growth control and environmental sensing that promotes growth cessation.

As evidence for this we show that increasing the level of nutrition available enabled cells overexpressing *RAS2* mutant alleles to escape quiescence in manner analogous to the co-expression with *PDE2.* Such a result may suggest that such cells are either incapable of taking up sufficient levels of nutrition, which yeast perceives as growth factors, or indeed that cells do not sense available nutrition. We propose that increasing the nutrient availability to cells overexpressing *RAS2* mutant alleles either through growth on nutrient rich media or through deletion of *CUP9* results in a rescue of the viability phenotype. This finding would tend to suggest to us that Ras mutant induced growth cessation occurs because of an inability to take up nutrition from the environment. Evidence for a role for Ras in this respect is further provided by our finding that *RAS2* overexpression improves viability on minimal media. Overall, our data suggests a link between Ras proteins, nutrient uptake, and growth cessation.

7.3 Genome-wide transcriptome analysis of wild type cells overexpressing *RAS2^{S225A}* or *RAS2^{S225E}*

We show that the overexpression of either *RAS2^{S225A}* or *RAS2^{S225E}* in wild type cells leads to growth defects and a loss of viability that we propose to be attributable to cell quiescence. We suggest that the slow growth phenotype is mediated through the Ras/cAMP/PKA pathway and that nutrient availability, or indeed the cells ability to acquire nutrition, appears to play an important role. Through genome-wide transcriptome analysis of wild type cells overexpressing either *RAS2^{S225A}* or *RAS2^{S225E}* we sought to investigate the gene expression

patterns that may govern the slow growth phenotype. Of interest was to ascertain whether mutant Ras2 expression led to changes in gene expression patterns that might be regarded as hallmarks of cell quiescence.

Unexpectedly, the overexpression of either *RAS2*^{S225A} or *RAS2*^{S225E} in wild type cells resulted in a significant upregulation of transcription, translation, and ribosomal biogenesis. Such an observation was unexpected as the pathways upregulated recapitulate those observed within exponentially growing cells [255]. However, upon analysis of the pathways downregulated upon the overexpression of these *RAS2* alleles we observe the downregulation of processes that govern cell division such as chromosome condensation and segregation, cell cycle phase transition, mitosis and transcription factors associated with cell cycle phase progression. The resulting effect of the downregulation of the pathways represent the fact that these cells are not engaged in the cell cycle and may provide an explanation for the loss in viability observed.

We hypothesize that the upregulation of transcription, translation and ribosomal biogenesis may be a result of increased PKA activity, as cells with enhanced PKA functions fail to undergo transcriptional reprogramming upon entry in diauxic growth [257]. However, constitutive PKA activity is usually correlated with a significant loss of viability that is attributed to cell death, as in seen cells expressing the *ras*^{val19} mutant [98]. The overexpression of either *RAS2*^{S225A} or *RAS2*^{S225E} also results in a loss of viability but which is not accompanied by cell death. We therefore propose that the overexpression of either *RAS2*^{S225A} or *RAS2*^{S225E} in wild type cells leads to an unreported slow phenotype that is characterized by an upregulation of transcriptional and translational machinery and a downregulation of nuclear and cellular division at a time when nutrient levels have depleted. Why mutant Ras cells are no longer able to re-engage growth when given fresh media of the same composition is unclear but

RNA-Seq data not included in this thesis suggests the deletion of *CUP9* in a *RAS2*^{S225A} background may reinstate cellular growth via the upregulation of a number of transporters that facilitate nutrient uptake.

7.4 Sequence alignment between Ras2 and human N-Ras suggests that Serine^{225} is conserved in human N-Ras at Serine^{S173}

We have shown that the Serine^{225} of the Ras2 protein is important for growth, viability, and the localisation and activity of Ras proteins. We hypothesized that this residue may be conserved in higher eukaryotes. To address this, sequence alignment between the Ras2 protein and the human N-Ras protein was performed *(Figure 93)*. Interestingly, although significant sequence divergence between the yeast and human Ras proteins outside of the GTPase domain and C terminal CAAX box, we discovered that Ras2 Serine^{225} was conserved in human N-Ras at Serine^{173} along with conservation of the surrounding region. The conservation of this serine residue in human Ras proteins may suggest an important role of this residue in higher eukaryotic systems, which could be exploited as a potential target for anti-Ras cancer therapy.

Figure 93. Sequence alignment of the Ras2 protein and human N-Ras shows that Serine[225] of Ras2p (circled) is conserved in N-Ras at Serine[173]

Interestingly, an independent group identified the Ser[226] residue in Ras1 to be an important residue for Ras1 phosphorylation, as mutating this residue to an alanine drastically diminishes the level of Ras1 phosphorylation [214]. Upon sequence alignment of yeast Ras1 and Ras2 *(Figure 13)* we show little sequence similarity outside of the GTPase domain. However, the serine site position in both Ras1 and Ras2 is similar suggesting that serine residues located around this position may play a conserved regulatory role within Ras proteins.

7.5 Targeting Ras membrane interaction as an anti-Ras cancer therapy

Investigations have estimated that ~50 % of all tumours are a result of mutations involved in the constitutive activation of Ras signalling [26]. Intensive sequencing of the cancer genome has revealed that, despite the identification of over 600 validated cancer genes (COSMIC v80; **http://cancer.sanger.ac.uk/cosmic**) , Ras oncogenes still constitute the most frequently mutated oncogene family in human cancers [258]. Despite decades of intensive effort, a

clinically effective anti-Ras therapy remains elusive, prompting the widely held perception that Ras proteins are 'undruggable' [259][260].

Initial approaches for the development of Ras inhibitors were guided by understanding the biochemical defects of mutant Ras proteins; *HRAS*, *KRAS4A*, *KRAS4B* and *NRAS* [261]. Unsuccessful attempts to develop anti-Ras drugs resulted from the misconception that the four Ras oncoproteins were identical in function [260]. With an ever increasing appreciation that different Ras proteins play unique roles in cancer, research has shifted its focus to *KRAS*, the isoform most frequently mutated in human cancer [262]. Sequence analyses have revealed the importance of the amino acids at positions 12, 13 and 61 in Ras proteins, mutations that cause the alternation of residues can lead to the over-activation of Ras via GAP impairment [41]. Mutations at these residues impair intrinsic and GAP-stimulated GTP hydrolysis rates and/or increase intrinsic exchange rates, favouring stimulus-independent formation of active Ras-GTP. As such, the earliest attempts of anti-Ras therapy centred on the formulation of small-molecule antagonists of GTP binding. Unfortunately, the picomolar affinity of Ras for GTP and the millimolar cellular concentrations of GTP render such attempts unsuccessful [262]. Small molecule mimetics of GAP activation on mutant Ras proteins was also unsuccessful due to the lack of well-defined hydrophobic pockets on the surface of Ras proteins [261]. As such many regarded Ras proteins as not tractable. This perception led to the pursuit of indirect strategies to target proteins that promote Ras membrane interaction.

With the recognition that Ras oncogenic activity is dependent on its association with the inner leaflet of the plasma membrane, and the subsequent identification of posttranslational modifications that modulate this association, came the next targeted anti-Ras therapy. Ras is synthesized in the cytosol and undergoes a series of posttranslational modification's that

promote its membrane association [263]. The initial modification is farnesyltransferase-catalyzed covalent addition of a farnesyl moiety to the cysteine residue of the CAAX motif. Followed by the proteolytic removal of the last three amino acids by Rec1 [263]. Lastly, isoprenylcysteine carboxyl methyltransferase (ICMT) facilitates methyl transfer to the C-terminal amino acid to negate the negative charge and prevent plasma membrane repulsion [263]. As the association of Ras proteins with the plasma membrane is essential for their function, targeting this requirement can be viewed as the functional equivalent not of turning off the defective switch that is oncogenic Ras, but of removing it and thereby destroying the circuit.

Due to the important role of the farnesyl lipid modification for posttranslational modifications and for Ras oncogenic activity, numerous farnyltransferase inhibitors were developed such as Ionafarnib and tipifarnib but disappointingly displayed no efficacy in the clinic. However, targeting other posttranslational modifications of Ras, such as phosphorylation, still display some promise as effective anti-Ras therapies [263][260][264]. Of these, phosphorylation of KRAS4B on serine^{181} can alter subcellular localisation of Ras, displacing the modified GTPase from the plasma membrane, and converting KRAS4B from growth-promoting to a growth-suppressing protein [77][265][266].

Like the phosphorylation of the Serine^{181} of KRAS4B, the modification of the phosphorylation site of Serine^{225} of Ras2p also alters the subcellular localisation of Ras proteins, displacing GTP-bound Ras from the plasma membrane to the nuclear envelope. Such localisation is correlated with a transition into a quiescence-like state that can be viewed as growth-supressing. We therefor hypothesize that modification of the equivalent serine residue in the NRAS oncoprotein, Serine^{173}, may also alter the subcellular localisation of Ras proteins and

convert NRAS from growth-promoting to a growth-suppressing protein. Providing more promise, is that the Serine^{173} residue of NRAS is in the variable domain of the protein, which makes this putative phosphorylation site an attractive drug target due to its accessibility.

Cosmic, the 'Catalogue of Somatic Mutations in Cancer' is an expert-curated database encompassing the wide variety of somatic mutation mechanisms causing human cancer. COSMIC contains details on millions of mutations across thousands of different cancer types. Hand-curation of key cancer genes provide in-depth detail on mutation distributions and effects, whilst semi-automated curation of cancer genomes provides broad somatic annotations toward target discovery. The COSMIC data provides details on the site and frequency of specific mutations.

Here we used the COSMIC data to investigate whether mutations located at the residue Ser^{173} of NRAS were recorded *(Figure 94)*. Interestingly, we observed that mutations have been found around the conserved serine residues, but mutations were not recorded at Ser^{173}. It would thus be interesting to investigate whether modification of the residues surrounding NRAS^{S173} lead to changes in Ras localisation.

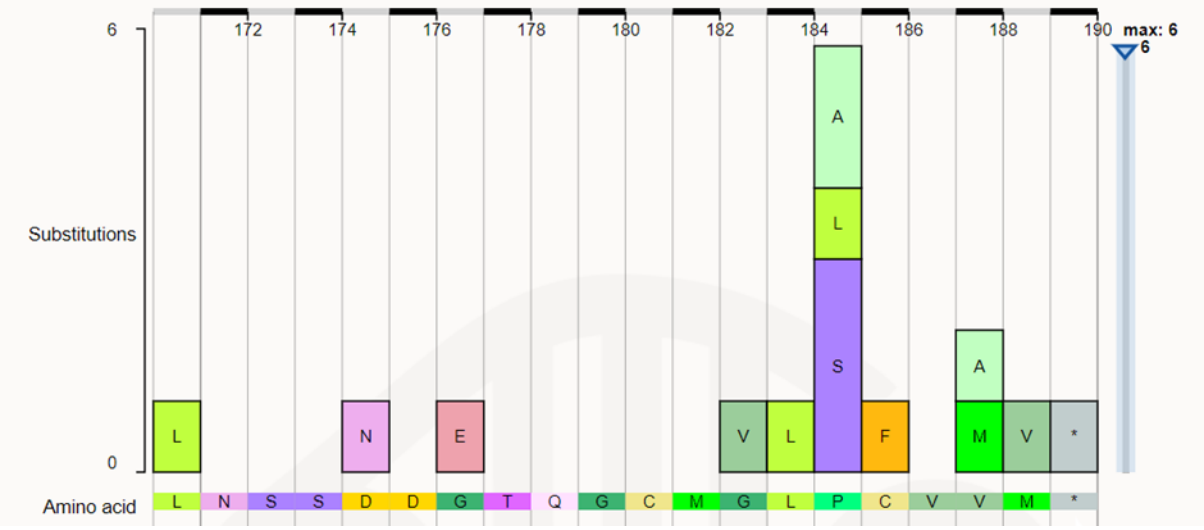

Figure 94. A graphical representation of the location and frequency of mutations surrounding the Ser^{173} of NRAS.
Mutations at NRAS^{S173} were absent but mutations were observed surrounding the conserved serine residue suggesting that these residues may be important for localisation and activity of Ras proteins.

7.6 Conclusions and future investigations

The work presented in this thesis suggests that the modification of the Ser^{225} residue of Ras2p is important for both localisation and activity of Ras proteins in yeast cells. We show that the miss localisation of active Ras proteins to the nuclear envelope of cells results in significant growth defects that are mediated through aberrant the Ras/cAMP/PKA signalling pathway. We suggest that enhanced PKA activity stimulated from active Ras populations on the nuclear envelope results in a decrease in viability which we attribute to premature cell cycle arrest, a phenotype previously not correlated with enhanced PKA activity. RNA-Seq analysis suggests that the slow growth phenotype does not recapitulate canonical quiescent transcription profiles but instead is characterised by an upregulation of transcriptional and translational machinery and a downregulation of nuclear and cellular division. The slow growth phenotype can be repressed through increasing nutrient availability to cells either through growth on

nutrient rich media or through deletion of *CUP9*. Sequence alignment between yeast Ras2 and human NRas, revealed that the Ser^{225} residue of Ras2 is conserved in human NRas at $Serine^{173}$. If modification of $NRAS^{173}$ in human cells results in the miss localisation of activated oncoproteins and induction in cell growth cessation. We suggest that this mechanism could be exploited as a potential anti-Ras cancer therapeutic if the precise nature of the effects of Ras redirection can be identified.

Further Work

- In cancer, a single mutation in just one copy of a gene can be enough to induce tumorigenesis. Dominant genes show their effect even if there is just one mutation in one copy of that gene pair [267]. This thesis has shown that the overexpression of either $RAS2^{S225A}$ or $RAS2^{S225E}$ in the presence of wild type *RAS2* resulted in a dominant phenotype. However, many of the experiments presented here have been conducted solely in a wild type background. While this thesis aimed to examine the effect of mutated *RAS2* expression in a system closely resembling that present in the human condition i.e. one wild type and one mutated gene. Limitations of this experimental design are that the effect of mutated Ras2 protein expression alone is not known, and therefor whether the presence of the wild type Ras2 protein confounds the phenotype observed upon the overexpression of either $RAS2^{S225A}$ or $RAS2^{S225E}$ in *S. cerevisiae.* To address this, all experiments investigating the expression of either $RAS2^{S225A}$ or $RAS2^{S225E}$ should be conducted in both wild type and *Δras2* yeast cells.
- We have observed significant differences in viability between yeast cells overexpressing *RAS2*, $RAS2^{S225A}$ or $RAS2^{S225E}$ and *NRAS*, $NRAS^{S173A}$ or $NRAS^{S173E}$; therefore, it would be interesting to investigate if similar growth defects and changes

in localisation of Ras and active Ras occur in a mammalian system. To address this, we would like to express *NRAS*, *NRAS*^{S173A} or *NRAS*^{S173E} in a human neuroblastoma cell line and conduct growth and viability assays. The human oncogene *NRAS* is linked to haematological malignancies particularly acute leukaemia [197][268]. Our data could therefore provide valuable information which might assist in developing new strategies for cancer treatment.

- We have shown that the reduction in viability induced by the overexpression of *RAS2*^{S225A} or *RAS2*^{S225E} in wild type cells can be reversed through the co-expression of *PDE2*. As aforementioned, Pde2 is a high-affinity cAMP phosphodiesterase which catalyses the degradation of cAMP[86]. The resulting effect of the overexpression of *PDE2*, is a decrease in intracellular levels of cAMP. We hypothesize that the overexpression of *RAS2*^{S225A} or *RAS2*^{S225E} in wild type cells leads to increase in intracellular cAMP levels and increased PKA activity. To attest this hypothesis, we would like to measure the intracellular levels of cAMP in wild type cells overexpressing *RAS2*^{S225A} or *RAS2*^{S225E} and compare levels to a wild type control. This would be achieved through a metabolite extraction protocol and measuring cAMP concentrations within cells.
- To investigate the global effects of the overexpression of either *RAS2*^{S225A} or *RAS2*^{S225E} in wild type cells we conducted a genome-wide transcriptome analysis. We have observed the global transcriptional changes induced upon the overexpression of *RAS2*^{S225A} or *RAS2*^{S225E} when compared to the wild type. It would be interesting to extract the RNA from wild type cells overexpressing wild type *RAS2* and perform RNA-Seq analysis to observe the changes in gene expression when the Serine^{225} is not

mutated. Such analysis would allow us to determine the genes up/downregulated and the gene sets enriched upon the modification of *RAS2*^{S225}.

- We observed that the overexpression of *RAS2*^{S225A} or *RAS2*^{S225E} in wild type cells had a dramatic effect on a wide array of cellular processes. By performing ribosomal profiling, we could observe a global profile of ribosomes in the cell allowing us to identify if they are being utilised for translation. In cells overexpressing either *RAS2*^{S225A} or *RAS2*^{S225E} we would anticipate that there should be an increase in 80S ribosomes, and polysomes if the overexpression of *RAS2* mutant alleles in the system is contributing to translation.
- Other lines of investigation would be to investigate whether the phosphorylation of Ras2^{S225} resulted in changes to the phosphorylation status of nearby serine residues – such as serine^{224}. Furthermore, we would like to examine whether mutating both serine^{225} and serine^{224} would lead to a further attenuation of growth and viability in yeast cells overexpressing these mutant alleles.
- It would be interesting to investigate why the loss of *CUP9* in cells overexpressing either *RAS2*^{S225A} or *RAS2*^{S225E} restore normal cell growth. Such insight could be achieved through comparing RNA-Seq data from wild type cells overexpressing *RAS2* mutant alleles to the expression of *RAS2* mutant alleles in a *Δcup9* background. Such analysis would allow us to determine the genes up/downregulated and the gene sets enriched upon the deletion of *CUP9* in cells overexpressing *RAS2*^{S225A} or *RAS2*^{S225E}.

References

1. Mager WH, and Winderickx J (**2005**). Yeast as a model for medical and medicinal research. **Trends Pharmacol Sci**. 26(5): 265–273. doi: 10.1016/j.tips.2005.03.004.

2. Goffeau A, Barrell BG, Bussey H, Davis RW, Dujon B, Feldmann H, Galibert F, Hoheisel JD, Jacq C, Johnston M, Louis EJ, Mewes HW, Murakami Y, Philippsen P, Tettelin H, and Oliver SG (**1996**). Life with 6000 Genes. **Science (80-)**. 274(October): 546–567. 8849441.

3. Connelly C, Dietrich F, Andre B, Dow S, Boeke J, Bakkoury M, Gentalen E, Foury F, Shoemaker D, Anderson K, Benito R, Bussey H, Chu A, Friend S, Winzeler E, Liang H, Davis K, Astromoff A, and Bangham R (**1999**). Functional Characterization of the S. cerevisiae Genome by Gene Deletion and Parallel Analysis. **Science (80-)**. 285(5429): 901–906.

4. Guri G, Chu AM, Li N, Carla C, Linda R, Steeve V, Dow S, Lucau-danila A, Anderson K, Arkin AP, Astromoff A, Bakkoury M El, Bangham R, Benito R, Brachat S, Andre B, Jaramillo DF, Kelly DE, Kelly SL, and Ko P (**2002**). Functional profiling of the Saccharomyces cerevisiae genome. **Nature**. 418(6896): 387–391.

5. Lequin S, Chassagne D, Bellat J-P, Huh W, Falvo J V, Gerke LC, Carroll AS, Howson RW, Weissman JS, and Shea EKO (**2003**). Global analysis of protein localization in budding yeast. **Nature**. 425(6959): 686–691.

6. Chemical C, Plant R, Plant P, Biol M, Ghaemmaghami S, Huh W, and Bower K (**2003**). Global analysis of protein expression in yeast. **Nature**. 108(1997): 737–741.

7. Foury F (**1997**). Human genetic diseases: A cross-talk between man and yeast. **Gene**. 195(1): 1–10. doi: 10.1016/S0378-1119(97)00140-6.

8. Heinicke S, Livstone MS, Lu C, Oughtred R, Kang F, Angiuoli S V., White O, Botstein D, and Dolinski K (**2007**). The Princeton Protein Orthology Database (P-POD): A comparative genomics analysis tool for biologists. **PLoS One**. 2(8). doi: 10.1371/journal.pone.0000766.

9. Laurent JM, Young JH, Kachroo AH, and Marcotte EM (**2016**). Efforts to make and apply humanized yeast. **Brief Funct Genomics**. 15(2): 155–163. doi: 10.1093/bfgp/elv041.

10. Zabrocki P, Pellens K, Vanhelmont T, Vandebroek T, Griffioen G, Wera S, Van Leuven F, and Winderickx J (**2005**). Characterization of α-synuclein aggregation and synergistic toxicity with protein tau in yeast. **FEBS J**. 272(6): 1386–1400. doi: 10.1111/j.1742-4658.2005.04571.x.

11. Bourne HR, Sanders DA, and McCormick F (**1990**). The GTPase superfamily: a conserved switch for diverse cell functions. **Nature**. 348(6297): 125–32. doi: 10.1038/348125a0.

12. Biou V, and Cherfils J (**2004**). Structural Principles for the Multispecificity of Small GTP-Binding Proteins. **Biochemistry**. 43(22): 6833–6840. doi: 10.1021/bi049630u.

13. Seabra MC, and Wasmeier C (**2004**). Controlling the location and activation of Rab GTPases. **Curr Opin Cell Biol**. 16(4): 451–457. doi: 10.1016/j.ceb.2004.06.014.

14. M Zerial, and H McBride (**2001**). Rab proteins as membrane organizers. **Nat Rev Mol Cell**

Biol. 2(2): 107–17.

15. Memon AR (**2004**). Erratum: The role of ADP-ribosylation factor and SAR1 in vesicular trafficking in plants (Biochimica et Biophysica Acta (2004) 1664 (9-30) PII: S0005-2736(04)00098-7 and DOI: 10.1016/j.bbamem.2004.04.005). **Biochim Biophys Acta - Biomembr**. 1665(1–2): 201. doi: 10.1016/j.bbamem.2004.08.007.

16. Ridley AJ (**2001**). Rho GTPases in cell migration. **J Cell Sci**. 114(July): 2713–2722. doi: 10.4161/sgtp.28997.

17. Ridley AJ (**2001**). Rho family proteins- coordinating cell responses. **Trends Cell Biol**. 11(12): 471–477.

18. Weis K (**2004**). Regulating Access to the Genome. **Cell**. 112(4): 441–451. doi: 10.1016/s0092-8674(03)00082-5.

19. Li H-Y, Cao K, and Zheng Y (**2003**). Ran in the spindle checkpoint: a new function for a versatile GTPase. **Trends Cell Biol**. 13(11): 553–557. doi: 10.1016/j.tcb.2003.09.003.

20. Boguski MS, and Frank B (**1993**). Proteins regulating Ras and its relatives. **Nature**. 366(December): 643–653.

21. Cox AD, and Der CJ (**2010**). Ras history: The saga continues. **Small GTPases**. 1(1): 2–27. doi: 10.4161/sgtp.1.1.12178.

22. Wennerberg K (**2005**). The Ras superfamily at a glance. **J Cell Sci**. 118(5): 843–846. doi: 10.1242/jcs.01660.

23. Bourne HR, DA S, and F. M (**1991**). The GTPase superfamily: conserved structure and molecular mechanism. **Nature**. 10: 117–27. 1898771.

24. Milburn M V, Tong L, Devos AM, Brunger A, Yamaizumi Z, Nishimura S, and Kim S (**1990**). Molecular switch for signal transduction: Structural differences between active and inactive forms of protooncogenic ras proteins. **Science (80-)**. 247(9): 939–945.

25. Almoh SC, Rapp G, Wilson K, Petratos K, Lentfer A, Wittinghofer A, Kabsch W, Pai EF, Petskoh GA, and Goody RS (**2000**). Time-resolved X-ray crystallographic study of the conformational change in Ha-Ras p21 protein on GTP hydrolysis. **Nature**. 345(May 1990): 309–315.

26. Bos JL, Rehmann H, and Wittinghofer A (**2007**). Review GEFs and GAPs : Critical Elements in the Control of Small G Proteins. **Cell**. 129: 865–877. doi: 10.1016/j.cell.200.

27. Rooij J De, and Bos JL (**1997**). Minimal Ras-binding domain of Raf1 can be used as an activation-specific probe for Ras. **Oncogene**. 14: 623–625.

28. Kataoka T, Powers S, Cameron S, Fasano O, Goldfarb M, Broach J, and Wigler M (**1985**). Functional homology of mammalian and yeast RAS genes. **Cell**. 40(1): 19–26. doi: 10.1016/0092-8674(85)90304-6.

29. Arozarena I, Calvo F, and Crespo P (**2011**). Ras, an actor on many Stages: Posttranslational modifications, Localization, and Site-Specified Events. **Genes and Cancer**. 2(3): 182–194. doi: 10.1177/1947601911409213.

30. Papageorge AG, Defeo-Jones D, Robinson P, Temeles G, and Scolnick EM (**1984**). Saccharomyces cerevisiae synthesizes proteins related to the p21 gene product of ras genes found in mammals. **Mol Cell Biol**. 4(1): 23–29. doi: 10.1128/mcb.4.1.23.

31. Wolfe KH (**2015**). Origin of the yeast whole-genome duplication. **PLoS Biol**. 13(8): 1–7. doi: 10.1371/journal.pbio.1002221.

32. Kataoka T, Powers S, McGill C, Fasano O, Strathern J, Broach J, and Wigler M (**1984**). Genetic analysis of yeast RAS1 and RAS2 genes. **Cell**. 37(2): 437–45. doi: 10.1016/0092-8674(84)90374-x.

33. Breviario D, Hinnebusch AG, and Dhar R (**1988**). Multiple regulatory mechanisms control the expression of the RAS1 and RAS2 genes of Saccharomyces cerevisiae. **EMBO J**. 7(6): 1805–1813. doi: 10.1002/j.1460-2075.1988.tb03012.x.

34. Tatchell K, Robinson LC, and Breitenbach M (**1985**). RAS2 of Saccharomyces cerevisiae is required for gluconeogenic growth and proper response to nutrient limitation. **Proc Nadl Acad Sci USA**. 82: 3785–3789.

35. Lisziewicz J, Brown J, Breviariol D, Sreenath T, Ahmed N, Koller R, and Dhar R (**1990**). Transcriptional regulatory elements of the RAS2 gene of Saccharomyces cerevisiae. **Nucleic Acids Res**. 18(14): 4167–4174.

36. Fraenkel DG (**1985**). On ras gene function in yeast. **Proc Natl Acad Sci**. 82(14): 4740–4744. doi: 10.1073/pnas.82.14.4740.

37. Marshall MS, Gibbs JB, Scolnick EM, and Sigal IS (**1987**). Regulatory function of the Saccharomyces cerevisiae RAS C-terminus. **Mol Cell Biol**. 7(7): 2309–2315. doi: 10.1128/mcb.7.7.2309.

38. Gibbs JB, Schaber MD, Allard WJ, Sigal IS, and Scolnick EM (**1988**). Purification of ras GTPase activating protein from bovine brain. **Proc Natl Acad Sci**. 85(14): 5026–5030. doi: 10.1073/pnas.85.14.5026.

39. Wang Y (**2001**). Alternative splicing of the K-RAS gene in mouse tissues and cell lines. **Exp Lung Res**. 27: 255–267.

40. Matallanas D, Arozarena I, Berciano MT, Aaronson DS, Pellicer A, Lafarga M, and Crespo P (**2003**). Differences on the Inhibitory Specificities of H-Ras, K-Ras, and N-Ras (N17) Dominant Negative Mutants Are Related to Their Membrane Microlocalization. **J Biol Chem**. 278(7): 4572–4581. doi: 10.1074/jbc.M209807200.

41. Campbell PM, and Der CJ (**2004**). Oncogenic Ras and its role in tumor cell invasion and metastasis. **Semin Cancer Biol**. 14(2): 105–114. doi: 10.1016/j.semcancer.2003.09.015.

42. Karnoub AE, and Weinberg RA (**2008**). Ras oncogenes: Split personalities. **Nat Rev Mol Cell Biol**. 9(7): 517–531. doi: 10.1038/nrm2438.

43. Rudolph J, and Stokoe D (**2014**). Selective inhibition of mutant ras protein through covalent binding. **Angew Chemie - Int Ed**. 53(15): 3777–3779. doi: 10.1002/anie.201400233.

44. Monahan AM, Callanan JJ, and Nally JE (**2008**). Proteomic analysis of post-translational modifications. **Microbiology**. 76(11): 4952–4958.

45. Fujiyama A, Matsumoto K, and Tamanoi F (**1987**). A novel yeast mutant defective in the processing of ras proteins: assessment of the effect of the mutation on processing steps. **EMBO J**. 6(1): 223–228.

46. Fujiyama A, and Tamanoi F (**1986**). Processing and fatty acid acylation of RAS1 and RAS2 proteins in Saccharomyces cerevisiae. **Proc Natl Acad Sci**. 83(5): 1266–1270. doi: 10.1073/pnas.83.5.1266.

47. Hancock JF, Cadwaller K, Paterson H, and Marshall CJ (**2003**). A CAAX or a CAAL motif and a second signal are sufficient for plasma membrane targeting of ras proteins. **Trends Cell Biol**. 2(3): 73. doi: 10.1016/0962-8924(92)90064-t.

48. Casey PJ, Solski PA, Der CJ, and Buss JE (**2006**). P21Ras Is Modified By a Farnesyl Isoprenoid. **Proc Natl Acad Sci**. 86(21): 8323–8327. doi: 10.1073/pnas.86.21.8323.

49. Rowell CA, Kowalczyk JJ, Lewis MD, and Garcia AM (**1997**). Direct Demonstration of Geranylgeranylation and Farnesylation of Ki-Ras in Vivo. **J Biol Chem**. 272(22): 14093–14097. doi: 10.1074/jbc.272.22.14093.

50. Choy E, Chiu VK, Silletti J, Feoktistov M, Morimoto T, Michaelson D, Ivanov IE, and Philips MR (**1999**). Endomembrane Trafficking of Ras. **Cell**. 98(1): 69–80. doi: 10.1016/S0092-8674(00)80607-8.

51. Schmidt WK, Tam A, Fujimura-Kamada K, and Michaelis S (**2002**). Endoplasmic reticulum membrane localization of Rce1p and Ste24p, yeast proteases involved in carboxyl-terminal CAAX protein processing and amino-terminal a-factor cleavage. **Proc Natl Acad Sci**. 95(19): 11175–11180. doi: 10.1073/pnas.95.19.11175.

52. Winter-Vann AM, and Casey PJ (**2005**). Post-prenylation-processing enzymes as new targets in oncogenesis. **Nat Rev Cancer**. 5(5): 405–412. doi: 10.1038/nrc1612.

53. Choy E, Chiu VK, Silletti J, Feoktistov M, Morimoto T, Michaelson D, Ivanov IE, and Philips MR (**1999**). Endomembrane trafficking of ras: The CAAX motif targets proteins to the ER and Golgi. **Cell**. 98(1): 69–80. doi: 10.1016/S0092-8674(00)80607-8.

54. Laude AJ, and Prior IA (**2008**). Palmitoylation and localisation of RAS isoforms are modulated by the hypervariable linker domain. **J Cell Sci**. 121(4): 421–427. doi: 10.1242/jcs.020107.

55. Eisenberg S, Laude AJ, Beckett AJ, Mageean CJ, Aran V, Hernandez-Valladares M, Henis YI, and Prior IA (**2013**). The role of palmitoylation in regulating Ras localization and function. **Biochem Soc Trans**. 41(1): 79–83. doi: 10.1042/BST20120268.

56. Rocks O (**2005**). An Acylation Cycle Regulates Localization and Activity of Palmitoylated Ras Isoforms. **Science (80-)**. 307(5716): 1746–1752. doi: 10.1126/science.1105654.

57. Chiu VK, Bivona T, Hach A, Sajous JB, Silletti J, Wiener H, Johnson RL, Cox AD, and Philips MR (**2002**). Ras signalling on the endoplasmic reticulum and the Golgi. **Nat Cell Biol**. 4(5): 343–350. doi: 10.1038/ncb783.

58. Shih TY, Weeks MO, Young HA, and Scolnick EM (**1979**). Identification of a sarcoma virus-coded phosphoprotein in nonproducer cells transformed by Kirsten or Harvey murine sarcoma virus. **Virology**. 96(1): 64–79. doi: 10.1016/0042-6822(79)90173-9.

59. Hancock JF, Magee AI, Childs JE, and Marshall CJ (**1989**). All ras proteins are polyisoprenylated but only some are palmitoylated. **Cell**. 57(7): 1167–1177. doi: 10.1016/0092-8674(89)90054-8.

60. Dong X, Mitchell DA, Lobo S, Zhao L, Bartels DJ, and Deschenes RJ (**2003**). Palmitoylation and Plasma Membrane Localization of Ras2p by a Nonclassical Trafficking Pathway in Saccharomyces cerevisiae. **Mol Cell Biol**. 23(18): 6574–6584. doi: 10.1128/MCB.23.18.6574.

61. Schafer WR, and Rine J (**1992**). PROTEIN PRENYLATION : .

62. Goodman LE, Judd SR, Farnsworth CC, Powers S, Gelb MH, Glomset JA, and Tamanoi F (**1990**). Mutants of Saccharomyces cerevisiae defective in the farnesylation of Ras proteins. **Proc Natl Acad Sci**. 87(24): 9665–9669. doi: 10.1073/pnas.87.24.9665.

63. Belotti F, Tisi R, Paiardi C, Rigamonti M, Groppi S, and Martegani E (**2012**). Localization of Ras signaling complex in budding yeast. **Biochim Biophys Acta - Mol Cell Res**. 1823(7): 1208–1216. doi: 10.1016/j.bbamcr.2012.04.016.

64. Vanoni M, Vavassori M, Frascotti G, Martegani E, and Alberghina L (**1990**). Overexpression of the CDC25 gene, an upstream element of the ras/adenylyl cyclase pathway in Saccharomyces cerevisiae, allows immunological identification and characterization of its gene product. **Biochem Biophys Res Commun**. 172(1): 61–69. doi: 10.1016/S0006-291X(05)80173-1.

65. Sobering AK, Romeo MJ, Vay HA, and Levin DE (**2003**). A Novel Ras Inhibitor, Eri1, Engages Yeast Ras at the Endoplasmic Reticulum. **Mol Cell Biol**. 23(14): 4983–4990. doi: 10.1128/mcb.23.14.4983-4990.2003.

66. Dong J, and Bai X (**2011**). The membrane localization of Ras2p and the association between Cdc25p and Ras2-GTP are regulated by protein kinase A (PKA) in the yeast *Saccharomyces cerevisiae*. **FEBS Lett**. 585(8): 1127–1134. doi: 10.1016/j.febslet.2011.03.057.

67. Belotti F, Tisi R, Paiardi C, Groppi S, and Martegani E (**2011**). PKA-dependent regulation of Cdc25 RasGEF localization in budding yeast. **FEBS Lett**. 585(24): 3914–3920. doi: 10.1016/j.febslet.2011.10.032.

68. Broggi S, Martegani E, and Colombo S (**2013**). Nuclear Ras2-GTP controls invasive growth in Saccharomyces cerevisiae. **PLoS One**. 8(11): e79274. doi: 10.1371/journal.pone.0079274.

69. Broggi S, Martegani E, and Colombo S (**2013**). Live-cell imaging of endogenous Ras-GTP shows predominant Ras activation at the plasma membrane and in the nucleus in Saccharomyces cerevisiae. **Int J Biochem Cell Biol**. 45(2): 384–394. doi: 10.1016/j.biocel.2012.10.013.

70. Leadsham JE, Miller K, Ayscough KR, Colombo S, Martegani E, Sudbery P, and Gourlay CW (**2009**). Whi2p links nutritional sensing to actin-dependent Ras-cAMP-PKA regulation and apoptosis in yeast. **J Cell Sci**. 122(Pt 5): 706–15. doi: 10.1242/jcs.042424.

71. Oliveira A, and Sauer U (**2012**). The importance of post-translational modifications in regulating Saccharomyces Cerevisiae metabolism. **FEMS Yeast Res**. 12(2): 104–117.

72. Cohen P (**2002**). The origins of protein phosphorylation. **Nat Cell Biol**. 4(5): 127–130.

73. Vlastaridis P, and Grigoris D (**2017**). Estimating the total number of phosphoproteins and phosphorylation sites in eukaryotic proteomes. **Gigascience**. 6(2): 1–11.

74. Whistler JL, and Rine J (**1997**). Ras2 and Ras1 protein phosphorylation is Saccharomyces cerevisiae. **J Biol Chem**. 272(30): 18790–18800. doi: 10.1074/jbc.272.30.18790.

75. Cobitz AR, Yim EH, Brown WR, Perou CM, and Tamanoi F (**2006**). Phosphorylation of RAS1 and RAS2 proteins in Saccharomyces cerevisiae. **Proc Natl Acad Sci**. 86(3): 858–862. doi: 10.1073/pnas.86.3.858.

76. Gibbs J, Ellis R, and Scolnick E (**1984**). Autophosphorylation of v-Ha-ras p21 is modulated by amino acid residue 12. **PNAS**. 81(9): 2674–2678.

77. Bivona TG, Quatela SE, Bodemann BO, Ahearn IM, Soskis MJ, Mor A, Miura J, Wiener HH, Wright L, Saba SG, Yim D, Fein A, Pérez De Castro I, Li C, Thompson CB, Cox AD, and Philips MR (**2006**). PKC regulates a farnesyl-electrostatic switch on K-Ras that promotes its association with Bcl-XL on mitochondria and induces apoptosis. **Mol Cell**. 21(4): 481–493. doi: 10.1016/j.molcel.2006.01.012.

78. Toda T, Uno I, Ishikawa T, Powers S, Kataoka T, Broek D, Cameron S, Broach J, Matsumoto K, and Wigler M (**1985**). In yeast, RAS proteins are controlling elements of adenylate cyclase. **Cell**. 40(1): 27–36. doi: 10.1016/0092-8674(85)90305-8.

79. Cazzaniga P, Pescini D, Besozzi D, Mauri G, Colombo S, and Martegani E (**2008**). Modeling and stochastic simulation of the Ras / cAMP / PKA pathway in the yeast Saccharomyces cerevisiae evidences a key regulatory function for intracellular guanine nucleotides pools. **J Biotechnol**. 133: 377–385. doi: 10.1016/j.jbiotec.2007.09.019.

80. Toda T, Cameron S, Sass P, Zoller M, Scott JD, McMullen B, Hurwitz M, Krebs EG, and Wigler M (**1987**). Cloning and characterization of BCY1, a locus encoding a regulatory subunit of the cyclic AMP-dependent protein kinase in Saccharomyces cerevisiae. **Mol Cell Biol**. 7(4): 1371–1377. doi: 10.1128/mcb.7.4.1371.

81. Toda T, Cameron S, Sass P, Zoller M, and Wigler M (**1987**). Three different genes in S. cerevisiae encode the catalytic subunits of the cAMP-dependent protein kinase. **Cell**. 50(2): 277–87. doi: 10.1016/0092-8674(87)90223-6.

82. Robertson LS, Causton HC, Young RA, and Fink GR (**2000**). The yeast A kinases differentially regulate iron uptake and respiratory function. **Proc Natl Acad Sci**. 97(11): 5984–5988. doi: 10.1073/pnas.100113397.

83. Robertson LS, and Fink GR (**1998**). The three yeast A kinases have specific signaling functions in pseudohyphal growth. **Genetic**. 95(November): 13783–13787.

84. Akada R, Yamamoto J, and Yamashita I (**1997**). Screening and identification of yeast sequences that cause growth inhibition when overexpressed. **Mol Gen Genet**. 254(3): 267–74. doi: 10.1007/s004380050415.

85. Nikawa J, Sass P, and Wigler M (**1987**). Cloning and characterization of the low-affinity cyclic AMP phosphodiesterase gene of Saccharomyces cerevisiae. **Mol Cell Biol**. 7(10): 3629–3636. doi: 10.1128/mcb.7.10.3629.

86. Sass P, Field J, Nikawa J, Toda T, and Wigler M (**1986**). Cloning and characterization of

the high-affinity cAMP phosphodiesterase of Saccharomyces cerevisiae. **Proc Natl Acad Sci**. 83(24): 9303–9307. doi: 10.1073/pnas.83.24.9303.

87. Wilson RB, and Tatchell K (**1988**). SRA5 Encodes the Low-KM Cyclic AMP phosphodiesterase of Saccharomyces cerevisiae. **Mol Cell Biol**. 8(1): 505–510.

88. Suoranta K, and Londesborough J (**1984**). Purification of intact and nicked forms of a zinc-containing, Mg2+-dependent, low K(m) cyclic AMP phosphodiesterase from bakers' yeast. **J Biol Chem**. 259(11): 6964–6971.

89. Wilson RB, Renault G, Jacquet M, and Tatchell K (**1993**). The pde2 gene of Saccharomyces cerevisiae is allelic to rcal and encodes a phosphodiesterase which protects the cell from extracellullar cAMP. **FEBS Lett**. 325(3): 191–195. doi: 10.1016/0014-5793(93)81071-7.

90. Damak F, Boy-marcotte E, Le-roscouet D, Guilbaud R, and Jacquet M (**1991**). SDC25 , a CDC25-Like gene Which Contains a RAS-Activating Domain and Is a Dispensable Gene of Saccharomyces cerevisiae. **Mol Cell Biol**. 11(1): 202–212.

91. Robinson L, Gibbs J, Marshall M, Sigal I, and Tatchell K (**1987**). CDC25: a component of the RAS-adenylate cyclase pathway in Saccharomyces cerevisiae. **Science (80-)**. 235(4793): 1218–1221. doi: 10.1126/science.3547648.

92. Jones S, Vignais ML, and Broach JR (**1991**). The CDC25 protein of Saccharomyces cerevisiae promotes exchange of guanine nucleotides bound to ras. **Mol Cell Biol**. 11(5): 2641–2646. doi: 10.1128/mcb.11.5.2641.

93. Tanaka K, Matsumoto K, and Toh-E A (**1989**). IRA1, an inhibitory regulator of the RAS-cyclic AMP pathway in Saccharomyces cerevisiae. **Mol Cell Biol**. 9(2): 757–768. doi: 10.1128/mcb.9.2.757.

94. Tanaka K, Nakafuku M, Tamanoi F, Kaziro Y, Matsumoto K, and Toh-e A (**1990**). IRA2, a second gene of Saccharomyces cerevisiae that encodes a protein with a domain homologous to mammalian ras GTPase-activating protein. **Mol Cell Biol**. 10(8): 4303–4313. doi: 10.1128/mcb.10.8.4303.

95. Tanaka K, Nakafuku M, Satoh T, Marshall MS, Gibbs JB, Matsumoto K, Kaziro Y, and Toh-e A (**1990**). S. cerevisiae genes IRA1 and IRA2 encode proteins that may be functionally equivalent to mammalian ras GTPase activating protein. **Cell**. 60(5): 803–807. doi: 10.1016/0092-8674(90)90094-U.

96. DeFeo-Jones D, Tatchell K, Robinson L, Sigal I, Vass W, Lowy D, and Scolnick E (**1985**). Mammalian and yeast ras gene products: biological function in their heterologous systems. **Science (80-)**. 228(4696): 179–184. doi: 10.1126/science.3883495.

97. Jacquet E, Parrini M, Bernardi A, Martegani E, and Parmeggiana A (**1994**). Properties of the catalytic domain of Cdc25, A yeast GDP/GTP exchange factor: Comparison of its activity on full-length and C-terminal truncated Ras2 proteins. **Biochem Biophys Res Commun**. 199(2): 497–503.

98. Mitts MR, Bradshaw-rouse J, and Heideman W (**1991**). Interactions between Adenylate Cyclase and the Yeast GTPase-Activating Protein IRAI. 11(9): 4591–4598.

99. Martegani E, Baroni MD, Frascotti G, and Alberghina L (**1986**). Molecular cloning and transcriptional analysis of the start gene CDC25 of Saccharomyces cerevisiae . **EMBO J**. 5(9): 2363–2369. doi: 10.1002/j.1460-2075.1986.tb04505.x.

100. Munder T, and Küntzel H (**1989**). Glucose-induced cAMP signaling in Saccharomyces cerevisiae is mediated by the CDC25 protein. **FEBS Lett**. 242(2): 341–345. doi: 10.1016/0014-5793(89)80498-3.

101. Schomerus C, Munder T, and Kuntzel H (**1990**). Site-directed mutagenesis of the Saccharomyces cerevisiae CDC25 gene: effects on mitotic growth and cAMP signalling. **MGG Mol Gen Genet**. 223(3): 426–432. doi: 10.1007/BF00264449.

102. Goldberg D, Segal M, and Levitzki A (**1994**). Cdc25 is not the signal receiver for glucose induced cAMP response in S. cerevisiae. **FEBS Lett**. 356(2–3): 249–254. doi: 10.1016/0014-5793(94)01273-3.

103. Rudoni S, Colombo S, Coccetti P, and Martegani E (**2001**). Role of guanine nucleotides in the regulation of the Ras/cAMP pathway in Saccharomyces cerevisiae. **Biochim Biophys Acta - Mol Cell Res**. 1538(2–3): 181–189. doi: 10.1016/S0167-4889(01)00067-2.

104. Garreau H, Geymonat M, Renault G, and Jacquet M (**1996**). Membrane-anchoring domains of Cdc25p, a Saccharomyces cerevisiae ras exchange factor. **Biol cell**. 86(2–3): 93–102. 8893498.

105. Gross E, Goldberg D, and Levitzki A (**1992**). Phosphorylation of the S. cerevisiae Cdc25 in response to glucose results in its dissociation from Ras. **Nature**. 360(6406): 762–5. doi: 10.1038/360762a0.

106. Jian D, Aili Z, Xiaojia B, Huansheng Z, and Yun H (**2010**). Feedback regulation of Ras2 guanine nucleotide exchange factor (Ras2-GEF) activity of Cdc25p by Cdc25p phosphorylation in the yeast Saccharomyces cerevisiae. **FEBS Lett**. 584(23): 4745–4750. doi: 10.1016/j.febslet.2010.11.006.

107. Li Y, and Wang Y (**2013**). Ras protein/cAMP-dependent protein kinase signaling is negatively regulated by a deubiquitinating enzyme, Ubp3, in yeast. **J Biol Chem**. 288(16): 11358–11365. doi: 10.1074/jbc.M112.449751.

108. Phan VT, Ding VW, Li F, Chalkley RJ, Burlingame A, and Mccormick F (**2010**). The RasGAP Proteins Ira2 and Neurofibromin Are Negatively Regulated by Gpb1 in Yeast and ETEA in Humans. **Mol Cell Biol**. 30(9): 2264–2279. doi: 10.1128/MCB.01450-08.

109. Zaman S, Lippman SI, Zhao X, and Broach JR (**2008**). How Saccharomyces Responds to Nutrients . **Annu Rev Genet**. 42(1): 27–81. doi: 10.1146/annurev.genet.41.110306.130206.

110. Santangelo GM (**2006**). Glucose Signaling in Saccharomyces cerevisiae. **Microbiol Mol Biol Rev**. 70(1): 253–282. doi: 10.1128/MMBR.70.1.253.

111. Xue Y, and Hirsch JP (**1996**). GPR1 encodes a putative G protein-coupled receptor that associates with the Gpa2p G α subunit and functions in a Ras-independent pathway. **EMBO J**. 17(7): 1996–2007.

112. Kraakman L, Lemaire K, Ma P, Teunissen a W, Donaton MC, Van Dijck P, Winderickx J, de Winde JH, and Thevelein JM (**1999**). A Saccharomyces cerevisiae G-protein coupled

receptor, Gpr1, is specifically required for glucose activation of the cAMP pathway during the transition to growth on glucose. **Mol Microbiol**. 32(5): 1002–12. 10361302.

113. Nakafuku M, Obara T, Kaibuchi K, Miyajima I, Miyajima A, Itoh H, Nakamura S, Arai K, Matsumoto K, and Kaziro Y (**1988**). Isolation of a second yeast Saccharomyces cerevisiae gene (GPA2) coding for guanine nucleotide-binding regulatory protein: studies on its structure and possible functions. **Proc Natl Acad Sci U S A**. 85(5): 1374–1378. doi: 10.1073/pnas.85.5.1374.

114. Lemaire K, Van De Velde S, Van Dijck P, and Thevelein JM (**2004**). Glucose and sucrose act as agonist and mannose as antagonist ligands of the G protein-coupled receptor Gpr1 in the yeast Saccharomyces cerevisiae. **Mol Cell**. 16(2): 293–299. doi: 10.1016/j.molcel.2004.10.004.

115. Colombo S, Ma P, Cauwenberg L, Winderickx J, Crauwels M, Teunissen A, Nauwelaers D, De Winde JH, Gorwa MF, Colavizza D, and Thevelein JM (**1998**). Involvement of distinct G-proteins, Gpa2 and Ras, in glucose- and intracellular acidification-induced cAMP signalling in the yeast Saccharomyces cerevisiae. **EMBO J**. 17(12): 3326–3341. doi: 10.1093/emboj/17.12.3326.

116. Dechant R, Binda M, Lee SS, Pelet S, Winderickx J, and Peter M (**2010**). Cytosolic pH is a second messenger for glucose and regulates the PKA pathway through V-ATPase. **EMBO J**. 29(15): 2515–2526. doi: 10.1038/emboj.2010.138.

117. Colombo S, Ronchetti D, Thevelein JM, Winderickx J, and Martegani E (**2004**). Activation state of the Ras2 protein and glucose-induced signaling in Saccharomyces cerevisiae. **J Biol Chem**. 279(45): 46715–22. doi: 10.1074/jbc.M405136200.

118. Rubio-Texeira M, Van Zeebroeck G, Voordeckers K, and Thevelein JM (**2010**). Saccharomyces cerevisiae plasma membrane nutrient sensors and their role in PKA signaling. **FEMS Yeast Res**. 10(2): 134–149. doi: 10.1111/j.1567-1364.2009.00587.x.

119. Klein C, and Struhl K (**1994**). Protein kinase A mediates growth-regulated expression of yeast ribosomal protein genes by modulating RAP1 transcriptional activity. **Mol Cell Biol**. 14(3): 1920–1928. doi: 10.1128/mcb.14.3.1920.

120. Neuman-Silberberg FS, Bhattacharya S, and Broach JR (**1995**). Nutrient availability and the RAS/cyclic AMP pathway both induce expression of ribosomal protein genes in Saccharomyces cerevisiae but by different mechanisms. **Mol Cell Biol**. 15(6): 3187–3196. doi: 10.1128/mcb.15.6.3187.

121. Wade JT, Hall DB, and Strahl K (**2004**). The transcription factor Ifh1 is a key regulator of yeast ribosomal protein genes. **Nature**. 432(7020): 1054–1058. doi: 10.1038/nature03175.

122. Hall DB, Wade JT, and Struhl K (**2006**). An HMG Protein, Hmo1, Associates with Promoters of Many Ribosomal Protein Genes and throughout the rRNA Gene Locus in Saccharomyces cerevisiae. **Mol Cell Biol**. 26(9): 3672–3679. doi: 10.1128/mcb.26.9.3672-3679.2006.

123. Martin DE, Soulard A, and Hall MN (**2004**). TOR regulates ribosomal protein gene expression via PKA and the Forkhead Transcription Factor FHL1. **Cell**. 119(7): 969–979. doi: 10.1016/j.cell.2004.11.047.

124. Schawalder SB, Kabani M, Howald I, Choudhury U, Werner M, and Shore D (**2004**). Growth-regulated recruitment of the essential yeast ribosomal protein gene activator Ifh1. **Nature**. 432(7020): 1058–1061. doi: 10.1038/nature03200.

125. Howard SC, Hester A, and Herman PK (**2003**). The Ras/PKA Signaling Pathway May Control RNA Polymerase II Elongation via the Spt4p/Spt5p Complex in Saccharomyces cerevisiae. **Genetics**. 165(3): 1059–1070.

126. Garrett S, Menold MM, and Broach JR (**1991**). The Saccharomyces cerevisiae YAK1 gene encodes a protein kinase that is induced by arrest early in the cell cycle. **Mol Cell Biol**. 11(8): 4045–4052. doi: 10.1128/mcb.11.8.4045.

127. Lee P, Paik SM, Shin CS, Huh WK, and Hahn JS (**2011**). Regulation of yeast Yak1 kinase by PKA and autophosphorylation-dependent 14-3-3 binding. **Mol Microbiol**. 79(3): 633–646. doi: 10.1111/j.1365-2958.2010.07471.x.

128. Lee P, Cho BR, Joo HS, and Hahn JS (**2008**). Yeast Yak1 kinase, a bridge between PKA and stress-responsive transcription factors, Hsf1 and Msn2/Msn4. **Mol Microbiol**. 70(4): 882–895. doi: 10.1111/j.1365-2958.2008.06450.x.

129. Boy-Marcotte E, Perrot M, Bussereau F, Boucherie H, and Jacquet M (**1998**). Msn2p and Msn4p control a large number of genes induced at the diauxic transition which are repressed by cyclic AMP in Saccharomyces cerevisiae. **J Bacteriol**. 180(5): 1044–1052.

130. Reinders A, Bürckert N, Boller T, Wiemken A, and De Virgilio C (**1998**). Saccharomyces cerevisiae cAMP-dependent protein kinase controls entry into stationary phase through the Rim15p protein kinase. **Genes Dev**. 12(18): 2943–2955. doi: 10.1101/gad.12.18.2943.

131. Cytryńska MI, Frajnt M, and Jakubowicz T (**2001**). Saccharomyces cerevisiae pyruvate kinase Pyk1 is PKA phosphorylation substrate in vitro. **FEMS Microbiol Lett**. 203(2): 223–227. doi: 10.1016/S0378-1097(01)00354-8.

132. Vaseghi S, Macherhammer F, Zibek S, and Reuss M (**2001**). Signal transduction dynamics of the protein kinase-A/phosphofructokinase-2 system in Saccharomyces cerevisiae. **Metab Eng**. 3(2): 163–172. doi: 10.1006/mben.2000.0179.

133. Gancedos C (**1983**). Fructose 2,6-Bisphosphate Activates the cAMP-dependent Phosphorylation of Yeast Fructose-1,6-bisphosphatase in Vitro. **J Biol Chem**. 10(August 1982): 4–6.

134. Lin K, Rath VL, Dai SC, Fletterick RJ, and Hwang PK (**1996**). A protein phosphorylation switch at the conserved allosteric site in GP. **Science (80-)**. 273(5281): 1539–1541. doi: 10.1126/science.273.5281.1539.

135. Hardy TA, and Roach PJ (**1993**). Control of yeast glycogen synthase-2 by COOH-terminal phosphorylation. **J Biol Chem**. 268(32): 23799–23805.

136. Busti S, Coccetti P, Alberghina L, and Vanoni M (**2010**). Glucose signaling-mediated coordination of cell growth and cell cycle in Saccharomyces Cerevisiae. **Sensors**. 10(6): 6195–6240. doi: 10.3390/s100606195.

137. Wang XW, and Zhang YJ (**2014**). Targeting mTOR network in colorectal cancer therapy. **World J Gastroenterol**. 20(15): 4178–4188. doi: 10.3748/wjg.v20.i15.4178.

138. Peeper DS, Upton TM, Ladha MH, Neuman E, Zalvide J, Bernards R, DeCaprio JA, and Ewen ME (**1997**). Ras signalling linked to the cell-cycle machinery by the retinoblastoma protein. **Nature**. 386(6621): 177–181. doi: 10.1038/386177a0.

139. Pruitt K, and Der CJ (**2001**). Ras and Rho regulation of the cell cycle and oncogenesis. **Cancer Lett**. 171(1): 1–10. doi: 10.1016/S0304-3835(01)00528-6.

140. Downward J (**2004**). Cell cycle: Routine role for Ras. **Curr Biol**. 7(4): R258–R260. doi: 10.1016/s0960-9822(06)00116-3.

141. Lord PG, and Wheals AE (**1983**). Rate of cell cycle initiation of yeast cells when cell size is not a rate-determining factor. **J Cell Sci**. 59: 183–201.

142. Hartwell L., and Unger M. (**1977**). Unequal division in Saccharomyces Cerevisiae and its implications for the control of cell division. **J Cell Biol**. 75: 422–435.

143. Vanoni M, Vai M, Popolo L, and Alberghina L (**1983**). Structural heterogeneity in populations of the budding yeast Saccharomyces cerevisiae. **J Bacteriol**. 156(3): 1282–1291.

144. Johnston GC, Ehrhardt CW, Lorincz A, and Carter BLA (**1979**). Regulation of cell size in the yeast Saccharomyces cerevisiae. **J Bacteriol**. 137(1): 1–5.

145. Baroni MD, Monti P, Lilia B, and Comparata B (**1994**). Repression of growth-regulated G1 cyclin expression by cyclic AMP in budding yeast. **Nature**. 371: 339–342.

146. Tokiwa G, Tyerst M, Volpe T, and Futchert B (**1994**). Inhibition of G1 cyclin activity by the Ras/cAMP pathway in yeast. **Nature**. 371(September): 342–345.

147. Mizunuma M, Tsubakiyama R, Ogawa T, Shitamukai A, Kobayashi Y, Inai T, Kume K, and Hirata D (**2013**). Ras/cAMP-dependent protein kinase (PKA) regulates multiple aspects of cellular events by phosphorylating the whi3 cell cycle regulator in budding yeast. **J Biol Chem**. 288(15): 10558–10566. doi: 10.1074/jbc.M112.402214.

148. Wood MD, and Sanchez Y (**2010**). Deregulated Ras signaling compromises DNA damage checkpoint recovery in S. cerevisiae. **Cell Cycle**. 9(16): 3353–3363. doi: 10.4161/cc.9.16.12713.

149. Gray J V, Petsko GA, Johnston GC, Ringe D, Singer RA, and Werner-washburne M (**2004**). “Sleeping Beauty”: Quiescence in Saccharomyces cerevisiae. **Microbiol Mol Biol Rev**. 68(2): 187–206. doi: 10.1128/MMBR.68.2.187.

150. Laporte D, Lebaudy A, Sahin A, Pinson B, Ceschin J, Daignan-Fornier B, and Sagot I (**2011**). Metabolic status rather than cell cycle signals control quiescence entry and exit. **J Cell Biol**. 192(6): 949–957. doi: 10.1083/jcb.201009028.

151. Coller HA, Sang L, and Roberts JM (**2006**). A new description of cellular quiescence. **PLoS Biol**. 4(3): 0329–0349. doi: 10.1371/journal.pbio.0040083.

152. Matson JP, and Cook JG (**2017**). Cell cycle proliferation decisions: the impact of single cell analyses. **FEBS J**. 284(3): 362–375. doi: 10.1111/febs.13898.

153. Smets B, Ghillebert R, De Snijder P, Binda M, Swinnen E, De Virgilio C, and Winderickx J (**2010**). Life in the midst of scarcity: Adaptations to nutrient availability in Saccharomyces cerevisiae. .

154. Thevelein JM, and de Winde JH (**1999**). Novel sensing mechanisms and targets for the cAMP-protein kinase A pathway in the yeast Saccharomyces cerevisiae. **Mol Microbiol**. 33(5): 904–18. 10476026.

155. Gourlay CW, Du W, and Ayscough KR (**2006**). Apoptosis in yeast - Mechanisms and benefits to a unicellular organism. **Mol Microbiol**. 62(6): 1515–1521. doi: 10.1111/j.1365-2958.2006.05486.x.

156. Carmona-Gutierrez D, Eisenberg T, Büttner S, Meisinger C, Kroemer G, and Madeo F (**2010**). Apoptosis in yeast: Triggers, pathways, subroutines. **Cell Death Differ**. 17(5): 763–773. doi: 10.1038/cdd.2009.219.

157. Fröhlich KU, Fussi H, and Ruckenstuhl C (**2007**). Yeast apoptosis-From genes to pathways. **Semin Cancer Biol**. 17(2): 112–121. doi: 10.1016/j.semcancer.2006.11.006.

158. Gourlay CW, and Ayscough KR (**2006**). Actin-Induced Hyperactivation of the Ras Signaling Pathway Leads to Apoptosis in Saccharomyces cerevisiae. **Mol Cell Biol**. 26(17): 6487–6501. doi: 10.1128/mcb.00117-06.

159. Pentland DR, Piper-Brown E, Mühlschlegel FA, and Gourlay CW (**2018**). Ras signalling in pathogenic yeasts. **Microb Cell**. 5(2): 63/73.

160. Santos J, Leão C, and Sousa MJ (**2013**). Ammonium-dependent shortening of CLS in yeast cells starved for essential amino acids is determined by the specific amino acid deprived, through different signaling pathways. **Oxid Med Cell Longev**. 2013. doi: 10.1155/2013/161986.

161. Santos J, Sousa MJ, and Leão C (**2012**). Ammonium is toxic for aging yeast cells, inducing death and shortening of the chronological lifespan. **PLoS One**. 7(5). doi: 10.1371/journal.pone.0037090.

162. Narasimhan ML, Damsz B, Ibeas I, Yun D, Coca MA, Pardo M, Hasegawa PM, and Lafayette W (**2001**). A Plant defence response effector induces microbial apoptosis. **Mol Cell**. 8(October): 921–930.

163. Fröhlich E, Madeo F, Sigrist SJ, Grey M, Ligr M, Fröhlich K-U, and Wolf DH (**2002**). Oxygen Stress: A Regulator of Apoptosis in Yeast. **J Cell Biol**. 145(4): 757–767. doi: 10.1083/jcb.145.4.757.

164. Silva RD, Sotoca R, Johansson B, Ludovico P, Sansonetty F, Silva MT, Peinado JM, and Côrte-Real M (**2005**). Hyperosmotic stress induces metacaspase- and mitochondria-dependent apoptosis in Saccharomyces cerevisiae. **Mol Microbiol**. 58(3): 824–834. doi: 10.1111/j.1365-2958.2005.04868.x.

165. Lastauskiene E, Zinkevičiene A, and Čitavičius D (**2014**). Ras/PKA signal transduction pathway participates in the regulation of Saccharomyces cerevisiae cell apoptosis in an acidic environment. **Biotechnol Appl Biochem**. 61(1): 3–10. doi: 10.1002/bab.1183.

166. Chen Y, and Klionsky DJ (**2010**). The regulation of autophagy - unanswered questions. **J Cell Sci**. 124(2): 161–170. doi: 10.1242/jcs.064576.

167. Stephan JS, Yeh Y-Y, Ramachandran V, Deminoff SJ, and Herman PK (**2009**). The Tor and PKA signaling pathways independently target the Atg1/Atg13 protein kinase complex to

control autophagy. **Proc Natl Acad Sci**. 106(40): 17049–17054. doi: 10.1073/pnas.0903316106.

168. Jacinto E, and Lorberg A (**2008**). TOR regulation of AGC kinases in yeast and mammals. **Biochem J**. 410(1): 19–37. doi: 10.1042/bj20071518.

169. Noda T, Ohsumi Y, and Tor (**1998**). Tor, a Phosphatidylinositol Kinase Homologue, Controls Autophagy in yeast. **J Biol Chem**. 273(7): 3963–3966.

170. Zaman S, Lippman SI, Schneper L, Slonim N, and Broach JR (**2009**). Glucose regulates transcription in yeast through a network of signaling pathways. **Mol Syst Biol**. 5(245): 1–14. doi: 10.1038/msb.2009.2.

171. Kingsbury JM, Sen ND, and Cardenas ME (**2015**). Branched-Chain Aminotransferases Control TORC1 Signaling in Saccharomyces cerevisiae. **PLoS Genet**. 11(12): 1–24. doi: 10.1371/journal.pgen.1005714.

172. Stracka D, Jozefczuk S, Rudroff F, Sauer U, and Hall MN (**2014**). Nitrogen source activates TOR (Target of Rapamycin) complex 1 via glutamine and independently of Gtr/Rag proteins. **J Biol Chem**. 289(36): 25010–25020. doi: 10.1074/jbc.M114.574335.

173. Sancak Y, Peterson TR, Shaul YD, Lindquist RA, Thoreen CC, Bar-peled L, and Sabatini DM (**2008**). The Rag GTPases bind raptor and nediate amino acid signaling in mTORC1. **Science (80-)**. 320(5882): 1496–1501. doi: 10.1126/science.1157535.The.

174. Binda M, Péli-Gulli MP, Bonfils G, Panchaud N, Urban J, Sturgill TW, Loewith R, and De Virgilio C (**2009**). The Vam6 GEF Controls TORC1 by Activating the EGO Complex. **Mol Cell**. 35(5): 563–573. doi: 10.1016/j.molcel.2009.06.033.

175. Rebsamen M, Pochini L, Stasyk T, De Araújo MEG, Galluccio M, Kandasamy RK, Snijder B, Fauster A, Rudashevskaya EL, Bruckner M, Scorzoni S, Filipek PA, Huber KVM, Bigenzahn JW, Heinz LX, Kraft C, Bennett KL, Indiveri C, Huber LA, and Superti-Furga G (**2015**). SLC38A9 is a component of the lysosomal amino acid sensing machinery that controls mTORC1. **Nature**. 519(7544): 477–481. doi: 10.1038/nature14107.

176. Wang S, Tsun Z-Y, Wolfson R, Shen K, Wyant GA, Plovanich ME, Yuan ED, Jones TD, Chantranupong L, Comb W, Wang T, Bar-Peled L, Zoncu R, Straub C, Kim C, Park J, Sabatini BL, and Sabatini DM (**2015**). The amino acid transporter SLC38A9 is a key component of a lysosomal membrane complex that signals arginine sufficiency to mTORC1. **Science (80-)**. 347(6218): 188–194. doi: 10.1126/science.1257132.

177. Averous J, Lambert-Langlais S, Mesclon F, Carraro V, Parry L, Jousse C, Bruhat A, Maurin AC, Pierre P, Proud CG, and Fafournoux P (**2016**). GCN2 contributes to mTORC1 inhibition by leucine deprivation through an ATF4 independent mechanism. **Sci Rep**. 6(June): 1–10. doi: 10.1038/srep27698.

178. Berlanga JJ, Santoyo J, and De Haro C (**1999**). Characterization of a mammalian homolog of the GCN2 eukaryotic initiation factor 2α kinase. **Eur J Biochem**. 265(2): 754–762. doi: 10.1046/j.1432-1327.1999.00780.x.

179. Cai H, Hauser M, Naider F, and Becker JM (**2007**). Differential regulation and substrate preferences in two peptide transporters of Saccharomyces cerevisiae. **Eukaryot Cell**. 6(10): 1805–1813. doi: 10.1128/EC.00257-06.

180. Perry JR, Basrai MA, Steiner H-Y, Naider F, and Becker " JM (**1994**). Isolation and Characterization of a Saccharomyces cerevisiae Peptide Transport Gene. **Mol Cell Biol**. 14(1): 104–115.

181. Alagramam K, Naider F, and Becker JM (**1995**). A recognition component of the ubiquitin system is required for peptide transport in Saccharomyces cerevisiae. **Mol Microbiol**. 15(2): 225–34. doi: 10.1111/j.1365-2958.1995.tb02237.x.

182. Island MD, Naider F, and Becker JM (**1987**). Regulation of dipeptide transport in Saccharomyces cerevisiae by micromolar amino acid concentrations. **J Bacteriol**. 169(5): 2132–2136. doi: 10.1128/jb.169.5.2132-2136.1987.

183. Varshavsky A (**1997**). The N-end rule pathway of protein degradation. **Genes to Cells**. 2(1): 13–28. doi: 10.1046/j.1365-2443.1997.1020301.x.

184. Varshavsky A (**1996**). The N-end rule: Functions, mysteries, uses. **Proc Natl Acad Sci U S A**. 93(22): 12142–12149. doi: 10.1073/pnas.93.22.12142.

185. Du F, Navarro-Garcia F, Xia Z, Tasaki T, and Varshavsky A (**2002**). Pairs of dipeptides synergistically activate the binding of substrate by ubiquitin ligase through dissociation of its autoinhibitory domain. **Proc Natl Acad Sci U S A**. 99(22): 14110–14115. doi: 10.1073/pnas.172527399.

186. Homann OR, Cai H, Becker JM, and Lindquist SL (**2005**). Harnessing Natural Diversity to Probe Metabolic Pathways. **PLoS Genet**. 1(6): e80. doi: 10.1371/journal.pgen.0010080.

187. Wiles AM, Cai H, Naider F, and Becker JM (**2006**). Nutrient regulation of oligopeptide transport in Saccharomyces cerevisiae. **Microbiology**. 152(10): 3133–3145. doi: 10.1099/mic.0.29055-0.

188. Martinelli E, De Palma R, Orditura M, De Vita F, and Ciardiello F (**2009**). Anti-epidermal growth factor receptor monoclonal antibodies in cancer therapy. **Clin Exp Immunol**. 158(1): 1–9. doi: 10.1111/j.1365-2249.2009.03992.x.

189. Normanno N, Tejpar S, Morgillo F, De Luca A, Van Cutsem E, and Ciardiello F (**2009**). Implications for KRAS status and EGFR-targeted therapies in metastatic CRC. **Nat Rev Clin Oncol**. 6(9): 519–527. doi: 10.1038/nrclinonc.2009.111.

190. Schulze WX, Deng L, and Mann M (**2005**). Phosphotyrosine interactome of the ErbB-receptor kinase family. **Mol Syst Biol**. 1(1): E1–E13. doi: 10.1038/msb4100012.

191. Downward J (**2003**). Targeting RAS signalling pathways in cancer therapy. **Nat Rev Cancer**. 3(1): 11–22. doi: 10.1038/nrc969.

192. Herrmann C (**2003**). Ras-effector interactions: After one decade. **Curr Opin Struct Biol**. 13(1): 122–129. doi: 10.1016/S0959-440X(02)00007-6.

193. KOLCH W (**2000**). Meaningful relationships: the regulation of the Ras/Raf/MEK/ERK pathway by protein interactions. **Biochem J**. 351(2): 289–305. doi: 10.1042/bj3510289.

194. Yung Y, Dolginov Y, Yao Z, Rubinfeld H, Michael D, Hanoch T, Roubini E, Lando Z, Zharhary D, and Seger R (**1997**). Detection of ERK activation by a novel monoclonal antibody. **FEBS Lett**. 408(3): 292–296. doi: 10.1016/S0014-5793(97)00442-0.

195. Scheid MP, and Woodgett JR (**2001**). Phosphatidylinositol 3' Kinase Signaling in Mammary Tumorigenesis. **J Mammary Gland Biol Neoplasia**. 6(1): 83–99. doi: 10.1023/A:1009520616247.

196. Hancock JF, Apolloni A, Yan J, Lane A, and Roy S (**2002**). Ras Isoforms Vary in Their Ability to Activate Raf-1 and Phosphoinositide 3-Kinase. **J Biol Chem**. 273(37): 24052–24056. doi: 10.1074/jbc.273.37.24052.

197. Rajalingam K, Schreck R, Rapp UR, and Albert Š (**2007**). Ras oncogenes and their downstream targets. **Biochim Biophys Acta - Mol Cell Res**. 1773(8): 1177–1195. doi: 10.1016/j.bbamcr.2007.01.012.

198. Powers S, Kataoka T, Fasano O, Goldfarb M, Strathem J, Broach J, and Wigler M (**1984**). Genes in S. cerevisiae encoding proteins with domains homologous to the mammalian ras proteins. **Cell**. 36(3): 607–612. doi: 10.1016/0092-8674(84)90340-4.

199. DeFeo-Jones D, Scolnick E, Koller R, and Dhar R (**1983**). Ras-related gene sequences identified and isolated from Saccharomyces cerevisiae. **Nature**. 306(5944): 707–709. doi: 10.1038/306707a0.

200. Clark S., McGrath J., and Levinson A. (**1985**). Expression of Normal and Activated Human Ha-ras cDNAs in Saccharomyces cerevisiae. **Mol Cell Biol**. 5(10): 2746–2752.

201. Fujiyama A, Matsumoto K, and Tamanoi F (**1987**). A novel yeast mutant defective in the processing of ras proteins: assessment of the effect of the mutation on processing steps. **EMBO J**. 6(1): 223–8. 3556161.

202. Afgan E, Baker D, Batut B, van den Beek M, Bouvier D, Cech M, Chilton J, Clements D, Coraor N, Grüning BA, Guerler A, Hillman-Jackson J, Hiltemann S, Jalili V, Rasche H, Soranzo N, Goecks J, Taylor J, Nekrutenko A, and Blankenberg D (**2018**). The Galaxy platform for accessible, reproducible and collaborative biomedical analyses: 2018 update. **Nucleic Acids Res**. 46(W1): W537–W544. doi: 10.1093/nar/gky379.

203. (2010). AS FASTQC: A quality control tool for high throughput sequence data. .

204. Krueger F (2012) Trim Galore!: A wrapper tool around Cutadapt and FastQC to consistently apply quality and adapter trimming to FastQ files, with some extra functionality for MspI-digested RRBS-type (Reduced Representation Bisufite-Seq) libraries. .

205. Kim D, Langmead B, and Salzberg SL (**2015**). HISAT : a fast spliced aligner with low memory requirements. 12(4). doi: 10.1038/nmeth.3317.

206. Liao Y, Smyth GK, and Shi W (**2014**). FeatureCounts: An efficient general purpose program for assigning sequence reads to genomic features. **Bioinformatics**. 30(7): 923–930. doi: 10.1093/bioinformatics/btt656.

207. Love MI, Huber W, and Anders S (**2014**). Moderated estimation of fold change and dispersion for RNA-seq data with DESeq2. **Genome Biol**. 15(12): 1–21. doi: 10.1186/s13059-014-0550-8.

208. Subramanian A, Tamayo P, Mootha VK, Mukherjee S, Ebert BL, Gillette M a, Paulovich A, Pomeroy SL, Golub TR, Lander ES, and Mesirov JP (**2005**). Gene set enrichment analysis: a knowledge-based approach for interpreting genome-wide expression profiles. **Proc Natl**

Acad Sci U S A. 102(43): 15545–50. doi: 10.1073/pnas.0506580102.

209. Gueldener U (**2002**). A second set of loxP marker cassettes for Cre-mediated multiple gene knockouts in budding yeast. **Nucleic Acids Res**. 30(6): 23e – 23. doi: 10.1093/nar/30.6.e23.

210. von der Haar T (**2007**). Optimized protein extraction for quantitative proteomics of yeasts. **PLoS One**. 2(10). doi: 10.1371/journal.pone.0001078.

211. Marshall M (**1995**). Interactions between Ras and Raf: key regulatory proteins in cellular transformation. **Mol Reprod Dev**. 42(4): 493–9. doi: 10.1002/mrd.1080420418.

212. Omerovic J, and Prior IA (**2009**). Compartmentalized signalling: Ras proteins and signalling nanoclusters. **FEBS J**. 276(7): 1817–1825. doi: 10.1111/j.1742-4658.2009.06928.x.

213. Xiaojia B, and Jian D (**2010**). Serine214 of Ras2p plays a role in the feedback regulation of the Ras-cAMP pathway in the yeast Saccharomyces cerevisiae. **FEBS Lett**. 584(11): 2333–2338. doi: 10.1016/j.febslet.2010.04.011.

214. Jin X, Starke S, Li Y, Sethupathi S, Kung G, Dodhiawala P, and Wang Y (**2016**). Nitrogen starvation-induced phosphorylation of Ras1 protein and its potential role in nutrient signaling and stress response. **J Biol Chem**. 291(31): 16231–16239. doi: 10.1074/jbc.M115.713206.

215. Herskowitz I (**1988**). Life cycle of the budding yeast Saccharomyces cerevisiae. **Microbiol Rev**. 52(4): 536–553.

216. Conrad M, Schothorst J, Kankipati HN, Van Zeebroeck G, Rubio-Texeira M, and Thevelein JM (**2014**). Nutrient sensing and signaling in the yeast *Saccharomyces cerevisiae*. **FEMS Microbiol Rev**. 38(2): 254–299. doi: 10.1111/1574-6976.12065.

217. Carmona-Gutierrez D et al. (**2018**). Guidelines and recommendations on yeast cell death nomenclature. **Microb Cell**. 5(1): 4–31. doi: 10.15698/mic2018.01.607.

218. Rinnerthaler M, Büttner S, Laun P, Heeren G, Felder TK, Klinger H, Weinberger M, Stolze K, Grousl T, Hasek J, Benada O, Frydlova I, Klocker A, Simon-Nobbe B, Jansko B, Breitenbach-Koller H, Eisenberg T, Gourlay CW, Madeo F, Burhans WC, and Breitenbach M (**2012**). Yno1p/Aim14p, a NADPH-oxidase ortholog, controls extramitochondrial reactive oxygen species generation, apoptosis, and actin cable formation in yeast. **Proc Natl Acad Sci U S A**. 109(22): 8658–8663. doi: 10.1073/pnas.1201629109.

219. Cebollero E, and Reggiori F (**2009**). Regulation of autophagy in yeast Saccharomyces cerevisiae. **Biochim Biophys Acta - Mol Cell Res**. 1793(9): 1413–1421. doi: 10.1016/j.bbamcr.2009.01.008.

220. Nakatogawa H, Ichimura Y, and Ohsumi Y (**2007**). Atg8, a Ubiquitin-like Protein Required for Autophagosome Formation, Mediates Membrane Tethering and Hemifusion. **Cell**. 130(1): 165–178. doi: 10.1016/j.cell.2007.05.021.

221. Kirisako T, Ichimura Y, Okada H, Kabeya Y, Mizushima N, Yoshimori T, Ohsumi M, Takao T, Noda T, and Ohsumi Y (**2000**). The Reversible Modification Regulates the Membrane-Binding State of Apg8/Aut7 Essential for Autophagy and the Cytoplasm to Vacuole Targeting Pathway. **J Cell Biol**. 151(2): 263–276. doi: 10.1083/jcb.151.2.263.

222. Cheong H, and Klionsky DJ (**2008**). Chapter 1 Biochemical Methods to Monitor Autophagy-Related Processes in Yeast. pp 1–26.

223. Shintani T, and Klionsky DJ (**2004**). Cargo Proteins Facilitate the Formation of Transport Vesicles in the Cytoplasm to Vacuole Targeting Pathway. **J Biol Chem**. 279(29): 29889–29894. doi: 10.1074/jbc.M404399200.

224. Leadsham JE, and Gourlay CW (**2010**). CAMP/PKA signaling balances respiratory activity with mitochondria dependent apoptosis via transcriptional regulation. **BMC Cell Biol**. 11(1): 92. doi: 10.1186/1471-2121-11-92.

225. Guaragnella N, Coyne LP, Chen XJ, and Giannattasio S (**2018**). Mitochondria-cytosol-nucleus crosstalk: Learning from Saccharomyces cerevisiae. **FEMS Yeast Res**. 18(8): 1–15. doi: 10.1093/femsyr/foy088.

226. de Virgilio C (**2012**). The essence of yeast quiescence. **FEMS Microbiol Rev**. 36(2): 306–339. doi: 10.1111/j.1574-6976.2011.00287.x.

227. Eraso P, and Gancedo JM (**1985**). Use of glucose analogues to study the mechanism of glucose-mediated cAMP increase in yeast. **FEBS Lett**. 191(1): 51–54. doi: 10.1016/0014-5793(85)80991-1.

228. FRANÇOIS J, ERASO P, and GANCEDO C (**1987**). Changes in the concentration of cAMP, fructose 2,6-bisphosphate and related metabolites and enzymes in Saccharomyces cerevisiae during growth on glucose. **Eur J Biochem**. 164(2): 369–373. doi: 10.1111/j.1432-1033.1987.tb11067.x.

229. BROACH J (**1991**). RAS genes in Saccharomyces cerevisiae: signal transduction in search of a pathway. **Trends Genet**. 7(1): 28–33. doi: 10.1016/0168-9525(91)90018-L.

230. Taylor WE, and Young ET (**1990**). CAMP-dependent phosphorylation and inactivation of yeast transcription factor ADR1 does not affect DNA binding. **Proc Natl Acad Sci U S A**. 87(11): 4098–4102. doi: 10.1073/pnas.87.11.4098.

231. Matsumoto K, Uno I, Oshima Y, and Ishikawa T (**1982**). Isolation and characterization of yeast mutants deficient in adenylate cyclase and cAMP-dependent protein kinase. **Proc Natl Acad Sci U S A**. 79(7 I): 2355–2359. doi: 10.1073/pnas.79.7.2355.

232. Toda T, Uno I, Ishikawa T, Powers S, Kataoka T, Broek D, Cameron S, Broach J, Matsumoto K, and Wigler M (**1985**). In yeast, RAS proteins are controlling elements of adenylate cyclase. **Cell**. 40(1): 27–36. doi: 10.1016/0092-8674(85)90305-8.

233. Kelliher CM, Foster MW, Motta FC, Deckard A, Soderblom EJ, Arthur Moseley M, and Haase SB (**2018**). Layers of regulation of cell-cycle gene expression in the budding yeast Saccharomyces cerevisiae. **Mol Biol Cell**. 29(22): 2644–2655. doi: 10.1091/mbc.E18-04-0255.

234. Clarke S, Vogel JP, Deschenes RJ, and Stock J (**1988**). Posttranslational modification of the Ha-ras oncogene protein: evidence for a third class of protein carboxyl methyltransferases [published erratum appears in Proc Natl Acad Sci U S A 1988 Oct;85(20):7556]. **Proc Natl Acad Sci U S A**. 85(13): 4643–4647.

235. Fujiyama A, and Tamanoi F (**1990**). RAS2 Protein of Saccharomyces cerevisiae

undergoes removal of methionine at N terminus and removal of three amino acids at C terminus. **J Biol Chem**. 265(6): 3362–3368.

236. Engelberg D, Simchen G, and Levitzki A (**1990**). In vitro reconstitution of cdc25 regulated S. cerevisiae adenylyl cyclase and its kinetic properties. **EMBO J**. 9(3): 641–651. doi: 10.1002/j.1460-2075.1990.tb08156.x.

237. Mitts MR, Grant DB, and Heideman W (**1990**). Adenylate cyclase in Saccharomyces cerevisiae is a peripheral membrane protein. **Mol Cell Biol**. 10(8): 3873–3883. doi: 10.1128/mcb.10.8.3873.

238. Hlavatá L, Aguilaniu H, Pichová A, and Nyström T (**2003**). The oncogenic RAS2val19 mutation locks respiration, independently of PKA, in a mode prone to generate ROS. **EMBO J**. 22(13): 3337–3345. doi: 10.1093/emboj/cdg314.

239. Johnson KE, Cameron S, Toda T, Wigler M, and Zoller MJ (**1987**). Expression in Escherichia coli of BCY1, the regulatory subunit of cyclic AMP-dependent protein kinase from Saccharomyces cerevisiae. Purification and characterization. **J Biol Chem**. 262(18): 8636–8642.

240. Edwards AS, and Scott JD (**2000**). A-kinase anchoring proteins: Protein kinase A and beyond. **Curr Opin Cell Biol**. 12(2): 217–221. doi: 10.1016/S0955-0674(99)00085-X.

241. Griffioen G, Branduardi P, Ballarini A, Anghileri P, Norbeck J, Baroni MD, and Ruis H (**2001**). Nucleocytoplasmic Distribution of Budding Yeast Protein Kinase A Regulatory Subunit Bcy1 Requires Zds1 and Is Regulated by Yak1-Dependent Phosphorylation of Its Targeting Domain. **Mol Cell Biol**. 21(2): 511–523. doi: 10.1128/mcb.21.2.511-523.2001.

242. Tudisca V, Recouvreux V, Moreno S, Boy-Marcotte E, Jacquet M, and Portela P (**2010**). Differential localization to cytoplasm, nucleus or P-bodies of yeast PKA subunits under different growth conditions. **Eur J Cell Biol**. 89(4): 339–348. doi: 10.1016/j.ejcb.2009.08.005.

243. Tamaki H (**2007**). Glucose-stimulated cAMP-protein kinase a pathway in yeast Saccharomyces cerevisiae. **J Biosci Bioeng**. 104(4): 245–250. doi: 10.1263/jbb.104.245.

244. Steyfkens F, Zhang Z, Van Zeebroeck G, and Thevelein JM (**2018**). Multiple Transceptors for Macro- and Micro-Nutrients Control Diverse Cellular Properties Through the PKA Pathway in Yeast: A Paradigm for the Rapidly Expanding World of Eukaryotic Nutrient Transceptors Up to Those in Human Cells. **Front Pharmacol**. 9: 191. doi: 10.3389/fphar.2018.00191.

245. Wiles AM, Cai H, Naider F, Becker JM, and Jeffrey Becker jbecker CM Nutrient regulation of oligopeptide transport in Saccharomyces cerevisiae. doi: 10.1099/mic.0.29055-0.

246. Hauser M, Narita V, Donhardt AM, Naider F, and Becker JM (**2001**). Multiplicity and regulation of genes encoding peptide transporters in *Saccharomyces cerevisiae*. **Mol Membr Biol**. 18(1): 105–112. doi: 10.1080/09687680010029374.

247. Thevelein JM, Cauwenberg L, Colombo S, De Winde JH, Donation M, Dumortier F, Kraakman L, Lemaire K, Ma P, Nauwelaers D, Rolland F, Teunissen A, Van Dijck P, Versele M, Wera S, and Winderickx J (**2000**). Nutrient-induced signal transduction through the protein kinase A pathway and its role in the control of metabolism, stress resistance, and growth in

yeast. **Enzyme Microb Technol**. 26(9–10): 819–825. doi: 10.1016/S0141-0229(00)00177-0.

248. Fuge EK, Braun EL, and Werner-Washburne M (**1994**). Protein synthesis in long-term stationary-phase cultures of Saccharomyces cerevisiae. **J Bacteriol**. 176(18): 5802–5813. doi: 10.1128/jb.176.18.5802-5813.1994.

249. Werner-Washburne M, Braun EL, Crawford ME, and Peck VM (**1996**). Stationary phase in Saccharomyces cerevisiae. **Mol Microbiol**. 19(6): 1159–66. doi: 10.1111/j.1365-2958.1996.tb02461.x.

250. Piñon R (**1978**). Folded chromosomes in non-cycling yeast cells: evidence for a characteristic g0 form. **Chromosoma**. 67(3): 263–74. doi: 10.1007/bf02569039.

251. Ewing B, Ewing B, Hillier L, Hillier L, Wendl MC, Wendl MC, Green P, and Green P (**2005**). Base-Calling of Automated Sequencer Traces Using. **Genome Res**. (206): 175–185. doi: 10.1101/gr.8.3.175.

252. Lever J, Krzywinski M, and Altman N (**2017**). Points of Significance: Principal component analysis. **Nat Methods**. 14(7): 641–642. doi: 10.1038/nmeth.4346.

253. Merico D, Isserlin R, Stueker O, Emili A, and Bader GD (**2010**). Enrichment map: A network-based method for gene-set enrichment visualization and interpretation. **PLoS One**. 5(11). doi: 10.1371/journal.pone.0013984.

254. Sagot I, and Laporte D (**2019**). The cell biology of quiescent yeast-a diversity of individual scenarios. doi: 10.1242/jcs.213025.

255. Boucherie H (**1985**). Protein synthesis during transition and stationary phases under glucose limitation in Saccharomyces cerevisiae. **J Bacteriol**. 161(1): 385–392.

256. Ju Q, and Warner JR (**1994**). Ribosome synthesis during the growth cycle ofSaccharomyces cerevisiae. **Yeast**. 10(2): 151–157. doi: 10.1002/yea.320100203.

257. Thevelein J, Bonini B, Castermans D, Haesendonckx S, Kriel J, Louwet W, Thayumanavan P, Popova Y, Rubio-Texeira M, Schepers W, Vandormael P, Zeebroeck G, Verhaert P, Versele M, and Voordeckers K (**2008**). Novel mechanisms in nutrient activation of the yeast Protein Kinase A pathway. **Acta Microbiol Immunol Hung**. 55(2): 75–89. doi: 10.1556/AMicr.55.2008.2.1.

258. Vogelstein B, Papadopoulos N, Velculescu VE, Zhou S, Diaz LA, and Kinzler KW (**2013**). Cancer genome landscapes. **Science (80-)**. 340(6127): 1546–1558. doi: 10.1126/science.1235122.

259. Stephen AG, Esposito D, Bagni RG, and McCormick F (**2014**). Dragging ras back in the ring. **Cancer Cell**. 25(3): 272–281. doi: 10.1016/j.ccr.2014.02.017.

260. Cox AD, Fesik SW, Kimmelman AC, Luo J, and Der CJ (**2014**). Drugging the undruggable RAS: Mission Possible? **Nat Rev Drug Discov**. 13(11): 828–851. doi: 10.1038/nrd4389.

261. Lazo JS, and Sharlow ER (**2016**). Drugging Undruggable Molecular Cancer Targets. **Annu Rev Pharmacol Toxicol**. 56(1): 23–40. doi: 10.1146/annurev-pharmtox-010715-103440.

262. Tsai FD, Lopes MS, Zhou M, Court H, Ponce O, Fiordalisi JJ, Gierut JJ, Cox AD, Haigis KM, and Philips MR (**2015**). K-Ras4A splice variant is widely expressed in cancer and uses a hybrid

membrane-targeting motif. **Proc Natl Acad Sci U S A**. 112(3): 779–784. doi: 10.1073/pnas.1412811112.

263. Ahearn IM, Haigis K, Bar-Sagi D, and Philips MR (**2012**). Regulating the regulator: Post-translational modification of RAS. **Nat Rev Mol Cell Biol**. 13(1): 39–51. doi: 10.1038/nrm3255.

264. Cox AD, Der CJ, and Philips MR (**2015**). Targeting RAS membrane association: Back to the future for anti-RAS drug discovery? **Clin Cancer Res**. 21(8): 1819–1827. doi: 10.1158/1078-0432.CCR-14-3214.

265. Plowman SJ, Ariotti N, Goodall A, Parton RG, and Hancock JF (**2008**). Electrostatic Interactions Positively Regulate K-Ras Nanocluster Formation and Function. **Mol Cell Biol**. 28(13): 4377–4385. doi: 10.1128/mcb.00050-08.

266. Sung PJ, Tsai FD, Vais H, Court H, Yang J, Fehrenbacher N, Foskett JK, and Philips MR (**2013**). Phosphorylated K-Ras limits cell survival by blocking Bcl-xL sensitization of inositol trisphosphate receptors. **Proc Natl Acad Sci U S A**. 110(51): 20593–20598. doi: 10.1073/pnas.1306431110.

267. Hanahan D, and Weinberg R (**2000**). The Hallmarks of Cancer. **Cell**. 1(100): 0092–8674. 10647931.

268. Mandalà M, Merelli B, and Massi D (**2014**). Nras in melanoma: Targeting the undruggable target. **Crit Rev Oncol Hematol**. 92(2): 107–122. doi: 10.1016/j.critrevonc.2014.05.005.

Appendix

RAS2^{S225A} vs EV- Cytoplasmic Translation- Upregulated

Gene Name	Rank in Gene List	Rank Metric Score	Running Enrichment Score
RPP0	25	2.342	0.0779
TMA19	56	1.975	0.1413
RPL30	121	1.675	0.1857
RPL29	140	1.606	0.2388
SSB1	195	1.461	0.278
SSA1	220	1.406	0.3225
SSB2	224	1.403	0.3721
THS1	278	1.315	0.4062
TMA7	311	1.265	0.4437
RPL28	373	1.181	0.4711
RPG1	404	1.133	0.5044
TIF11	426	1.1	0.5387
SSZ1	523	1.001	0.5511
TIF35	531	0.993	0.585
TIF3	535	0.989	0.6197
HYP2	596	0.918	0.6379
TRM7	771	0.778	0.6231
TAE1	1061	0.585	0.5732
RBG1	1112	0.558	0.5809
PRT1	1175	0.525	0.5846
HCR1	1262	0.483	0.5808
FES1	1388	0.428	0.5655
FUN12	1803	0.267	0.4736
CLU1	1941	0.213	0.4476
TIF34	2035	0.16	0.4305
TMA46	2238	-0.234	0.3894
RPM2	3373	-0.601	0.1329
MTG2	3405	-0.614	0.1473
AFG3	3551	-0.679	0.1361

Cytosolic Ribosome

Gene Name	Rank in Gene List	Rank Metric Score	Running Enrichment Score
RPP0	25	2.342	0.0505
ASC1	49	2.05	0.0944
RPS12	79	1.818	0.1312
RPS5	85	1.784	0.1731
RPS3	120	1.677	0.2053
RPL30	121	1.675	0.2458
RPS31	138	1.615	0.2809
RPL29	140	1.606	0.3195
RPL39	179	1.513	0.3467
RPL5	208	1.425	0.3743
RPL3	232	1.381	0.4021
RPL38	257	1.345	0.4287
RPS20	279	1.313	0.4553
RPL25	294	1.286	0.4829
RPL32	300	1.278	0.5126
RPS13	305	1.273	0.5424
RLI1	318	1.253	0.5697
SIS1	327	1.246	0.5979
RPS2	363	1.193	0.6182
RPL28	373	1.181	0.6445
YEF3	378	1.174	0.6719
RPL10	452	1.072	0.6799
NAT1	571	0.946	0.6738
HYP2	596	0.918	0.6901
MAP1	605	0.909	0.7101
SQT1	678	0.848	0.7129
ARD1	709	0.825	0.7255
SNL1	1030	0.605	0.6615
FES1	1388	0.428	0.5841
NAT5	1632	0.33	0.5323
NMD3	1733	0.293	0.5148
FUN12	1803	0.267	0.5043
LSG1	1943	0.212	0.4753
JJJ1	2216	-0.226	0.4139
HEF3	2692	-0.367	0.3061
RQC1	3116	-0.5	0.2142
RRP14	3137	-0.507	0.2215
BUD27	3546	-0.676	0.1376

Pre-ribosome

Gene Name	Rank in Gene List	Rank Metric Score	Running Enrichment Score
SNU13	23	2.41	0.025
RPP0	25	2.342	0.0547
RPS5	85	1.784	0.0627
NOP58	100	1.74	0.0814
KRR1	103	1.73	0.103
RPS3	120	1.677	0.1204
HCA4	148	1.59	0.1339
RPL3	232	1.381	0.1308
NIP7	242	1.365	0.146
YVH1	249	1.355	0.1618
EMG1	283	1.307	0.1702
NOP13	285	1.303	0.1866
RPS13	305	1.273	0.1981
ENP1	317	1.256	0.2114
RLI1	318	1.253	0.2274
NOP56	357	1.203	0.2332
RPS2	363	1.193	0.2472
RPL28	373	1.181	0.2601
MRT4	411	1.123	0.2651
UTP13	430	1.095	0.2746
NOP1	431	1.094	0.2886
MAK16	498	1.034	0.2853
NOC2	525	0.999	0.2915
NEW1	534	0.991	0.3021
DIM1	560	0.958	0.3081
UTP4	564	0.953	0.3195
HAS1	579	0.936	0.328
IMP3	597	0.918	0.3354
RRS1	598	0.917	0.3472
UTP10	608	0.903	0.3564
RPF2	629	0.886	0.3627
CBF5	634	0.881	0.373
NSA2	640	0.876	0.3829
PRP43	652	0.866	0.3912
SQT1	678	0.848	0.3958
DBP3	696	0.833	0.4022

CIC1	708	0.827	0.41
NOP7	717	0.821	0.4185
UTP14	739	0.806	0.4235
DBP5	759	0.787	0.4288
NUG1	790	0.768	0.4311
MAK21	803	0.757	0.4378
IPI1	807	0.755	0.4466
RRP1	832	0.737	0.45
KRE33	847	0.727	0.4558
ROK1	866	0.715	0.4605
SLX9	889	0.701	0.4639
BFR2	896	0.696	0.4713
UTP21	925	0.677	0.4729
CGR1	1001	0.626	0.4621
UTP6	1031	0.605	0.4626
SAS10	1045	0.596	0.4669
SPB1	1072	0.578	0.4678
FCF1	1132	0.548	0.46
CKB2	1159	0.534	0.4604
NOP2	1193	0.517	0.4587
ERB1	1205	0.512	0.4625
RIX7	1219	0.507	0.4657
CKB1	1231	0.5	0.4693
NSA1	1251	0.489	0.4708
NOG1	1255	0.486	0.4763
NOP9	1324	0.455	0.465
RRP12	1334	0.452	0.4686
UTP7	1366	0.441	0.4664
RRP36	1394	0.425	0.4651
NOP4	1422	0.413	0.4636
NOG2	1466	0.397	0.4579
DBP8	1488	0.388	0.4576
CKA2	1528	0.364	0.4525
BUD20	1536	0.361	0.4554
RSA3	1543	0.359	0.4584
PWP2	1566	0.351	0.4574
UTP22	1602	0.34	0.453
SSF1	1687	0.31	0.4359
RRP7	1699	0.306	0.4371
NMD3	1733	0.293	0.4326
TIF6	1786	0.276	0.4231
NOP6	1787	0.275	0.4266

FUN12	1803	0.267	0.4262
RRP5	1819	0.261	0.4258
UTP23	1828	0.258	0.4271
CMS1	1839	0.254	0.4278
SQS1	1871	0.239	0.4231
UTP5	1885	0.235	0.4229
RLP24	1887	0.234	0.4256
UTP15	1906	0.227	0.424
RRP9	1909	0.227	0.4264
NOP15	1981	0.198	0.4111
YTM1	2015	0.179	0.4052
UTP18	2117	-0.189	0.3823
RLP7	2137	-0.196	0.3801
DIP2	2158	-0.205	0.3777
TSR1	2162	-0.206	0.3795
CRM1	2184	-0.215	0.377
JJJ1	2216	-0.226	0.3722
NOP16	2232	-0.232	0.3714
SPB4	2319	-0.258	0.3531
UTP20	2386	-0.28	0.3402
ENP2	2464	-0.303	0.3248
NOP19	2586	-0.335	0.2988
UTP30	2642	-0.352	0.2895
RRP15	2662	-0.358	0.2893
UTP11	2710	-0.375	0.2823
MRD1	2754	-0.386	0.2765
LAS1	2803	-0.4	0.2696
EBP2	2806	-0.4	0.2742
LTV1	2974	-0.451	0.2381
KRI1	2995	-0.458	0.239
ECM1	3114	-0.5	0.2158
DBP6	3234	-0.544	0.193
MDN1	3321	-0.579	0.1788
CKA1	3440	-0.627	0.1573
IMP4	3634	-0.722	0.1182

Ribosome Assembly

Gene Name	Rank in Gene List	Rank Metric Score	Running Enrichment Score
RPP0	25	2.342	0.0885
REX4	91	1.75	0.1433
RPS31	138	1.615	0.1972
IPI3	143	1.598	0.2608
NSR1	180	1.508	0.3129
RPL5	208	1.425	0.3638
RPL3	232	1.381	0.414
YVH1	249	1.355	0.4648
RPL25	294	1.286	0.5059
MRT4	411	1.123	0.5229
RPL10	452	1.072	0.5564
RPF2	629	0.886	0.549
SQT1	678	0.848	0.5715
MAK21	803	0.757	0.5717
IPI1	807	0.755	0.6014
RIA1	815	0.75	0.63
RSA4	1222	0.505	0.5509
RSA1	1519	0.368	0.4933
RSA3	1543	0.359	0.5021
SSF1	1687	0.31	0.4796
RRP7	1699	0.306	0.4893
FUN12	1803	0.267	0.4748
LSG1	1943	0.212	0.4493
SPB4	2319	-0.258	0.3678
MRD1	2754	-0.386	0.2771
MDN1	3321	-0.579	0.1617
MRH4	3681	-0.753	0.1042

Ribosome Biogenesis

Gene Name	Rank in Gene List	Rank Metric Score	Running Enrichment Score
SNU13	23	2.41	0.0107
RPP0	25	2.342	0.0266
RPS5	85	1.784	0.0238
REX4	91	1.75	0.0346
NOP58	100	1.74	0.0446

KRR1	103	1.73	0.056
RPS3	120	1.677	0.0635
RPL30	121	1.675	0.075
RPS31	138	1.615	0.0821
IPI3	143	1.598	0.0921
HCA4	148	1.59	0.102
NSR1	180	1.508	0.1045
TSR2	194	1.463	0.1113
SSB1	195	1.461	0.1213
RPS15	201	1.446	0.13
RPL5	208	1.425	0.1383
EFG1	213	1.417	0.1471
SSB2	224	1.403	0.1542
RPL3	232	1.381	0.1619
GSP1	235	1.379	0.171
RRB1	236	1.374	0.1804
NIP7	242	1.365	0.1886
YVH1	249	1.355	0.1964
RPS20	279	1.313	0.198
EMG1	283	1.307	0.2063
RPL25	294	1.286	0.2126
RPS13	305	1.273	0.2188
ENP1	317	1.256	0.2247
RLI1	318	1.253	0.2333
NOP56	357	1.203	0.2319
RPS2	363	1.193	0.2388
SRD1	400	1.139	0.2374
GAR1	402	1.136	0.245
MRT4	411	1.123	0.2507
UTP13	430	1.095	0.2537
NOP1	431	1.094	0.2612
RPL10	452	1.072	0.2635
ESF1	481	1.051	0.2635
MAK5	482	1.051	0.2708
MAK16	498	1.034	0.2741
SSZ1	523	1.001	0.2748
NOC2	525	0.999	0.2815
NEW1	534	0.991	0.2863
DIM1	560	0.958	0.2865
UTP4	564	0.953	0.2923
HAS1	579	0.936	0.2951
NHP2	585	0.931	0.3003

SKI6	588	0.927	0.3062
IMP3	597	0.918	0.3104
RRS1	598	0.917	0.3168
ZUO1	604	0.91	0.3218
UTP10	608	0.903	0.3272
RAI1	622	0.89	0.33
RPF2	629	0.886	0.3346
CBF5	634	0.881	0.3397
NSA2	640	0.876	0.3444
PRP43	652	0.866	0.3476
RPP1	676	0.849	0.3476
SQT1	678	0.848	0.3532
RRP46	681	0.845	0.3585
DBP3	696	0.833	0.3606
TMA20	715	0.823	0.3617
NOP7	717	0.821	0.3671
PWP1	728	0.813	0.3702
FYV7	738	0.806	0.3734
UTP14	739	0.806	0.379
DBP9	750	0.798	0.3819
NUG1	790	0.768	0.3772
FAP7	793	0.763	0.382
MAK21	803	0.757	0.3849
IPI1	807	0.755	0.3893
RIA1	815	0.75	0.3927
RRP1	832	0.737	0.3937
KRE33	847	0.727	0.3951
ROK1	866	0.715	0.3954
RNT1	888	0.701	0.3949
SLX9	889	0.701	0.3997
RRP42	895	0.696	0.4032
BFR2	896	0.696	0.408
NUP85	898	0.694	0.4126
SRM1	917	0.682	0.4127
UTP21	925	0.677	0.4155
RRP43	933	0.673	0.4184
RRP40	936	0.669	0.4225
CGR1	1001	0.626	0.4104
UTP6	1031	0.605	0.4071
SAS10	1045	0.596	0.4079
YAR1	1054	0.59	0.4099
RRP3	1070	0.579	0.4101

SPB1	1072	0.578	0.4138
GRC3	1097	0.566	0.4115
RCM1	1128	0.549	0.4076
FCF1	1132	0.548	0.4106
PUF6	1166	0.531	0.4058
POP7	1178	0.524	0.4066
NOP2	1193	0.517	0.4066
SYO1	1204	0.512	0.4076
ERB1	1205	0.512	0.4111
RIX7	1219	0.507	0.4113
RSA4	1222	0.505	0.4142
CAM1	1226	0.5	0.4169
MTR4	1250	0.489	0.4144
NSA1	1251	0.489	0.4178
NOG1	1255	0.486	0.4203
HCR1	1262	0.483	0.4221
MPP6	1304	0.466	0.4148
NOP9	1324	0.455	0.4131
RRP12	1334	0.452	0.4139
UTP7	1366	0.441	0.409
PUS7	1381	0.432	0.4084
RRP36	1394	0.425	0.4082
NOP4	1422	0.413	0.4042
REX3	1445	0.404	0.4013
RNA1	1448	0.403	0.4036
NOG2	1466	0.397	0.4019
DBP8	1488	0.388	0.3992
RSA1	1519	0.368	0.3941
BUD20	1536	0.361	0.3925
RSA3	1543	0.359	0.3934
RNH70	1555	0.356	0.393
URB2	1565	0.352	0.3932
PWP2	1566	0.351	0.3956
TRM112	1598	0.341	0.39
UTP22	1602	0.34	0.3916
MTR3	1631	0.33	0.3867
RRP4	1668	0.313	0.3796
SSF1	1687	0.31	0.3771
RRP7	1699	0.306	0.3764
NMD3	1733	0.293	0.3699
SDA1	1774	0.28	0.3616
LTO1	1784	0.276	0.3612

TIF6	1786	0.276	0.3628
NOP6	1787	0.275	0.3647
FUN12	1803	0.267	0.3627
RRP8	1816	0.262	0.3615
RRP5	1819	0.261	0.3628
UTP23	1828	0.258	0.3625
SQS1	1871	0.239	0.3534
UTP5	1885	0.235	0.3516
RLP24	1887	0.234	0.353
LCP5	1888	0.234	0.3546
UTP15	1906	0.227	0.3518
RRP9	1909	0.227	0.3529
FCF2	1913	0.224	0.3536
NOP53	1934	0.216	0.35
LSG1	1943	0.212	0.3494
NOP15	1981	0.198	0.3413
REX2	1994	0.192	0.3395
NGL2	2014	0.179	0.3359
YTM1	2015	0.179	0.3371
SEN1	2039	0.153	0.3323
TMA23	2056	-0.159	0.3293
NIC96	2098	-0.183	0.32
SAC3	2115	-0.189	0.3172
UTP18	2117	-0.189	0.3183
RLP7	2137	-0.196	0.3147
NUP49	2138	-0.197	0.3161
DIP2	2158	-0.205	0.3126
TSR1	2162	-0.206	0.3133
PUS5	2169	-0.208	0.3132
CRM1	2184	-0.215	0.3111
JJJ1	2216	-0.226	0.3047
NOP16	2232	-0.232	0.3024
RMP1	2243	-0.236	0.3015
POP6	2262	-0.242	0.2986
SPB4	2319	-0.258	0.286
YAE1	2371	-0.274	0.2748
UTP20	2386	-0.28	0.2731
YRB2	2408	-0.288	0.2697
LSM7	2422	-0.293	0.2684
MRM2	2448	-0.3	0.264
ENP2	2464	-0.303	0.2623
RAT1	2488	-0.309	0.2585

NOP19	2586	-0.335	0.2359
UTP30	2642	-0.352	0.2242
RRP15	2662	-0.358	0.2218
UTP11	2710	-0.375	0.2124
POP1	2717	-0.376	0.2134
RIO2	2752	-0.385	0.2073
MRD1	2754	-0.386	0.2098
RSP5	2785	-0.393	0.2048
LAS1	2803	-0.4	0.2032
EBP2	2806	-0.4	0.2054
BCP1	2807	-0.4	0.2082
RRP6	2921	-0.435	0.1822
LTV1	2974	-0.451	0.1719
KRI1	2995	-0.458	0.17
RRP17	3012	-0.465	0.1691
HIT1	3049	-0.478	0.1631
PAF1	3094	-0.492	0.1552
ECM1	3114	-0.5	0.1538
RRP14	3137	-0.507	0.1517
TSR3	3142	-0.508	0.1541
SNU66	3221	-0.539	0.1378
DBP6	3234	-0.544	0.1385
DIS3	3240	-0.546	0.141
MDN1	3321	-0.579	0.1245
LRP1	3332	-0.581	0.1259
SPT5	3358	-0.591	0.1236
NUP116	3447	-0.63	0.1053
MOT1	3514	-0.658	0.0929
TOR2	3521	-0.663	0.096
RRP45	3569	-0.69	0.0887
IMP4	3634	-0.722	0.0772
MRH4	3681	-0.753	0.0706
TOR1	3689	-0.757	0.0741
NUP1	3707	-0.774	0.0751
TOM1	3754	-0.812	0.0689
SNM1	3878	-0.92	0.0436
DBP7	3933	-0.984	0.0366
NME1	4005	-1.098	0.0259

RAS2^{S225A} vs EV- Cell Cycle- Downregulated

Gene Name	Rank in Gene List	Rank Metric Score	Running Enrichment Score
KIN4	938	0.667	-0.1891
MAD2	1015	0.615	-0.1701
HHT2	1155	0.536	-0.1714
LTE1	1301	0.467	-0.1784
CDC20	1424	0.413	-0.1831
TPD3	1718	0.298	-0.2367
BMH1	1961	0.205	-0.2835
CTF3	2277	-0.246	-0.3456
CDC55	2383	-0.279	-0.3543
RTS1	2598	-0.339	-0.3861
IPL1	2720	-0.377	-0.3927
FIN1	2941	-0.442	-0.4196
MPS1	3205	-0.534	-0.4514
BUB3	3224	-0.54	-0.4228
BUD2	3250	-0.55	-0.3953
ULP2	3297	-0.571	-0.3717
GAC1	3368	-0.599	-0.3522
MAD1	3406	-0.614	-0.3238
DOC1	3489	-0.65	-0.3042
SWM1	3524	-0.664	-0.2719
CEP3	3570	-0.69	-0.2408
BFA1	3733	-0.791	-0.2322
BIR1	3826	-0.874	-0.2013
DMA2	3895	-0.934	-0.1609
CDH1	3970	-1.039	-0.1155
CHL4	3982	-1.053	-0.0539
CTF19	4076	-1.374	0.0074

Condensed Chromosome

Gene Name	Rank in Gene List	Rank Metric Score	Running Enrichment Score
SPO16	406	1.13	-0.0782
RFA3	635	0.881	-0.1173
REC104	710	0.825	-0.1192
RFA2	765	0.783	-0.117
MEI4	799	0.76	-0.11
MCD1	805	0.755	-0.0962
SMC3	965	0.646	-0.1228
YCS4	1000	0.627	-0.1187

PDS5	1011	0.619	-0.1089
MAD2	1015	0.615	-0.0973
MCM16	1028	0.606	-0.0882
SMC6	1179	0.524	-0.115
SMC1	1192	0.517	-0.1077
MTW1	1228	0.5	-0.1064
HSK3	1229	0.5	-0.0964
NSE5	1383	0.431	-0.1258
DUO1	1473	0.393	-0.1401
DAD1	1581	0.347	-0.1597
CSM1	1622	0.333	-0.163
YCG1	1689	0.309	-0.1732
STU2	1741	0.29	-0.1801
IRR1	1751	0.287	-0.1766
SMC4	1797	0.271	-0.1824
LRS4	1872	0.239	-0.196
TOP2	1956	0.208	-0.2124
NSE1	2172	-0.209	-0.2616
CTF3	2277	-0.246	-0.2825
ZIP1	2300	-0.252	-0.283
KRE29	2459	-0.302	-0.3162
CST9	2483	-0.307	-0.3158
PLC1	2512	-0.316	-0.3164
CBF2	2556	-0.328	-0.3205
MEC3	2581	-0.334	-0.3198
RTS1	2598	-0.339	-0.317
MCM22	2600	-0.34	-0.3105
NUF2	2644	-0.352	-0.3142
DAM1	2698	-0.369	-0.32
IPL1	2720	-0.377	-0.3177
ASK1	2863	-0.419	-0.3446
PPH3	2912	-0.432	-0.3479
FIN1	2941	-0.442	-0.346
CSE4	2956	-0.446	-0.3406
REC102	2958	-0.446	-0.3319
RED1	3163	-0.518	-0.3722
MCM21	3166	-0.52	-0.3624
MPS1	3205	-0.534	-0.3611
BUB3	3224	-0.54	-0.3548
DAD3	3225	-0.541	-0.3441
ZIP2	3378	-0.603	-0.3698
AME1	3445	-0.63	-0.3736

SCM3	3460	-0.636	-0.3644
NNF1	3469	-0.641	-0.3536
NSE4	3501	-0.653	-0.3482
ECM11	3503	-0.655	-0.3354
REC107	3531	-0.666	-0.3289
CEP3	3570	-0.69	-0.3245
REC114	3656	-0.741	-0.3309
CTF13	3668	-0.748	-0.3187
MMS21	3753	-0.812	-0.3233
MND1	3765	-0.823	-0.3097
RAD51	3795	-0.85	-0.2999
REC8	3796	-0.85	-0.283
BIR1	3826	-0.874	-0.2727
UBC9	3861	-0.901	-0.2632
SLK19	3917	-0.963	-0.2577
MIF2	3925	-0.975	-0.24
OKP1	3929	-0.979	-0.2212
DSN1	3941	-0.998	-0.204
SPO13	3950	-1.009	-0.1859
DMC1	3963	-1.029	-0.1684
CHL4	3982	-1.053	-0.1518
NDC80	3988	-1.059	-0.132
KRE28	4004	-1.091	-0.1139
BRN1	4016	-1.125	-0.0942
TFC3	4037	-1.199	-0.0753
CTF19	4076	-1.374	-0.0573
SPC24	4095	-1.573	-0.0304
MEI5	4099	-1.652	0.0017

Kinetechore

Gene Name	Rank in Gene List	Rank Metric Score	Running Enrichment Score
MAD2	1015	0.615	-0.2262
MCM16	1028	0.606	-0.206
MTW1	1228	0.5	-0.2358
HSK3	1229	0.5	-0.2167
DUO1	1473	0.393	-0.2615
DAD1	1581	0.347	-0.2745
CSM1	1622	0.333	-0.2716
STU2	1741	0.29	-0.2896
LRS4	1872	0.239	-0.3124

CRM1	2184	-0.215	-0.3807
CTF3	2277	-0.246	-0.3939
PLC1	2512	-0.316	-0.4394
CBF2	2556	-0.328	-0.4375
RTS1	2598	-0.339	-0.4346
MCM22	2600	-0.34	-0.4219
WIP1	2638	-0.351	-0.4175
NUF2	2644	-0.352	-0.4053
DAM1	2698	-0.369	-0.4042
IPL1	2720	-0.377	-0.395
CNN1	2767	-0.388	-0.3914
ASK1	2863	-0.419	-0.3988
FIN1	2941	-0.442	-0.4008
CSE4	2956	-0.446	-0.3872
MCM21	3166	-0.52	-0.4188
MPS1	3205	-0.534	-0.4077
BUB3	3224	-0.54	-0.3914
DAD3	3225	-0.541	-0.3708
MAD1	3406	-0.614	-0.3916
AME1	3445	-0.63	-0.3768
NNF1	3469	-0.641	-0.358
CEP3	3570	-0.69	-0.3562
CTF13	3668	-0.748	-0.3514
BIR1	3826	-0.874	-0.3566
SLK19	3917	-0.963	-0.3419
MIF2	3925	-0.975	-0.3064
OKP1	3929	-0.979	-0.2696
CBF1	3939	-0.996	-0.2338
DSN1	3941	-0.998	-0.1958
CHL4	3982	-1.053	-0.1654
NDC80	3988	-1.059	-0.1261
KRE28	4004	-1.091	-0.0881
CTF19	4076	-1.374	-0.053
SPC24	4095	-1.573	0.0027

Microtubule based processes

Gene Name	Rank in Gene List	Rank Metric Score	Running Enrichment Score
ACT1	353	1.214	-0.063
SPC29	379	1.169	-0.0455

SPC98	646	0.872	-0.0938
CRN1	672	0.853	-0.0828
CMD1	713	0.824	-0.076
CLB4	725	0.814	-0.0622
RHO2	769	0.78	-0.057
TUB4	890	0.7	-0.0726
ESP1	1022	0.61	-0.0928
LDB18	1041	0.597	-0.0851
CLB1	1096	0.566	-0.0871
LIA1	1127	0.549	-0.0834
ARP1	1191	0.517	-0.0885
HSK3	1229	0.5	-0.0876
TVP38	1232	0.498	-0.0779
CDC28	1377	0.434	-0.1049
DUO1	1473	0.393	-0.1205
DYN2	1505	0.377	-0.1205
NDC1	1574	0.349	-0.1304
DAD1	1581	0.347	-0.1248
STU2	1741	0.29	-0.1584
BUD6	1815	0.262	-0.1712
HCM1	1895	0.231	-0.1861
BER1	1929	0.219	-0.1899
DSK2	1935	0.216	-0.1868
MYO2	1991	0.193	-0.1965
DYN1	2157	-0.205	-0.2333
NAP1	2164	-0.207	-0.2306
ATS1	2341	-0.264	-0.269
RRD1	2375	-0.274	-0.2716
KIP3	2435	-0.297	-0.2802
BBP1	2494	-0.311	-0.2883
CBF2	2556	-0.328	-0.2968
SPO1	2578	-0.333	-0.2953
RTS1	2598	-0.339	-0.2931
SFI1	2627	-0.347	-0.293
NUF2	2644	-0.352	-0.2898
CLB3	2653	-0.355	-0.2846
DAM1	2698	-0.369	-0.288
SPC42	2699	-0.369	-0.2805
IPL1	2720	-0.377	-0.2779
SHE1	2753	-0.386	-0.278
ASK1	2863	-0.419	-0.2965
KIP2	2866	-0.42	-0.2885

FIN1	2941	-0.442	-0.2979
BNI1	2962	-0.447	-0.2938
NIP100	2972	-0.45	-0.2869
MLP2	2998	-0.46	-0.2838
CDC5	3007	-0.462	-0.2764
POM34	3090	-0.491	-0.2868
CLB5	3092	-0.491	-0.2771
MPS1	3205	-0.534	-0.2941
DAD3	3225	-0.541	-0.2878
GPA1	3229	-0.543	-0.2775
SHP1	3235	-0.544	-0.2677
JNM1	3246	-0.549	-0.2591
NDL1	3262	-0.554	-0.2516
STU1	3369	-0.599	-0.2657
AME1	3445	-0.63	-0.2716
NUM1	3562	-0.687	-0.2864
CDC31	3573	-0.691	-0.2749
CDC14	3604	-0.705	-0.268
ASE1	3808	-0.859	-0.301
BIR1	3826	-0.874	-0.2875
KAR3	3828	-0.876	-0.27
UBC9	3861	-0.901	-0.2596
IRC15	3867	-0.91	-0.2424
DMA2	3895	-0.934	-0.2301
MPS2	3908	-0.953	-0.2138
SLK19	3917	-0.963	-0.1962
MIF2	3925	-0.975	-0.1782
OKP1	3929	-0.979	-0.1591
DSN1	3941	-0.998	-0.1416
DYN3	3953	-1.012	-0.1237
CDH1	3970	-1.039	-0.1066
NDC80	3988	-1.059	-0.0894
MPS3	4049	-1.261	-0.0787
CTF19	4076	-1.374	-0.0572
SPC24	4095	-1.573	-0.0298
CIK1	4096	-1.59	0.0025

Sister Chromatid Segregation

Gene Name	Rank in Gene List	Rank Metric Score	Running Enrichment Score
POL30	166	1.548	-0.0072
MCD1	805	0.755	-0.1489
TOF1	879	0.705	-0.1516
KIN4	938	0.667	-0.1513
SMC3	965	0.646	-0.1436
YCS4	1000	0.627	-0.1383
PDS5	1011	0.619	-0.1272
MAD2	1015	0.615	-0.1145
ESP1	1022	0.61	-0.1026
MCM16	1028	0.606	-0.0906
HHT2	1155	0.536	-0.1101
SMC1	1192	0.517	-0.1077
CTF18	1215	0.509	-0.102
LTE1	1301	0.467	-0.1128
CDC20	1424	0.413	-0.1341
CHL1	1508	0.376	-0.1464
YCG1	1689	0.309	-0.1843
MRC1	1708	0.304	-0.1821
TPD3	1718	0.298	-0.1778
IRR1	1751	0.287	-0.1794
SMC4	1797	0.271	-0.1846
BMH1	1961	0.205	-0.2206
DYN1	2157	-0.205	-0.2644
CTF3	2277	-0.246	-0.2885
POL2	2313	-0.257	-0.2916
APC2	2322	-0.26	-0.2879
CDC55	2383	-0.279	-0.2967
ELG1	2404	-0.286	-0.2954
SGS1	2469	-0.303	-0.3046
RTS1	2598	-0.339	-0.3289
MCM22	2600	-0.34	-0.3217
IPL1	2720	-0.377	-0.3429
GPN2	2765	-0.388	-0.3454
CTF8	2825	-0.411	-0.351
RDH54	2843	-0.415	-0.3461
MMS22	2888	-0.425	-0.3477
TOP1	2931	-0.44	-0.3485
FIN1	2941	-0.442	-0.3411

CSE4	2956	-0.446	-0.3348
ESC2	3000	-0.46	-0.3353
APC1	3076	-0.486	-0.3433
SCC2	3095	-0.492	-0.337
MCM21	3166	-0.52	-0.3429
MPS1	3205	-0.534	-0.3407
BUB3	3224	-0.54	-0.3333
BUD2	3250	-0.55	-0.3275
ULP2	3297	-0.571	-0.3264
CSM3	3360	-0.594	-0.3287
GAC1	3368	-0.599	-0.3173
ECO1	3382	-0.605	-0.3073
RMI1	3400	-0.613	-0.2981
MAD1	3406	-0.614	-0.2859
SRC1	3454	-0.635	-0.2837
DOC1	3489	-0.65	-0.2779
SWM1	3524	-0.664	-0.2717
RAD30	3535	-0.667	-0.2596
CEP3	3570	-0.69	-0.2529
BFA1	3733	-0.791	-0.2758
REC8	3796	-0.85	-0.2725
SOH1	3818	-0.869	-0.2587
BIR1	3826	-0.874	-0.2413
KAR3	3828	-0.876	-0.2224
IRC15	3867	-0.91	-0.2118
SCC4	3880	-0.922	-0.1946
DMA2	3895	-0.934	-0.1776
TOP3	3902	-0.946	-0.1584
DSN1	3941	-0.998	-0.146
SPO13	3950	-1.009	-0.1258
CDH1	3970	-1.039	-0.1078
CHL4	3982	-1.053	-0.0875
BRN1	4016	-1.125	-0.071
MPS3	4049	-1.261	-0.0513
CTF19	4076	-1.374	-0.0276
CIK1	4096	-1.59	0.0025

U2 Splicesome Complex

Gene Name	Rank in Gene List	Rank Metric Score	Running Enrichment Score
PRP11	633	0.882	-0.1141
PRP39	1358	0.443	-0.2712
NTR2	1486	0.389	-0.2841
CWC22	1520	0.368	-0.2749
SMB1	1611	0.337	-0.2811
SPP382	1710	0.302	-0.291
PRP16	2132	-0.195	-0.3853
SNU56	2303	-0.253	-0.4151
CWC25	2335	-0.263	-0.4104
CEF1	2377	-0.276	-0.4075
CWC24	2402	-0.286	-0.3999
LUC7	2492	-0.31	-0.4072
SNU71	2592	-0.337	-0.4156
SNP1	2626	-0.347	-0.4074
CWC15	2873	-0.421	-0.448
LEA1	2900	-0.43	-0.4341
CWC27	2920	-0.435	-0.4183
PRP45	2982	-0.455	-0.4119
SYF1	3060	-0.481	-0.4082
CUS1	3080	-0.487	-0.3899
CLF1	3084	-0.489	-0.3676
YHC1	3143	-0.51	-0.3578
YJU2	3322	-0.579	-0.3743
MUD1	3339	-0.584	-0.3507
PRP9	3361	-0.594	-0.3279
SLU7	3372	-0.601	-0.3021
SNT309	3391	-0.608	-0.2778
SMD2	3443	-0.63	-0.2607
NAM8	3451	-0.633	-0.2326
HSH49	3457	-0.635	-0.2039
PRP40	3467	-0.64	-0.1759
CWC2	3505	-0.656	-0.1541
PRP22	3693	-0.764	-0.1641
SMD1	3789	-0.844	-0.1477
PRP18	3802	-0.854	-0.1104
CWC21	3819	-0.869	-0.0734
PRP2	3924	-0.974	-0.0531
CWC23	3951	-1.01	-0.0119
SYF2	3986	-1.056	0.0295

RAS2^{S225E} vs EV- Cytoplasmic Translation- Upregulated

Gene Name	Rank in Gene List	Rank Metric Score	Running Enrichment Score
RPP0	17	3.703	0.0675
RPL30	22	3.58	0.1352
TMA19	35	3.425	0.1983
SSB2	98	2.756	0.2387
SSB1	100	2.735	0.2909
SSA1	122	2.54	0.3353
TMA7	132	2.496	0.3813
RPL28	216	2.164	0.4062
RPL29	236	2.101	0.4427
THS1	274	2.01	0.4738
TIF35	281	1.996	0.5108
SSZ1	289	1.967	0.547
RPG1	295	1.936	0.5831
TIF3	410	1.68	0.5926
TIF11	453	1.616	0.6152
TRM7	663	1.312	0.599
RBG1	827	1.161	0.5889
PRT1	848	1.143	0.6068
HYP2	858	1.134	0.6267
CLU1	1250	0.815	0.5649
RBG2	1444	0.68	0.5397
FUN12	1495	0.657	0.5424
FES1	1606	0.601	0.5321
SLH1	1714	0.546	0.5214
TIF34	1762	0.527	0.5222
TAE1	1810	0.501	0.5224
MTF2	1826	0.491	0.5289
HCR1	2033	0.4	0.4957
TIF5	2391	0.235	0.4296
GIR2	2418	0.225	0.4287
SRO9	3107	-0.451	0.3012
MTG2	3375	-0.581	0.2594
RPM2	3503	-0.65	0.2467
TMA46	3726	-0.784	0.2178
AFG3	4181	-1.13	0.1495
RDN5-1	4548	-1.548	0.1067

Cytosolic Ribosome

Gene Name	Rank in Gene List	Rank Metric Score	Running Enrichment Score
RPP0	17	3.703	0.0459
RPL30	22	3.58	0.0927
RPS3	31	3.465	0.1372
RPS12	42	3.291	0.179
ASC1	53	3.165	0.2191
RPL3	61	3.052	0.2583
YEF3	66	3.013	0.2976
RPS31	85	2.857	0.3321
RPS5	95	2.81	0.3676
RPS2	156	2.38	0.3874
RPS13	174	2.314	0.4148
RPL39	199	2.233	0.4397
RPL28	216	2.164	0.4654
RPL25	219	2.155	0.4936
RPL29	236	2.101	0.5184
RPL10	238	2.096	0.5461
RPS20	256	2.061	0.5701
RLI1	261	2.053	0.5967
RPL32	271	2.021	0.6218
RPL5	280	1.998	0.6468
RPL38	284	1.984	0.6726
NAT1	556	1.456	0.6382
MAP1	626	1.35	0.6425
SIS1	757	1.215	0.6328
ARD1	765	1.207	0.6475
ARX1	822	1.163	0.6519
HYP2	858	1.134	0.66
SQT1	951	1.047	0.6557
SNL1	1081	0.935	0.6426
NMD3	1105	0.913	0.6501
GCN20	1362	0.735	0.6091
CDC48	1461	0.675	0.5987
FUN12	1495	0.657	0.6009
NAT5	1570	0.615	0.5944
FES1	1606	0.601	0.5954
LSG1	1616	0.595	0.6016
GCN1	2111	0.36	0.5084
REI1	2132	0.353	0.5091
YGR054W	2166	0.341	0.5071
TIF5	2391	0.235	0.4658
PAT1	2414	0.226	0.4644

RQC1	2553	-0.169	0.4393
JJJ1	3714	-0.776	0.2196
RRP14	4240	-1.182	0.1312
BUD27	4246	-1.19	0.146
RDN5-1	4548	-1.548	0.1069

Pre-ribosome

Gene Name	Rank in Gene List	Rank Metric Score	Running Enrichment Score
SNU13	11	4.043	0.0243
RPP0	17	3.703	0.0475
RPS3	31	3.465	0.0676
NIP7	60	3.074	0.0821
RPL3	61	3.052	0.1021
NOP58	78	2.895	0.1178
KRR1	94	2.814	0.1332
RPS5	95	2.81	0.1516
UTP13	130	2.504	0.1611
NOP13	150	2.401	0.173
RPS2	156	2.38	0.1876
RPS13	174	2.314	0.1993
NEW1	178	2.295	0.2138
YVH1	204	2.212	0.2232
EMG1	210	2.189	0.2365
RPL28	216	2.164	0.2497
NOP1	218	2.157	0.2636
UTP10	250	2.068	0.2709
ENP1	254	2.066	0.2838
RLI1	261	2.053	0.2961
NOP56	263	2.044	0.3093
ROK1	292	1.959	0.3165
NOC2	305	1.906	0.3265
NUG1	336	1.845	0.3325
CBF5	345	1.818	0.3428
HAS1	356	1.804	0.3526
NSA2	376	1.756	0.3603
HCA4	378	1.753	0.3716
NOG1	382	1.744	0.3824
CIC1	394	1.708	0.3914
KRE33	404	1.699	0.4007
RIX7	443	1.632	0.4037

UTP4	469	1.593	0.4091
PRP43	475	1.589	0.4185
UTP14	489	1.56	0.4261
DBP3	502	1.547	0.4338
DIM1	504	1.544	0.4437
MRT4	511	1.54	0.4526
UTP21	513	1.538	0.4625
RPF2	515	1.535	0.4723
IPI1	540	1.484	0.4772
MAK21	562	1.442	0.4824
MAK16	577	1.417	0.4889
RRP12	638	1.339	0.4855
NOP7	644	1.332	0.4932
SPB1	687	1.284	0.4932
BFR2	696	1.272	0.4999
NOP2	754	1.217	0.4964
SAS10	779	1.198	0.4994
UTP6	781	1.195	0.507
RRP1	788	1.19	0.5136
ARX1	822	1.163	0.5145
SLX9	826	1.161	0.5215
DBP5	850	1.14	0.5244
IMP3	857	1.134	0.5306
PWP2	895	1.091	0.5303
NOG2	900	1.089	0.5366
RRS1	947	1.054	0.5342
ERB1	948	1.053	0.5411
SQT1	951	1.047	0.5476
RRP36	982	1.015	0.5482
NSA1	984	1.012	0.5546
RRP5	1025	0.979	0.5529
UTP7	1033	0.976	0.5579
TIF6	1041	0.967	0.5628
YTM1	1045	0.964	0.5685
NOP4	1096	0.92	0.5645
NMD3	1105	0.913	0.5688
NOP12	1190	0.859	0.5575
NOP9	1193	0.857	0.5627
CKB1	1194	0.856	0.5683
UTP5	1264	0.804	0.5597
BUD20	1279	0.797	0.5621
NOP15	1285	0.794	0.5662

NOC4	1303	0.78	0.5679
SSF1	1349	0.744	0.5637
UTP15	1414	0.697	0.5554
MPP10	1480	0.668	0.5466
DBP8	1493	0.659	0.5485
FUN12	1495	0.657	0.5526
UTP22	1519	0.645	0.5522
ARB1	1532	0.641	0.554
ECM16	1581	0.611	0.5483
RLP24	1719	0.542	0.5242
NAN1	1727	0.54	0.5263
CKB2	1736	0.536	0.5282
RRP9	1743	0.534	0.5305
SOF1	1776	0.521	0.5275
BMS1	1888	0.467	0.5081
UTP25	1981	0.42	0.4923
SQS1	2031	0.4	0.485
NOC3	2032	0.4	0.4877
TSR1	2035	0.397	0.4899
DIP2	2076	0.377	0.4843
UTP23	2083	0.374	0.4855
DBP10	2119	0.358	0.4808
NOP14	2124	0.357	0.4823
REI1	2132	0.353	0.4832
CGR1	2146	0.348	0.4829
FCF1	2156	0.344	0.4833
CMS1	2184	0.328	0.48
UTP20	2192	0.325	0.4807
BUD21	2219	0.312	0.4775
RSA3	2245	0.3	0.4744
UTP9	2249	0.295	0.4758
RRP7	2315	0.269	0.4644
YBL028C	2332	0.264	0.4629
HMO1	2339	0.261	0.4634
BRX1	2361	0.251	0.4608
RCL1	2374	0.241	0.46
AFG2	2389	0.236	0.4587
MRD1	2423	0.223	0.4535
NOB1	2464	0.201	0.4467
DRS1	2520	0.158	0.4366
CKA2	2522	0.158	0.4375
LAS1	2561	-0.172	0.4309

LOC1	2589	-0.193	0.4268
RPF1	2636	-0.222	0.4189
UTP30	2802	-0.303	0.3876
BUD22	2838	-0.324	0.3827
NOP6	2930	-0.365	0.3667
UTP11	3076	-0.434	0.3403
LTV1	3291	-0.541	0.3006
ECM1	3450	-0.627	0.2728
NOP19	3453	-0.628	0.2765
NOP16	3659	-0.74	0.24
IMP4	3699	-0.762	0.2371
JJJ1	3714	-0.776	0.2394
EBP2	3720	-0.781	0.2435
RRP15	3808	-0.837	0.2314
DBP6	4227	-1.172	0.1547
KRI1	4409	-1.365	0.1272
CKA1	4487	-1.446	0.1211

Ribosome assembly

Gene Name	Rank in Gene List	Rank Metric Score	Running Enrichment Score
RPP0	17	3.703	0.0826
RPL3	61	3.052	0.145
NSR1	64	3.03	0.215
RPS31	85	2.857	0.2774
REX4	147	2.407	0.3212
IPI3	185	2.274	0.3667
YVH1	204	2.212	0.4145
RPL25	219	2.155	0.4618
RPL10	238	2.096	0.507
RPL5	280	1.998	0.5453
RIA1	402	1.7	0.5608
MRT4	511	1.54	0.5752
RPF2	515	1.535	0.6103
IPI1	540	1.484	0.64
MAK21	562	1.442	0.6694
RSA4	636	1.342	0.6861
SQT1	951	1.047	0.6483
RSA1	1223	0.832	0.614
RIX1	1237	0.824	0.6306

SSF1	1349	0.744	0.6259
FUN12	1495	0.657	0.6125
LSG1	1616	0.595	0.6026
BMS1	1888	0.467	0.5598
DRS2	2081	0.375	0.5305
RSA3	2245	0.3	0.5052
RRP7	2315	0.269	0.4978
MAK11	2353	0.255	0.4964
BRX1	2361	0.251	0.5009
TIF5	2391	0.235	0.5006
MRD1	2423	0.223	0.4996
DRS1	2520	0.158	0.4843
RPF1	2636	-0.222	0.4667
MRH4	3713	-0.774	0.2718

Ribosome Biogenesis

Gene Name	Rank in Gene List	Rank Metric Score	Running Enrichment Score
SNU13	11	4.043	0.0125
RPP0	17	3.703	0.0249
RPL30	22	3.58	0.0371
RPS3	31	3.465	0.0481
NIP7	60	3.074	0.0535
RPL3	61	3.052	0.0646
NSR1	64	3.03	0.0753
NOP58	78	2.895	0.0831
RPS31	85	2.857	0.0923
KRR1	94	2.814	0.1009
RPS5	95	2.81	0.1111
SSB2	98	2.756	0.1208
SSB1	100	2.735	0.1305
UTP13	130	2.504	0.1337
REX4	147	2.407	0.1391
RPS2	156	2.38	0.1461
RPS13	174	2.314	0.1511
RRB1	176	2.298	0.1592
NEW1	178	2.295	0.1674
IPI3	185	2.274	0.1744
GSP1	202	2.229	0.1792
YVH1	204	2.212	0.1871

EMG1	210	2.189	0.194
NOP1	218	2.157	0.2004
RPL25	219	2.155	0.2083
RPL10	238	2.096	0.2122
UTP10	250	2.068	0.2175
ENP1	254	2.066	0.2244
RPS20	256	2.061	0.2317
RLI1	261	2.053	0.2383
NOP56	263	2.044	0.2456
RPL5	280	1.998	0.2496
SSZ1	289	1.967	0.2551
ROK1	292	1.959	0.2618
NOC2	305	1.906	0.2663
SKI6	308	1.903	0.2728
TSR2	314	1.893	0.2786
ESF1	330	1.85	0.2823
NUG1	336	1.845	0.288
CBF5	345	1.818	0.2929
EFG1	349	1.814	0.2989
HAS1	356	1.804	0.3043
MAK5	358	1.803	0.3106
NSA2	376	1.756	0.3135
HCA4	378	1.753	0.3197
NOG1	382	1.744	0.3254
NHP2	390	1.72	0.3303
RIA1	402	1.7	0.3342
KRE33	404	1.699	0.3402
GAR1	426	1.658	0.3419
RIX7	443	1.632	0.3445
SYO1	448	1.627	0.3496
UTP4	469	1.593	0.3513
RNT1	473	1.59	0.3564
PRP43	475	1.589	0.362
UTP14	489	1.56	0.365
DBP3	502	1.547	0.3682
DIM1	504	1.544	0.3736
RPS15	506	1.544	0.379
MRT4	511	1.54	0.3838
UTP21	513	1.538	0.3892
RPF2	515	1.535	0.3946
RAI1	538	1.491	0.3955
IPI1	540	1.484	0.4007

PUF6	541	1.484	0.4061
MTR4	560	1.444	0.4076
MAK21	562	1.442	0.4127
MAK16	577	1.417	0.4149
RRP3	613	1.37	0.4127
PWP1	625	1.351	0.4153
RSA4	636	1.342	0.4182
RRP12	638	1.339	0.4228
NOP7	644	1.332	0.4267
ZUO1	676	1.292	0.425
DBP2	678	1.292	0.4295
BMT6	682	1.289	0.4335
SPB1	687	1.284	0.4374
DBP9	690	1.281	0.4417
BFR2	696	1.272	0.4453
PUS7	738	1.237	0.4413
NOP2	754	1.217	0.4426
RRP43	764	1.209	0.4452
SAS10	779	1.198	0.4466
UTP6	781	1.195	0.4508
RRP1	788	1.19	0.4539
ARX1	822	1.163	0.4513
NUP85	825	1.161	0.4551
SLX9	826	1.161	0.4593
URB2	840	1.15	0.4608
IMP3	857	1.134	0.4617
RRP42	874	1.112	0.4624
RCM1	893	1.094	0.4627
PWP2	895	1.091	0.4664
DHR2	898	1.09	0.47
NOG2	900	1.089	0.4738
BMT5	904	1.087	0.4771
RPP1	907	1.086	0.4806
RRS1	947	1.054	0.4764
ERB1	948	1.053	0.4803
SQT1	951	1.047	0.4837
RRP36	982	1.015	0.4812
NSA1	984	1.012	0.4846
RRP5	1025	0.979	0.4799
TMA20	1032	0.976	0.4823
UTP7	1033	0.976	0.4858
FAP7	1040	0.967	0.4881

TIF6	1041	0.967	0.4916
YTM1	1045	0.964	0.4945
SDA1	1047	0.96	0.4978
NOP4	1096	0.92	0.4912
SRD1	1104	0.913	0.4931
NMD3	1105	0.913	0.4964
RRP4	1130	0.892	0.4947
RRP46	1139	0.888	0.4963
NUP159	1144	0.886	0.4987
RRP40	1155	0.882	0.4998
NOP12	1190	0.859	0.4959
NOP9	1193	0.857	0.4987
SRM1	1222	0.834	0.4959
RSA1	1223	0.832	0.4989
FCF2	1232	0.827	0.5003
RIX1	1237	0.824	0.5025
RNH70	1259	0.806	0.5011
UTP5	1264	0.804	0.5032
REX3	1268	0.801	0.5055
BUD20	1279	0.797	0.5063
NOP15	1285	0.794	0.5082
NOC4	1303	0.78	0.5075
SSF1	1349	0.744	0.5009
URB1	1397	0.707	0.4938
TIF4631	1410	0.699	0.4938
UTP15	1414	0.697	0.4957
GLC7	1426	0.691	0.496
POP7	1456	0.678	0.4925
MPP10	1480	0.668	0.4901
DBP8	1493	0.659	0.49
FUN12	1495	0.657	0.4922
YAR1	1505	0.652	0.4927
UTP22	1519	0.645	0.4924
ARB1	1532	0.641	0.4923
FYV7	1547	0.633	0.4917
ECM16	1581	0.611	0.4871
NSP1	1582	0.61	0.4893
SGD1	1598	0.603	0.4884
LSG1	1616	0.595	0.4871
RNA1	1699	0.553	0.4721
LCP5	1711	0.547	0.4718
RLP24	1719	0.542	0.4724

NAN1	1727	0.54	0.4729
RRP9	1743	0.534	0.4717
LSM6	1761	0.527	0.4701
SOF1	1776	0.521	0.4691
CAM1	1791	0.515	0.4681
RVB2	1792	0.514	0.47
MTR3	1803	0.504	0.4698
MPP6	1823	0.493	0.4676
RRP8	1829	0.491	0.4684
TMA108	1846	0.48	0.4668
BMS1	1888	0.467	0.46
UTP25	1981	0.42	0.4425
SQS1	2031	0.4	0.4339
NOC3	2032	0.4	0.4353
HCR1	2033	0.4	0.4368
TSR1	2035	0.397	0.438
NGL2	2058	0.386	0.4349
DIP2	2076	0.377	0.4327
DRS2	2081	0.375	0.4333
UTP23	2083	0.374	0.4344
GRC3	2086	0.373	0.4354
DBP10	2119	0.358	0.4301
NOP14	2124	0.357	0.4305
REI1	2132	0.353	0.4304
CGR1	2146	0.348	0.429
FCF1	2156	0.344	0.4284
UTP20	2192	0.325	0.4223
BUD21	2219	0.312	0.4181
RSA3	2245	0.3	0.414
UTP9	2249	0.295	0.4144
NOP8	2285	0.279	0.4082
RRP7	2315	0.269	0.4032
MAK11	2353	0.255	0.3965
BRX1	2361	0.251	0.3959
RCL1	2374	0.241	0.3943
RTC6	2386	0.237	0.3929
AFG2	2389	0.236	0.3934
TIF5	2391	0.235	0.394
MRD1	2423	0.223	0.3884
NOB1	2464	0.201	0.3809
GEP3	2476	0.196	0.3793
NOP53	2501	0.18	0.375

DRS1	2520	0.158	0.3719
RAT1	2540	-0.13	0.3684
JIP5	2545	-0.152	0.3681
LAS1	2561	-0.172	0.3657
NIC96	2570	-0.181	0.3647
POP4	2586	-0.192	0.3623
LOC1	2589	-0.193	0.3626
RPF1	2636	-0.222	0.3539
DIS3	2637	-0.222	0.3547
RSP5	2647	-0.226	0.3536
CSL4	2665	-0.233	0.351
PUS5	2711	-0.26	0.3426
REX2	2728	-0.271	0.3403
UTP30	2802	-0.303	0.3263
FAL1	2833	-0.319	0.3213
BUD22	2838	-0.324	0.3216
SPT5	2846	-0.326	0.3214
LTO1	2917	-0.358	0.3082
NOP6	2930	-0.365	0.307
SAC3	3000	-0.401	0.2942
HIT1	3022	-0.409	0.2914
LSM7	3026	-0.411	0.2922
UTP11	3076	-0.434	0.2837
NUP120	3100	-0.448	0.2806
TOM1	3175	-0.483	0.267
HRR25	3224	-0.506	0.259
TOR2	3252	-0.52	0.2553
NUP49	3256	-0.522	0.2565
LTV1	3291	-0.541	0.2515
RMP1	3446	-0.625	0.2219
ECM1	3450	-0.627	0.2236
NOP19	3453	-0.628	0.2255
MTR2	3510	-0.653	0.2163
BUD23	3594	-0.704	0.2017
POP6	3607	-0.709	0.2018
NUP116	3628	-0.724	0.2003
YAE1	3644	-0.734	0.1998
RIO2	3657	-0.74	0.2
NOP16	3659	-0.74	0.2025
RRP45	3696	-0.761	0.1979
TMA23	3698	-0.762	0.2004
IMP4	3699	-0.762	0.2032

MRH4	3713	-0.774	0.2033
JJJ1	3714	-0.776	0.2062
EBP2	3720	-0.781	0.208
YRB2	3786	-0.821	0.1975
TOR1	3799	-0.83	0.1981
RRP15	3808	-0.837	0.1995
DBP7	3827	-0.848	0.1988
MOT1	3875	-0.878	0.1923
PAF1	3903	-0.894	0.19
RRP17	3935	-0.922	0.187
SNU66	3972	-0.95	0.183
TSR3	4108	-1.055	0.1589
SNM1	4207	-1.152	0.1428
DBP6	4227	-1.172	0.1432
RRP14	4240	-1.182	0.145
LRP1	4369	-1.317	0.1233
NUP1	4382	-1.33	0.1257
KRI1	4409	-1.365	0.1253
RNP1	4508	-1.479	0.1104
NME1	4925	-2.497	0.0335

Translation Elongation

Gene Name	Rank in Gene List	Rank Metric Score	Running Enrichment Score
EFT1	18	3.69	0.0853
TEF2	29	3.473	0.1669
TEF1	39	3.308	0.2447
EFT2	56	3.152	0.3174
YEF3	66	3.013	0.3881
SSB2	98	2.756	0.4483
SSB1	100	2.735	0.514
EFB1	126	2.524	0.5698
RPS2	156	2.38	0.6213
STM1	200	2.233	0.6666
TEF4	248	2.07	0.7071
SSZ1	289	1.967	0.7466
ZUO1	676	1.292	0.7015
HYP2	858	1.134	0.693
GCN20	1362	0.735	0.6114
TUF1	1708	0.549	0.5565
CAM1	1791	0.515	0.5527

GCN1	2111	0.36	0.4983
SUA5	2151	0.346	0.499
OAZ1	2300	0.275	0.4764
DHH1	3517	-0.658	0.2521
CTK2	3535	-0.665	0.2647
CTK1	3555	-0.676	0.2772
CTK3	4091	-1.042	0.1967

RAS2^{S225E} vs EV- Chromosome Segredatation- Downregulated

Gene Name	Rank in Gene List	Rank Metric Score	Running Enrichment Score
NDJ1	266	2.036	-0.0401
SCP160	322	1.864	-0.0387
RFC5	551	1.462	-0.075
TPD3	587	1.4	-0.0726
RFC4	729	1.243	-0.0927
POL30	906	1.086	-0.121
SMC3	1001	1.002	-0.1333
INO80	1249	0.815	-0.1778
SPO16	1275	0.798	-0.1775
KIN3	1317	0.769	-0.1806
GLC7	1426	0.691	-0.1978
CDC48	1461	0.675	-0.2001
SPO22	1539	0.637	-0.2114
HOP1	1732	0.539	-0.2467
FOB1	1765	0.526	-0.2496
TOF1	1833	0.486	-0.2599
KIN4	1914	0.458	-0.273
SMC4	1918	0.457	-0.2705
CHL1	1923	0.451	-0.2683
SMC6	1940	0.442	-0.2685
LRS4	1997	0.415	-0.2771
LTE1	2057	0.386	-0.2864
DCC1	2087	0.372	-0.2898
CDC20	2243	0.3	-0.3191
BUR2	2259	0.289	-0.3202
MND2	2305	0.274	-0.3275
MAD2	2358	0.252	-0.3363

HDA3	2379	0.24	-0.3387
NPA3	2412	0.227	-0.3437
PAT1	2414	0.226	-0.3423
RFC2	2450	0.21	-0.348
PPH21	2467	0.201	-0.3499
CDC28	2494	0.186	-0.3539
MCK1	2576	-0.185	-0.3691
MMS22	2587	-0.193	-0.3698
STS1	2590	-0.193	-0.3689
IRR1	2690	-0.248	-0.3872
SLI15	2734	-0.274	-0.3941
DMA1	2753	-0.283	-0.3958
MCD1	2778	-0.291	-0.3987
MAD3	2797	-0.3	-0.4003
SPC72	2801	-0.303	-0.3989
RAD61	2813	-0.309	-0.399
CTF4	2835	-0.322	-0.4011
CTF18	2851	-0.329	-0.4019
RTS1	2871	-0.337	-0.4035
ESP1	2918	-0.359	-0.4104
HFM1	2950	-0.375	-0.4141
SMC2	2973	-0.388	-0.416
IML3	2991	-0.398	-0.4167
GPN2	3014	-0.407	-0.4184
CIN8	3031	-0.413	-0.4189
CEP3	3055	-0.426	-0.4207
RTT102	3065	-0.43	-0.4196
YPI1	3083	-0.437	-0.4201
ELG1	3091	-0.442	-0.4185
SGS1	3097	-0.446	-0.4165
RED1	3145	-0.467	-0.4229
CDC55	3160	-0.478	-0.4225
DAD2	3202	-0.496	-0.4274
NUP170	3203	-0.496	-0.4241
HRR25	3224	-0.506	-0.4247
SCC2	3234	-0.51	-0.4231
BUB1	3237	-0.511	-0.42
GIP3	3273	-0.53	-0.4235
CTF3	3335	-0.557	-0.4321
MCM21	3383	-0.585	-0.4377
STH1	3463	-0.632	-0.4494
SIZ1	3475	-0.637	-0.4474

HHT2	3483	-0.641	-0.4444
RMI1	3486	-0.641	-0.4405
APC1	3491	-0.644	-0.437
IES6	3519	-0.658	-0.438
BUB2	3522	-0.66	-0.4339
MTW1	3541	-0.667	-0.4331
WIP1	3570	-0.685	-0.4341
IRC15	3630	-0.725	-0.4412
BIM1	3655	-0.74	-0.441
POL2	3663	-0.744	-0.4374
MAD1	3668	-0.746	-0.4332
ZIP1	3712	-0.774	-0.4367
RDH54	3721	-0.782	-0.433
FIN1	3746	-0.795	-0.4325
DUO1	3753	-0.801	-0.4283
BMH1	3760	-0.806	-0.4241
RSC2	3771	-0.813	-0.4206
CNN1	3779	-0.816	-0.4165
PDS5	3787	-0.822	-0.4124
RAD30	3815	-0.843	-0.4121
SRC1	3849	-0.863	-0.413
CSE4	3850	-0.863	-0.4072
KIP1	3898	-0.89	-0.4107
AMA1	3943	-0.924	-0.4134
SHP1	3970	-0.947	-0.4122
TOP1	4017	-0.983	-0.4149
SPC25	4040	-1.001	-0.4126
CBF2	4045	-1.003	-0.4066
DMA2	4092	-1.044	-0.4089
NUD1	4095	-1.047	-0.4022
CDC5	4118	-1.065	-0.3995
DAM1	4122	-1.071	-0.3928
BFA1	4124	-1.075	-0.3858
SGO1	4134	-1.086	-0.3803
BUD2	4152	-1.097	-0.3763
DAD4	4162	-1.105	-0.3707
SCC4	4166	-1.108	-0.3638
MPS1	4193	-1.145	-0.3613
REC8	4214	-1.16	-0.3575
CSM4	4250	-1.195	-0.3566
GLC8	4255	-1.201	-0.3493
SWM1	4258	-1.203	-0.3415

ULP2	4259	-1.203	-0.3334
SFH1	4288	-1.227	-0.3308
NBL1	4289	-1.228	-0.3225
ASK1	4298	-1.243	-0.3157
SPC34	4310	-1.255	-0.3095
AME1	4312	-1.257	-0.3012
CTF8	4332	-1.281	-0.2964
ZIP2	4381	-1.33	-0.2971
PDS1	4421	-1.38	-0.2957
BUB3	4453	-1.408	-0.2925
CSM3	4466	-1.422	-0.2853
ECO1	4584	-1.599	-0.2982
VIK1	4608	-1.627	-0.2918
CDH1	4620	-1.641	-0.283
IPL1	4627	-1.657	-0.273
TOP3	4650	-1.701	-0.266
BIR1	4652	-1.703	-0.2547
SCM3	4680	-1.76	-0.2482
DMC1	4685	-1.776	-0.2371
CDC14	4713	-1.823	-0.2302
NFI1	4723	-1.852	-0.2195
BRN1	4746	-1.899	-0.2112
CHL4	4748	-1.91	-0.1985
DAD3	4765	-1.943	-0.1886
GAC1	4766	-1.946	-0.1754
NNF1	4771	-1.964	-0.163
CBF1	4792	-2.026	-0.1533
CTF19	4845	-2.194	-0.149
NDC80	4847	-2.199	-0.1344
KAR3	4849	-2.21	-0.1197
MIF2	4858	-2.23	-0.1062
OKP1	4876	-2.305	-0.0941
SLK19	4886	-2.343	-0.0801
MPS3	4919	-2.483	-0.0698
SOH1	4931	-2.508	-0.0551
DSN1	4950	-2.595	-0.0412
SPO13	4960	-2.647	-0.0251
CIK1	5039	-3.286	-0.0187
SPC24	5081	-4.182	0.0012

Condensed Chromosome

Gene Name	Rank in Gene List	Rank Metric Score	Running Enrichment Score
NSE5	761	1.212	-0.14
REC104	914	1.08	-0.1595
SMC3	1001	1.002	-0.1666
SPO16	1275	0.798	-0.2131
GLC7	1426	0.691	-0.2361
SPO22	1539	0.637	-0.2521
PSY2	1584	0.61	-0.2548
HOP1	1732	0.539	-0.2787
SMC4	1918	0.457	-0.3111
RFA2	1921	0.452	-0.307
SMC6	1940	0.442	-0.3061
LRS4	1997	0.415	-0.3131
TOP2	2144	0.348	-0.3388
RFA3	2190	0.326	-0.3445
NSE3	2225	0.308	-0.3482
RAD17	2248	0.297	-0.3496
MAD2	2358	0.252	-0.3689
NSE1	2510	0.173	-0.3973
PLC1	2573	-0.184	-0.4079
IRR1	2690	-0.248	-0.4286
MCD1	2778	-0.291	-0.443
RAD61	2813	-0.309	-0.4467
RTS1	2871	-0.337	-0.4547
RFA1	2886	-0.34	-0.4541
SMC2	2973	-0.388	-0.4674
IML3	2991	-0.398	-0.4668
CIN8	3031	-0.413	-0.4704
CEP3	3055	-0.426	-0.4707
SMT3	3073	-0.433	-0.4698
RED1	3145	-0.467	-0.4792
DAD2	3202	-0.496	-0.4854
HRR25	3224	-0.506	-0.4845
BUB1	3237	-0.511	-0.4818
STU2	3272	-0.53	-0.4832
CTF3	3335	-0.557	-0.49
MCM21	3383	-0.585	-0.4935
MTW1	3541	-0.667	-0.5182
MEC3	3598	-0.706	-0.5223
PPH3	3603	-0.708	-0.516
ZIP1	3712	-0.774	-0.5298
FIN1	3746	-0.795	-0.5283

DUO1	3753	-0.801	-0.5215
PDS5	3787	-0.822	-0.5198
CSE4	3850	-0.863	-0.5235
SPC25	4040	-1.001	-0.5512
CBF2	4045	-1.003	-0.5419
CTF13	4064	-1.019	-0.5352
DAM1	4122	-1.071	-0.5358
SGO1	4134	-1.086	-0.5271
DAD4	4162	-1.105	-0.5213
MPS1	4193	-1.145	-0.5158
REC8	4214	-1.16	-0.5081
NSE4	4220	-1.165	-0.4974
ASK1	4298	-1.243	-0.5002
SPC34	4310	-1.255	-0.4898
AME1	4312	-1.257	-0.4773
ZIP2	4381	-1.33	-0.4775
REC107	4385	-1.336	-0.4647
REC114	4394	-1.347	-0.4527
UBC9	4427	-1.385	-0.4451
SAE3	4438	-1.397	-0.433
REC102	4445	-1.404	-0.4201
BUB3	4453	-1.408	-0.4073
RAD51	4510	-1.482	-0.4036
GMC2	4559	-1.556	-0.3975
IPL1	4627	-1.657	-0.3942
BIR1	4652	-1.703	-0.3818
SCM3	4680	-1.76	-0.3695
DMC1	4685	-1.776	-0.3524
BRN1	4746	-1.899	-0.3453
CHL4	4748	-1.91	-0.3262
TFC3	4754	-1.921	-0.3078
DAD3	4765	-1.943	-0.2903
NNF1	4771	-1.964	-0.2715
KRE28	4796	-2.036	-0.2557
MMS21	4806	-2.052	-0.2369
CTF19	4845	-2.194	-0.2224
NDC80	4847	-2.199	-0.2004
MND1	4851	-2.22	-0.1786
MIF2	4858	-2.23	-0.1573
OKP1	4876	-2.305	-0.1375
SLK19	4886	-2.343	-0.1157
DSN1	4950	-2.595	-0.1021

ECM11	4952	-2.599	-0.0762
SPO13	4960	-2.647	-0.0509
MEI5	5042	-3.347	-0.0333
SPC24	5081	-4.182	0.0012

Microtubule Based Processes

Gene Name	Rank in Gene List	Rank Metric Score	Running Enrichment Score
ACT1	180	2.293	-0.013
CMD1	324	1.862	-0.023
LDB18	681	1.291	-0.0813
CLB4	795	1.184	-0.092
CRN1	810	1.172	-0.0831
LIA1	967	1.027	-0.104
ARP1	1133	0.891	-0.1281
CDC48	1461	0.675	-0.1868
TVP38	1661	0.574	-0.2208
NDC1	1690	0.559	-0.2208
BUD6	1724	0.541	-0.222
RRD2	2067	0.381	-0.2867
DSK2	2183	0.33	-0.3064
DYN2	2216	0.313	-0.3096
BER1	2296	0.276	-0.3227
CDC28	2494	0.186	-0.3602
CDC15	2736	-0.276	-0.4057
DMA1	2753	-0.283	-0.4061
SPC72	2801	-0.303	-0.4124
ATS1	2804	-0.305	-0.4098
CLB5	2829	-0.318	-0.4114
RTS1	2871	-0.337	-0.4162
ESP1	2918	-0.359	-0.4218
KAR1	2939	-0.37	-0.4221
YHR127W	2995	-0.399	-0.4291
JNM1	3007	-0.404	-0.4273
CIN8	3031	-0.413	-0.4277
PAC11	3052	-0.425	-0.4275
DAD2	3202	-0.496	-0.4523
HRR25	3224	-0.506	-0.4515
BUB1	3237	-0.511	-0.4487
SPC97	3260	-0.524	-0.4479

STU2	3272	-0.53	-0.4448
NBP1	3322	-0.552	-0.449
CLB3	3354	-0.567	-0.4496
HCM1	3356	-0.568	-0.4441
BNI1	3387	-0.586	-0.4442
SPC110	3396	-0.593	-0.4398
RRD1	3412	-0.606	-0.4368
KIP3	3490	-0.643	-0.4457
NUM1	3500	-0.646	-0.441
SWE1	3578	-0.692	-0.4495
ABM1	3587	-0.699	-0.4441
MLP2	3599	-0.707	-0.4392
IRC15	3630	-0.725	-0.4379
BIM1	3655	-0.74	-0.4353
NIP100	3666	-0.745	-0.4299
FIN1	3746	-0.795	-0.4377
DUO1	3753	-0.801	-0.4309
KIP1	3898	-0.89	-0.4508
SHP1	3970	-0.947	-0.4555
GPA1	3976	-0.954	-0.4469
SPC25	4040	-1.001	-0.4495
CBF2	4045	-1.003	-0.4402
DMA2	4092	-1.044	-0.4389
NUD1	4095	-1.047	-0.4288
KIP2	4102	-1.052	-0.4195
NDL1	4105	-1.054	-0.4093
CDC5	4118	-1.065	-0.401
DAM1	4122	-1.071	-0.3909
SGO1	4134	-1.086	-0.3822
DAD4	4162	-1.105	-0.3765
STU1	4185	-1.132	-0.3696
MPS1	4193	-1.145	-0.3595
ASK1	4298	-1.243	-0.3678
SPC34	4310	-1.255	-0.3574
AME1	4312	-1.257	-0.345
MPS2	4328	-1.272	-0.3353
ASE1	4342	-1.294	-0.3249
BBP1	4358	-1.304	-0.3148
POM34	4372	-1.321	-0.3042
UBC9	4427	-1.385	-0.3011
CDC31	4484	-1.442	-0.2978
SPC42	4543	-1.532	-0.2941

SHE1	4581	-1.596	-0.2855
VIK1	4608	-1.627	-0.2744
CDH1	4620	-1.641	-0.2601
IPL1	4627	-1.657	-0.2447
BIR1	4652	-1.703	-0.2324
DYN3	4693	-1.797	-0.2224
CDC14	4713	-1.823	-0.2079
DAD3	4765	-1.943	-0.1986
CTF19	4845	-2.194	-0.1924
NDC80	4847	-2.199	-0.1706
KAR3	4849	-2.21	-0.1486
MIF2	4858	-2.23	-0.1278
OKP1	4876	-2.305	-0.1081
SLK19	4886	-2.343	-0.0864
MPS3	4919	-2.483	-0.0679
DSN1	4950	-2.595	-0.0479
CIK1	5039	-3.286	-0.0325
SPC24	5081	-4.182	0.0012

Nuclear Division

Gene Name	Rank in Gene List	Rank Metric Score	Running Enrichment Score
YVH1	204	2.212	-0.0308
RCK1	228	2.127	-0.0248
NDJ1	266	2.036	-0.0221
SCP160	322	1.864	-0.0241
WTM1	396	1.708	-0.0305
BFR1	398	1.706	-0.0221
PSE1	452	1.619	-0.0248
TPD3	587	1.4	-0.0453
KAR4	616	1.362	-0.0442
MSH2	661	1.314	-0.0466
AMN1	673	1.296	-0.0424
CLB4	795	1.184	-0.0613
SPO23	816	1.168	-0.0595
POL30	906	1.086	-0.0723
REC104	914	1.08	-0.0683
SMC3	1001	1.002	-0.081
RCK2	1181	0.864	-0.1134
MSH5	1197	0.855	-0.1122
SPO16	1275	0.798	-0.124

CPR1	1294	0.788	-0.1237
GLC7	1426	0.691	-0.1471
TRS85	1487	0.661	-0.1561
KAP104	1511	0.649	-0.1576
SPO22	1539	0.637	-0.1599
RTT101	1559	0.622	-0.1607
PSY2	1584	0.61	-0.1625
BRE1	1667	0.572	-0.1765
HOP1	1732	0.539	-0.1869
CDC10	1819	0.497	-0.2021
TOF1	1833	0.486	-0.2023
MRE11	1840	0.484	-0.2011
RAD50	1855	0.478	-0.2016
RAD1	1908	0.46	-0.21
KIN4	1914	0.458	-0.2087
SMC4	1918	0.457	-0.207
RFA2	1921	0.452	-0.2051
CHL1	1923	0.451	-0.2031
LRS4	1997	0.415	-0.216
DOT1	2020	0.405	-0.2185
RME1	2025	0.403	-0.2173
MLH1	2039	0.396	-0.2179
LTE1	2057	0.386	-0.2195
CDC42	2060	0.385	-0.218
CDC7	2062	0.384	-0.2162
DCC1	2087	0.372	-0.2193
TOP2	2144	0.348	-0.229
RFA3	2190	0.326	-0.2366
SHS1	2194	0.324	-0.2356
CDC20	2243	0.3	-0.244
RAD17	2248	0.297	-0.2433
BUR2	2259	0.289	-0.2439
XRS2	2269	0.286	-0.2443
MND2	2305	0.274	-0.2501
SKI8	2345	0.258	-0.2568
MAD2	2358	0.252	-0.258
NPA3	2412	0.227	-0.2678
SKP1	2429	0.221	-0.27
PPH21	2467	0.201	-0.2765
CDC28	2494	0.186	-0.2809
HAC1	2511	0.171	-0.2834
MCK1	2576	-0.185	-0.2956

MMS22	2587	-0.193	-0.2967
KEL1	2674	-0.239	-0.3131
IRR1	2690	-0.248	-0.315
SNF3	2694	-0.251	-0.3143
RIM8	2706	-0.258	-0.3153
FPR3	2722	-0.268	-0.317
CDC15	2736	-0.276	-0.3183
SPO12	2748	-0.28	-0.3191
DMA1	2753	-0.283	-0.3185
PDR16	2760	-0.286	-0.3183
MCD1	2778	-0.291	-0.3204
STE20	2790	-0.298	-0.3211
MAD3	2797	-0.3	-0.3209
RAD10	2798	-0.301	-0.3193
SPC72	2801	-0.303	-0.3182
RAD61	2813	-0.309	-0.3189
CLB5	2829	-0.318	-0.3204
CTF4	2835	-0.322	-0.3198
MLH3	2845	-0.326	-0.32
CTF18	2851	-0.329	-0.3194
RAD52	2867	-0.336	-0.3208
RTS1	2871	-0.337	-0.3197
RFA1	2886	-0.34	-0.3209
ESP1	2918	-0.359	-0.3254
HFM1	2950	-0.375	-0.3299
SMC2	2973	-0.388	-0.3325
NDT80	2976	-0.39	-0.3309
IML3	2991	-0.398	-0.3318
SAC3	3000	-0.401	-0.3314
GPN2	3014	-0.407	-0.3321
KEL2	3019	-0.409	-0.3308
CIN8	3031	-0.413	-0.331
CEP3	3055	-0.426	-0.3336
RMR1	3057	-0.426	-0.3316
YPI1	3083	-0.437	-0.3346
NPR3	3085	-0.439	-0.3326
ELG1	3091	-0.442	-0.3314
SGS1	3097	-0.446	-0.3302
RED1	3145	-0.467	-0.3375
CDC55	3160	-0.478	-0.3379
GIC2	3166	-0.482	-0.3365
RAD6	3169	-0.482	-0.3345

TOM1	3175	-0.483	-0.3331
HRR25	3224	-0.506	-0.3404
SCC2	3234	-0.51	-0.3397
BUB1	3237	-0.511	-0.3376
MSH6	3295	-0.543	-0.3465
CTF3	3335	-0.557	-0.3517
RIM101	3345	-0.563	-0.3508
BNS1	3351	-0.565	-0.349
CLB3	3354	-0.567	-0.3465
SET3	3357	-0.568	-0.3441
MCM21	3383	-0.585	-0.3463
MUM2	3431	-0.619	-0.3528
IDS2	3444	-0.624	-0.3521
STH1	3463	-0.632	-0.3526
HHT2	3483	-0.641	-0.3533
RMI1	3486	-0.641	-0.3505
KIP3	3490	-0.643	-0.3479
APC1	3491	-0.644	-0.3446
BUB2	3522	-0.66	-0.3475
RAD57	3527	-0.662	-0.345
MSC3	3562	-0.678	-0.3486
TGS1	3571	-0.686	-0.3467
RIM15	3573	-0.689	-0.3435
SWE1	3578	-0.692	-0.3408
HOS2	3589	-0.701	-0.3394
SIN3	3592	-0.703	-0.3362
PPH3	3603	-0.708	-0.3347
IRC15	3630	-0.725	-0.3364
BIM1	3655	-0.74	-0.3376
POL2	3663	-0.744	-0.3353
MAD1	3668	-0.746	-0.3324
SET2	3681	-0.753	-0.3311
DON1	3706	-0.769	-0.3321
SSN8	3711	-0.774	-0.329
ZIP1	3712	-0.774	-0.3252
EBP2	3720	-0.781	-0.3227
RDH54	3721	-0.782	-0.3187
MSH4	3725	-0.784	-0.3154
FIN1	3746	-0.795	-0.3155
BMH1	3760	-0.806	-0.3141
TEM1	3780	-0.817	-0.3139
PDS5	3787	-0.822	-0.311

TOR1	3799	-0.83	-0.3091
NIS1	3813	-0.84	-0.3075
RAD30	3815	-0.843	-0.3035
SRC1	3849	-0.863	-0.3059
CSE4	3850	-0.863	-0.3016
PAP2	3878	-0.878	-0.3027
KIP1	3898	-0.89	-0.3022
IME1	3941	-0.923	-0.3061
AMA1	3943	-0.924	-0.3017
NUP53	3965	-0.945	-0.3013
CAK1	4014	-0.982	-0.3062
TOP1	4017	-0.983	-0.3016
IME2	4068	-1.021	-0.3068
DBF4	4084	-1.034	-0.3047
DMA2	4092	-1.044	-0.3008
NUD1	4095	-1.047	-0.296
SPO11	4098	-1.048	-0.2911
CDC5	4118	-1.065	-0.2897
BFA1	4124	-1.075	-0.2853
CDC24	4133	-1.085	-0.2815
SGO1	4134	-1.086	-0.276
BUD2	4152	-1.097	-0.274
ALK1	4160	-1.104	-0.2699
DBF20	4164	-1.106	-0.2649
SCC4	4166	-1.108	-0.2596
MPS1	4193	-1.145	-0.2591
SAE2	4199	-1.149	-0.2544
REC8	4214	-1.16	-0.2514
RIM4	4232	-1.176	-0.249
CSM4	4250	-1.195	-0.2465
HOS4	4252	-1.196	-0.2407
SWM1	4258	-1.203	-0.2357
ULP2	4259	-1.203	-0.2296
GMC1	4327	-1.271	-0.237
CTF8	4332	-1.281	-0.2313
WTM2	4359	-1.305	-0.2301
ARP10	4360	-1.305	-0.2236
ZIP2	4381	-1.33	-0.221
REC107	4385	-1.336	-0.2149
REC114	4394	-1.347	-0.2097
PDS1	4421	-1.38	-0.2081
SAE3	4438	-1.397	-0.2044

REC102	4445	-1.404	-0.1986
BUB3	4453	-1.408	-0.1929
CSM3	4466	-1.422	-0.1882
RAD51	4510	-1.482	-0.1896
PCH2	4540	-1.53	-0.1879
GMC2	4559	-1.556	-0.1837
ECO1	4584	-1.599	-0.1806
VIK1	4608	-1.627	-0.1772
CDH1	4620	-1.641	-0.1712
IPL1	4627	-1.657	-0.1641
TOP3	4650	-1.701	-0.16
BIR1	4652	-1.703	-0.1517
DMC1	4685	-1.776	-0.1493
CDC14	4713	-1.823	-0.1457
BRN1	4746	-1.899	-0.1427
CHL4	4748	-1.91	-0.1333
SLZ1	4755	-1.925	-0.1249
MOB1	4757	-1.931	-0.1154
GAC1	4766	-1.946	-0.1072
UME6	4811	-2.067	-0.1059
CTF19	4845	-2.194	-0.1016
KAR3	4849	-2.21	-0.0911
MND1	4851	-2.22	-0.0801
SLK19	4886	-2.343	-0.0753
MPS3	4919	-2.483	-0.0694
SOH1	4931	-2.508	-0.0591
DSN1	4950	-2.595	-0.0497
ECM11	4952	-2.599	-0.0368
SPO13	4960	-2.647	-0.025
CIK1	5039	-3.286	-0.0244
MEI5	5042	-3.347	-0.008
IME4	5045	-3.39	0.0086

Organelle Fission

Gene Name	Rank in Gene List	Rank Metric Score	Running Enrichment Score
YVH1	204	2.212	-0.031
RCK1	228	2.127	-0.0252
NDJ1	266	2.036	-0.0227
SCP160	322	1.864	-0.0248
WTM1	396	1.708	-0.0313
BFR1	398	1.706	-0.0231
PSE1	452	1.619	-0.0259
TPD3	587	1.4	-0.0466
KAR4	616	1.362	-0.0456
MSH2	661	1.314	-0.0481
AMN1	673	1.296	-0.044
CLB4	795	1.184	-0.063
SPO23	816	1.168	-0.0613
POL30	906	1.086	-0.0742
REC104	914	1.08	-0.0703
SMC3	1001	1.002	-0.083
RCK2	1181	0.864	-0.1156
MSH5	1197	0.855	-0.1144
SPO16	1275	0.798	-0.1263
CPR1	1294	0.788	-0.1261
GLC7	1426	0.691	-0.1496
TRS85	1487	0.661	-0.1587
KAP104	1511	0.649	-0.1602
SPO22	1539	0.637	-0.1626
RTT101	1559	0.622	-0.1634
PSY2	1584	0.61	-0.1653
BRE1	1667	0.572	-0.1793
HOP1	1732	0.539	-0.1898
CDC10	1819	0.497	-0.205
TOF1	1833	0.486	-0.2053
MRE11	1840	0.484	-0.2041
RAD50	1855	0.478	-0.2047
CAF4	1865	0.473	-0.2042
RAD1	1908	0.46	-0.2105
KIN4	1914	0.458	-0.2093
SMC4	1918	0.457	-0.2076
RFA2	1921	0.452	-0.2058
CHL1	1923	0.451	-0.2038
PEX11	1945	0.439	-0.2059
LRS4	1997	0.415	-0.2143
DOT1	2020	0.405	-0.2169

RME1	2025	0.403	-0.2157
MLH1	2039	0.396	-0.2164
LTE1	2057	0.386	-0.218
CDC42	2060	0.385	-0.2165
CDC7	2062	0.384	-0.2148
DCC1	2087	0.372	-0.2179
TOP2	2144	0.348	-0.2277
RFA3	2190	0.326	-0.2353
SHS1	2194	0.324	-0.2343
RPN11	2239	0.302	-0.2419
CDC20	2243	0.3	-0.241
RAD17	2248	0.297	-0.2404
BUR2	2259	0.289	-0.241
XRS2	2269	0.286	-0.2414
MND2	2305	0.274	-0.2473
SKI8	2345	0.258	-0.254
MAD2	2358	0.252	-0.2552
NPA3	2412	0.227	-0.265
SKP1	2429	0.221	-0.2672
PPH21	2467	0.201	-0.2738
CDC28	2494	0.186	-0.2782
HAC1	2511	0.171	-0.2807
MCK1	2576	-0.185	-0.2929
MMS22	2587	-0.193	-0.294
KEL1	2674	-0.239	-0.3105
IRR1	2690	-0.248	-0.3124
SNF3	2694	-0.251	-0.3117
RIM8	2706	-0.258	-0.3127
FPR3	2722	-0.268	-0.3145
CDC15	2736	-0.276	-0.3158
SPO12	2748	-0.28	-0.3167
DMA1	2753	-0.283	-0.3161
PDR16	2760	-0.286	-0.3159
MCD1	2778	-0.291	-0.3179
STE20	2790	-0.298	-0.3187
MAD3	2797	-0.3	-0.3185
RAD10	2798	-0.301	-0.317
SPC72	2801	-0.303	-0.3159
RAD61	2813	-0.309	-0.3166
CLB5	2829	-0.318	-0.3181
CTF4	2835	-0.322	-0.3176
MLH3	2845	-0.326	-0.3178

CTF18	2851	-0.329	-0.3172
RAD52	2867	-0.336	-0.3186
RTS1	2871	-0.337	-0.3176
RFA1	2886	-0.34	-0.3188
ESP1	2918	-0.359	-0.3234
FIS1	2944	-0.372	-0.3267
HFM1	2950	-0.375	-0.3258
SMC2	2973	-0.388	-0.3284
NDT80	2976	-0.39	-0.3269
IML3	2991	-0.398	-0.3278
SAC3	3000	-0.401	-0.3275
GPN2	3014	-0.407	-0.3281
KEL2	3019	-0.409	-0.3269
CIN8	3031	-0.413	-0.3271
CEP3	3055	-0.426	-0.3298
RMR1	3057	-0.426	-0.3279
YPI1	3083	-0.437	-0.3308
NPR3	3085	-0.439	-0.3289
ELG1	3091	-0.442	-0.3277
SGS1	3097	-0.446	-0.3265
RED1	3145	-0.467	-0.3339
CDC55	3160	-0.478	-0.3344
GIC2	3166	-0.482	-0.333
RAD6	3169	-0.482	-0.331
TOM1	3175	-0.483	-0.3297
HRR25	3224	-0.506	-0.337
SCC2	3234	-0.51	-0.3364
BUB1	3237	-0.511	-0.3342
MSH6	3295	-0.543	-0.3433
CTF3	3335	-0.557	-0.3485
RIM101	3345	-0.563	-0.3476
BNS1	3351	-0.565	-0.3458
CLB3	3354	-0.567	-0.3434
SET3	3357	-0.568	-0.341
MCM21	3383	-0.585	-0.3433
MUM2	3431	-0.619	-0.3499
IDS2	3444	-0.624	-0.3493
STH1	3463	-0.632	-0.3498
HHT2	3483	-0.641	-0.3506
RMI1	3486	-0.641	-0.3478
KIP3	3490	-0.643	-0.3452
APC1	3491	-0.644	-0.342

NUM1	3500	-0.646	-0.3405
BUB2	3522	-0.66	-0.3415
RAD57	3527	-0.662	-0.3391
MSC3	3562	-0.678	-0.3427
TGS1	3571	-0.686	-0.3409
RIM15	3573	-0.689	-0.3377
SWE1	3578	-0.692	-0.3351
HOS2	3589	-0.701	-0.3337
SIN3	3592	-0.703	-0.3306
PPH3	3603	-0.708	-0.3292
IRC15	3630	-0.725	-0.3309
BIM1	3655	-0.74	-0.3322
POL2	3663	-0.744	-0.33
MAD1	3668	-0.746	-0.3271
SET2	3681	-0.753	-0.3258
DON1	3706	-0.769	-0.3269
SSN8	3711	-0.774	-0.3239
ZIP1	3712	-0.774	-0.3201
EBP2	3720	-0.781	-0.3177
RDH54	3721	-0.782	-0.3138
MSH4	3725	-0.784	-0.3105
VPS1	3736	-0.79	-0.3087
FIN1	3746	-0.795	-0.3066
BMH1	3760	-0.806	-0.3053
TEM1	3780	-0.817	-0.3051
PDS5	3787	-0.822	-0.3023
TOR1	3799	-0.83	-0.3004
NIS1	3813	-0.84	-0.2989
RAD30	3815	-0.843	-0.295
SRC1	3849	-0.863	-0.2975
CSE4	3850	-0.863	-0.2932
PAP2	3878	-0.878	-0.2944
KIP1	3898	-0.89	-0.2939
IME1	3941	-0.923	-0.298
AMA1	3943	-0.924	-0.2936
NUP53	3965	-0.945	-0.2932
CAK1	4014	-0.982	-0.2982
TOP1	4017	-0.983	-0.2938
IME2	4068	-1.021	-0.299
DBF4	4084	-1.034	-0.297
DMA2	4092	-1.044	-0.2932
NUD1	4095	-1.047	-0.2884

SPO11	4098	-1.048	-0.2837
CDC5	4118	-1.065	-0.2823
BFA1	4124	-1.075	-0.278
CDC24	4133	-1.085	-0.2743
SGO1	4134	-1.086	-0.2689
BUD2	4152	-1.097	-0.2669
ALK1	4160	-1.104	-0.2629
DBF20	4164	-1.106	-0.258
SCC4	4166	-1.108	-0.2528
MPS1	4193	-1.145	-0.2524
SAE2	4199	-1.149	-0.2478
REC8	4214	-1.16	-0.2449
RIM4	4232	-1.176	-0.2426
CSM4	4250	-1.195	-0.2402
HOS4	4252	-1.196	-0.2344
SWM1	4258	-1.203	-0.2295
ULP2	4259	-1.203	-0.2235
GMC1	4327	-1.271	-0.231
CTF8	4332	-1.281	-0.2255
WTM2	4359	-1.305	-0.2244
ARP10	4360	-1.305	-0.2179
ZIP2	4381	-1.33	-0.2154
REC107	4385	-1.336	-0.2094
REC114	4394	-1.347	-0.2044
PDS1	4421	-1.38	-0.2029
SAE3	4438	-1.397	-0.1993
REC102	4445	-1.404	-0.1936
BUB3	4453	-1.408	-0.188
CSM3	4466	-1.422	-0.1835
RAD51	4510	-1.482	-0.185
PCH2	4540	-1.53	-0.1833
GMC2	4559	-1.556	-0.1793
ECO1	4584	-1.599	-0.1763
VIK1	4608	-1.627	-0.173
CDH1	4620	-1.641	-0.1671
IPL1	4627	-1.657	-0.1602
TOP3	4650	-1.701	-0.1563
BIR1	4652	-1.703	-0.148
DMC1	4685	-1.776	-0.1458
CDC14	4713	-1.823	-0.1423
BRN1	4746	-1.899	-0.1395
CHL4	4748	-1.91	-0.1302

SLZ1	4755	-1.925	-0.1219
MOB1	4757	-1.931	-0.1126
GAC1	4766	-1.946	-0.1046
UME6	4811	-2.067	-0.1034
CTF19	4845	-2.194	-0.0993
KAR3	4849	-2.21	-0.089
MND1	4851	-2.22	-0.0782
SLK19	4886	-2.343	-0.0736
MPS3	4919	-2.483	-0.0678
SOH1	4931	-2.508	-0.0577
DSN1	4950	-2.595	-0.0485
ECM11	4952	-2.599	-0.0358
SPO13	4960	-2.647	-0.0242
CIK1	5039	-3.286	-0.0239
MEI5	5042	-3.347	-0.0077
IME4	5045	-3.39	0.0086

Sister Chromatid Segregation

Gene Name	Rank in Gene List	Rank Metric Score	Running Enrichment Score
TPD3	587	1.4	-0.0999
POL30	906	1.086	-0.15
SMC3	1001	1.002	-0.1563
GLC7	1426	0.691	-0.2324
TOF1	1833	0.486	-0.3076
KIN4	1914	0.458	-0.3178
SMC4	1918	0.457	-0.3127
CHL1	1923	0.451	-0.3079
LTE1	2057	0.386	-0.3297
DCC1	2087	0.372	-0.3309
CDC20	2243	0.3	-0.3581
BUR2	2259	0.289	-0.3575
MND2	2305	0.274	-0.3631
MAD2	2358	0.252	-0.3703
NPA3	2412	0.227	-0.3781
PPH21	2467	0.201	-0.3864
MCK1	2576	-0.185	-0.4057
MMS22	2587	-0.193	-0.4053
IRR1	2690	-0.248	-0.4226
DMA1	2753	-0.283	-0.4314
MCD1	2778	-0.291	-0.4326

MAD3	2797	-0.3	-0.4325
SPC72	2801	-0.303	-0.4293
RAD61	2813	-0.309	-0.4276
CTF4	2835	-0.322	-0.4278
CTF18	2851	-0.329	-0.4267
RTS1	2871	-0.337	-0.4263
ESP1	2918	-0.359	-0.431
SMC2	2973	-0.388	-0.437
IML3	2991	-0.398	-0.4354
GPN2	3014	-0.407	-0.4348
CIN8	3031	-0.413	-0.4328
CEP3	3055	-0.426	-0.4321
YPI1	3083	-0.437	-0.432
ELG1	3091	-0.442	-0.4279
SGS1	3097	-0.446	-0.4234
CDC55	3160	-0.478	-0.4298
SCC2	3234	-0.51	-0.438
BUB1	3237	-0.511	-0.4321
CTF3	3335	-0.557	-0.4445
MCM21	3383	-0.585	-0.4466
HHT2	3483	-0.641	-0.4584
RMI1	3486	-0.641	-0.4508
APC1	3491	-0.644	-0.4436
BUB2	3522	-0.66	-0.4414
IRC15	3630	-0.725	-0.4537
BIM1	3655	-0.74	-0.4493
POL2	3663	-0.744	-0.4414
MAD1	3668	-0.746	-0.4329
RDH54	3721	-0.782	-0.4336
FIN1	3746	-0.795	-0.4284
BMH1	3760	-0.806	-0.421
PDS5	3787	-0.822	-0.4159
RAD30	3815	-0.843	-0.4108
SRC1	3849	-0.863	-0.4067
CSE4	3850	-0.863	-0.3959
KIP1	3898	-0.89	-0.3942
TOP1	4017	-0.983	-0.4056
DMA2	4092	-1.044	-0.4073
BFA1	4124	-1.075	-0.4001
SGO1	4134	-1.086	-0.3884
BUD2	4152	-1.097	-0.3781
SCC4	4166	-1.108	-0.3669

MPS1	4193	-1.145	-0.3578
REC8	4214	-1.16	-0.3473
SWM1	4258	-1.203	-0.3409
ULP2	4259	-1.203	-0.3259
CTF8	4332	-1.281	-0.3244
PDS1	4421	-1.38	-0.3248
BUB3	4453	-1.408	-0.3134
CSM3	4466	-1.422	-0.2981
ECO1	4584	-1.599	-0.3015
VIK1	4608	-1.627	-0.2858
CDH1	4620	-1.641	-0.2676
IPL1	4627	-1.657	-0.2481
TOP3	4650	-1.701	-0.2313
BIR1	4652	-1.703	-0.2103
BRN1	4746	-1.899	-0.2052
CHL4	4748	-1.91	-0.1816
GAC1	4766	-1.946	-0.1607
CTF19	4845	-2.194	-0.149
KAR3	4849	-2.21	-0.122
MPS3	4919	-2.483	-0.1048
SOH1	4931	-2.508	-0.0757
DSN1	4950	-2.595	-0.047
SPO13	4960	-2.647	-0.0158
CIK1	5039	-3.286	0.0096